JPL NO. 9950 – 892

DRL No. 157
DRD No. SE-3
Item #4

WAESD-TR-83-1007
DOE/JPL 955909-83/[redacted]11
Distribution Category UC-63

N84-34017 63/44

LOW COST SOLAR ARRAY PROJECT

CELL AND MODULE FORMATION RESEARCH AREA

PROCESS RESEARCH OF NON-CZ SILICON MATERIAL

F I N A L   R E P O R T

November 26, 1980 to September 30, 1983

CONTRACT NO. 955909

The JPL Low-Cost Silicon Array Project is sponsored by the U. S. Department of Energy and forms part of the Solar Photovoltaic Conversion Program to initiate a major effort toward the development of low-cost solar arrays. This work was performed for the Jet Propulsion Laboratory, California Institute of Technology, by agreement between NASA and DOE.

Advanced Energy Systems Division
WESTINGHOUSE ELECTRIC CORPORATION
P. O. Box 10864
Pittsburgh, Pennsylvania 15236

LOW COST SOLAR ARRAY PROJECT
Cell and Module Formation Research Area

PROCESS RESEARCH OF NON-CZ SILICON MATERIAL

FINAL REPORT
November 26, 1980 to September 30, 1983

Contract No. 955909

The JPL Low-Cost Silicon Array Project is sponsored by the U. S. Department of Energy and forms part of the Solar Photovoltaic Conversion Program to initiate a major effort toward the development of low-cost solar arrays. This work was performed for the Jet Propulsion Laboratory, California Institute of Technology, by agreement between NASA and DOE.

Approved:

C. M. Rose

C. M. Rose, Manager
Photovoltaic Pilot Operations

Advanced Energy Systems Division
WESTINGHOUSE ELECTRIC CORPORATION
P. O. Box 10864
Pittsburgh, Pennsylvania 15236

9950-392

TECHNICAL CONTENT STATEMENT

3

ACKNOWLEDGMENTS

This work was sponsored by the United States Department of Energy under JPL Contract 955909.

Mr. C. M. Rose was the Program Manager, and Dr. R. B. Campbell was the Principal Investigator.

The authors would like to thank Dr. D. Meier of the Westinghouse R&D Center for the dark IV and spectral response measurements and Drs. Meier and A. Rohatgi for stimulating discussions.

The measurements were made by Messrs. J. McNally, S. Karako, F. S. Younk (Dark IV) and D. Schmidt (spreading resistivity).

9950-892

TABLE OF CONTENTS

Page No.

I. CONTRACT GOALS AND OBJECTIVES 1
  A. Liquid Junction Technical Feasibility Study 1
  B. Liquid Diffusion Mask Feasibility Study 1
  C. Application Studies of Antireflective (AR) Material Using a Meniscus Coater 1
  D. Ion Implantation Compatibility/Feasibility Study. . . . 2
  E. Cost Analysis 2

II. INTRODUCTION. 3

III. TECHNICAL RESULTS 4
  A. P^+P Junction Formation Using Liquid Boron Solutions . . 4
    1. Process Sequence and Application of Liquid. 4
    2. Initial Experiments 7
    3. Dark IV Measurements. 10
    4. Verification Tests. 12
    5. Belt Furnace Feasibility Investigation. 22
  B. Liquid Diffusion Mask 25
  C. Test of Various Boron and SiO_2 Containing Liquids . . . 30
  D. Cell Evaluation 33
    1. Evaluation of High Efficiency Runs. 33
    2. Evaluation of Low Efficiency Cells. 35
  E. Application of Liquid with a Meniscus Coater. 38
  F. Liquid Phosphorus Dopants for N^+P Front Junction. . . . 43
    1. Introduction and Initial Experiments. 43
    2. Determination of Diffusion Parameters 46
    3. Tests Using the Meniscus Coater 54
    4. Analysis of Cell Parameters 69
  G. Cost Analysis 75
    1. Introduction. 75
    2. Definition of Process Step on Format A. 75
    3. Format A Inputs 79

5

9950-892

TABLE OF CONTENTS (Continued)

Page No.

4. IPEG 2 Calculations 79
5. Conclusions 79

H. Ion Implantation. 82

I. Pelletized Silicon for Replenishment During Web Growth. . . 83

6

LIST OF TABLES

Page No.

1. Solar Cell Junction Formation Process Steps: Baseline vs Various Liquid Dopant Sequences. 5
2. Process Sequence for Fabrication of Solar Cells using Liquid Boron and Liquid Diffusion Masks 6
3. Liquid Boron Diffusion - Time/Temperature Study 8
4. Liquid Boron Dopant vs BBr_3 Baseline Process. 11
5. Dark IV Measurements on Cells Produced in Initial Liquid Boron Experiment. 14
6. Liquid Dopant/Liquid Mask Verification Results. 16
7. Overall Data from Liquid Dopant/Liquid Mask Verification Runs. 17
8. Summary of Liquid Boron/Liquid SiO_2 vs Baseline Cell Efficiency Comparisons. 20
9. Long-Term Comparison of Baseline Process with Liquid SiO_2/Liquid Boron Process 21
10. Data from Belt Furnace Junction Formation Experiment. 23
11. Effects of Web Strip Orientation, Temperature, and Ambient Conditions during Belt Furnace Diffusion. 24
12. Efficiencies Measured on Cells Processed in Standard Silox/Liquid SiO_2/Standard (Gaseous) BBr_3/Liquid Boron Matrix Experiment 27
13. Comparisons of Efficiencies of Cells Produced from a Single Web Crystal Produced using Various Diffusion Drive and Mask Process. 28
14. CVD Silox - Liquid SiO_2 Diffusion Mask Comparison Experiment. 29
15. Alternate Liquid Solutions Investigated 31
16. Results using Various Liquid SiO_2 and Liquid Boron Solutions 32
17. High Efficiency Liquid Boron/Liquid Diffusion Mask Processing Run. 34
18. Data from Reject Cells Analysis 37
19. Meniscus Coater Acceptance Test Data: Thickness of AR Coated Strips 42
20. Data from Cells Processed with AR coating Applied by Meniscus Coater 44

LIST OF TABLES (Continued)

Page No.

21. Process Sequence for Fabrication of Solar Cells using Liquid Dopants and Liquid Diffusion Masks 47
22. Initial Data from Liquid Phosphorus Doped Silicon Dendritic Web Strips. 48
23. Variation of Diffusion Parameters for N^+P Junctions 49
24. Comparison of Lighted IV Data from Liquid Diffusant Source Cells vs $POCl_3$ Diffused Cells 51
25. Lighted IV Cell Data from Initial Meniscus Coater, Liquid Phosphorus Experiment 57
26. Expanded Cell Data from First Meniscus Coater, Liquid Phosphorus Experiment 58
27. N^+P Junction Depth Measurements on Several Liquid Junction Cells. 59
28. Yield Data from Initial Meniscus Coater, Liquid Phosphorus Experiment. 61
29. Effect of Meniscus Coater Applicator Speed on Film Thickness 63
30. Sheet Resistivity of Liquid Coated Strips from Second Meniscus Coater Liquid Phosphorus Experiment. 64
31. Experimental Conditions and Measured Sheet Resistivity for Third Meniscus Coater Test. 66
32. Lighted IV Cell Data on Web Crystal Pairs 68
33. Dark IV Data - Comparison of Front Junction using Liquid Diffusants vs $POCl_3$ 70
34. Process Steps Analyzed. 76
35. Junction Formation Steps Costed 77
36. Assumptions used in Cost Analysis 78
37. IPEG (Interim Price Estimate Guide) 80
38. Cost Summary. 81
39. Average Efficiencies of Cells Grown in Runs using AESD Silicon Shot as Replenishment Material. 90
40. Average Efficiencies of Cells Grown in Runs using Outside Vendor Silicon Pellets as Replenishment Material. 93

8

7950-392

LIST OF FIGURES

Page No.

1. P^+P Junction Profiles in a Liquid Diffused Cell and a Standard Gaseous BBr_3 Diffused Cell 9
2. Generalized Dark IV Curve Segments for Bulk and Junction Currents of Solar Cells 13
3. Efficiency Histogram of 1.6 cm x 9.4 cm Cells Fabricated in Liquid Boron/Liquid SiO_2 Verification Runs 18
4. Efficiency Histogram of 2.0 cm x 9.8 cm Cells Fabricated in Liquid Boron/Liquid SiO_2 Verification Runs 19
5. Schematic Drawing of Meniscus Coater Liquid Application Device. 39
6. Meniscus Coater Web Holding Fixture 40
7. Meniscus Coater after Installation in the Westinghouse Pre-Pilot Facility. 45
8. N^+P Diffusion Profiles for Cell 91A - Liquid Diffusion Source and Cell 92A - $POCl_3$ Diffusion Source. 52
9. Sketch of Mechanism for Low Shunt Resistance Observed in First Liquid Phosphorus Experiment. 56
10. Quantum Efficiency vs Wavelength Plot of $POCl_3$ Diffused Cell and Liquid Diffused Cell. $POCl_3$ Diffused Cell Superior to Liquid Diffused Cell. 73
11. Quantum Efficiency vs Wavelength Plot of $POCl_3$ Diffused Cell and Liquid Diffused Cell. Cells of Equal Quality. . . 74
12. Silicon Pellet Shot Tower after Assembly at Westinghouse. . . 85
13. Normalized Efficiency Distribution of Cells Produced from Web Grown from Runs using AESD Silicon Shot Replenishment 91

I. CONTRACT GOALS AND OBJECTIVES

The primary objective of this contract, in its final form, was to investigate high-risk, high-payoff research areas associated with the Westinghouse process for producing photovoltaic modules using non-CZ sheet material. All investigations were performed using dendritic web silicon, but all process steps studied are directly applicable to other ribbon forms of sheet material. The final contract was separated into the following tasks.

A. Liquid Junction Technical Feasibility Study

The objective of this task was to determine the technical feasibility of forming front and back junctions in non-CZ silicon using liquid dopant techniques. Numerous commercially available liquid phosphorus and boron dopant solutions were investigated. Optimal diffusion parameters required for this process step using liquid dopants were determined.

B. Liquid Diffusion Mask Feasibility Study

The objective of this task was to determine the technical feasibility of forming a liquid applied diffusion mask to replace the more costly chemical vapor deposited SiO_2 diffusion mask. Parameters investigated included SiO_2 containing liquids procured from various vendors, temperature-time profiles for baking liquid masks, film thickness relationship with masking capabilities, identification of etching solutions, process parameters for post-diffusion removal of masks, and methods of liquid mask application.

C. Application Studies of Antireflective (AR) Material Using a Meniscus Coater

The objective of this task was to determine the technical feasibility of applying liquid antireflective solutions using meniscus coating equipment. Film thickness relationships with antireflective capabilities were investigated. The AR films formed were shown to have uniform thickness along the web and possess the required antireflective properties.

10

D. Ion Implantation Compatibility/Feasibility Study

In this task, the feasibility of producing uniform high efficiency solar cells from non-CZ silicon using ion implantation junction formation techniques was studied. This task included an investigation of process variations between processing ion implanted cells and processing gaseous diffused cells using a standard gaseous diffusion process as a baseline and a comparison of cell efficiencies of ion implanted cells with gaseous diffused cells using a standard gaseous diffusion process as a baseline.

E. Cost Analysis

In this task, quantity production cost improvements associated with process improvements under investigation were quantified using IPEG methodology. In addition, Format A, B, and C data have been prepared and are included with this report for SAMICS analyses.

II. INTRODUCTION

Work on JPL Contract 955909 was initiated on November 26, 1980. The initial contract was a technical readiness demonstration program entitled "Module Experimental Process System Development Unit" (MEPSDU). On February 10, 1982, the program was completely restructured to an investigation of high-risk, high-payoff research areas associated with the Westinghouse process for producing photovoltaic modules using non-CZ sheet material. The restructuring was required by the contractor, JPL, to comply with modified Department of Energy guidelines for funding research projects.

A Summary Technical Report was prepared to cover work completed on the MEPSDU technical readiness demonstration contract prior to the redirection. For completeness, the Summary Report is included as Appendix A to this Final Report.

The remainder of this report covers work completed after February 10, 1982. At this time, the contract title was changed to "Process Research of Non-CZ Silicon Material." All tasks identified in Section I of this report were completed as defined in the contract Statement of Work with the exception of the Ion Implantation Compatibility/Feasibility Study. Westinghouse had planned to process web cells after ion implantation of junctions by a separate JPL subcontract. However, no implanted cells were received; and this effort was redirected to other program tasks.

In the Process Research Program, JPL funds were used to define, evaluate, and report results on experiments discussed in this report. All technician and material costs were borne by Westinghouse

Throughout the report, the terms such as liquid boron solution, liquid phosphorus solution, liquid dopant, and liquid SiO_2 mask solution are used. These terms are to be understood as meaning organic solutions containing known concentrations of boron, phosphorus, or SiO_2 compounds, which when applied to the silicon surface and properly dried will act as a diffusant source or a diffusion mask. The terms above are used in the interest of brevity.

12

III. TECHNICAL RESULTS

A. P^+P Junction Formation Using Liquid Boron Solutions

1. Process Sequence and Application of Liquid

The Westinghouse baseline process for fabricating solar cells from dendritic web silicon includes the gaseous diffusion of boron and phosphorus to form the P^+P and N^+P junctions respectively in the N^+PP^+ junction structure. During the gaseous diffusion step, the side of the silicon not being diffused is protected with a chemical vapor deposited SiO_2 film (CVD SiO_2). This gaseous diffusion process has produced high efficiency cells but required relatively expensive capital equipment (e.g., quartz tube diffusion furnaces) and a multi-step processing sequence.

The use of liquid dopants to form the junctions as an alternative to gaseous diffusion would reduce costs by requiring less expensive chemicals and equipment, less involved procedures with simplified controls, and would eliminate several cleaning steps. The purpose of this phase of the program was to demonstrate that cells produced using liquid dopants have as high an efficiency as cells produced using the gaseous diffusion baseline process.

Table 1 shows the junction formation process steps for the baseline and various liquid dopant sequences. This table shows time and material saving since fewer steps are involved. In addition, it also indicates compatibility of the various steps within the baseline sequence.

Table 2 shows the process step using liquid mask + liquid boron + liquid mask + gaseous $POCl_3$ in greater detail.

During the program, several techniques were investigated for applying the liquid dopants. Due to the high aspect ratio rectangular shape of the dendritic web (~3 cm x 33 cm) and the presence of dendrites, a spin on application process is not feasible. Painting on application techniques were attempted without success due to streaking and uncovered areas. The best method of manual application found was to use a sponge and squeegee to apply the liquid onto the

TABLE 1

SOLAR CELL JUNCTION FORMATION PROCESS STEPS:
BASELINE VS VARIOUS LIQUID DOPANT SEQUENCES

Step No.	Process	Baseline	CVD SiO_2 + Liquid Boron	Liquid Mask + Liquid Boron + Liquid Mask + Gaseous $POCl_3$	CVD SiO_2 + Liquid Boron + CVD SiO_2 + Liquid Phosphorus	Liquid Mask + Liquid Boron + Liquid Mask + Liquid Phosphorus
1	CVD SiO_2 N^+ Side	•	•		•	
1A	Apply Liquid Mask and Bake			•		•
1B	Apply Liquid Boron and Bake		•	•	•	•
2	HF Etch	•	•		•	
3	Pre-Diffusion Clean	•				
4	Diffuse P^+	•	•	•	•	•
5	Oxide Etch	•	•	•	•	•
5A	Apply Liquid Phosphorus and Bake				•	•
6	CVD SiO_2 P^+ Side	•	•		•	
6A	Apply Liquid Mask and Bake			•		•
7	HF Etch	•	•			
8	Pre-Diffusion Clean	•	•	•		
9	Diffuse N^+	•	•	•	•	•
10	Oxide Etch	•	•	•	•	•

NOTE: Starting Point - All web pre-diffusion cleaned.

14

TABLE 2

PROCESS SEQUENCE FOR FABRICATION OF SOLAR CELLS
USING LIQUID BORON AND LIQUID DIFFUSION MASKS

1. Pre-diffusion clean (standard chelating).
2. Apply liquid SiO_2 to designated N^+ side of web.
3. Dry under heat lamp for 5 minutes (about 80°C).
4. Apply liquid boron dopant to designated P^+ side of web.
5. Dry under heat lamp for 5 minutes (about 80°C).
6. Load strips in boat with SiO_2 side facing SiO_2 side and P^+ side facing P^+ side. Pre-bake in oven for 15 minutes at 200°C.
7. Place loaded boat in front end of diffusion furnace and bake strips for 5 minutes at approximately 300°C.
8. Move boat into furnace and diffuse for 30 minutes at 960°C. Slow cool furnace to 700°C at 3°C/minute.
9. Strip oxides in 2:1 H_2O:HF.
10. Repeat Step 1.
11. Apply liquid SiO_2 to boron diffused side.
12. Repeat Step 3.
13. Load strips into boat with SiO_2 side facing SiO_2 side.
14. Place boat into front end of $POCl_3$ diffusion tube and bake strips for 5 minutes at approximately 300°C.
15. Move boat into furnace and diffuse in gaseous $POCl_3$ for 20 minutes at 850°C (baseline conditions). Slow cool furnace to 700°C at 3°C/minute.
16. Strip oxides and complete baseline process.

web. When done properly, a uniform layer with no contamination of the opposite side can be routinely obtained.

Experiments conducted early in the program indicated that the liquids used in dendritic web processing for front and back junctions, diffusion masks, AR coatings, and photoresist coatings could be uniformly applied using a meniscus coater, manufactured by Integrated Technologies, Acushnet, MA. Accordingly, a meniscus coater (trade name "CAVEX") was placed on order with Westinghouse capital funds. The testing and verification of this unit is discussed in Section IIIE of this report.

2. Initial Experiments

The primary tool for determining the quality of the diffused junctions is a four-point probe sheet resistivity measurement. The sheet resistivity is a measure of both the surface concentration of the dopant atoms as well as the junction depth. The baseline dendritic web process specifies a sheet resistivity of 40 ±10 Ω/□ for the P^+P junctions and 60 ±10 Ω/□ for the N^+P junction. After achieving sheet resistivities in the proper range, spreading resistance measurements are made to determine actual dopant concentration profiles on the junction regions of the cells. Finally, cells are fabricated from liquid doped web for evaluation using lighted and dark IV measurements.

Initial experiments studied the optimization of the time/temperature boron diffusant drive-in. In all cases, the boron diffusant was applied with a sponge-squeegee. Table 3 shows data from these experiments. With the liquid dopant, it was found necessary to diffuse at 20°C higher temperature and/or a longer time to achieve the proper sheet resistivity.*

Figure 1 shows a boron concentration profile in a cell diffused with liquid boron compared to the profile in a cell processed using the standard gaseous BBr_3 diffusion. Spreading resistance measurements were used to determine concentration profiles in both cases. As is quite evident in the data, both the

*Solution used was Filmtronics Corporation B201.

TABLE 3

LIQUID BORON DIFFUSION - TIME/TEMPERATURE STUDY

Diffusion Temperature (°C)	Diffusion Time (min)	Sheet Resistivity (Ω/□)
925	20	90
925	30	80
960	20	65
960	30	50
960	40	48
980	15	75
980	30	55
980	45	45
980	60	30

NOTES:
1. Baseline BBr_3 gaseous diffusion carried out at 960°C for 20 minutes.
2. Baseline process specification for boron doped p+p junction = 40Ω/□ ±10Ω/□.

17

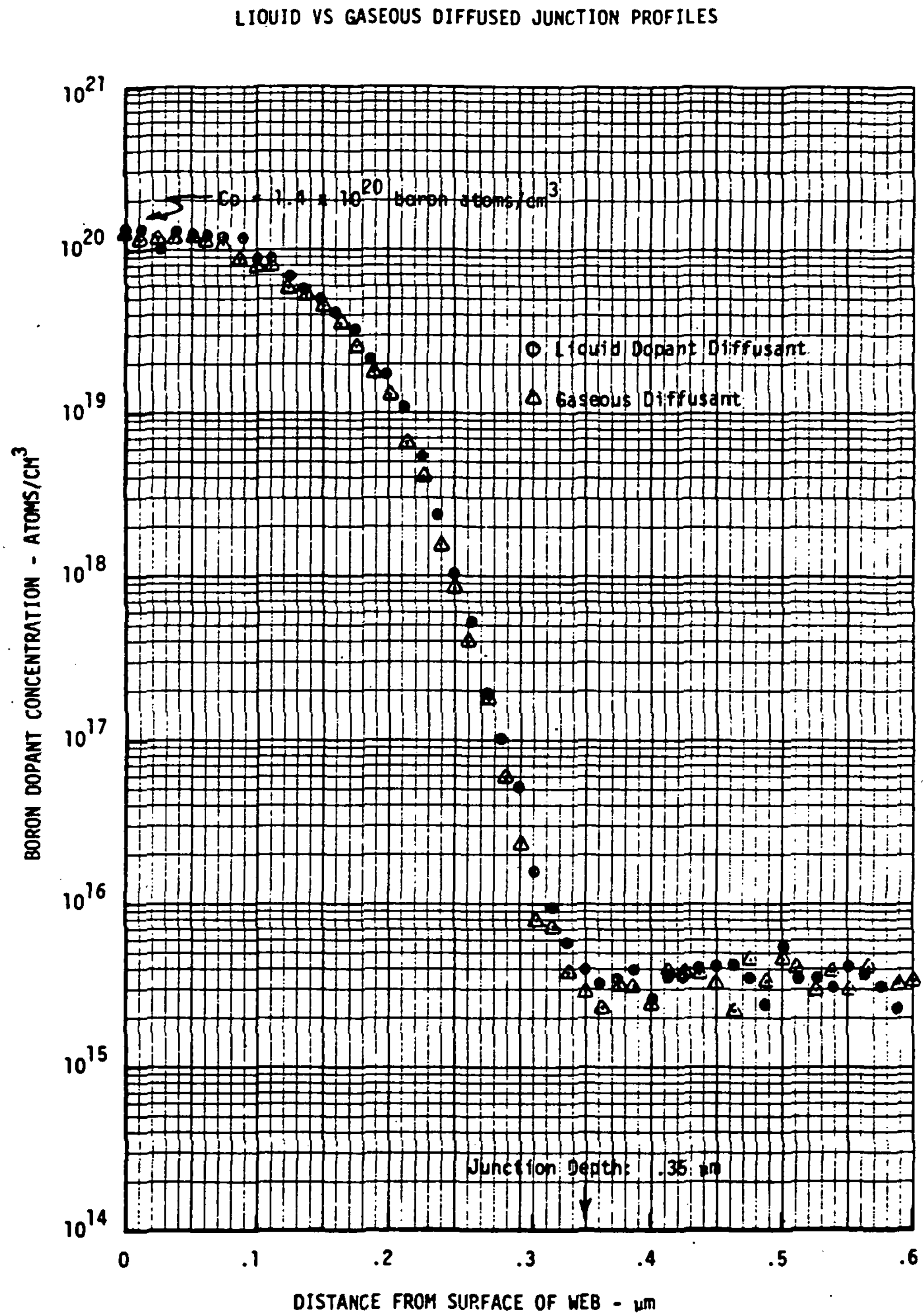

Figure 1. P^+P Junction Profiles in a Liquid Diffused Cell and a Standard Gaseous BBr_3 Diffused Cell

18

surface boron concentration and the junction depths are identical in the two processes. The surface concentration ($\sim 1.4 \times 10^{20}$) and junction depth (0.35 μm) are within the limits set for the baseline process.

Subsequently, a number of experiments were run using both standard diffusion of gaseous BBr_3 and a liquid boron process. All of these runs used the standard Westinghouse baseline process sequence including the CVD SiO_2 (Silox) diffusion mask and $POCl_3$ gaseous diffusion process. Evaluation of cells produced in these runs show that liquid boron diffusion produces cells that are comparable in performance to those produced using the standard BBr_3 baseline process. In these runs, the liquid boron dopant solution was also applied using a sponge squeegee. Table 4 shows the results on a typical run. Efficiency data is shown on 23 (2.0 cm x 9.8 cm) cells. On direct comparison of strips processed from the same dendritic web crystal, it is seen that there is no significant difference in the two processes. The large standard deviations noted for the liquid diffused lots are not considered significant due to the small sample size.

3. Dark IV Measurements

In addition to measuring the lighted IV parameters on all cells, selected cells were analyzed using dark IV measurements. In this measurement, the diode characteristics of the cell are measured in the dark; and from this measurement, series and shunt resistances can be determined as well as the contributions of the junction recombination and bulk current to the dark saturation current.

The dark IV curve for a solar cell can be expressed as:

$$J(V) = J_{01}\, e^{V/V_T} + J_{02}\, e^{V/nV_T}$$

where $V_T = \frac{kT}{q}$. k is the Boltzman constant, T is the absolute temperature, q is the electron charge, V is the cell voltage, and n is the diode factor.

The J_{01} term arises from current flow by carrier diffusion through the bulk. The J_{02} term describes current flow by recombination in the junction depletion

19

TABLE 4

LIQUID BORON DOPANT VS BBr_3 BASELINE PROCESS
(Standard CVD-SiO_2 Diffusion Mask)

- **Overall Run**

BBr_3 Baseline Process - 12 cells

η_{av} = 12.7% ±0.7%

η_{max} = 14.0%

η_{min} = 11.3%

Liquid Boron Dopant - 11 cells

η_{av} = 13.1% ±1.5%

η_{max} = 15.5%

η_{min} = 10.3%

- **Direct Comparison - Cells from the Same Web Crystal**

	Average Efficiency	
Web Crystal No.	Liq. Boron	BBr_3
4.122-18.3	10.8 ±0.8%	
4.122-18.4		12.4 ±0.2%
4.122-16.3	12.6%	
4.122-16.4		12.6 ±0.3%
1.157-1.3	14.9 ±0.6%	
1.157-1.4		13.9 ±0.2%

20

region. The components (J_{01}, J_{02}) of the total current are sketched in Figure 2. Significant increases in the junction (J_{02}) current indicate junction degradation due to improper diffusion, impurity segregation, etc., which are noted by a lowered shunt resistance. Shifts in the bulk current (J_{01}) indicate bulk lifetime changes due to improper diffusion or impurities in the bulk or emitter (N^+) region.

It is important to note that the solar cell parameters of Voc, Isc, and efficiency can be affected by independent changes in the J_{01} and J_{02} currents. Therefore, this dark IV technique can be used as a diagnostic tool to study solar cell structure, material and processing quality.

Two cells, processed in the initial experiments discussed in Section A2, were tested in this way to determine any differences in junction structure of the BBr_3 diffused and the liquid boron diffused cells. Data on the two cells is summarized in Table 5. The very low values of J_{02} indicate high quality junctions, and the bulk lifetimes are close to that measured for good quality float-zone material.

4. Verification Tests

These initial experiments indicated that high quality cells could be fabricated using the liquid boron dopant. The next task was to carry out several verification runs using the the liquid dopant to obtain a larger data base for comparison to the baseline diffused cells.

The first verification test was made during a one week period when all cell processing runs made on the Westinghouse pre-pilot facility used a liquid boron diffusant source to prepare the P^+P junction and a liquid SiO_2 diffusion mask during both the boron and phosphorus (gaseous $POCl_3$) diffusions. The purpose of these runs was: (1) to verify that this techniqe is suitable for diffusing P^+P junctions and for producing high efficiency solar cells, and (2) to increase the data base as required to statistically quantify any improvements with this technique as opposed to the baseline gaseous diffusion process. The process sequence and materials used in this one week processing experiment were presented previously in Table 2. During this test period, a B201ET boron source

21

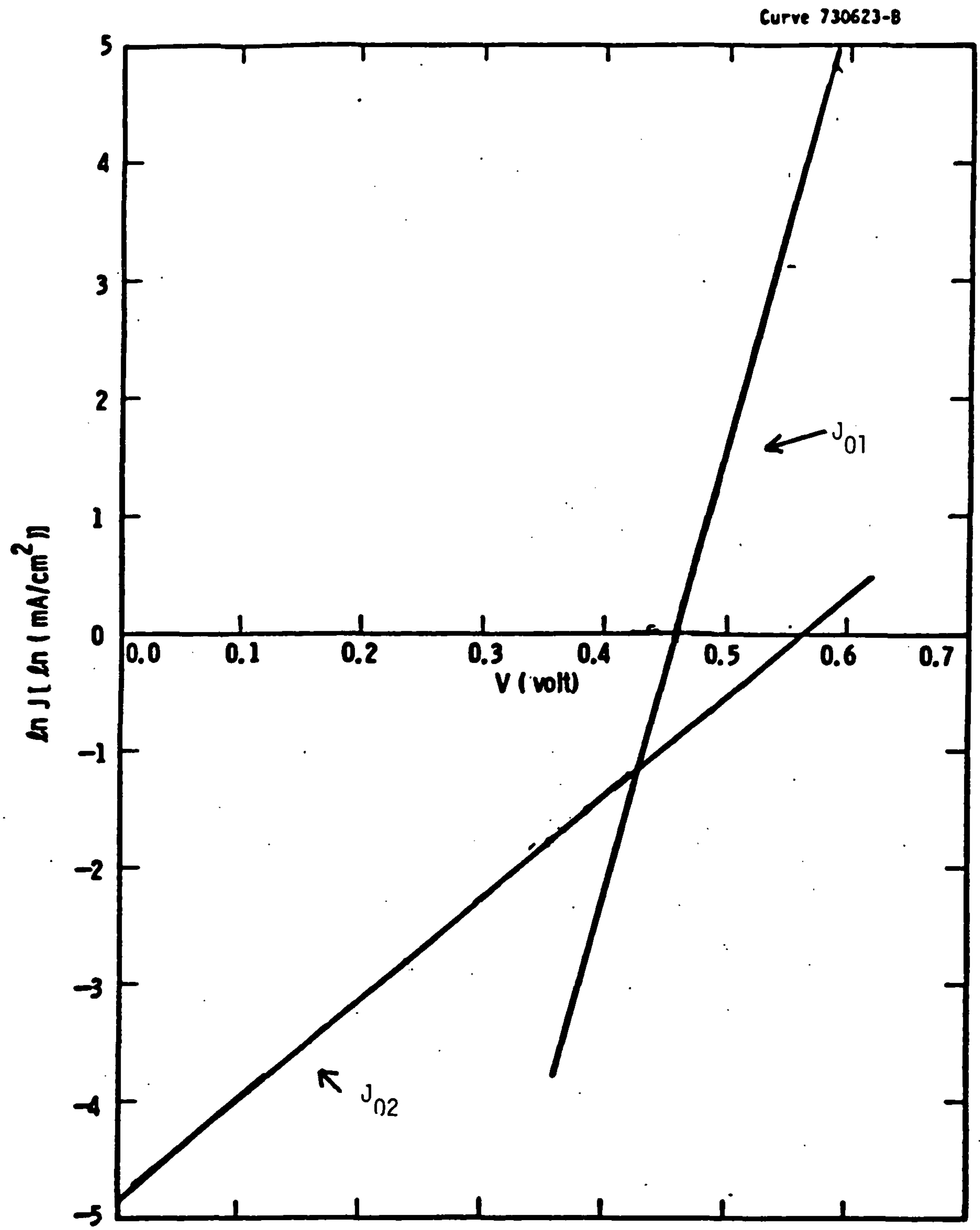

Figure 2. Generalized Dark IV Curve Segments for Bulk and Junction Currents of Solar Cells

23

TABLE 5

DARK IV MEASUREMENTS ON CELLS PRODUCED IN INITIAL LIQUID BORON EXPERIMENT

Cell ID	Cell Area cm^2	T Bulk μsec	J_{sc} ma/cm^2	V_{oc} Volts	Fill Factor	η %	R_S Series Resistance Ω-cm	R_{SH} Shunt Resistance kΩ-cm^2	J_{02} A/cm^2	Remarks
2102-15C	19.6	434	33.8	0.578	0.798	15.6	0.31	68	3.2×10^{-7}	Liq.Boron/$POCl_3$ Process
2090-36C	19.6	339	32.5	0.578	0.802	15.1	0.44	31	6.2×10^{-8}	Std $B(BBr_3)/POCL_3$ Process

(The bulk lifetime calculated from the dark I-V measurements cannot be directly compared to the OCD lifetime. It is, however, a good relative measure of cell quality.)

9950-892

and an SiO_2-700A mask source, both from Filmtronics Company in Butler, PA, were used. Twenty-one standard batches were processed during this same period. Of these batches, ten contained 1.6 cm x 9.4 cm cells while eleven contained 2.0 cm x 9.8 cm cells. Table 6 gives the efficiency data on the individual runs, and Table 7 gives data on the 21 runs with a breakdown as a function of cell size. Figures 3 and 4 show the efficiency distribution of the 1.6 x 9.4 cm and 2.0 x 9.8 cm cells respectively.

After this first, one week verification test was completed, the Westinghouse pre-pilot facility reverted back to the baseline gaseous process.

Data from cells fabricated using this gaseous baseline process during a 10 day period are shown in Table 8. For ease of reference, the results of the one week verification test (from Table 7) are also shown.

On a direct comparison basis, it appears that the baseline cells were slightly higher in efficiency than the liquid dopant cells. However, considering the fact that the liquid dopant process is different and the application method (i.e., hand applicator squeegee) is not optimum, the difference was not considered to be significant.

Therefore, a second series of liquid boron/liquid SiO_2 process runs were initiated. All processing runs were made using a liquid boron diffusant source to prepare the P^+P junction and a liquid SiO_2 diffusion mask for both the boron and phosphorus diffusions. The process sequence used for the second series of liquid dopant experiments is shown in Table 2. During this test period, a B201ET boron source and an SiO_2-700A mask source, both from Filmtronics Company in Butler, PA, were used. All processing runs were made in the Westinghouse AESD Pre-Pilot Facility. Table 9 summarizes the data obtained on 9,265 cells fabricated over an extended period using the liquid boron/liquid SiO_2 process. These data are compared to cells processed with the baseline CVD SiO_2/BBr_3 gaseous process. There was no significant difference in the average efficiency of cells produced using the two junction formation processes.

24

TABLE 6

LIQUID DOPANT/LIQUID MASK VERIFICATION RESULTS

Run #	# Cells	Avg. Efficiency	Max/Min. Efficiency
1*	32	11.9	14.2/10.7
2*	35	12.4	13.9/10.3
3	52	12.7	13.9/9.6
4	43	11.9	13.3/10.6
5	43	12.3	13.6/10.8
6	39	12.0	13.8/10.3
7	51	12.3	13.7/10.6
8*	47	12.2	14.2/10.0
9*	46	12.4	14.5/10.8
10	42	13.1	14.1/11.0
11*	56	13.1	14.7/11.8
12*	56	12.7	13.6/11.3
13	41	12.5	14.1/10.1
14*	48	13.0	14.2/11.8
15	23	12.1	13.4/10.0(process problem)
16	43	11.0	12.6/8.7 (process problem)
17*	39	12.6	13.9/11.0
18	47	13.6	14.9/12.2
19	36	12.7	14.6/10.9
20*	51	12.5	14.5/11.3
21*	48	12.5	14.4/10.8

*1.6 x 9.4 cm cells (all other cells 2.0 x 9.8 cm)

TABLE 7

OVERALL DATA FROM LIQUID DOPANT/LIQUID MASK VERIFICATION RUNS

No. of Runs - 21
No. of Cells Tested - 918

Average Efficiency - 12.5 ±0.8%

Overall Yield: $\left(\frac{\text{Cells Tested}}{\text{Total Possible \# of Cells}} \times 100\right) = 61\%$

CELL PARAMETERS MEASURED FOR TWO DISCRETE CELL SIZES

Cell Size (cm x cm)	# Runs	# Cells	Average Values V_{oc} (V)	J_{sc} $\left(\frac{mA}{cm^2}\right)$	Efficiency (%)
1.6 x 9.4	10	437	0.534 ±0.008	29.9 ±0.8	12.6 ±0.8
2.0 x 9.8	11	481	0.534 ±0.007	29.4 ±1.0	12.4 ±0.9

26

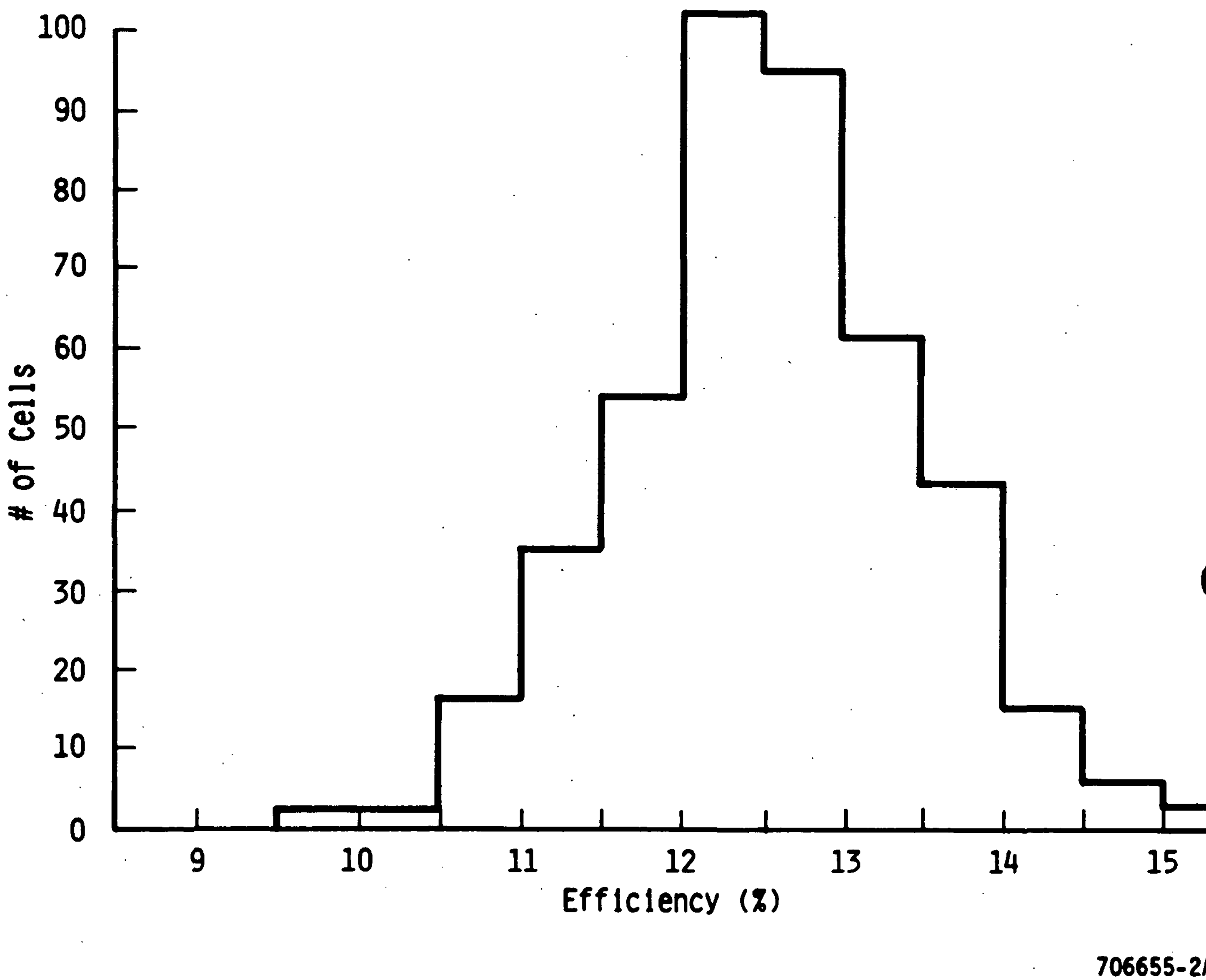

Figure 3. Efficiency Histogram of 1.6 cm x 9.4 cm Cells Fabricated in Liquid Boron/Liquid SiO_2 Verification Runs

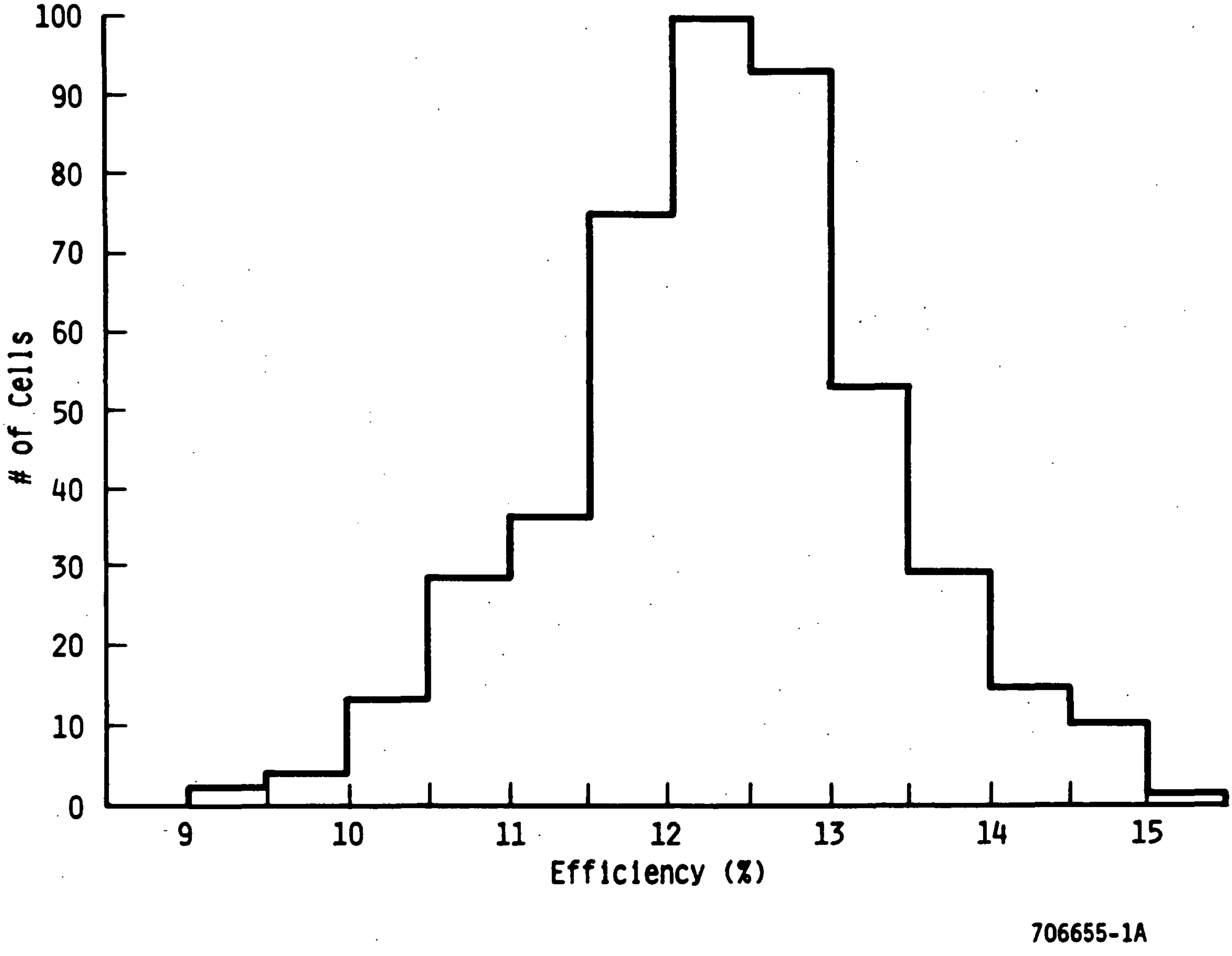

Figure 4. Efficiency Histogram of 2.0 cm x 9.8 cm Cells Fabricated in Liquid Boron/Liquid SiO_2 Verification Runs

TABLE 8

SUMMARY OF LIQUID BORON/LIQUID SIO_2
VS BASELINE CELL EFFICIENCY COMPARISONS

Technique	Cell Size cm x cm	# Cells	Average Efficiency %
Baseline Process	1.6 x 9.4	453	12.9
	2.0 x 9.8	343	12.7
*Liquid Boron Liquid SiO_2	1.6 x 9.4	437	12.6
	2.0 x 9.8	481	12.4

*Presented previously in Table 7 and given here for comparison with baseline runs.

TABLE 9

LONG-TERM COMPARISON OF BASELINE PROCESS
WITH LIQUID SIO_2/LIQUID BORON PROCESS

Baseline Process		Liquid SiO_2/Liquid Boron Process	
# Cells	Av. Eff.(%)	# Cells	Av. Eff.(%)
6161	12.6	9265	12.7

NOTES:

1. Period Covered - July 1, 1982 - November 24, 1982
2. Baseline Process - CVD SiO_2 + BBr_3 / CVD SiO_2 + $POCl_3$ — See May 1982 Quarterly Report (Westinghouse TME 3150)
3. Liquid Process - Liquid SiO_2 + Liquid Boron / Liquid SiO_2 + $POCl_3$ — See Table 2 of this report.
4. Data includes cells of different areas (15.7 cm^2; 19.6 cm^2; and 24.5 cm^2).

30

9950-89?

This experiment provided statistical verification that the low cost junction formation process could produce cell efficiencies equal to those of the baseline process.

5. Belt Furnace Feasibility Investigation

An important related experiment was conducted to determine the feasibility of using a belt furnace to diffuse junctions in dendritic web strips with liquid dopants applied. A belt furnace of a given capacity is substantially less expensive than the tube-type diffusion furnace specified by the Westinghouse baseline process sequence. In addition, belt furnace operations are inherently more continuous, hence, more automatable and cost effective than diffusion furnace operations. Development of a high quality belt furnace junction formation process using liquid dopants could be a benefit to processing virtually all ribbon sheet materials.

For this experiment, which was conducted at the facilities of Radiant Technologies, Inc., at Cerritos, CA, a total of 96 strips of silicon web were processed. The JPL contract monitor for the Westinghouse program was present for the diffusion runs made at Radiant Technologies.

Half of the strips were taken to Radiant Technologies, coated with liquid SiO_2/liquid boron, and processed through their belt furnace in four separate runs. The ambients used in these runs were 100% O_2, 50% O_2 and 50% N_2, and pure dry air. The diffusion temperatures were 950°C and 980°C. All diffusions were for 30 minutes with a slow furnace cool to 750°C at 4°C/min. The remaining half of these strips were diffused in the Westinghouse pre-pilot tube type diffusion facility using the liquid SiO_2/liquid boron. These strips were generally crystal pairs of the samples diffused in the belt furnace. Results of the experiment are tabulated in Table 10.

Cells diffused in the belt furnace using the various atmospheres described above yielded similar electrical results; however, cells diffused in a pure O_2 ambient produced the most acceptable appearances in that post-diffusion surface stains were minimized.

31

TABLE 10

DATA FROM BELT FURNACE JUNCTION FORMATION EXPERIMENT

1. Overall Results

	Belt Furnace Junction Formation (Liq B/Liq SiO_2)		Tube Diffusion Furnace Junction Formation (Liq B/Liq SiO_2)	
Cell Run #*	No. of Cells	Av. Eff.**	No. of Cells	Av. Eff.**
924-1W	36	12.4	18	12.3
924-24W	18	12.9	25	12.4
924-49W	25	12.8	28	12.5
924-72W	17	12.9	15	12.6

*This cell run number defines the original group of web strips selected for test. Portions of each run were diffused at AESD and at Radiant Technologies, Inc.

**Four cells with efficiencies less than 11% not included in average.

2. Details of V_{oc}, I_{sc}, and FF measurements (averages for all cells)

	V_{oc} (V)	I_{sc} (A)	FF
Processed in Belt Furnace	0.544 ±.010	.578 ±.027	0.780 ±.023
Processed in Tube Diffusion Furnace	0.542 ±.008	.578 ±.028	0.778 ±.029

32

TABLE 11

EFFECTS OF WEB STRIP ORIENTATION, TEMPERATURE, AND AMBIENT CONDITIONS DURING BELT FURNACE DIFFUSION

Diffusion Conditions		Avg. Efficiency (%)	
Temperature	Ambient	Strip Lying Flat	Strip Standing Up
980°C	100% O_2	13.1	12.6
980°C	50% O_2-50% N_2	13.2	12.6
960°C	50% O_2-50% N_2	12.5	12.9
960°C	Dry Air	12.3	12.7

In addition to the ambient atmosphere and diffusion temperature variables, the effects of web strip orientation in the belt furnace during diffusion were examined. In each diffusion run, half of the strips were laid flat on quartz plates with the liquid boron side facing upward. The remaining strips were processed in a standing position using a standard diffusion boat. Data are presented in Table 11.

Although some differences are observed, the variations are too small to allow definite conclusions to be drawn. When small variations such as these are encountered, it is absolutely necessary to use paired strips from a single crystal to eliminate crystal-to-crystal variations which produce variations of some magnitude.

Although optimum temperatures, ambients, and orientations were not determined from these tests, the feasibility of substituting a belt furnace for the standard tube-type diffusion furnace has been established. If there are performance penalties associated with the use of belt furnaces, the penalties do not appear prohibitive. More statistical data using matched strips from a single crystal will be required to optimize diffusion parameters and to quantify performance differences between the two techniques for driving junctions in dendritic web silicon.

B. Liquid Diffusion Mask

Concurrent with the liquid boron doping experiments described in Section IIIA, the use of a liquid diffusion mask was investigated. In this section of the report, the experiments carried out to verify the applicability of this mask will be discussed.

In order to evaluate liquid SiO_2 as a diffusion mask, detailed experiments were run to evaluate liquid SiO_2, baseline CVD SiO_2, liquid boron, and BBr_3 in various combinations. The matrix used in one such experiment was as follows:

Liq SiO_2 Liq B	Liq SiO_2 BBr_3
Std SiO_2 Liq B	Std SiO_2 BBr_3

The overall results are summarized in Table 12, and comparisons of cells produced from a single web crystal are presented in Table 13. The results indicated that standard CVD Silox with liquid boron yields the highest efficiencies, but in this initial experiment there were some difficulties encountered removing the liquid SiO_2 layer after boron diffusion. Therefore, the results are suspect due to these application and removal problems. Another similar experiment was then performed using standard CVD Silox and two different liquid SiO_2 solutions to resolve the diffusion mask issue. The two liquid SiO_2 solutions were designated 700A* and 700B*, with the main difference in the viscosity of the solution. One run of 24 pieces of web strips was chosen for this experiment: 8 pieces were coated with CVD SiO_2, 8 pieces were coated with liquid SiO_2 700A, and 8 pieces were coated with liquid SiO_2 700B solution. Liquid boron dopant solution was used on all the pieces to produce the P^+ back surface. Results of this run are summarized in Table 14. It is seen in using the two SiO_2 solutions that there is no significant difference in the cell efficiencies. Since 700B is a thicker solution, it is more difficult to strip after diffusion. Based on these observations, it was decided that later verification runs would be made using the SiO_2 700A solution. However, it should be noted that this experiment established that the SiO_2 700B solution can also be used quite effectively as a diffusion mask.

These data indicate that a liquid diffusion mask can be used to protect one side of the web during diffusion. The processing runs shown previously in Table 9 (liquid boron verification run) used a liquid diffusion mask.

The detailed results of the liquid boron and liquid mask experiments were summarized in two topical reports which are attached to this report as Appendices B and C. These reports were previously submitted to JPL.

---

*Filmtronics Corporation designations.

TABLE 12

EFFICIENCIES MEASURED ON CELLS PROCESSED IN STANDARD SILOX/LIQUID SiO_2/STANDARD (GASEOUS) BBr_3/LIQUID BORON MATRIX EXPERIMENT

	Efficiency (pct); Measured with AR Coating			
Cell No.	Standard Silox/ Standard Boron	Liquid SiO_2/ Standard Boron	Standard Silox/ Liquid Boron	Liquid SiO_2/ Liquid Boron
1	12.19	12.29	13.52	12.29
2	12.34	12.24	14.23	12.39
3	10.81	11.83	11.38	8.41
4	10.71	11.83	10.26	7.95
5	11.27	7.65	12.81	12.04
6	12.50	7.34	12.35	12.04
7	12.60	12.34	12.70	10.96
8	12.29	12.55	13.72	11.42
9	12.60	11.27	14.28	12.34
10	12.70	12.39	14.85	12.39
11	12.85	11.78	15.56	10.86
12	12.60	11.88		11.17
13	13.82	11.98		11.53
14	14.03	8.57		11.68
15				10.96
16				12.14
17				13.01
18				13.06
Average	12.38 ±0.92	11.04 ±1.74	13.24 ±1.48	11.48 ±1.33

36

TABLE 13

COMPARISONS OF EFFICIENCIES OF CELLS PRODUCED FROM A SINGLE WEB CRYSTAL PRODUCED USING VARIOUS DIFFUSION DRIVE AND MASK PROCESS

1. Standard Silox Diffusion Mask

Crystal No.	Diffusion Drive	Cell No.	Cell Efficiency (%)
4-122-18	Liquid Boron	6A	11.38
4-122-18	Liquid Boron	6B	10.26
4-122-18	BBr_3	7A	12.50
4-122-18	BBr_3	7B	12.60
4-122-18	BBr_3	7C	12.29
4-122-16	Liquid Boron	11A	12.81
4-122-16	Liquid Boron	11B	12.35
4-122-16	Liquid Boron	11C	12.70
4-122-16	BBr_3	10A	12.6
1-157-1	Liquid Boron	15A	14.28
1-157-1	Liquid Boron	15B	14.85
1-157-1	Liquid Boron	15C	15.56
1-157-1	BBr_3	16A	13.82
1-157-1	BBr_3	16B	14.03

2. Liquid SiO_2 Diffusion Mask

Crystal No.	Diffusion Drive	Cell No.	Cell Efficiency (%)
4-122-13	Liquid Boron	54A	12.34
4-122-13	Liquid Boron	54B	12.39
4-122-13	BBr_3	55AX	12.29
4-122-13	BBr_3	55BX	12.24
1-156-23	Liquid Boron	66A	11.68
1-156-23	Liquid Boron	66B	10.96
1-156-23	BBr_3	65AX	12.34
1-156-23	BBr_3	65BX	12.55
7-131-3	Liquid Boron	68A	12.14
7-131-3	Liquid Boron	68B	13.01
7-131-3	Liquid Boron	68C	13.06
7-131-3	BBr_3	69AX	11.27
7-131-3	BBr_3	69BX	12.55
7-131-3	BBr_3	69CX	12.39

37

TABLE 14

CVD SILOX - LIQUID SIO_2
DIFFUSION MASK COMPARISON EXPERIMENT

• Total Cells

	CVD Silox	Liquid SiO_2 700A*	Liquid SiO_2 700B*
No. of Cells	15	14	19
Average Efficiency	12.18%	11.99%	12.29%
Maximum Efficiency	13.0%	13.87%	14.74%
Minimum Efficiency	11.68%	11.12%	11.27%

• Direct Comparison of Efficiencies of Cells from Same Web Crystal or Furnace Run

Run #1	12.13%	11.33%	11.32%
Run #2	12.34%	12.59%	12.13%

NOTE: Liquid boron diffusion process used on all cells.

*Filmtronics Corporation designations.

38

C. Test of Various Boron and SiO_2 Containing Liquids

The data presented in Sections IIIA and IIIB were obtained using Filmtronics Corporation FB201 and 700B (boron and SiO_2 respectively) and Diffusion Technology P8 and U1A (boron and SiO_2 respectively) solutions.

A subsequent program task involved investigation of alternate diffusant and mask solutions from various vendors. Table 15 presents a list of alternate liquids used in this study. In all experiments, the baseline diffusion temperatures and gas flows were used.

Table 16 shows the results of these tests. The first eight columns identify the runs and the dopants together with sheet resistivity data. All of the samples produced cells with suitable sheet resistivity. The next three columns give the average Voc and efficiency data and the number of cells in the run. The last column (electrical rejects) are cells of the type discussed in Section IIIC of this report. The major cause of rejection was a low shunt resistance. The number of electrical rejects is a measure of the efficiency of the diffusion mask in preventing this shunting.

In general, all the dopants tested were capable of producing good back surface fields which in conjunction with the $POCl_3$ diffusion yield high efficiency cells.

Only one liquid SiO_2 solution (X600, in Items 3 and 4) yielded cells with a very large number of reject cells. However, Item 5 which was the same process as Item 4 showed above average efficiencies with few rejects. Since this is an experimental product, there may be an unknown problem in preparing the diffusion mask.

The data also suggest that the mask is much less important during $POCl_3$ diffusion than during the back surface diffusion. For example, Items 6, 7, and 8 used the standard U1A for the boron diffusion and the X600 for the $POCl_3$ diffusion. In all cases, these runs yielded good cells.

The XB-150 appears to be a suitable boron dopant when used with U1A.

TABLE 15

ALTERNATE LIQUID SOLUTIONS INVESTIGATED

Supplier	Liquid Mask Solution	Liquid Boron Solution
Filmtronics	700A	FB201
Emulsitone	B100	B201
Allied Chemical	X600*	XB150*
Diffusion Technology	U1A	B60

*These are experimental products.

TABLE 16

RESULTS USING VARIOUS LIQUID SIO_2 AND LIQUID BORON SOLUTIONS

Item No.	Proc. Run No.	P^+P Mask	P^+P Diffusant	P^+P Sheet Res. (Ω/□)	N^+P Mask	N^+P Diffusant	N^+P Sheet Res. (Ω/□)	IV (Avg. Values) Voc(V)	IV (Avg. Values) η (%)	YIELD No. of Cells Tested	YIELD No. of Electrical Rejects
1	217-73W	700A	FB201	40-50	700A	$POCl_3$	43-54	.571	14.2	58	7
2	217-49W	B100	B201	40-47	B100	$POCl_3$	45-57	.575	14.2	53	1
3	217-1W	X600	XB150	40-50	X600	$POCl_3$	45-55	.548	11.4	45	41
4	210-73W	X600	B60	30-40	X600	$POCL_3$	45-55	.556	13.1	51	27
5	214-73W	X600	B60	32-36	X600	$POCl_3$	44-52	.558	13.8	53	3
6	210-49W	U1A	B60	31-36	X600	$POCl_3$	44-55	.566	13.6	45	2
7	310-1M	U1A	B60	31-35	X600	$POCl_3$	48-52	.564	14.3	55	0
8	310-25M	U1A	B60	31-35	X600	$POCl_3$	45-58	.568	14.4	51	4
9	303-25M	U1A	XB150	42-50	U1A	$POCl_3$	45-55	.563	15.1	17	0
10	303-25M	U1A	B60	30-35	U1A	$POCl_3$	45-55	.565	13.8	25	0

41

9950-892

D. Cell Evaluation

1. Evaluation of High Efficiency Runs

During the period of the second verification run for the liquid boron/liquid mask process sequence, eleven processing runs, representative of runs with high average efficiency, were analyzed to determine the effectiveness of the liquid boron diffused back surface field.

Table 17 gives the compiled data on eleven runs processed between December 15, 1982, and January 15, 1983. These runs were chosen as being representative of runs having high average efficiencies. In addition to the efficiency data, the average open circuit voltage and number of cells in the run are given. The open circuit voltage is a good measure of the quality of the back surface field due to the P^+P junction.

The presence of a high-low junction (i.e., P^+P) at the back surface of an N^+P cell structure will increase the short circuit current but mainly enhances the open circuit voltage. One important factor in limiting the efficiency of a solar cell is a high minority carrier recombination velocity at the cell surfaces. The back surface field reduces the back surface recombination velocity due to a potential energy barrier between the two regions (P^+P) which effectively causes a built-in field. This field reduces the loss of photogenerated carriers, enhancing the quantum efficiency of the base region of the cell and thereby increasing the open circuit voltage.

In Table 17, the average Voc for all cells is 0.562V. The maximum Voc measured was 0.598V. Hovel* gives calculated values of Voc for N^+P cells (i.e., no back surface field) fabricated on 1 Ω-cm and 10 Ω-cm silicon of 0.600V and 0.545V respectively. The cells reported here are fabricated on 4-8 Ω-cm material, and the calculated Voc should be 0.555. Thus, the 0.562V average reported and the 0.598V maximum indicate an effective back surface field.

---

*H. J. Hovel, "Semiconductors and Semimetals," Vol. 11 - Solar Cells Academic Press, New York, 1955.

42

TABLE 17

HIGH EFFICIENCY LIQUID BORON/LIQUID DIFFUSION MASK PROCESSING RUN

Run ID	Cell Area (cm^2)	No. of Cells	Av. V_{oc}(V)	Av. Eff. (%)	Correlation Coeff. r
1108-49M	15.68	46	.556	14.8	.77
1118-1M	15.68	48	.559	14.4	.70
1127-1M	15.68	48	.560	14.7	.74
1209-49M	15.68	45	.569	14.2	.64
1126-25M	15.68	53	.563	13.9	.89
1126-49M	15.68	32	.570	15.0	.75
1201-25W	19.60	53	.558	14.1	.73
1201-73W	19.60	37	.560	14.4	.92
1210-73W	19.60	43	.576	14.3	.79
1201-1W	19.60	47	.557	14.3	.96
2234-49E	24.80	21	.557	13.5	.93
TOTALS	---	473	.562	14.3	--

The last column in Table 17 is the correlation coefficient between the Voc and efficiency of the cells in the given runs. This coefficient in all cases is above 0.6 where 1.0 is perfect correlation and 0 is no correlation.

Dark IV measurements, as described in Section IIIA of this report, were made on selected cells from this group. All cells tested showed low J_{01} and J_{02} values. The series and shunt resistance were below 0.5 $\Omega\text{-cm}^2$ and above 10K $\Omega\text{-cm}^2$ respectively. These data indicate that there were good cells with excellent junction characteristics.

In summary, the data presented here show an operating back surface field which enhances the Voc and where the cell efficiency is controlled to a great extent by the open circuit voltage.

2. Evaluation of Low Efficiency Cells

During the period the liquid dopant process sequence has been investigated, a number of cells were fabricated with very low efficiencies (in the 1% - 10% range). As a part of this overall effort, 150 of these reject cells were analyzed to determine the cause of the low efficiencies.

Based on the measured lighted IV parameters, the 150 reject cells can be divided into 3 groups:

<u>Group 1</u> (about 15% of the reject cells)

This group contained cells having the following lighted IV properties:

Voc > 0.5V
Jsc - variable
FF - variable
Efficiency - variable but less than 10%

These cells were mechanical failures for reasons such as: very thin or no copper plating, non-adherent grid fingers, broken or cracked cells, grid lines not completely opened, and a light copper flash over the entire surface. Thus, these cells could have been rejected prior to testing as mechanical failures.

44

Group 2 (about 5% of the reject cells)

These cells had no cosmetic defects with lighted IV properties as follows:

Voc > 0.5V
Jsc > 20 mA/cm^2
FF < 0.6
Efficiency - 6-10%

Dark IV properties of representative cells from this group showed mediocre bulk lifetimes (10-30 μsec) and adequate junctions ($J_{02} < 10^{-6}A$) but with high series resistance or low shunt resistances. These spurious resistances cause the low fill factor and low efficiency. These resistance problems are related to processing problems.

Group 3 (about 80% of the reject cells)

These cells also showed no cosmetic defects. The lighted IV properties are listed below:

Voc < 0.4V
Jsc < 20 mA/cm^2
FF < 0.6
Efficiency - 1-6%

Dark IV measurements showed normal series resistance with a low shunt resistance. The bulk lifetime was less than 1 microsecond, and the junction current density exceeded 10^{-4} A/cm^2.

Eight cells were selected from this group, and the contact metals and antireflective coatings were removed. The sheet resistivity and conductivity type were then measured on these bare cells. This data, shown in Table 18, indicates the back (P^+) surface was not at fault. The sheet resistivity was within specification, and the conductivity is strongly P-type. Analysis of the front surface, however, indicated considerable problems. The sheet resistivities are quite variable, and the conductivity varies from N to P over the surface.

These results indicate that during the initial boron diffusion, the sun side of the cell (protected by the liquid SiO_2 mask) became contaminated with boron

TABLE 18

DATA FROM REJECT CELLS ANALYSIS

Cell No.	Avg. Sheet Resistivity (Ω/□) Front	Back	Conductivity Type Front	Back
4A	55	45	Spotty N & P	Strong P
77C	100	44	Spotty N & P	Strong P
59A	95	40	Spotty N & P	Strong P
79C	90	35	N	Strong P
88A	30-100	35	Heavy P in spots	Strong P
66B	65	40	P	Strong P
44C	65	40	Spotty N & P	Strong P
53A	80	40	Spotty N & P	Strong P

46

which shorted out the (later diffused) N^+P junction. These shorted regions would account for the low shunt resistance and very low bulk lifetime.

This front surface contamination may have occurred during the liquid boron application where the liquid "wicked" by capillary action to the sun side and was subsequently driven in. A second more probable cause of contamination is that the protective liquid SiO_2 mask contains small pinholes through which boron (in the furnace tube ambient) diffuses.

In either case, the integrity of the liquid mask must be questioned. In fact, several runs made in late 1982 used a liquid SiO_2 mask with BBr_3 diffusant gas. These runs had a significantly large number of rejects. This result is consistent with the theory of pinholes in the SiO_2 mask.

From this analysis, it is concluded that the liquid SiO_2 mask will, on occasion, permit boron to diffuse through and thus degrade the sun side surface of the cell.

Since the liquid mask is applied using a sponge-squeegee, it is quite possible that non-uniform thickness and coating techniques can lead to pinholes. The problem may be obviated when the liquid SiO_2 can be applied with a meniscus coater which has been shown to give uniform layers.

However, it should be noted that in a vast majority of cells, the SiO_2 mask performed quite well.

E. Application of Liquid with a Meniscus Coater

A complete description of the operation of a meniscus coater is discussed in the MEPSDU Summary Technical Report, TME 3148, July 1982, attached as an appendix to this report. Basically, the coater pumps the fluid into a porous stainless steel cylinder so that a meniscus is formed on the cylinder as shown in Figure 5. The cylinder moves under the web strip held in a fixture as shown in Figure 6, so that just the meniscus touches the web. The coating thickness is proportional to the speed of the cylinder.

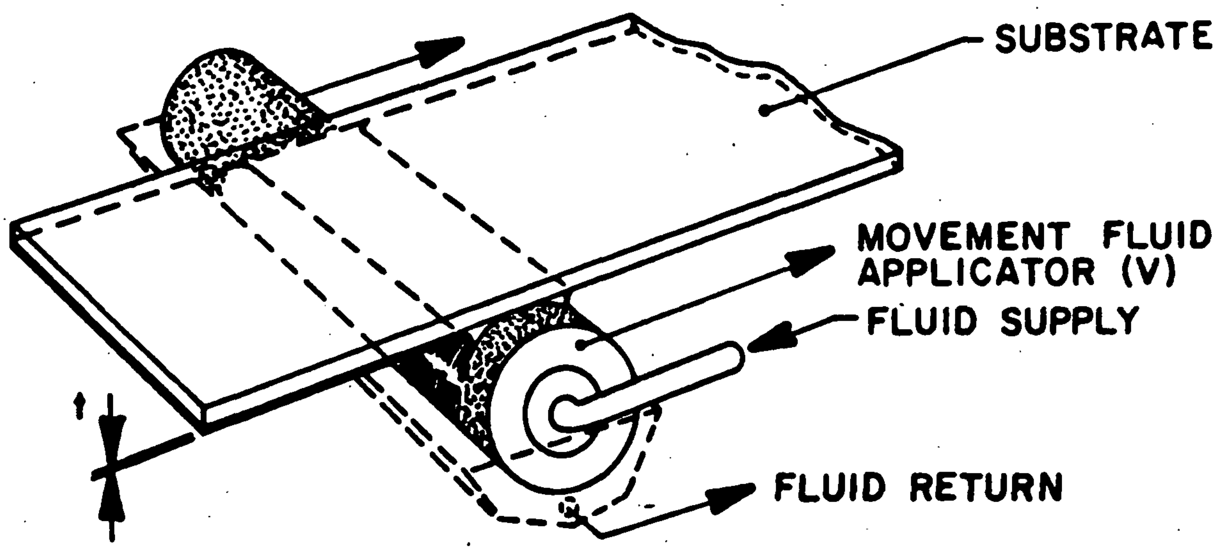

Figure 5. Schematic Drawing of Meniscus Coater Liquid Application Device

98

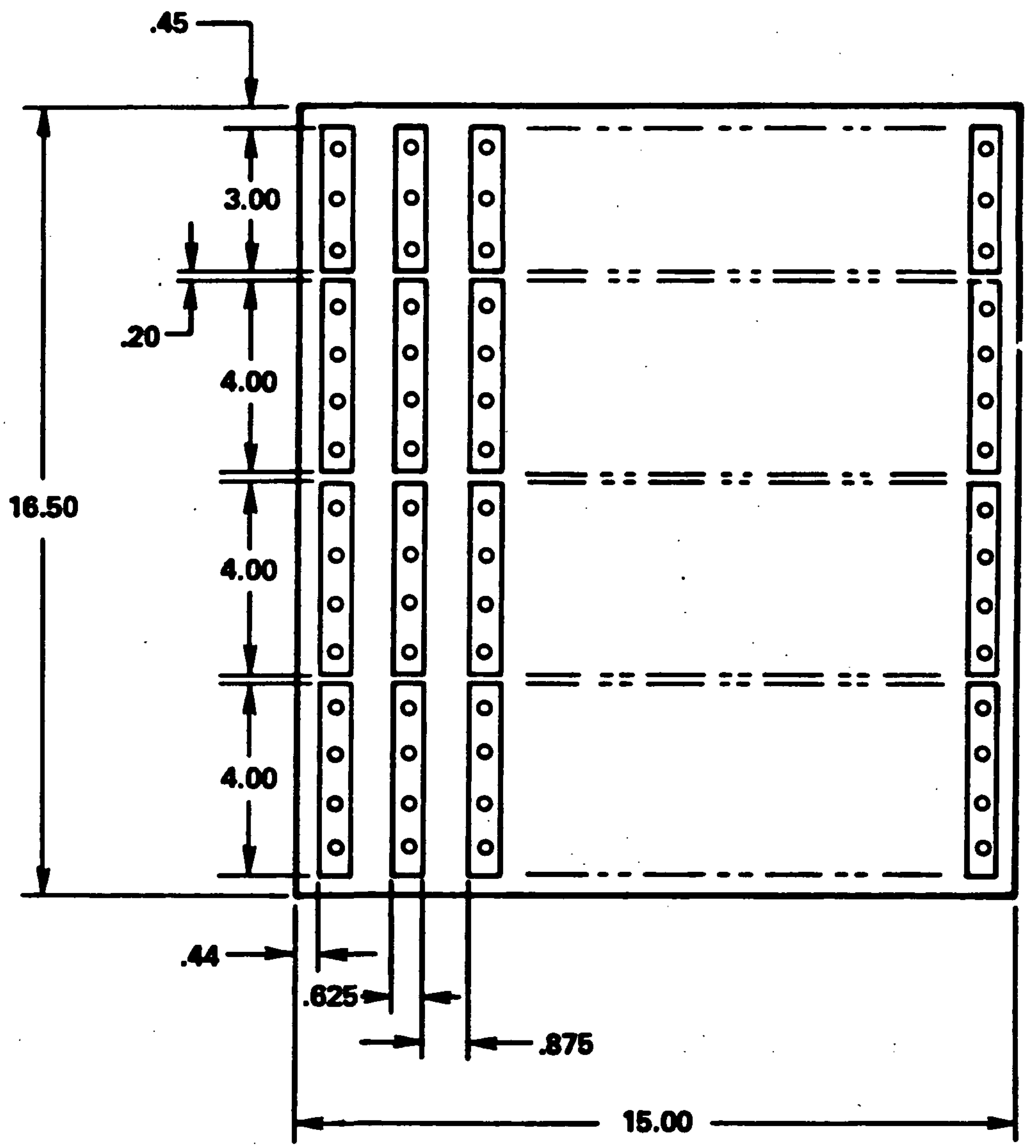

Figure 6. Meniscus Coater Web Holding Fixture

An acceptance test on this unit was carried out in the vendor's plant. These tests used an antireflective coating solution. This solution was selected because it allows the most rapid assessment of coating thickness and uniformity. In the test, fifteen web strips, each 33 cm, were coated with a standard AR coating solution. The coating speed was 21-24 inches/min. After coating, the strips were baked at 400°C for 15 minutes in air. The general appearance of all strips was good, and three strips (numbered 25, 44, and 47) were selected for further study.

General Appearance of Strips:

#25 - only 28 cm coated due to break on end of strip. This strip was etched in KOH at Integrated Technologies before coating. Color was light blue and was acceptably uniform over the surface.

#44 - Coated entire length, deep purple-blue, slight variation in color over surface noted.

#47 - Coated entire length, deep purple-blue except at one end where there was a gold colored stripe. This was caused by the web not being held firmly in the vacuum chuck.

On all samples, there was no significant carryover of the AR coating on the uncoated side.

The three strips were sent to Westinghouse R&D Center where the thickness was measured at 20 uniformly spaced positions along the length of the web using an ellipsometer. The measurements were taken within ±1 cm of the centerline of the web. The data is shown in Table 19.

50

TABLE 19

MENISCUS COATER ACCEPTANCE TEST DATA: THICKNESS OF AR COATED STRIPS

Strip #	Coating Thickness Along Length (Å)	Strip #	Coating Thickness Along Length (Å)	Strip #	Coating Thickness Along Length (Å)
25	847	44	712	47	716
	857		714		703
	848		707		724
	834		698		742
	838		713		739
	832		701		695
	835		683		602*
	827		679		648*
	833		711		721
	845		700		718
	809		683		724
	799		709		718
	798		703		730
	815		707		700
	840		691		687
	815		687		726
	819		699		718
	819		690		711
	818		690		724
			720		689
	Av = 828 ±17		Av = 700 ±12		Av = 707 ±33

On Strip #47, the two thickness values (marked with an asterisk) correspond to the noted gold colored stripe. If these two values are neglected, the average for #47 is 716 ±16.

It is estimated that an AR coating thickness variation of ±20A is suitable for the process sequence.

These three strips along with the 12 others were part of a cell processing run. After the thickness measurements were made, all strips were merged with the original run and the processing completed. Table 20 gives data on this run.

The data in Tables 19 and 20 indicate that the "CAVEX" meniscus coater is suitable for applying an antireflective coating. Since the thickness control of the AR coating is the most critical of all liquids applied to dendritic web silicon during processing operations and the meniscus coater can achieve this control, the coater was deemed suitable for the other applications planned, e.g., liquid SiO_2 deposition and liquid dopant deposition.

Figure 7 is a photograph of the meniscus coater after its receipt at AESD. The unit was placed in the diffusion area of the Westinghouse pre-pilot facility. In the photograph, the web holding fixture portion of the machine, which will simultaneously support up to ten strips of web during liquid application operations, is shown in the upright (half-open) position. Final assembly and checkout of this equipment was completed in early March, and the unit was then used to complete the liquid phosphorus diffusion tasks specified in the contract and discussed in the next section of this report.

F. Liquid Phosphorus Dopants for N^+P Front Junction

1. Introduction and Initial Experiments

The requirements for the front N^+P junction are more stringent than for the back P^+P junction. Since the radiation is incident on the N^+ surface, the diffusion front should be uniform and free of spikes and pinholes. After diffusion, the liquid dopant material should be completely removable so that no stain is left on the surface.

During the time the liquid boron diffusant and liquid mask experiments and verification tests were underway, scoping experiments were carried out using a liquid phosphorus dopant to form the front junction.

52

TABLE 20

DATA FROM CELLS PROCESSED WITH AR COATING APPLIED BY MENISCUS COATER

A. Cell Run No: 1313-1

B. Efficiency Data Comparison

AR Application Technique	No. of Cells	Avg. Efficiency
Dip/Withdrawal	12	12.0%
Meniscus Coater	35	12.2%

C. AR Enhancement Factor* of Meniscus Coated Cells

$$\frac{V_{oc}\ \text{(coated)}}{V_{oc}\ \text{(uncoated)}} = 1.01 \pm 0$$

$$\frac{I_{sc}\ \text{(coated)}}{I_{sc}\ \text{(uncoated)}} = 1.44 \pm 0.02$$

$$\frac{\text{FF (coated)}}{\text{FF (uncoated)}} = 1.01 \pm 0.03$$

$$\frac{\text{Efficiency (coated)}}{\text{Efficiency (uncoated)}} = 1.46 \pm 0.03$$

*The enhancement factor was determined by measuring the IV properties of the cell, removing the AR in a dilute HF solution, and remeasuring the cell. Six cells were tested in this way.

Figure 7. Meniscus Coater after Installation in the Westinghouse Pre-Pilot Facility

These tests were designed to determine approximate diffusion parameters to achieve the required sheet resistivity and the necessary conditions to achieve a clean surface after diffusion.

In tests conducted at the vendor's facility, it was shown that the meniscus coater (Section IIIE) did apply a uniform layer of dopant that was removable after diffusion. However, these initial experiments were carried out with the dopant applied using a sponge-squeegee as discussed in the liquid boron dopant section (IIIA).

The process sequence used in these and later tests is given in Table 21.

The results of the first tests are shown in Table 22. These data indicated the need for oxygen in the nitrogen diffusion ambient in order to achieve a clean surface after removal of the diffusion glass.

It was noted in these tests that in a number of cases there was a wide variation of resistivity along the length of the web, with some areas being as high as 300-400 $\Omega/\square$. This variability was seen in most of the tests and was probably related to a non-uniform coating of the phosphorus liquid, leading to variable diffusant source concentrations on the surface. Some of the strips from these experiments were processed through the baseline process and made into cells with efficiencies from 10-14%.

2. Determination of Diffusion Parameters

After these initial tests, a series of experiments were conducted to determine the optimum diffusion time and temperature and gas flow and composition to achieve cells with efficiencies equal to or higher than the baseline cells. These tests used two liquid dopants: Diffusion Technology P8 and Allied Chemical PX10. The dopants were applied using a sponge-squeegee.

Table 23 shows the diffusion parameters and the sheet resistivity measured for these experimental runs. As is shown, the sheet resistivity continued to show a wide variation.

55

TABLE 21

PROCESS SEQUENCE FOR FABRICATION OF SOLAR CELLS
USING LIQUID DOPANTS AND LIQUID DIFFUSION MASKS

1. Raw web clean (including hot H_2SO_4 treatment).
2. Pre-diffusion clean (standard chelating).
3. Apply liquid SiO_2 to designated N^+ side of web.
4. Dry under heat lamp for 5 minutes (about 80°C).
5. Apply liquid boron dopant to designated P^+ side of web.
6. Dry under heat lamp for 5 minutes (about 80°C).
7. Load strips in boat with SiO_2 side facing SiO_2 side and P^+ side facing P^+ side. Pre-bake in oven for 15 minutes at 200°C.
8. Place loaded boat in front end of diffusion furnace and bake strips for 5 minutes at approximately 300°C.
9. Move boat into furnace and diffuse for 30 minutes at 960°C. Slow cool furnace to 700°C at 3°C/minute.
10. Strip oxides in 2:1 H_2O:HF.
11. Repeat Step 2.
12. Apply liquid SiO_2 to boron diffused side.
13. Repeat Step 4.
14. Apply liquid phosphorus on designated N^+ side of web.
15. Dry under heat lamp for 5 minutes (about 80°C).
16. Load strips in boat with SiO_2 side facing SiO_2 side and P^+ side facing P^+ side. Pre-bake in oven for 15 minutes at 200°C.
17. Load boat into furnace and diffuse at predetermined conditions. Slow cool furnace to 700°C at 3°C/minute.
18. Strip oxides and complete baseline process.

TABLE 22

INITIAL DATA FROM LIQUID PHOSPHORUS DOPED SILICON DENDRITIC WEB STRIPS

Run #	Diffusion Temp./Time	Gas Mixture	ρ_s (Ω/□)	Remarks
1	900°C/30 min.	100% O_2	≥100	Surface Clean after Stripping
2	950°C/30 min	50% O_2 50% N_2	7-8	Surface Clean after Stripping
3	900°C/30 min	50% O_2 50% N_2	25-28	Surface Clean after Stripping
4	900°C/30 min	30% O_2 70% N_2	26-41	Surface Clean after Stripping
5	900°C/30 min	20% O_2 80% N_2	33-50	Slight Stain after Stripping
6	900°C/30 min	5% O_2 95% N_2	21-27	Slight Stain after Stripping
7	900°C/20 min	5% O_2 95% N_2	24-29	Slight Stain after Stripping

TABLE 23

VARIATION OF DIFFUSION PARAMETERS FOR N^+P JUNCTIONS

Test No.	Run ID	Diffusion Temp. (°C)	Diffusion Time (Min)	Dopant	Gas Flow & Comp. (cc/min)	Sheet Resistivity (Ω/□) Range	Avg.
1	315-49M	870	20	P8	2200-O_2	80-300	
3	405-73W	900	20	P8	2200-O_2	50-300	
4	411-49W	910	20	P8	2200-O_2	25-45	
5	409-49W	900	40	P8	2200 O_2/200 N_2	36-50	
6	507-49W	900	20	P8	400 O_2/2000 N_2	20-30	
8	1217-49E	900	30	PX10	2200 O_2/2200 N_2	24-50	34
9	502-1M	900	30	P8	2200 O_2/2200 N_2	18-30	21
10	1217-1E	885	20	PX10	2200 O_2/2200 N_2	36-90	58
				P8-Old(1)		40-80	57
11	608-73W	885	30	P8-New(2)	2200 O_2/2200 N_2	25-35	32
12	617-25E	885	30	P8	200 O_2/2200 N_2	18-25	21
13	617-73W	875	30	P8	2200 O_2/2200 N_2	30-160	50
14	611-49W	875	30	PX10	2200 O_2/2200 N_2	31-52	37
18	113-25E	860	20	P8	2200 O_2/2200 N_2	100-150	130
19	718-1W	860	20	PX10	2200 O_2/2200 N_2	47-180	85
20	113-49E	860	20	PX10	400 O_2/2200 N_2	60-116	88
22	113-73E	870	20	PX10	2200 O_2/2200 N_2	40-135	79
24	721-49E	870	30	PX10	2200 O_2/2200 N_2	45-100	72
25	721-25E	875	30	PX10	2200 O_2/2200 N_2	48-120	75
26	731-7.8	880	20	PX10	2200 O_2/2200 N_2	40-95	65
27	731-7.8	880	20	Dil.PX10(3)	2200 O_2/2200 N_2	45-1000	190
29	733-5.3	860	20	Dbl.PX10(4)	2200 O_2/2200 N_2	75-110	92
30	729-4.1	865	20	Dbl.PX10(4)	2200 O_2/2200 N_2	80-200	125

NOTES: (1) P8 solution was 8 weeks old.
(2) P8 solution was 1 week old.
(3) PX10 diluted 1/1 with propanol.
(4) Strip coated, dried and recoated with PX10.

In Table 23, Test Nos. 10 and 11 show the effect of age on the liquid source diffusant, with the newer material giving a much lower sheet resistivity. This effect (sheet resistivity dependent on age of diffusant source) would make it difficult to achieve reproducible results. (The P8 used in #9 was only several weeks old and, as such, behaved as new material.)

In these runs, the web strips were separated into crystal pairs* with matched pairs being diffused with the baseline $POCl_3$ and liquid dopant. In this way, the effectiveness of the liquid dopant process could be directly compared to the baseline process.

Table 24 shows lighted IV data on cells from these runs with the parameters of the liquid diffused cells compared to the baseline cells. The columns marked "Ratio of IV Parameters Liq/$POCl_3$" contain data from the crystal pairs included in the process experiment. The last two columns "Avg. Eff. (%)" give the average efficiency for all the liquid doped and $POCl_3$ diffused cells in the run.

Spreading resistance measurements to determine the surface concentration and junction depth were made on selected cells. Figure 8 shows the N^+P diffusion profile of two representative cells from the same web growth run and processing run. Cell 91A was a liquid phosphorus diffused cell while 92A was a gaseous $POCl_3$ diffused cell. The curves are practically coincident. The small difference in Co is negligible.

Since only a very small portion of a cell is measured during this test, no conclusions can be drawn regarding the overall uniformity of the junction in either cell. The curves do show, however, that the junction profile of a liquid diffused cell is not significantly different from a gaseous $POCl_3$ diffused cell.

*The dendritic web is grown in long (2-6 meters) single crystals. Crystal pairs, as used above, means that the multiple web strips were cut from the same single crystal.

TABLE 24

COMPARISON OF LIGHTED IV DATA FROM LIQUID DIFFUSANT SOURCE CELLS VS $POCL_3$ DIFFUSED CELLS

Test No.	No. of Cells Liq.	No. of Cells $POCl_3$	Dopant	Cell Area (cm^2)	Ratio of IV Parameters Liq/$POCl_3$ Voc	Isc	Eff.	Avg. Eff. (%) Liq.	Avg. Eff. (%) $POCl_3$
1	14	25	P8	15.68	.95	.95	.88	12.6 ±.7	13.4 ±.8
3	17	45	P8	19.6	.97	.92	.86	11.7 ±.8	13.5 ±.8
4	12	50	P8	19.6	.98	.93	.90	12.1 ±.7	13.2 ±1.0
5	12	26	P8	19.6	.94	.98	.97	10.6 ±1.8	13.1 ±1.0
6	15	39	P8	19.6	1.0	.96	.97	11.6 ±.3	12.3 ±.8
8	12	33	PX10	24.5	.96	.94	.88	11.2 ±.9	12.8 ±1.0
9	13	37	P8	15.68	.99	.92	.91	11.3 ±1.0	12.4 ±.9
10	12	31	PX10	24.5	.95	.92	.88	11.3 ±.6	12.6 ±.8
11	12	38	P8	19.6	.96	.91	.87	11.9 ±.6	13.7 ±1.0
12	9	44	P8	24.5	.99	.89	.90	12.1 ±1.0	13.5 ±.9
13	7	26	P8	19.6	.97	.92	.88	11.1 ±1.5	13.5 ±.7
14	10	38	PX10	19.6	.98	.94	.95	12.2 ±.4	13.0 ±.8
18	13	34	P8	24.5	.97	.97	.94	12.4 ±1.0	12.9 ±.8
19	10	38	PX10	19.6	.98	.96	.94	12.3 ±.7	12.8 ±.6
20	12	37	PX10	24.5	.99	.98	.97	12.2 ±.7	12.4 ±.8
22	12	43	PX10	24.5	.97	.96	.93	11.9 ±.8	12.7 ±.6
24	9	31	PX10	24.5	.99	.96	.96	11.8 ±.6	12.2 ±.6
25	10	31	PX10	24.5	.98	.97	.96	12.3 ±.8	12.6 ±.7
26 } 1proc	5	22	Dil.PX10	24.5	.98	.99	.98	12.9 ±.8	13.2 ±.7
27 } run	11	22	PX10	24.5	.98	.98	.96	12.5 ±.5	13.2 ±.7
29	4	43	Dbl.PX10	19.6	1.0	.99	.99	13.4 ±.7	13.4 ±1.0
30	7	34	Dbl.PX10	15.68	.99	.99	.98	12.4 ±.7	12.5 ±.8

60

9950-8??

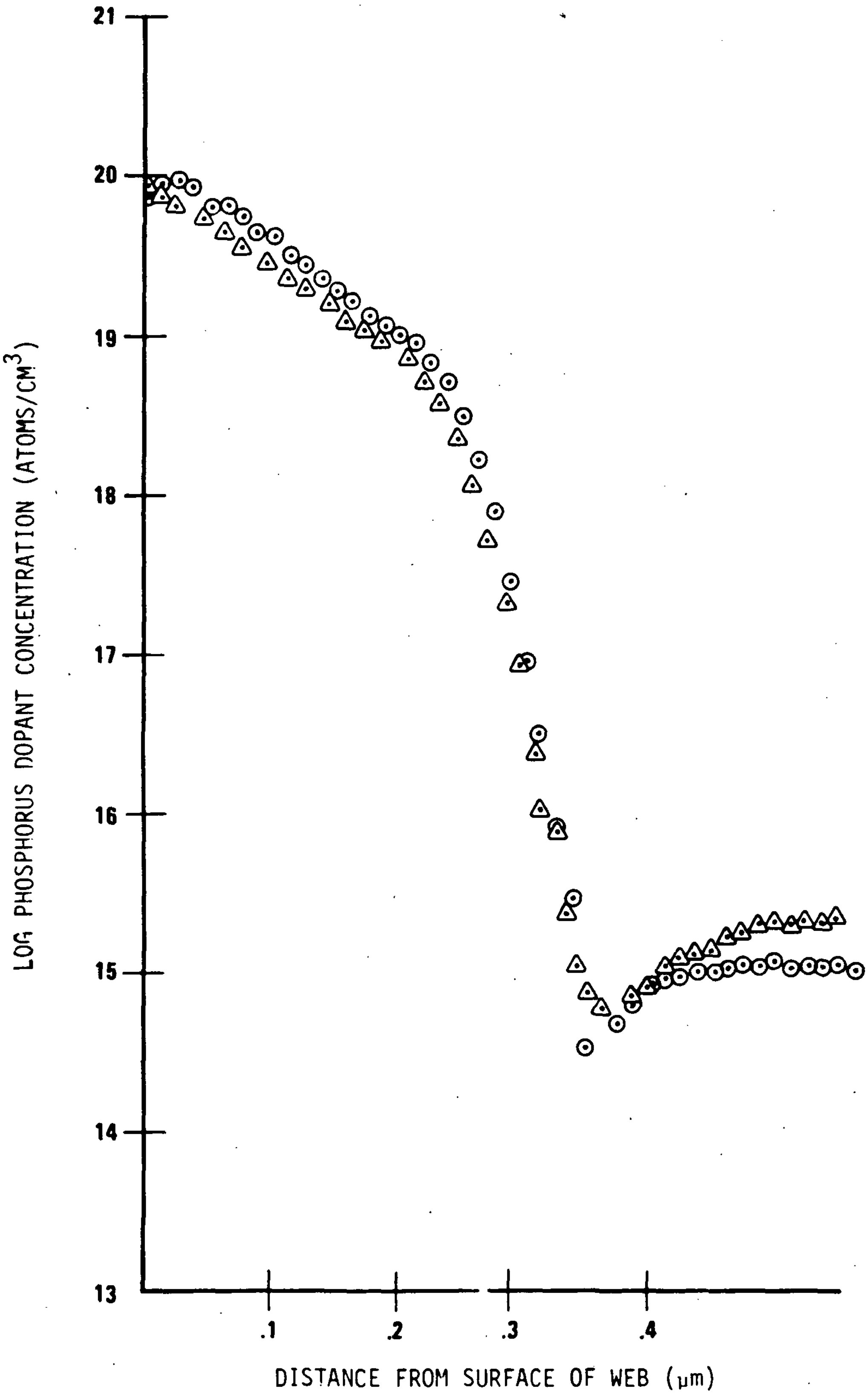

Figure 8. N^+P Diffusion Profiles for Cell 91A - Liquid Diffusion Source (△) and Cell 92A - $POCl_3$ Diffusion Source (⊙)

61

Of especial interest in Table 24 are Items 29 and 30 where a double coating of the liquid dopant was applied to the web before diffusion. In these two runs, the overall efficiency of the liquid diffused cells was equal to the $POCl_3$ diffused cells. In a number of cases in these runs, the liquid cells were superior to the $POCl_3$ diffused cells.

In Items 26 and 28, the liquid dopant was diluted one to one with isopropyl alcohol to determine any effect if the dopant was diluted for use in the meniscus coater. The data indicate there should not be an efficiency penalty if the diluted material is used.

The IV data of Table 24 shows the liquid source diffused cells have lower average efficiencies than the baseline diffused cells, although some individual liquid diffused cells had efficiencies equal to the baseline cells. In general, if the N^+ sheet resistivity of the cell was above 100 $\Omega/\square$ or lower than 40 $\Omega/\square$, the efficiency of the cells was lower than the baseline cell. Those liquid diffused cells having the highest average efficiency had sheet resistivities in the 60-90 $\Omega/\square$ range.

Dark IV data (See Section IIIA3) and other diagnostic tests on various crystal pairs of cells from these experiments will be given in a later section.

3. Tests Using the Meniscus Coater

Three experiments were carried out using the meniscus coater to apply the liquid phosphorus dopant. Two of these tests used P8 as the dopant source while the third used PX10.

Two 24 strip batches of dendritic web were chosen for the first test using the meniscus coater to apply liquid phosphorus. Twenty-four strips were coated with Diffusion Technology P8 liquid phosphorus solution using the meniscus coater, and 24 strips were given the baseline $POCl_3$ gaseous diffusion. Where possible, matched web crystal pairs were liquid coated and $POCl_3$ diffused. All cells had a liquid boron diffused P^+P junction, and a liquid SiO_2 mask was used. Runs used were designated 0203-1W and 0203-25W. All cells processed in the baseline sequence had sheet resistivities within specification, and no abnormalities were noted.

The results from the coating and diffusion portion of the test were:

a. Problems were encountered with coating the strips with the P8. The strips did not coat uniformly across the holding fixture, and it was necessary to raise the porous stainless steel cylinder. (This in spite of the fact the unit was originally aligned using an antireflective solution.) Because of this, several strips (or portions thereof) were coated more than once. The cause of this problem was the high viscosity of the P8 solution which caused a low and irregular meniscus across the porous cylinder.

b. After application of P8, the strips were baked for 15 minutes at 150°C. After drying, the strips had a white-powdery surface.

c. The strips were diffused for 20 minutes at 850°C in an 80% N_2 - 20% O_2 ambient. The powdery surface was still evident after diffusion.

63

d. After stripping (10% HF in deionized water), the N^+ surface appeared clean; but there were small, lightly adherent particles which could be brushed off.

e. After the strips were coated, the residual P8 solution removed from the meniscus coater was distinctly yellow - as opposed to the original water-white color.

The sheet resistivity on the coated strips was measured after diffusion and showed a wide variability with a number of the strips having resistivities in excess of 1000 Ω/□ (the specification is 60 ±10 Ω/□). The high sheet resistivity noted was presumably due to (1) very thin or nonexistent coating on some strips or portions thereof, or (2) coating flaked off areas of strips during bake cycle. This would also cause a low shunt resistance. Figure 9 is a sketch which shows how shunting could occur.

After diffusion, processing of all strips both gaseous $POCl_3$ and liquid P8 diffused was completed using baseline processes. Table 25 shows a comparison of lighted IV data from liquid P8 diffused cells and gaseous $POCl_3$ diffused cells fabricated on the same web crystal. Of the 10 web crystal pairs listed, in five cases the liquid P8 cells had significantly higher properties. In one case, the $POCl_3$ diffused cell was superior; and in four cases, the cells were essentially equal. When the liquid source diffused cells have higher efficiencies than the $POCl_3$ diffused cells, the major difference is a larger short circuit current.

Table 26 shows lighted and dark IV data on 3 cells selected from this initial experiment. Note that the all-liquid source diffused cell (3B) has excellent junction properties and bulk lifetime. Cell 10C was also a liquid source diffused cell but had a high sheet resistivity and a very low shunt resistance.

Table 27 shows spreading resistivity measurements made on these same three cells to determine the N^+P junction depth. The slightly shallower junction with the liquid phosphorus diffused cell should increase current collection

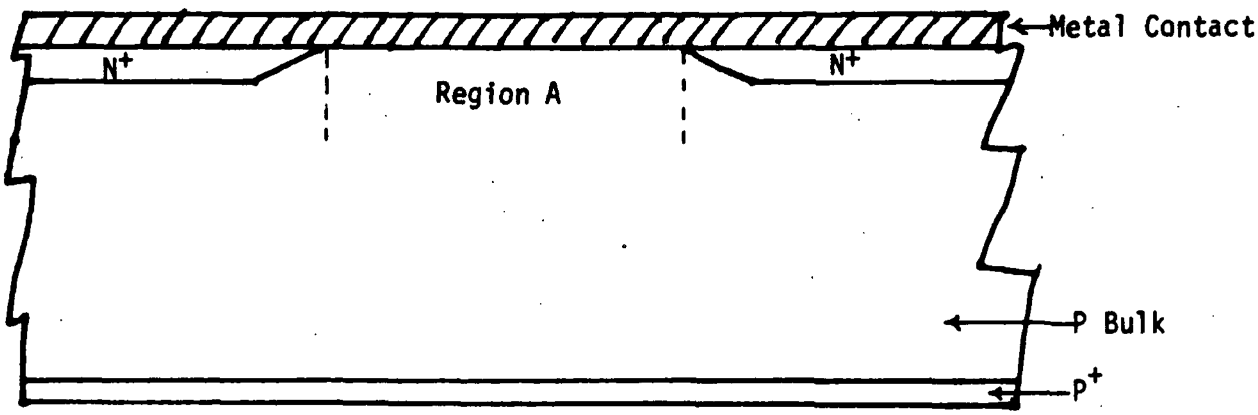

<u>NOTE</u>: No N^+ diffusion or very shallow diffusion in Region A. Metal contact shorts N^+ and P regions giving a low R_{shunt}.

Figure 9. Sketch of Mechanism for Low Shunt Resistance Observed in First Liquid Phosphorus Experiment

TABLE 25

LIGHTED IV CELL DATA FROM INITIAL MENISCUS COATER, LIQUID PHOSPHORUS EXPERIMENT

(Process Runs 0203-1W and 0203-25W)

Web Crystal	Junction* Process	No. of Cells	Av. V_{oc} (V)	Av. I_{sc} (A)	Av. FF	Av. Eff. (%)
5.206-16	Liq P8	3	.574	.614	.786	14.1
	$POCl_3$	2	.578	.639	.782	14.8
1.224-15	Liq P8	3	.541	.577	.787	12.6
	$POCl_3$	3	.545	.579	.786	12.7
5.206-17	Liq P8	3	.568	.616	.774	13.8
	$POCl_3$	3	.568	.596	.773	13.3
1.224-18	Liq P8	5	.545	.604	.754	12.9
	$POCl_3$	1	.546	.626	.723	12.6
7.196-3	Liq P8	2	.562	.619	.786	13.9
	$POCl_3$	3	.552	.584	.795	13.3
1.225-3	Liq P8	3	.560	.610	.781	13.6
	$POCl_3$	1	.544	.575	.797	12.8
2.188-4	Liq P8	1	.537	.503	.810	11.0
	$POCl_3$	2	.525	.522	.783	10.9
1.207-2	Liq P8	1	.558	.600	.752	12.9
	$POCl_3$	2	.550	.584	.793	13.1
7.196-5	Liq P8	2	.577	.637	.779	14.6
	$POCl_3$	1	.550	.576	.783	12.7
4.188-6	Liq P8	3	.551	.596	.762	12.8
	$POCl_3$	2	.523	.530	.769	10.9

*Liq P8 = Diffusion Technology P8 phosphorus solution applied using meniscus coater.
$POCL_3$ = Baseline $POCl_3$ diffusion.

TABLE 26

EXPANDED CELL DATA FROM FIRST MENISCUS COATER, LIQUID PHOSPHORUS EXPERIMENT

LIGHTED AND DARK IV DATA: ALL LIQUID JUNCTION CELLS VS $POCl_3$ BASELINE CELL

Web Crystal	Process	Cell No.	$V_{oc}(V)$	$J_{sc}(mA)$	FF	$\eta(\%)$	$R_s(\Omega\text{-cm}^2)$	$R_{sh}(\Omega\text{-cm}^2)$	$\tau(\mu sec)$	$J_{01}(\frac{A}{cm^2})$	$J_{02}(\frac{A}{cm^2})$
5.206-17	$POCl_3$	9A	.569	30.5	.765	13.3	0.11	7.6×10^3	69	6.6×10^{-12}	9.1×10^{-7}
5.206-16	Liq P8	3B	.577	31.3	.805	14.5	0.45	712.5×10^3	124	5.0×10^{-12}	8.4×10^{-8}
1.224-16	Liq P8	10C	.217	18.5	.564	2.3	-3.2	0.02×10^{-3}	Not calculated, out of range.		

Cell 9A has good junctions and adequate bulk lifetime; both R_s and R_{sh} are good.

Cell 3B has exceptional junctions and bulk lifetime; R_s and R_{sh} are good.

Cell 10C was a reject cell, with high sheet resistivity after N^+ diffusion; cell shows very low shunt resistance.

TABLE 27

N^+P JUNCTION DEPTH MEASUREMENTS ON SEVERAL LIQUID JUNCTION CELLS

Web No.	Cell No.	Process	Junction Depth (N^+P) (μm)	Surface Conc. (atoms/cm^3)
5.206-17	9A	$POCl_3$ Baseline	0.38	9×10^{19}
5.206-16	3B	Liquid P8	0.32	2.9×10^{19}
1.224-16	10C	Liquid P8	0.24	1.9×10^{19}

while the lower surface concentration would decrease the heavy doping (lattice strain) effects. The shallow junction depth on cell 10C reinforces the possible shunting mechanism discussed above and depicted in Figure 9.

Table 28 presents overall yield data from those runs which indicates no apparent yield penalty with the all liquid diffusion process.

This first test on the meniscus coater showed that high quality cells can be fabricated from liquid source diffusions. However, the uniformity of the coating required improvement. In addition, the diffusion temperature and time and the ambient gas composition required optimization to obtain the required sheet resistance.

A second meniscus coater test was then carried out to study coating results when the dopant solution viscosity and the application speed were varied. Again, the dopant solution used was Diffusion Technology P8.

Since it was noted previously that the as-received dopant solution did not form a full meniscus over the top of the porous stainless steel cylinder, the liquid dopant was diluted by adding 25% (by volume) of isopropyl alcohol. Although improved, the coating applied to the strips along the width of the holding fixture was still not completely uniform. Adding an additional 25% of isopropyl alcohol increased the meniscus height sufficiently to produce a uniform coating. The remainder of the test run was made using this 50% isopropyl alcohol/50% as-received P8 solution.

For the second experiment, three batches of 24 strips of dendritic web were identified. These batches were first diffused to form a P^+P back junction using Diffusion Technology B60 liquid dopant. Prior to applying the liquid phosphorus on the meniscus coater, the strips were manually coated with a liquid SiO_2 diffusion mask using a sponge-squeegee.

Where possible, individual strips in each batch were again separated into crystal pairs, and approximately one-half of the pairs were diffused using

TABLE 28

YIELD DATA FROM INITIAL MENISCUS COATER, LIQUID PHOSPHORUS EXPERIMENT
Runs 0203-1W and 0203-25W

	No. of Cells Started	No. of Cells Tested	Mechanical Yield
Liquid Phosphorus	72	49	68%
Baseline $POCl_3$	72	49	68%
TOTAL	144	98	68%

70

the baseline $POCl_3$ process to obtain comparative data. The baseline cells showed a sheet resistivity within specification and an average efficiency of 13.9% for 53 cells. The remainder of the pairs were separated into four groups and coated with the diluted P8 solution in the meniscus coater at application speeds of 7.5, 18, 28, and 36 cm/min. After coating, the strips were baked under a heat lamp for 10 minutes at 80°C and in a drying oven for 15 minutes at 200°C. Immediately before diffusion, they were held at the mouth of the furnace tube for 10 minutes at about 350°C.

Table 29 shows the effect of coating speed on the liquid dopant thickness as determined after the 200°C bake. These results are similar to those observed when an antireflective coating is applied to web material by withdrawing the strip from a liquid. That is, the slower the withdrawal speed, the thinner the coating.

Two of the three experimental batches were diffused at 870°C for 20 minutes in a gas flow of 225 cc/min O_2 and 100 cc/min N_2. The third batch was diffused at 877°C for 20 minutes in the same gas flow. After diffusion, the diffusion glass was removed from the strips and the sheet resistivity measured. Table 30 shows the results of these measurements. As was seen in the first meniscus coater test, the sheet resistivity varied greatly both along the strip and among the different strips. There was no obvious correlation between sheet resistivity and coating speed (thickness).

The average efficiency of all the liquid diffusant coated cells (about 10.5%) was significantly lower than the baseline processed cells. However, several of the liquid cells had properties equal to the $POCl_3$ diffused cells.

One major difference between these two runs was the use of the diluted P8 solution, and this is suggested as being the cause of the generally lower cell efficiency in this test.

71

TABLE 29

EFFECT OF MENISCUS COATER APPLICATOR SPEED ON FILM THICKNESS

Applicator Speed (cm/min)	Estimated Thickness
7.5	<200 nm - colorless
18	red - green
28	≈~300-700 nm, some white powdery areas
36	Thick, no color when dry, ≈1 μm, white powdery surface

72

TABLE 30

SHEET RESISTIVITY OF LIQUID COATED STRIPS FROM SECOND MENISCUS COATER LIQUID PHOSPHORUS EXPERIMENT

Strip No.	Coating Speed (cm/min)	Sheet Resistivity Range along Strip (Ω/□)
RUN 305-1W (Diffused at 870°C - 20 min.)		
1	18	120-2000
3	36	250-2000
5	18	700-1000
7	36	700-1000
9	18	50-200
14	18	44-500
15	18	90-2000
19	18	300-1500
21	36	500-2000
24	18	650-900
RUN 305-25W (Diffused at 870°C - 20 min.)		
25	28	700-800
27	28	600-1000
29	18	600-1200
33	28	500-800
36	18	400-1000
37	28	700-2000
38	28	38-1500 (P type surf.)
41	28	35-2000 (P type surf.)
43	28	34-2000 (P type surf.)
45	28	150-900
47	28	180-600
48	28	53-270
RUN 308-73W (Diffused at 877°C - 20 min.)		
73	7.5	45-750
74	7.5	35-1700
78	7.5	120-500
84	28	260-750
87	28	70-980
89	28	180-730
91	7.5	35-77
92	28	35-160
94	28	35-460
96	28	80-950

73

From this second meniscus coater test, the following conclusions were drawn:

- The meniscus coater can be used to apply uniform coatings of the liquid phosphorus containing solution of varying thicknesses.

- Although the overall average of the front junction liquid doped cells was lower than on the first test, several cells were equal to the baseline processed cells. The average lower cell efficiency is believed due to the use of the diluted P8.

In the third meniscus coater experiment, PX10 was used as the liquid dopant. The solution was used undiluted, and coating speeds of 18 cm/min, 28 cm/min, 32 cm/min, and 36 cm/min were used. Four processing runs were used in the test, and these runs were separated into crystal pairs for baseline $POCl_3$ diffusion and meniscus coated liquid phosphorus diffusion.

Table 31 gives the diffusion conditions and sheet resistivity range for the steps in this test.

After the strips were coated and baked, the coating appeared adherent and uniform in color. There were no areas of powdery coating as noted in the second run. The variability in sheet resistivity was somewhat less than noted in the previous runs. In addition, there was a rough correlation between coating speed (film thickness) and sheet resistivity, with the slower coating speed (thicker film) having the lower sheet resistivity.

These strips along with the $POCl_3$ diffused crystal pairs were finished baseline processed and tested.

74

TABLE 31

EXPERIMENTAL CONDITIONS AND MEASURED SHEET RESISTIVITY
FOR THIRD MENISCUS COATER TEST

I. Run #812-49M, Diffused 20 min. at 870°C; 2200 cc/min O_2; 2200 cc/min N_2

Strip No.	Coating Speed	Sheet Resistivity Range Along Strip (Ω/□)
49	28	60-105
50	28	100-270
56	18	100-135
57	28	90-200
58	18	70-115
64	28	115-170
65	28	75-170
70	28	75-150

II. Run #811-73E, Diffused 20 min. at 870°C; 2200 cc/min O_2; 2200 cc/min N_2

74	36	70-135
75	36	100-700
78	36	70-140
80	18	90-140
84	18	50-100
86	36	70-140
88	36	75-155
90	36	75-110
92	36	85-150
94	28	85-120
95	36	100-150
96	28	65-250

III. Run #1220-25E, Diffused 30 min. at 875°C; 2200 cc/min O_2; 2200 cc/min N_2

25	32	180-700
27	18	80-170
28	28	95-250
32	28	80-110
34	28	100-190
38	18	150-280
40	18	75-95
46	28	100-140

IV. Run #813-1W, Diffused 30 min. at 875°C; 2200 cc/min O_2; 2200 cc/min N_2

1	34	90-110
3	18	100-240
6	18	130-200
8	28	95-120
13	34	100-450
15	34	150-320
17	34	250-330
19	28	200-280
20	34	300-600
22	18	65-95

75

Table 32 gives the data on the crystal pairs in the test. In this table, on an overall basis, the efficiencies of the liquid diffused cells are lower than the baseline $POCl_3$ cells; although in 4 cases, the liquid diffused cells are superior. Also there is no one-to-one correlation between the measured sheet resistivity and the cell efficiency. This factor should be studied more carefully, but the lack of correlation may be due to the overall variation of sheet resistivity along the length of the web.

This variability of sheet resistivity has been noted in both the meniscus coater tests and the tests discussed in Table 23. We have no simple explanation for this effect at this time, but it may be related to a non-uniform distribution of phosphorus atoms over the web surface, even when the overal coating appears to be uniform.

From this third test, we conclude:

- Undiluted PX10 can be used in the meniscus coater to give uniform layers of the dopant.
- High efficiency cells can be fabricated using the meniscus coater to apply the dopant.
- Further experiments are required to increase the overall average of the process.

TABLE 32

LIGHTED IV CELL DATA ON WEB CRYSTAL PAIRS

Web Crystal	Junction Process	Avg. Voc (V)	Avg.Jsc (ma/cm^2)	Avg.Eff. (%)	ρ_S(Ω/□)
4.236-15	L	.559	29.4	13.1	100-200
	P	.574	30.9	13.8	*
3.126-4	L	.561	28.4	13.2	130-200
	P	.575	29.8	13.7	
3.126-5	L	.564	28.8	13.5	95-120
	P	.566	28.3	13.2	
3.126-6	L	.555	30.2	13.5	250-350
	P	.571	29.2	13.2	
3.126-7	L	.567	26.4	12.0	250-330
	P	.585	26.1	12.0	
1.255-2	L	.543	28.8	12.5	300-600
	P	.571	30.2	14.0	
1.255-3	L	.579	24.7	11.4	65-95
	P	.588	26.4	12.1	
7.190-7	L	.563	29.5	13.2	100
	P	.583	30.8	14.3	
5.202-6	L	.556	28.8	12.5	150
	P	.570	30.5	13.7	
4.183-7	L	.554	28.8	12.7	120
	P	.548	27.3	12.3	
4.214-2	L	.545	27.7	11.8	70-140
	P	.566	29.9	13.6	
4.214-3	L	.553	28.1	12.3	90-140
	P	.544	26.5	11.3	
2.216-6	L	.579	25.6	12.8	50-100
	P	.582	28.2	13.7	
3.126-6	L	.564	29.9	13.3	75-150
	P	.574	30.1	13.9	
3.126-7	L	.575	25.8	12.5	85-120
	P	.583	26.5	12.5	

*All $POCl_3$ diffused strips were within the specified 60 ±10 Ω/□ range.

77

4. Analysis of Cell Parameters

The lighted IV data given in the preceding sections (IIIF2 and IIIF3) show that except for several experiments, the cells fabricated with a liquid phosphorus front junction have, on the average, lower efficiencies than the $POCl_3$ diffused cells. In this section, we report the results of various diagnostic tests which were made to investigate the cause of the lower efficiency.*

Dark IV data, i.e., data taken in the diode forward direction in the dark, can give information regarding the junction quality, carrier lifetime, and series and shunt resistances. From these data, inferences can be drawn regarding the device. The dark IV measurements were discussed in some detail in Section IIIA3.

Table 33 shows dark IV data for a number of selected cells fabricated with liquid phosphorus and $POCl_3$ diffusions. In the table, data is given on web crystal pairs so that a one to one comparison of the liquid vs $POCl_3$ junctions can be seen.

The first conclusion to be drawn is that the lower efficiency in the liquid diffused cells is not related to the web material since in most cases the $POCl_3$ diffusion results in high efficiency cells.

When the efficiency of the liquid diffused cell is lower than the $POCl_3$ diffused cell, the minority carrier lifetime of the liquid diffused cell is also lower. This is generally mirrored in a higher bulk saturation current density, J_{01}, for the liquid diffused cell. By the same token, when the two types of cells have generally equal efficiencies, the lifetimes and bulk saturation current densities are nearly equal.

A depressed lifetime is usually due to recombination centers in either the bulk or emitter regions of the cell.

---

*As discussed in these sections, a number of individual cells from the experiments had efficiencies equal to the baseline $POCl_3$ cells.

9950-892

TABLE 33

DARK IV DATA - COMPARISON OF FRONT JUNCTION USING LIQUID DIFFUSANTS VS $POCL_3$

	Item No. & Web Run	Proc. Run No.	Cell No.	Diffusant	Eff.(%)	τ_B (μsec)	R_s (Ωcm^2)	R_{sh} ($K\Omega cm^2$)	$J_{01}\left(\frac{A}{cm^2}\right)$
1.	3.091-9	1217-49E	58A	PX10	12.8	45	.20	82	8.1×10^{-12}
	3.091-9	1217-49E	59A	$POCl_3$	13.4	95	.12	1.7	5.7×10^{-12}
2.	4.203-6	502-1M	1A	P8	10.4	22	.10	1	1.2×10^{-11}
	4.203-6	502-1M	2B	$POCl_3$	13.2	120	.14	30	5.1×10^{-12}
3.	3.116-7	502-1M	10A	P8	13.1	50	.15	34	7.8×10^{-12}
	3.116-7	502-1M	11A	$POCl_3$	13.2	40	.18	320	9.1×10^{-12}
4.	3.120-7	611-73W	88B	P8	12.0	25	1.1	429	1.0×10^{-11}
	3.120-7	611-73W	89A	$POCl_3$	14.2	205	.67	224	3.8×10^{-12}
5.	1.245-5	611-73W	94B	P8	12.8	63	.61	315	7.0×10^{-12}
	1.245-5	611-73W	95A	$POCl_3$	13.9	96	1.0	2	5.6×10^{-12}
6.	7.193-8	113-25E	33C	P8	13.7	90	.24	540	5.9×10^{-12}
	7.193-8	113-25E	36B	P8	11.7	14	.13	.7	1.4×10^{-11}
	7.193-8	113-25E	35B	$POCl_3$	13.7	200	.16	570	3.9×10^{-12}
7.	2.186-10	113-25E	40C	P8	10.4	3	1.5	28	3.1×10^{-11}
	2.186-10	113-25E	42C	$POCl_3$	12.9	50	.04	5	7.9×10^{-12}
8.	7.193-7	113-25E	25B	P8	13.7	80	0.1	380	6.2×10^{-12}
	7.193-7	113-25E	26A	$POCl_3$	13.2	76	0.8	50	6.2×10^{-12}
9.	5.232-5	718-1W	2B	PX10	13.5	75	.19	15	6.4×10^{-12}
	5.232-5	718-1W	1C	$POCl_3$	13.6	100	.26	21	5.6×10^{-12}
10.	1.248-1	718-1W	23B	PX10	12.1	30	.28	58	1.0×10^{-11}
	1.248-1	718-1W	24B	$POCl_3$	13.1	60	.47	9	7.2×10^{-12}
11.	4.211-8	722-73W	95B	PX10	13.2	80	.44	50	6.1×10^{-12}
	4.211-8	722-73W	96B	$POCl_3$	13.6	100	.92	40	5.5×10^{-12}
12.	5.236-6	733-1W	6-2A	PX10	14.0	350	.18	14	2.9×10^{-12}
	5.236-6	733-1W	6-3B	$POCl_3$	13.7	200	.16	13	3.9×10^{-12}
13.	7.194-1	113-73E	95B	PX10	11.7	25	.35	180	1.1×10^{-11}
	7.194-1	113-73E	94B	$POCl_3$	13.1	50	.26	16	8×10^{-12}

79

Of especial interest in Table 32 are the three cells of Item 6. The two liquid diffused cells, 33C and 36B, are from the same web crystal and from the same processing run. However, they have vastly different cell properties with 33C being essentially equal to 35B, the $POCl_3$ diffused cell. Cell 36B has a low lifetime and a high saturation current density. This set of data indicates that the overall processing of the cell (e.g., diffusion, metallization, etc.) are not the cause of the lower efficiency since these cells were processed as a group. (The 700 Ωcm^2 shunt resistance of cell 36B, although low, cannot account for the measured differences in cell parameters.)

By the same token, the lower efficiency is probably not due to impurities in the liquid phosphorus diffusant since the cells were coated at one time using the same lot of liquid diffusant.

One possibility for the poorer cells produced using the liquid dopant is that the phosphorus containing layer may be non-uniform or incomplete; and after diffusion, regions of low concentration of N type doping may be present on the surface. This irregular N^+P junction may act as though there were recombination sites in the emitter region.

Referring back to Table 24, Items 29 and 30 were double coated with the liquid source; and thus should have a more complete coating of the diffusant. In these two experiments, the liquid diffused cells have the same average efficiency as the $POCl_3$ diffused cells.

If the coating (thickness or uniformity) is a problem and causes the lower efficiency of the liquid diffused cells, one would expect the effect to be most noticeable in the emitter portion of the saturation current density.

The saturation current is composed of two parts, J_{OB} (bulk portion) and J_{OE} (emitter portion), or

$$J_{01} = J_{OB} + J_{OE}$$

To separate the bulk and emitter portions of the saturation current, spectral response measurements were obtained on a number of the cells in Table 33. From

80

these data, quantum efficiency curves vs wavelength were derived for each cell. Quantum efficiency curves for Items 13 and 8 in Table 33 are shown in Figures 10 and 11. Each figure shows the quantum efficiency vs wavelength curve of a $POCl_3$ diffused cell and a liquid diffused cell from the same web crystal and processing run. For these cells, spreading resistance data showed similar junction depths. In the figures, P = $POCl_3$ diffused and L = liquid dopant diffused.

These figures show that when the liquid diffused cell is of poorer quality than the $POCl_3$ diffused cell (Figure 10, Item 13 in Table 33), the loss in response is mainly in the short wavelength region (i.e., wavelengths which are generally absorbed in the emitter region). However, when the cells are of equal quality (Figure 11, Item 8 in Table 33), the quantum efficiency curves are nearly coincident.

Thus, Figure 10 indicates that the liquid diffused cell is controlled by the emitter region; and thus, the coating uniformity may well be the problem with the liquid diffused cells. This conclusion is borne out by the data of Table 24, Items 29 and 30.

81

32

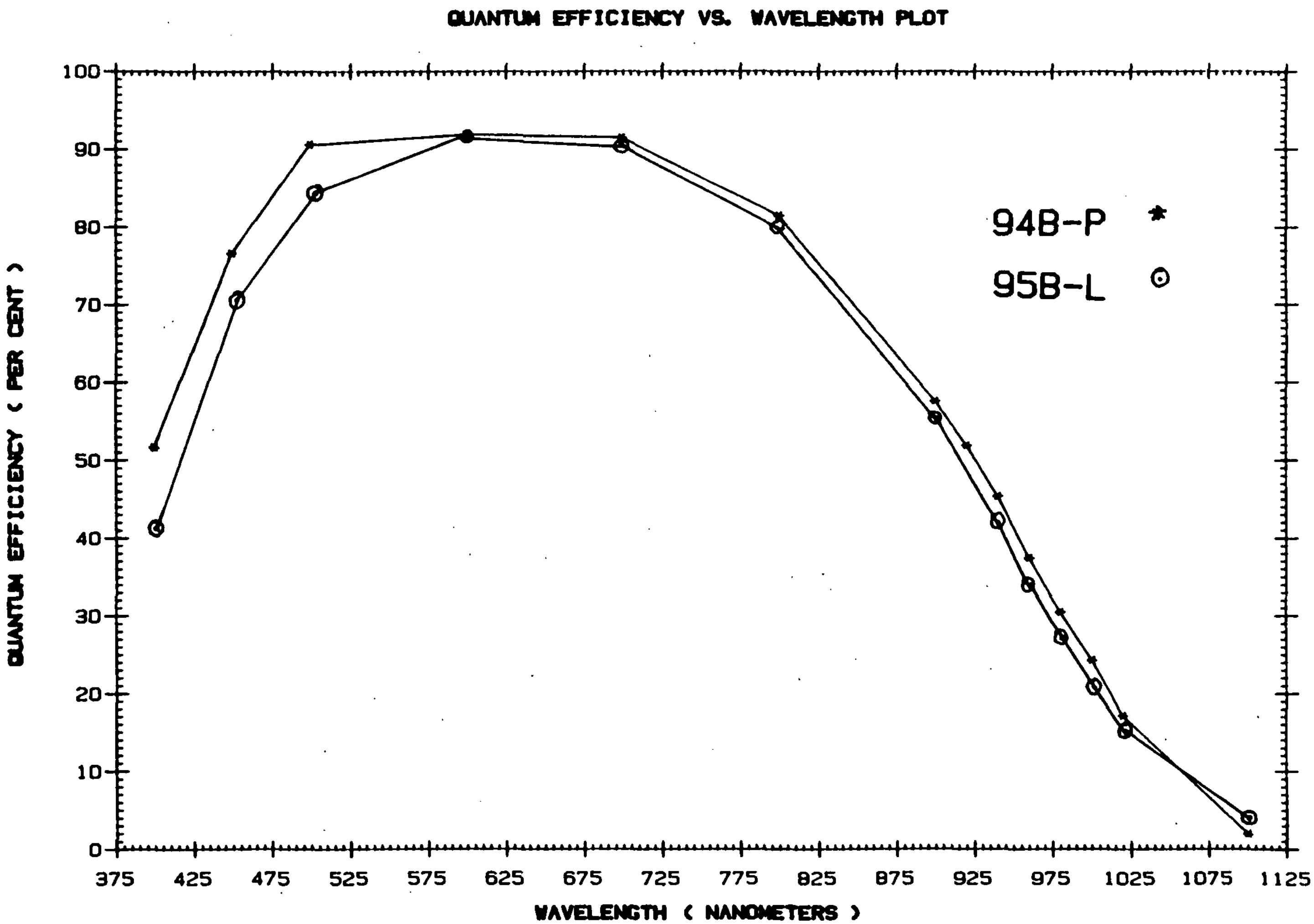

Figure 10. Quantum Efficiency vs Wavelength Plot of $POCl_3$ Diffused Cell and Liquid Diffused Cell. $POCl_3$ Diffused Cell Superior to Liquid Diffused Cell.

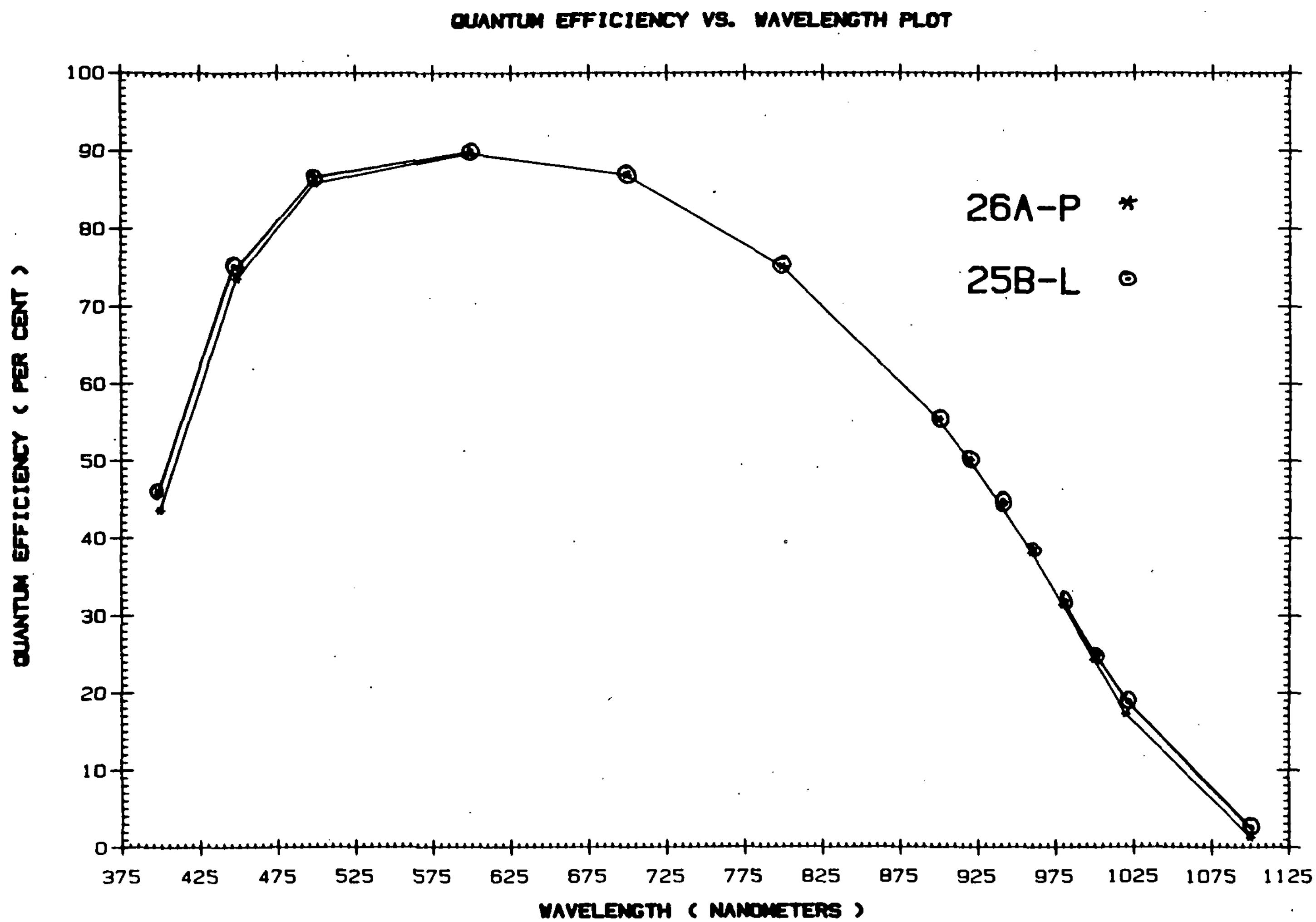

Figure 11. Quantum Efficiency vs Wavelength Plot of $POCl_3$ Diffused Cell and Liquid Diffused Cell. Cells of Equal Quality.

G. Cost Analysis

1. Introduction

The fifth milestone of JPL Contract 955909 is to perform a cost analysis of the junction formation step in the processing of solar cells from dendritic web silicon when the diffusant source and mask source are obtained from liquids.

In this section, we give the results of this analysis and compare these results with the junction formation step when the Westinghouse baseline gaseous diffusion process is used. The analyses were carried out for 1 MW/yr and 25 MW/yr production facilities.

For the analysis, IPEG-2 was used to obtain these costs. Copies of Formats A, B, and C are also included for a SAMICS simulation.

2. Definition of Process Step on Format A

Table 34 lists the process steps given in the Format A's*, and Table 35 lists the six junction formation processes that were costed.

The Format A's retain the referents used in the previous SAMICS simulation of the Westinghouse baseline process sequence, and thus the data can be used as input into the existing SAMIS program.

In the Format A's, the prefix M refers to a process step with a throughput of approximately 1 MW/yr. We have assumed a 12% efficient module; therefore, the area throughput for the M process is about 200 cm^2 of dendritic web per minute. Similarly, the prefix P refers to a process step with a throughput of 25 MW/yr and an area throughput of 5000 cm^2/min, again for a 12% module.

Table 36 gives further assumptions made in preparing data for the Format A's.

---

*The various formats used in the calculation are attached as Appendix D.

TABLE 34

PROCESS STEPS ANALYZED

Facility Throughput	Process Referent	Process
1 MW/yr	M2	Baseline CVD SiO_2 + Gaseous BBr_3 Diffusion
1 MW/yr	M3	Baseline CVD SiO_2 + Gaseous $POCl_3$ Diffusion
1 MW/yr	M12	Liq Mask + Liq Boron Source
1 MW/yr	M13	Liq Mask + $POCl_3$ Source
1 MW/yr	M23	Liq Mask + Liq Phosphorus Source
25 MW/yr	P2	Baseline CVD SiO_2 + Gaseous BBr_3 Diffusion
25 MW/yr	P3	Baseline CVD SiO_2 + Gaseous $POCl_3$ Diffusion
25 MW/yr	P12	Liq Mask + Liq Boron Source
25 MW/yr	P13	Liq Mask + $POCl_3$ Source
25 MW/yr	P23	Liq Mask + Liq Phosphorus Source

TABLE 35

JUNCTION FORMATION STEPS COSTED

1.	M2 + M3	(Baseline Gaseous Diffusion, CVD SiO_2 Mask Process)
2.	M12 + M13	(Liq Mask + Liq B Source + Liq Mask + $POCl_3$)
3.	M12 + M23	(Liq Mask + Liq B Source + Liq Mask + Liq Phos Source)
4.	P2 + P3	(Baseline Gaseous Diffusion, CVD SiO_2 Mask Process)
5.	P12 + P13	(Liq Mask + Liq B Source + Liq Mask + $POCL_3$)
6.	P12 + P23	(Liq Mask + Liq B Source + Liq Mask + Liq Phos Source)

TABLE 36

ASSUMPTIONS USED IN COST ANALYSIS

1. 3 shift, 7 days per week, 345 days/yr operation. (4.97×10^5 operating minutes/yr).

2. In M-Process, the throughput rate at the last station is 200 cm^2/min of usable web (99.4×10^2 M^2/yr).

3. In the P-Process, the throughput rate at the last station is 5000 cm^2/min of usable web (2.485×10^5 M^2/yr).

4. The strips of dendritic web silicon input into the line are 42 cm long by 2.7 cm wide. From these strips, four 2.5 cm x 10.0 cm cells will be fabricated.

5. The modules fabricated are a nominal 16" x 48" (120 cm x 40 cm) and produce 60 watts at 28°C and 100 mW/cm^2 insolation. This relates to a module efficiency of 12.1% with a nominal cell efficiency of 14%.

6. Yields for the process sequence are taken into account in each step in the process. The assumed yields are based on semiconductor industry experience.

7. The operational uptime of all equipment is based on industry experience. The various pieces of equipment have been sized such that the required throughput can be obtained including downtime for maintenance. Major maintenance may also be carried out during the 20 days/year downtime.

8. Waste organics and acids are disposed of by a local contractor. The Format A input relates to the quote for this service.

3. Format A Inputs

The Format A's give our estimates for capital equipment, labor, space, and materials for the process steps.

When possible, all material, labor, and space costs were obtained from the SAMICS Cost Accounting Catalog. Items not included in the Cost Accounting Catalog are listed in the "New Expense Item" sheet. These costs are based on vendor quotes. For large scale production, larger quantity prices are vendor budgetary estimates.

The capital equipment costs are vendor estimates or are based on recently purchased equipment. In all cases, a 7 year lifetime was used for the capital equipment.

All formats are attached to this report as Appendix D.

4. IPEG 2 Calculations

The IPEG equation is given in Table 37. The inputs to this equation were obtained from the Format A's.

Table 38 gives the cost data for the six different junction formation processes shown in Table 34. The column marked "SAMICS" gives the results obtained in a previous SAMICS simulation for the two baseline junction formation processes.

5. Conclusions

The cost analyses show that the liquid processes are significantly less expensive than the baseline gaseous diffusion process. The major cost saving is in capital equipment and material costs. The 2¢/watt saving in the 25 MW/yr process represents a 3% reduction in the overall process sequence cost, i.e., cell production and module fabrication.

Further savings would be realized if a simultaneous diffusion process were used where both the front and back junctions were diffused at the same time.

TABLE 37

IPEG (INTERIM PRICE ESTIMATE GUIDE)

$$\text{Cost} = \frac{C_1\ (\text{Eqpt.}) + C_2\ (\text{Space}) + C_3\ (\text{Dir.Lab.}) + C_4\ (\text{Materials}) + C_5\ (\text{Utilities})}{\text{Quantity}}$$

C_1 varies with depreciation rate of eqpt. = 0.57 for 7 yr. life

C_2 = \$110.6

C_3 = 2.8

C_4 = 1.2

C_5 = 1.2

Eqpt. = cost in constant dollars of capital eqpt. + installation - salvage

Space = required floor space (sq. ft.)

Dir. Lab. = cost of direct labor only - in constant dollars

$\left.\begin{array}{l}\text{Materials}\\ \text{Utilities}\end{array}\right\}$ cost in constant dollars

89

TABLE 38

COST SUMMARY
(All Costs in 1980$/Watt)

Process Step	IPEG Cost	IPEG Junction Formation Cost	SAMICS Cost	
M2	0.162	0.318	0.197	0.386
M3	0.153		0.189	
M12	0.156	0.293		
M13	0.137			
M12	0.156	0.261		
M23	0.105			
P1	0.035	0.059	0.036	0.060
P2	0.024		0.024	
P12	0.0209	0.0446		
P13	0.0237			
P12	0.0209	0.0402		
P23	0.0193			

90

H. Ion Implantation

Ion implantation is a process which can be used for the direct introduction of dopants to form the N^+ and P^+ regions of the N^+PP^+ solar cell. The inherent technical features of implantation relate to uniformity, reproducibility, versatility, and control. The purpose of this task was to demonstrate that uniform, high efficiency solar cells could be produced from dendritic web silicon using ion implantation junction formation techniques.

The task involved dendritic web growth and preparation at Westinghouse, shipment of the web blanks to Spire Corporation for ion implantation, cell processing completion, testing, and evaluation by Westinghouse. Actual ion implantation of the material was performed by Spire for JPL under separate contract.

A baseline for the dendritic web ion implantation process optimization had been established previously by Spire under direct Westinghouse funding. In this effort, 15 cm^2 dendritic web silicon blanks were processed into complete solar cells using standard ion implantation techniques developed for (100) Czochralski grown wafers. In this effort, Spire-processed cells, metallized with the Westinghouse contact configuration, had average efficiencies of 12.8 percent.

A second part of the baseline effort was junction formation by ion implantation and annealing at Spire followed by cell completion at Westinghouse. This task showed that ion implantation appears to be compatible with the remainder of the Westinghouse process sequence. Average cell efficiency of 12.7 percent was obtained, and this was about 1/2 percent above average efficiencies of baseline processed cells at the time. These results, obtained without process optimization, indicated the advantages of ion implantation and forms the basis for work included in this task. It was hoped that this task would produce cells whose average efficiency exceeded the current 13.5% average of baseline processed cells.

The first phase of work on this contract task involved preparation of dendritic web sheet material suitably sized for ion implantation. Accordingly, 100 pieces of dendritic web material were grown on the AESD web growth furnaces and cut

91

into 2.1 cm x 5.0 cm blanks. These blanks were shipped to JPL in November, 1982. Initial ion implantation experiments were completed on these web blanks by Spire Corporation, and the results reported in their first quarterly report*.

Due to concerns relative to cleaning procedures used prior to ion implantation, these initial results were suspect. Accordingly, a second batch of dendritic web material grown in the AESD web growth furnaces was cleaned using standard Westinghouse procedures, cut into 2.1 cm x 5.0 cm blanks, and shipped directly to Spire Corporation for further ion implantation work. The web pieces submitted were from crystals which had produced cells with efficiencies in excess of 13% using the baseline diffusion process.

Twenty-five of these blanks were returned to Westinghouse after ion implantation for processing into cells using the baseline sequence.

The performance of these cells was essentially the same as given in the Spire report in that the cells exhibited low open circuit voltages and short circuit currents.

The causes for the relatively poor performance of these cells are not known, and no further work is recommended. It is obvious that a concerted program is required to investigate ion implantation for fabrication of solar cells from dendritic web silicon.

I. Pelletized Silicon for Replenishment During Web Growth

Cost effective growth of dendritic web silicon crystals demands continuous replenishment of polycrystal silicon into the growth furnaces during crystal pulling operations to maintain equilibrium growth conditions. This replenishment is best achieved by the continuous introduction of pelletized silicon into the furnace crucible during growth operations.

---

*Quarterly Report QR-10085-01 from JPL Contract 956381.

In July 1982, a silicon shot tower which was developed for JPL by Kayex Corporation under subcontract to Union Carbide Company was transferred to this contract. The transfer was made on a "no-cost" basis to JPL. The purpose of the transfer was to facilitate an evaluation of dendritic web silicon grown from small Si pellets produced by the shot tower. This evaluation was made by processing dendritic web grown from shot into cells both at Westinghouse and at JPL.

The initial phase of this effort was completed by Kayex Corporation under Westinghouse contract. A Westinghouse engineer visited Kayex, took pictures of the shot tower, witnessed critical component disassembly operations by Kayex personnel, and obtained drawings and operational manuals. After disassembly, the unit was shipped to Westinghouse AESD in Pittsburgh.

The shot tower was then re-installed at AESD in a building capable of handling the unit's 40 foot long drop tube. Figure 12 is a photograph of the shot tower after installation. The heated zone of the device is located on the upper platform. Also visible in the forefront of the photograph is the RF power supply. The drop tube extends from the bottom of the heated zone downward to the floor of the building. The tube continues through a hole in the floor into a pit. A 10 foot extension tube was added to the lower end of the drop tower at the recommendation of Kayex personnel. Neither the bottom of the drop tube nor the shot collection basis are visible in the photograph.

After connection of water, electrical, and gas lines to the unit, shakedown operations were initiated. Several modifications, incorporated to improve controls and to reduce the operating accoustical noise level from the extremely high levels reported by Kayex-Hamco to acceptable levels, proved to be more than adequate.

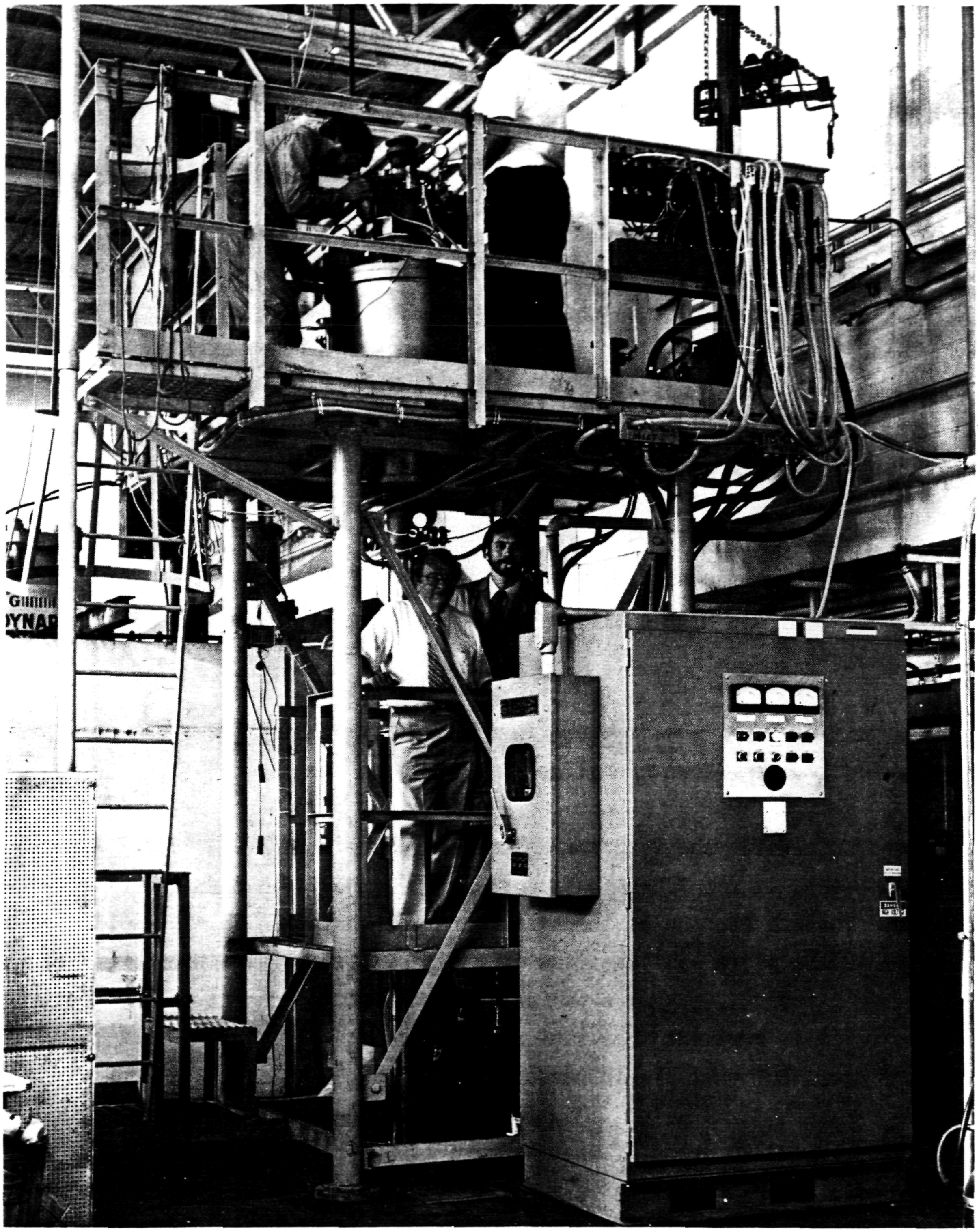

Figure 12. Silicon Pellet Shot Tower after Assembly at Westinghouse

Initial shotting run attempts were unsuccessful due to water leaks in the system or freezing of the silicon in the crucible nozzle. The following changes were made to correct conditions observed during these shakedown runs:

1. The length of the crucible nozzle was reduced to prevent silicon freezing.

2. Wherever possible, all coolant connections were moved from inside the capacitor bank to the outside. High pressure, high temperature hose was used to replace the reinforced Tygon tube previously used.

3. Helium flow was reversed so as to enter at the top of the drop tube and exit from the collection tank.

4. The operating procedures were modified to run the heat-up part of the cycle with static helium in the drop tube until shotting begins.

A Kayex test engineer who is shown in the photograph assisted and supervised in assembly and shakedown operations.

The first successful shotting run was made in late September, 1982. After shotting began, it was found to be necessary to provide a pressure drop between the furnace section of the system and the shot tube in excess of 1 psi to maintain the molten silicon flow in a steady stream. The pressure drop was maintained between 1.3 and 1.8 psi and appeared to yield shot of the proper diameter. It is apparent that shot size can be altered by manipulating the pressure drop, but only within narrow limits.

The run yielded 2350 grams of what appears to be good shot. Input material weighed 2523 grams, resulting in a net yield of 94%.

Prior to initiation of a second run, the following additional system modifications were made.

1. An argon cover gas supply and graphite wool blanket was added to the furnace area of the system to reduce heat losses, hence, power requirements.

2. Water cooling coils were added to the top of the collection drum and to the short end tube of the shot tube assembly to improve shot cooling.

3. The helium flow in the shot tube was modified so that cool gas enters at the top and bottom of the drop tube and is exhausted at the center of the tube and at the bottom of the collection tank. This produces additional cooling in the tube required to complete solidification of pellets prior to contact with the collection tank. (The initial run produced evidence that many of the pellets had not totally solidified prior to impact in the collection tank.)

4. An oxygen monitor and hygrometer were installed in the system to allow monitoring and recording of oxygen and water vapor levels prior to initiating a shotting run.

5. A Grafoil radiation shield was installed to replace the molybdenum shield in the furnace area of the shot tower, thereby eliminating potential molybdenum contamination of the silicon produced.

After completion of modifications, a second production run was made. This run produced 2325 grams of silicon shot (92% yield) made up as follows: 530 grams over 2 mm diameter; 1450 grams from 1 to 2 mm dia.; 215 grams from .6 to 1 mm dia.; and 130 grams less than .6 mm dia. During the run it became obvious that the operator can impose a considerable influence on shot size by varying the pressure drop across the furnace chamber and the shot tube receiver section.

96

While the product of this run appeared acceptable, further system changes were implemented to assure shotting at a lower temperature. Data indicated that the nozzle temperature at the exit end was significantly lower than the temperature of the melt and that the silicon coming through the orifice was too cold for optimum flow. Thus the crucible nozzle was further reduced in length so that it ends inside the cavity provided in the susceptor, rather than being flush with it as in the original configuration.

A significant operational modification was also incorporated. To improve shot purity, the system was evacuated to .07 psi before backfilling with gas. This not only reduces the amount of free oxygen in the system but also reduces the water content. To extend the anti-oxidant protection, the system was filled with argon before removing the furnace lid.

A sufficient quantity of high purity, 0.6 to 2 mm, silicon shot was then produced in the shot tower to initiate growth runs in which silicon shot is automatically introduced into the melt as dendritic web crystals are being withdrawn from web growth furnaces at AESD. These growth runs, made during the last two weeks of November, were to evaluate the response of two different furnace lid and shield configurations to the feeding mode of operation, to acquaint the web growers with the set-up and operation of the furnaces in the feeding mode, and to identify areas for further development in order to consistently sustain continuous crystal growth.

Eight web growth furnace runs were made in December, 1982, to evaluate the silicon shot produced in the shot tower installed at AESD. In general, several crystals were grown from the melts before the shot was introduced. Crystals were grown during the remainder of the run using AESD silicon shot as the replenishment material. With this procedure, the first web crystals grown were composed of the standard semiconductor grade silicon. The later web crystals, due to replenishment, contained increasingly more silicon melted from shot material.

These web strips were then processed into cells using the Westinghouse baseline process sequence, and data from these cells were anlayzed. Both 1.6 x 9.8 cm and 2.0 x 9.8 cm cells were produced in these runs.

The average efficiencies of cells made from web grown from the initial melt and after the introduction of shot into the melt as replenishment material are given in Table 39. The small differences in these averages are believed due to the inclusion of this web in many processing batches (some of which were part of ongoing experiments). A normalized distribution of cell efficiencies is shown in Figure 13. Considering the small number of cells in this sample, this distribution is not significantly different than that obtained in normal processing (including experimental batches). Although a larger data base is required, it is tentatively concluded that the material made in the shot tower installed at AESD does not degrade cell properties; and the shot produced qualify as silicon melt replenishment material for solar cell production.

During the silicon shot evaluation program, Westinghouse was approached by a potential supplier of silicon pellets manufactured using an approach that did not employ a shot tower. The pellet sizes appeared equally applicable to the pellet feed mechanism currently in use on several of the pre-pilot line furnaces. A significant aspect of this manufacturer's material is that it can be procured in large quantities at a much lower price than semiconductor grade silicon. Since more expensive commercially available polycrystalline boules must first be sliced to smaller sizes and then used as input to the shot tower, the potential cost savings is very large.

To allow an evaluation of the material, a sufficiently large sample was left by the supplier to make numerous web growth runs. Web grown using some of the material has been processed into cells that can now be compared to cells produced from web grown from the standard silicon charge. For this evaluation, several web crystals were grown in the furnace melts prior to the introduction of pellets. Crystals were then grown during the remainder of the furnace runs using the pellets as replenishment material. With this procedure, the first web crystals grown were composed of the standard semiconductor grade silicon.

TABLE 39

AVERAGE EFFICIENCIES OF CELLS GROWN IN RUNS USING AESD SILICON SHOT AS REPLENISHMENT MATERIAL

Condition	Cell Size (cm x cm)	No. of Cells	Average Efficiency, %
Initial Melt	1.6 x 9.8	25	13.8 ±1.7
After Replenishment	1.6 x 9.8	73	13.2 ±2.2
Initial Melt	2.0 x 9.8	34	12.9 ±1.9
After Replenishment	2.0 x 9.8	62	12.7 ±2.0

99

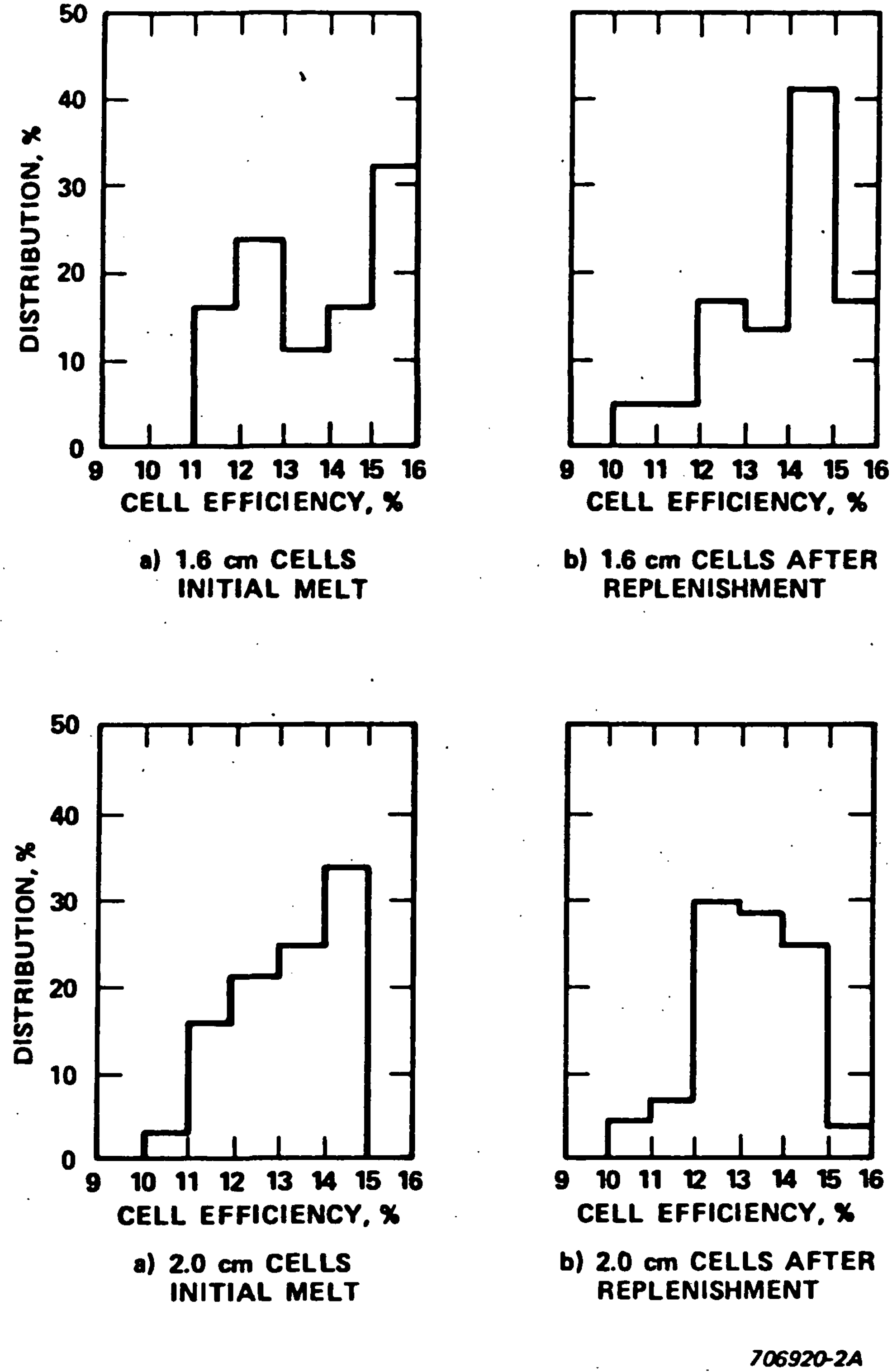

Figure 13. Normalized Efficiency Distribution of Cells Produced from Web Grown from Runs using AESD Silicon Shot Replenishment

The later web crystals, due to replenishment, contained an increasing fraction of silicon melted from the pellets. The crystals were then processed into solar cells using standard procedures.

The average efficiencies of cells made from web grown from the initial melt and after the introduction of pellets into the melt as replenishment material are given in Table 40. This web was included in many processing batches (some of which were part of ongoing experiments) and provided a relatively small population of cells. Although a larger data base is required, it is tentatively concluded that this replenishment material is of excellent quality. Further use and evaluation of this material is continuing at Westinghouse.

TABLE 40

AVERAGE EFFICIENCIES OF CELLS GROWN IN RUNS USING OUTSIDE VENDOR SILICON PELLETS AS REPLENISHMENT MATERIAL

Condition	Cell Size (cm x cm)	No. of Cells	Average Efficiency, %
Initial Melt	1.6 x 9.8	17	12.6 ±2.4
After Replenishment	1.6 x 9.8	48	13.6 ±1.9
Initial Melt	2.0 x 9.8	21	12.2 ±2.1
After Replenishment	2.0 x 9.8	43	13.2 ±1.5

9950-892

A P P E N D I X   A

SUMMARY TECHNICAL REPORT

103

9930-322

DRL No. 157
DRD No. SE-3
Item #5

TME 3149
DOE/JPL 955909-82/1
Distribution Category UC-63

LOW COST SOLAR ARRAY PROJECT

PROCESS RESEARCH TASK

A MODULE EXPERIMENTAL PROCESS SYSTEM DEVELOPMENT UNIT (MEPSDU)

SUMMARY TECHNICAL REPORT

November 26, 1980 to February 10, 1982

CONTRACT NO. 955909

The JPL Low-Cost Silicon Array Project is sponsored by the U. S. Department of Energy and forms part of the Solar Photovoltaic Conversion Program to initiate a major effort toward the development of low-cost solar arrays. This work was performed for the Jet Propulsion Laboratory, California Institute of Technology, by agreement between NASA and DOE.

Advanced Energy Systems Division
WESTINGHOUSE ELECTRIC CORPORATION
P. O. Box 10864
Pittsburgh, Pennsylvania 15236

4

LOW COST SOLAR ARRAY PROJECT
Production Process and Equipment Task

A MODULE EXPERIMENTAL PROCESS SYSTEM DEVELOPMENT UNIT (MEPSDU)

SUMMARY TECHNICAL REPORT

November 26, 1980 to February 10, 1982

Contract No. 955909

The JPL Low-Cost Silicon Array Project is sponsored by the U. S. Department of Energy and forms part of the Solar Photovoltaic Conversion Program to initiate a major effort toward the development of low-cost solar arrays. This work was performed for the Jet Propulsion Laboratory, California Institute of Technology, by agreement between NASA and DOE.

Approved:

C. M. Rose

C. M. Rose, Project Manager
Photovoltaic Components

Advanced Energy Systems Division
WESTINGHOUSE ELECTRIC CORPORATION
P. O. Box 10864
Pittsburgh, Pennsylvania 15236

TECHNICAL CONTENT STATEMENT

9950-300

TABLE OF CONTENTS

				Page
I.	CONTRACT GOALS AND OBJECTIVES			1
II.	SUMMARY			2
III.	SELECTION OF INPUT SHEET MATERIAL			5
IV.	MEPSDU Module			11
	A.	Module Design		11
		1.	Mechanical	11
		2.	Interface	14
		3.	Electrical Design	16
	B.	Module Performance Evaluation		24
	C.	Environmental Testing		31
		1.	Hailstone Impact Tests	31
		2.	Wind Load Testing	31
		3.	Thermal and Humidity Cyclic Tests	32
		4.	Loss of Cell Contact Pad Electrical Connection	41
		5.	Cell Shading Tests	44
V.	PROCESS SEQUENCE DESIGN			48
	A.	Baseline Process Sequence		48
	B.	Alternate Process Sequence Steps		55
		1.	Alternate Metallization Procedures	55
		2.	Dry Processing Experiments	57
		3.	Liquid Precursor Films for Diffusion Masks	61
		4.	Liquid Dopant Diffusant Studies	62
VI.	MEPSDU Design			67
	A.	General		67
	B.	Pre-Diffusion Cleaning		67
	C.	Junction Formation Station		68
	D.	Antireflective (AR) and Photoresist (PR) Application Stations		69
	E.	Expose/Develop/Etch Station		71
	F.	Metallization Box Coater		72
	G.	Metal Rejection/Plating Station		74
	H.	Cell Separation Station		76
	I.	Cell/Module Test Stations		80

107

9950-893

TABLE OF CONTENTS (Continued)

		Page
VII.	KULICKE AND SOFFA SUBCONTRACT	82
	A. General	82
	B. Bonder	84
	C. Cassette Unload Station	89
	D. Bond Stations	89
	E. String Conveyor	92
	F. Control System	93
	G. Design Review	94
VIII.	ECONOMIC ANALYSES	96
	A. Background	96
	B. Assumptions Used in SAMICS Cost Analyses	98
	C. Results and Conclusions	99
IX.	DOCUMENTATION	104

108

9950-392

LIST OF TABLES

Page

1. A Comparison of Candidate Sheet Forms for MEPSDU. 6
2. Specification for Polycrystalline Silicon to be Used in Westinghouse MEPSDU Sheet Material 10
3. MEPSDU Dendritic Web Input Sheet Material Specification (Preliminary). 11
4. Major Westinghouse MEPSDU Module Design Innovations 13
5. Calculated MEPSDU Module Performance Parameters 29
6. Layup of Small Modules Used for Environmental Testing 33
7. Pre- and Post-Lamination Measurements of Cell String Characteristics. 37
8. Measurements Made on Thermally Cycled Test Modules. 39
9. Measurements Made on Environmental Test Modules 40
10. Output Power from Solar Cell as Function of Interconnect Pads Contacted 43
11. Plasma Etching of Raw Web 60
12. Comparison of Cells Produced Using the Baseline Process (Gaseous Diffusion) and Liquid Dopants 64
13. Metallization Box Coater Specification Highlights 73
14. Rejection/Plating Station Treatment Cycle 75
15. Novel Features of the Westinghouse MEPSDU Facility Laser Scribe . . 78
16. MEPSDU Laser Scribe Automatic Alignment System Features 79
17. Laser Scribe Time Budgets 81
18. Processes and Referents Used in SAMICS Cost Analyses. 97
19. SAMICS Cost Analysis (1MW/yr Production Facility) 100
20. SAMICS Cost Analysis (25 MW/yr Production Facility) 102
21. SAMICS Cost Analysis. 103
22. MEPSDU Programmable Documentation Submittal Status. 105

109

LIST OF FIGURES

Page

1. Westinghouse Dendritic Web being Removed from the Dendritic Web Growth Furnace. 7
2. Westinghouse MEPSDU Module Assembly Drawing. 12
3. Prototype MEPSDU Module Fabricated in Westinghouse Pre-Pilot Facility. 15
4. Glass Panelled Wall Utilizing Structural Adhesive Supports 17
5. Geometry of Ultrasonic Bonds, Dark Side. 19
6. Cell Interconnection Geometry. 21
7. Layup Materials and Dimensions of the Westinghouse MEPSDU Module . . 26
8. Calculated MEPSDU Module V_{oc} and I_{sc} as Functions of Ambient Temperature 27
9. Calculated MEPSDU Module Power and Efficiency as Functions of Ambient Temperature 28
10. I-V Test Curve of Prototype MEPSDU Module. 30
11. Environmental Test Module G-2 (10 cm x 9 cm) 35
12. Environmental Test Modules in Humidity Test Fixture. 36
13. Environmental Test Data from Minimodule G-2. 42
14. Test System Used for Cell Shading Tests. 45
15. Shadowed Cell Heating Effects under Module Short Circuit Conditions. 46
16. Westinghouse MEPSDU Overall Process Sequence 49
17. Westinghouse MEPSDU Baseline Process Sequence Flow Chart 50
18. Westinghouse MEPSDU Module Assembly Flow Chart 53
19. Meniscus Coating of Precursor Fluids to Dendritic Web Silicon. . . . 66
20. Automated Laser Scribe 77
21. Westinghouse MEPSDU Automated Cell Interconnect Station. 83
22. Rotary Ultrasonic Seam Bonding 85
23. Rolling Spot Ultrasonic Bonding. 86
24. Bonding Mechanism for First Bond Station 88
25. Mockup of Cassette Unload Station. 90
26. Interconnect Feed Station (Minus Ribbon Transfer Mechanism). 91
27. Interconnect Station Control Structure 95

I. CONTRACT GOALS AND OBJECTIVES

The objective of this contract, as it was originally written, was to determine technical feasibility of the production of photovoltaic modules designed to meet all environmental specifications described in JPL Document 5101-138, fabricated using single crystal silicon dendritic web sheet material, and meeting JPL's 1986 production cost goals of 70¢/peak watt (1980$). This determination of technical feasibility was to be accomplished by:

A. The design of a flat plate photovoltaic module utilizing dendritic web sheet material and meeting all environmental specifications contained in JPL Document 5101-138,

B. The selection, design, and implementation of a solar cell processing and photovoltaic assembly sequence for fabricating modules of the specified design (Item A above) in a Module Experimental Process System Development Unit (MEPSDU),

C. Performance of technical feasibility experiments in which a sufficient number of modules were to be produced in the MEPSDU facility to allow assessment of production costs,

D. Passing of acceptance and qualification tests by modules produced during the demonstration runs, and

E. Projection of a 1986 module FOB mass production cost in a fully automated, 25 MW/yr capacity facility using the MEPSDU process sequence as calculated by SAMICS using cost data generated during completion of the demonstration runs (Item C above).

II. SUMMARY

Work on the Westinghouse MEPSDU contract was initiated on November 26, 1980. This report summarizes all technical progress made on the contract from the initiation date until a stop work order was received from JPL on February 10, 1982. In the stop work order, the contract was restructured from a technical readiness demonstration program to an investigation of high-risk, high-payoff research areas associated with the Westinghouse process for producing photovoltaic modules using non-CZ sheet material. It was emphasized in the JPL stop work order that the "restructuring in no way reflects adversely upon the contractual performance of Westinghouse, but is intended to comply with the Department of Energy guidelines for funding high-risk, high-payoff research projects."

Prior to the stop work order, two contract modifications had been effected by JPL which reduced program expenditure rates from those of the original contract. However, in all cases the contract goals and objectives as presented in Section I of this report remained unchanged.

The first major program milestone, Preliminary Design Review (PDR), was met as scheduled with a formal presentation at JPL on March 4 and 5, 1981. This was preceded by the submittal of the Preliminary Design Review Data Package consisting of:

- A Preliminary Specification for MEPSDU Input Sheet Material (Dendritic Web Silicon),

- A MEPSDU Module Preliminary Design Layout Drawing and all associated detail drawings,

- Analysis of the performance of the MEPSDU module over a range of operating conditions,

- Definition of all steps in the Baseline Process Sequence,

- Equipment Specifications for all long-lead time items in the MEPSDU,

- Preliminary design of the cassette unload element and interconnect feed elements of the automated cell interconnect station, and

- The Preliminary Quality Assurance Plan.

The second major program milestone, Final MEPSDU Module Design Review (MDR), was a formal presentation at JPL on July 14, 1981. This was preceded by the Design Review Data Package submittal consisting of:

- Copies of viewgraph materials,
- All module drawings,
- The module materials selection sheet,
- Performance predictions, and
- Module manufacturing flow information.

The module design matured substantially between the PDR and the MDR. Many of the improvements stemmed from comments received from JPL personnel at the PDR. The most significant improvement was the deletion of the module frame in favor of a "frameless" design which provides a substantially improved cell packing factor, hence overall efficiency. Also, a modification was made in the cell series/parallel electrical interconnect configuration to eliminate potential shaded cell damage resulting from operation into a short circuit.

Through work on this contract, a Baseline Process Sequence was identified for the fabrication of modules using the selected dendritic web sheet material. This baseline process was incorporated in the Westinghouse Pre-Pilot Photovoltaic Module Production Facility. Although this facility is a non-automated, limited volume facility, prototype modules of the MEPSDU design were fabricated using the baseline process sequence. (The assembly work was completed as part of a non-Government funded project.) Subsequently, extensive tests on full-size and mini-size prototype modules verified compliance of the basic layup configuration with environmental specifications of JPL Document 5101-138. In addition,

113

performance data from prototype modules fabricated using the baseline process sequence demonstrated that an overall module efficiency level of 12% projected at the beginning of the contract was achieved.

Economic evaluations of the Westinghouse Baseline Process Sequence have been completed, using formal Solar Array Manufacturing Industry Costing Standards (SAMICS) techniques. These evaluations were performed in close coordination with JPL personnel who completed similar but parallel economic analyses of the Westinghouse MEPSDU process sequence. Results of these analyses have verified that the process sequence defined in this program for manufacturing photovoltaic modules from dendritic web silicon can meet the JPL long range cost objectives of 70¢/peak watt (1980$) in a fully automated production facility.

When the Westinghouse MEPSDU contract stop work order was received from JPL, all technical and documentation tasks were on the schedule defined in the contract program plan. Referring to the contract goals and objectives listed in Section I of this report, Item A (module design) was complete; and Item B (MEPSDU facility design) was essentially complete.

The baseline process sequence had been established and verified, and nearly all equipment required for a 1 MW/yr demonstration facility had been formally specified. Some long lead equipment (i.e., laser scribe, semi-automated cell and module test equipment, and automated cell interconnect station) had been placed on order.

Based on the success of this program, Westinghouse Electric Corporation, which had previously committed to procure the capital equipment required for the 1 MW/yr demonstration facility, has decided to complete the design, procurement, and installation tasks with corporate funding. JPL funding will continue for two highly developmental, but promising, research and development tasks that could result in substantial improvement in the cost effectiveness of the baseline process sequence.

MEPSDU project costs were consistent with budget projections at the time of the stop work order issuance. The remaining research tasks are being completed on a significantly reduced budget level.

III. SELECTION OF INPUT SHEET MATERIAL

The first technical milestone of the MEPSDU contract was the selection of input sheet material to be used for the manufacture of solar cells produced in the MEPSDU facility.

A study of the significant parameters of all candidate sheet forms was made, and Table 1 summarizes the results of this analysis. As is shown in Table 1, each of the sheet input forms has favorable characteristics. However, the Westinghouse dendritic web excels in nearly every category and is the clear-cut front runner in providing the high efficiency, high reliability, and low cost demanded by the low cost solar array program objectives. Thus, single crystal dendritic web silicon was selected as the Westinghouse MEPSDU input sheet material.

Figure 1 shows a length of dendritic web silicon in the as-grown condition being removed from a growth furnace at the Westinghouse pre-pilot facility. The shape of the dendritic web is determined by a combination of crystallographic and surface tension forces as it is formed from the molten silicon. The absence of any die material precludes contamination and die material inclusions which are known problems with other ribbon growth techniques. Cells fabricated on dendritic web have shown efficiencies comparable to cells fabricated on Czochralski wafers (15 to 17%). The process conserves expensive silicon since the as-grown material is thin - 110 to 170 μm - and the smooth surface does not require extensive treatment prior to cell fabrication.

The natural rectangular shape of cells fabricated on dendritic web permits high module packing factors which contributes to high module efficiency.

Investigations in the production and application of photovoltaic modules have confirmed that high module efficiency has many benefits ranging from decreased module encapsulation costs to significant balance of system and installation cost savings. In the area of module fabrication alone, a cost saving of six cents per watt is associated with each 1% increase in module efficiency. High quality starting material is essential to producing high efficiency cells and

TABLE 1

A COMPARISON OF CANDIDATE SHEET FORMS FOR MEPSDU

Parameter	Westinghouse Dendritic Web	EFG	CZ	HEM	SEMIX
Demonstrated Cell Efficiency	High	Medium	High	Medium	Medium
Module Efficiency	12-16%	7-10%	8-16%	8-11%	7-10%
Cell Interconnection Redundancy	High	High	Low	Medium	High
Growth Rate	Medium	High	Medium	High	High
Crystal Quality	Single	Poly	Single	Poly	Poly
Module Packing Fraction	High	High	Low	Medium	High
Silicon Utilization	3 kg/kw	8 kg/kw	12 kg/kw	12 kg/kw	8 kg/kw
Slicing Requirement	No	No	Yes	Yes	Yes
SAMICS Cost Catalog	$30/m^2$	$27/m^2$	$47/m^2$	$40/m^2$	

EFG - Edge Defined Film Fed Growth (Mobil Tyco)
Cz - Czochralski Wafers
HEM - Heat Exchanger Method (Crystal Systems)

116

ORIGINAL PAGE
BLACK AND WHITE PHOTOGRAPH

Figure 1. Westinghouse Dendritic Web being Removed from the Dendritic Web Growth Furnace

17

modules. Dendritic web is high quality, single crystal silicon, and has already been used in fabricating photovoltaic cells with efficiencies greater than 15% and modules with efficiencies greater than 12%.

A preliminary material specification for the polycrystalline silicon used as a feed stock in the dendritic web furnaces has been prepared and is shown in Table 2. Table 3 shows the preliminary material specification for the dendritic web silicon sheet input.

118

TABLE 2

SPECIFICATION FOR POLYCRYSTALLINE SILICON TO BE USED
IN WESTINGHOUSE MEPSDU SHEET MATERIAL

- Boule to be 5-10 cm in diameter
- Random lengths acceptable, but length must be in excess of 15 cm
- Less than 0.3 PPBA (parts per billion atoms) boron concentration
- Less than 0.5 PPBA phosphorous concentration
- Less than 10 PPBA aluminum concentration
- Total of all other metals less than 5 PPBA concentration

TABLE 3

MEPSDU DENDRITIC WEB INPUT SHEET MATERIAL SPECIFICATION
(PRELIMINARY)

I. Chemical

A. Single crystal silicon with [111] web surface orientation

B. P-type material with boron based dopant providing a resistivity in the range 3 to 12 ohm cm

II. Physical

A. Thickness of web: 140 ±30 μm

B. Width of web: Equal to or greater than 2.55 cm excluding dendrites

C. Length* of web: 43 ±.5 cm

D. Surface striations across web not to exceed 1 μm height as measured by a thickness monitor such as "Taly-Step" or "Data-Trak"

E. Etch pit density (determined after 5 min. Sirtl etch) not to exceed $3 \times 10^4/cm^2$

F. Flatness: No twist or bow as determined by visual inspection

---

*Shorter lengths are acceptable but will produce less than 4 cells/strip, thus reducing yield of all cell processing operations.

120

IV. MEPSDU MODULE

A. Module Design

1. Mechanical

The second technical milestone of the MEPSDU contract was the design of a flat plate photovoltaic module meeting all environmental specifications contained in JPL Document 5101-138.

The MEPSDU Preliminary Design Review was held at JPL on March 4 and 5, 1981. A preliminary module design was presented at that time. The Prototype Module Design Review was conducted at JPL on July 14, 1981. In general, the design was well received. Some concern was expressed by JPL personnel for the unprotected edges of the tempered glass superstrate in the Westinghouse frameless module design. Resolution of this concern was deferred pending completion of hail impact tests which were conducted after the design review and which confirmed that the glass could withstand corner impacts without damage. These and other environmental tests are discussed below.

The assembly drawing of the prototype Westinghouse MEPSDU module (Westinghouse Drawing 712J927) is shown in Figure 2. The most significant innovations included in the design are summarized in Table 4.

The MEPSDU module assembly drawing specifies a superstrate of 1/8 inch thick tempered glass with an iron content of less than 0.03%. With this low iron content, the solar transmittance in the 0.4 to 1.2 μm wavelength range is 91%. This is a significant improvement over standard tempered glass which transmits less than 87%. The remaining loss in transmittance is mainly (≈80-90%) a reflection loss.

Working with a vendor after completion of the module assembly drawing, an even greater transmittance was achieved through a proprietary surface treatment. This treatment is based on work initiated on an ERDA program[1] and improved by later industry studies[2]. The treatment consists of etching the glass in

---

[1] Phase II Final Report, COO-2930-12 to ERDA from Honeywell Corporation.
[2] Zuel Corporation, St. Paul, Minnesota.

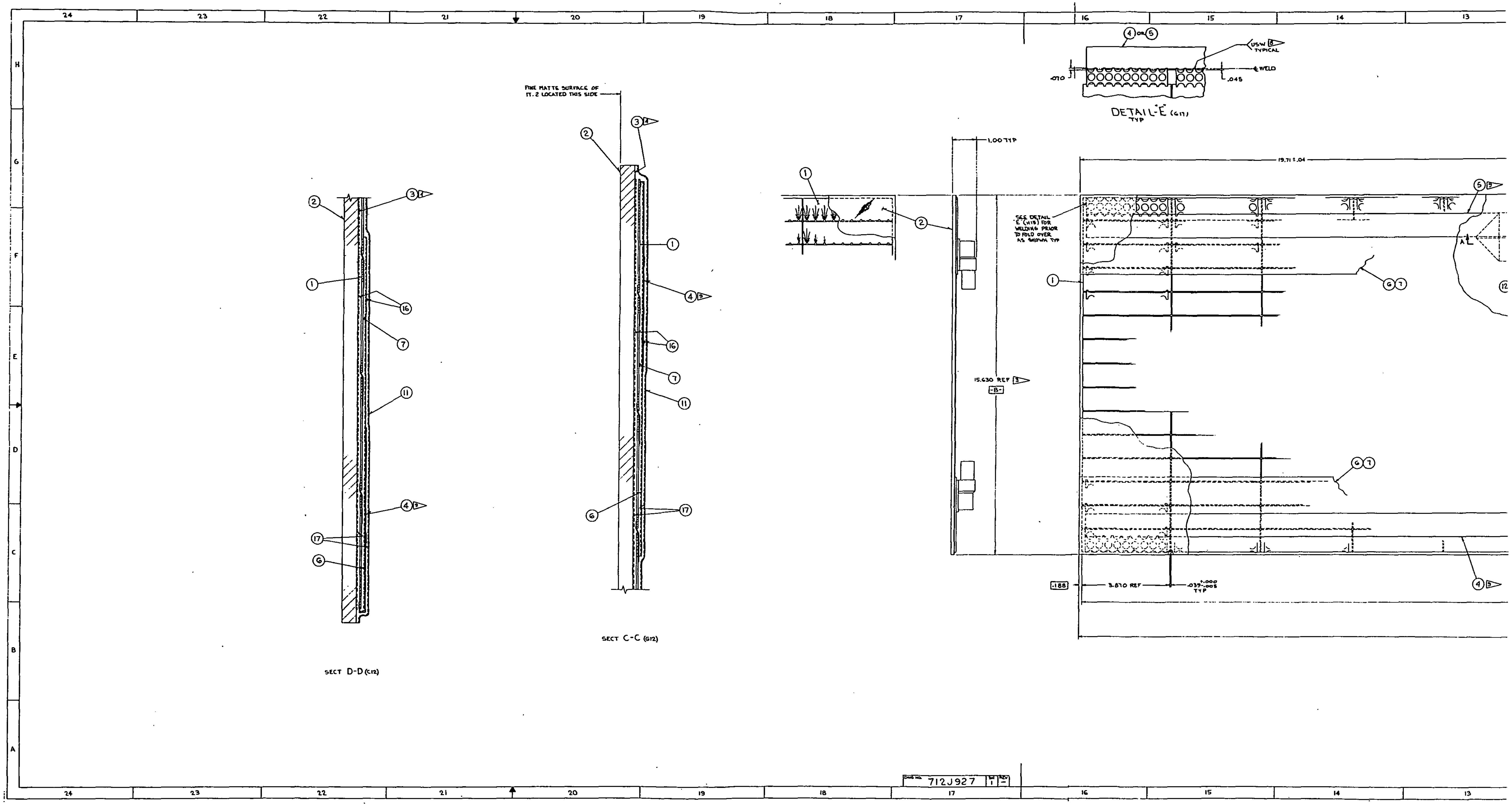
FINE MATTE SURFACE OF IT. 2 LOCATED THIS SIDE
DETAIL E (G11) TYP
USW TYPICAL
WELD
.045
1.00 TYP
19.71 ±.04
SEE DETAIL E (H18) FOR WELDING PRIOR TO FOLD OVER AS SHOWN TYP
15.630 REF
-B-
.188
3.870 REF
SECT C-C (G12)
SECT D-D (C12)
712J927

12'

9950-892

FOLDOUT FRAME 1.

FOLDOUT FRAME 2.

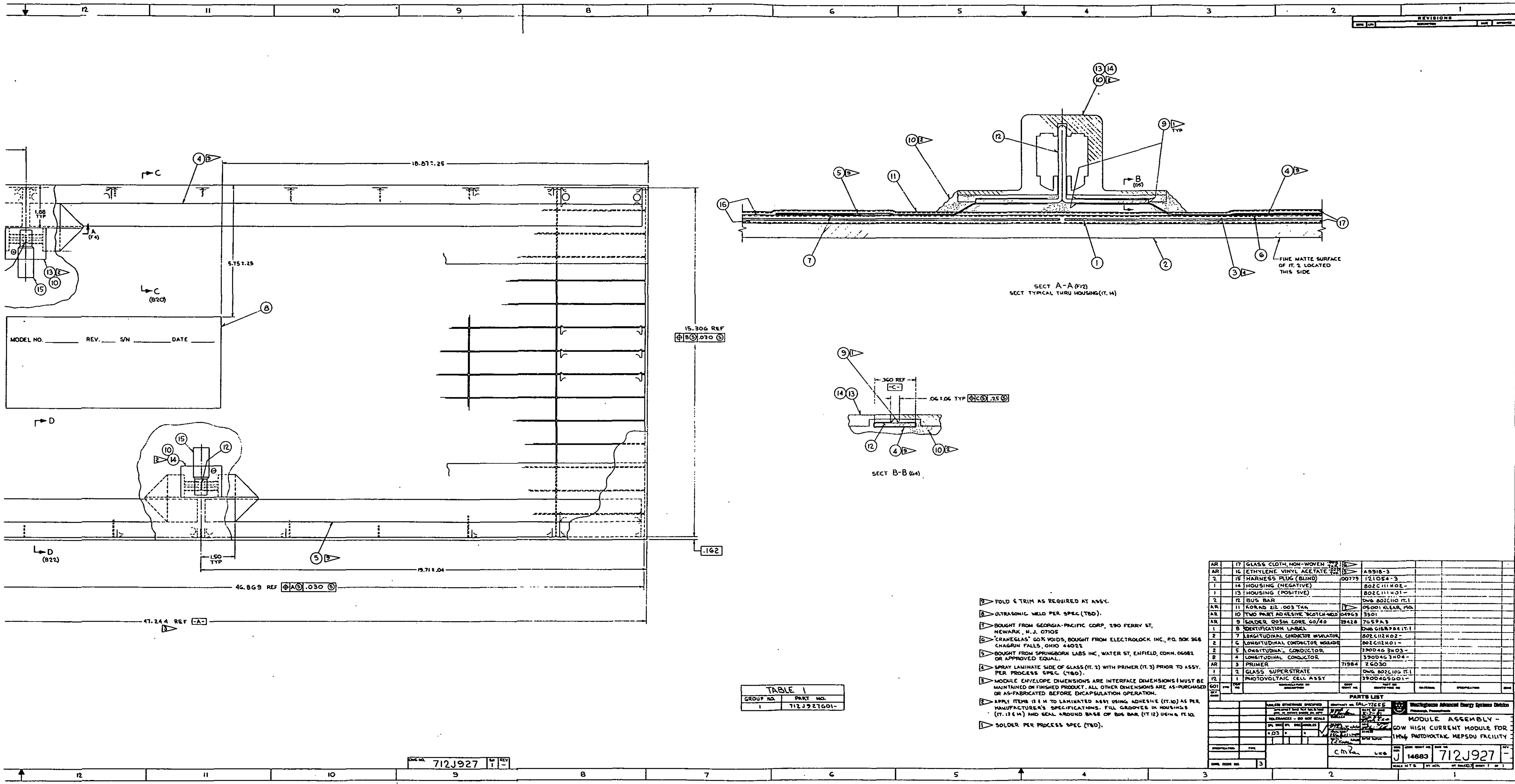

Figure 2. Westinghouse MEPSDU Module Assembly Drawing

TABLE 4

MAJOR WESTINGHOUSE MEPSDU MODULE DESIGN INNOVATIONS

- Use of dendritic web single-crystal silicon
- Use of high aspect ratio (3.9:1) rectangular photovoltaic cells
- Tempered glass superstrate
- Antireflectance treated front glass surface
- Frameless construction
- Elimination of solder joints inside the encapsulation envelope
- High cell interconnect redundancy
- 12 parallel cell circuits

a controlled manner to produce micro-pores on the surface (10-30Å across) which act as an antireflective coating. The index of refraction of this surface matches the glass-air interface and reduces reflection losses.

Samples of this glass with this surface treatment have been on test at the Los Alamos Test Center for over 12 months, and no degradation in transmittance has been noted.

Several pieces of module sized glass (nominal 16" x 48"), prepared with the antireflective surface treatment, were procured for test purposes. The treated surfaces show a bluish tint as would be noted with a very thin antireflective coating. Tests indicate that this treated glass increases the transmittance from 91% to 96%. On a high efficiency module (≈12%), this increased transmittance translates into about 0.5% absolute increase in module efficiency.

Several laminations were carried out using this glass without difficulty. Subsequently, all modules fabricated on the Westinghouse pre-pilot facility have incorporated this glass treatment.

Figure 3 is a photograph of one of the first prototype MEPSDU modules fabricated in the Westinghouse Pre-Pilot Facility. Visible in the photograph is the 12 x 15 array of solar cells. Each cell is nominally 1 in. (2.5 cm) by 4 in. (9.83 cm), and the nominal module dimensions are 16 in. (39.7 cm) by 48 in. (119.9 cm). Nominal output power of the module is 55 watts (peak).

2. Interface

Perhaps the most significant innovation of the Westinghouse module is the elimination of a module frame. This design allows placement of photovoltaic cells under a much larger percentage of the superstrate surface than is possible when using a frame. The modules are to be attached to and supported from the array structure, test rack, or roof structure through a structural adhesive system. The adhesive system consists of two components: strips or patches of double-faced polyurethane adhesive tape and a silicone adhesive/sealant. The tape provides immediate low strength attachment and stand-off of the module to the

125

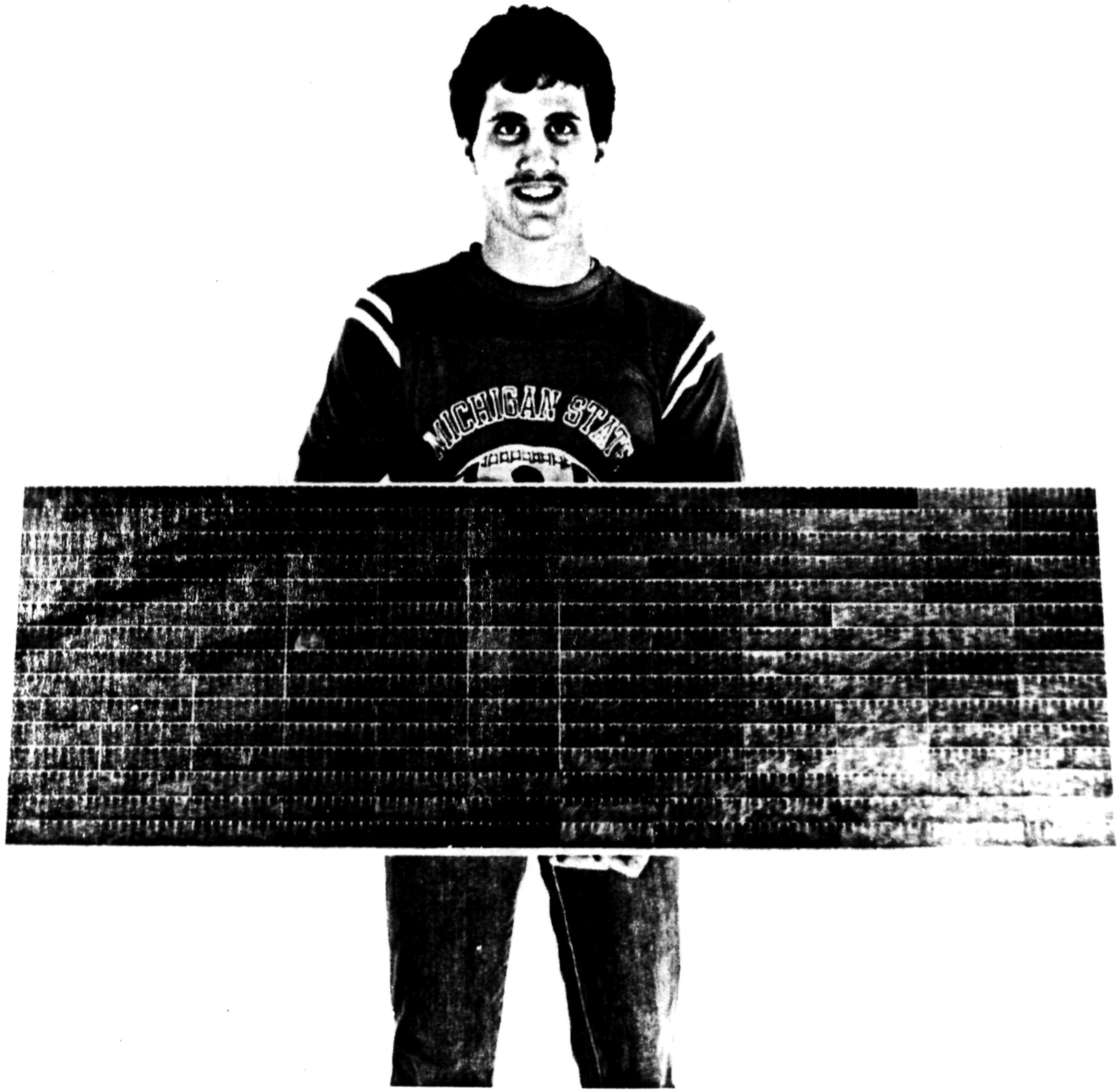

Figure 3. Prototype MEPSDU Module Fabricated in Westinghouse Pre-Pilot Facility

support structure. The adhesive/sealant fills the gaps between the support structure and module and provides a high strength intermediate modulus attachment when cured under ambient conditions. A significant feature of this support system is that application of the adhesive is a field operation rather than a shop operation. No silicones will be present in the shop environment prior to lamination, and the lamination operation is completed several days to several weeks before the module encounters the silicone adhesive.

Although this support system has never been used (to our knowledge) on photovoltaic module arrays, it has been used successfully in architectural applications. One installation in the Pittsburgh area is shown in Figure 4. These glass panels are much larger and heavier than the modules (approximately 5 x 7 feet, 1/4 inch thick) and are supported only by the two-component adhesive system. Most of the panels are vertical, but the top course is inclined approximately 15° back from the vertical while the bottom course is inclined the same amount in the opposite sense so that these panels are suspended. This installation was designed to survive an 80 mph wind. This particular installation is four years old and has no indications of damage from wind, winter temperatures as low as -20°F, summer temperatures up to 100°F, and severe rain and snow storms.

3. Electrical Design

A second important design innovation is the use of twelve parallel strings of fifteen series connected cells. This is a much higher number of parallel connected strings that is commonly found in photovoltaic modules. This arrangement provides two significant advantages:

- If any single cell becomes a nonconducting cell because of cracking, connection separation, or other open circuit failure, the output of only one series out of twelve is lost. With this arrangement and under the cell failure conditions specified, the module output is reduced only 8.33%. This clearly satisfies the specification of JPL Document 5101-138 which calls for the module output to be reduced no more than 10% under these conditions.

Figure 4. Glass Panelled Wall Utilizing Structural Adhesive Supports

- If any single cell becomes a nonconducting cell because of shading, the potential available to force current through it in its high resistance condition is that produced by only 14 cells. Calculations and tests described below verified that one shaded cell in a series of 15 will survive short circuit operation indefinitely without damage. This design eliminates the need for incorporation of costly blocking diodes to prevent cell damage during short circuit/shaded operation. These diodes have been found to have been the cause of some module field failures.

The Westinghouse MEPSDU module is unique in its approach to the electrical interconnection of cells. Each cell has a front surface grid pattern that collects current and directs it to eight .040" x .060" copper interconnect pads evenly spaced near the edge of the long cell dimension. Cell-to-cell interconnection is achieved by bonding .0015 inch thick aluminum foil with circular punched-out holes to the interconnect pads on the front surface of each cell and to the metallized back (dark) side of the adjacent cell. The geometry of the interconnection scheme is shown in Figure 5.

Thus, there are eight individual bonds made to each side of each individual cell providing a higher degree of redundancy than is found in any other photovoltaic module design. Since interconnect failure has been found to be a major cause of module field failures, this redundancy is felt to be highly desirable.

Because of the large number of bonds required in the Westinghouse design, a high speed bonding technique is required. For this reason, an ultrasonic bonding scheme was developed to replace the standard reflow solder joining technique. The ultrasonic bonding technique eliminates cell heating during the bond operation, eliminates flux application and removal requirements and provides substantially improved mechanical and electrical bonds. Automation of the bonding operation is described in a separate section of this report.

The necessity for (or the desirability of) a strain relief, such as an S-bend, in the aluminum electrical interconnections between photovoltaic cells has

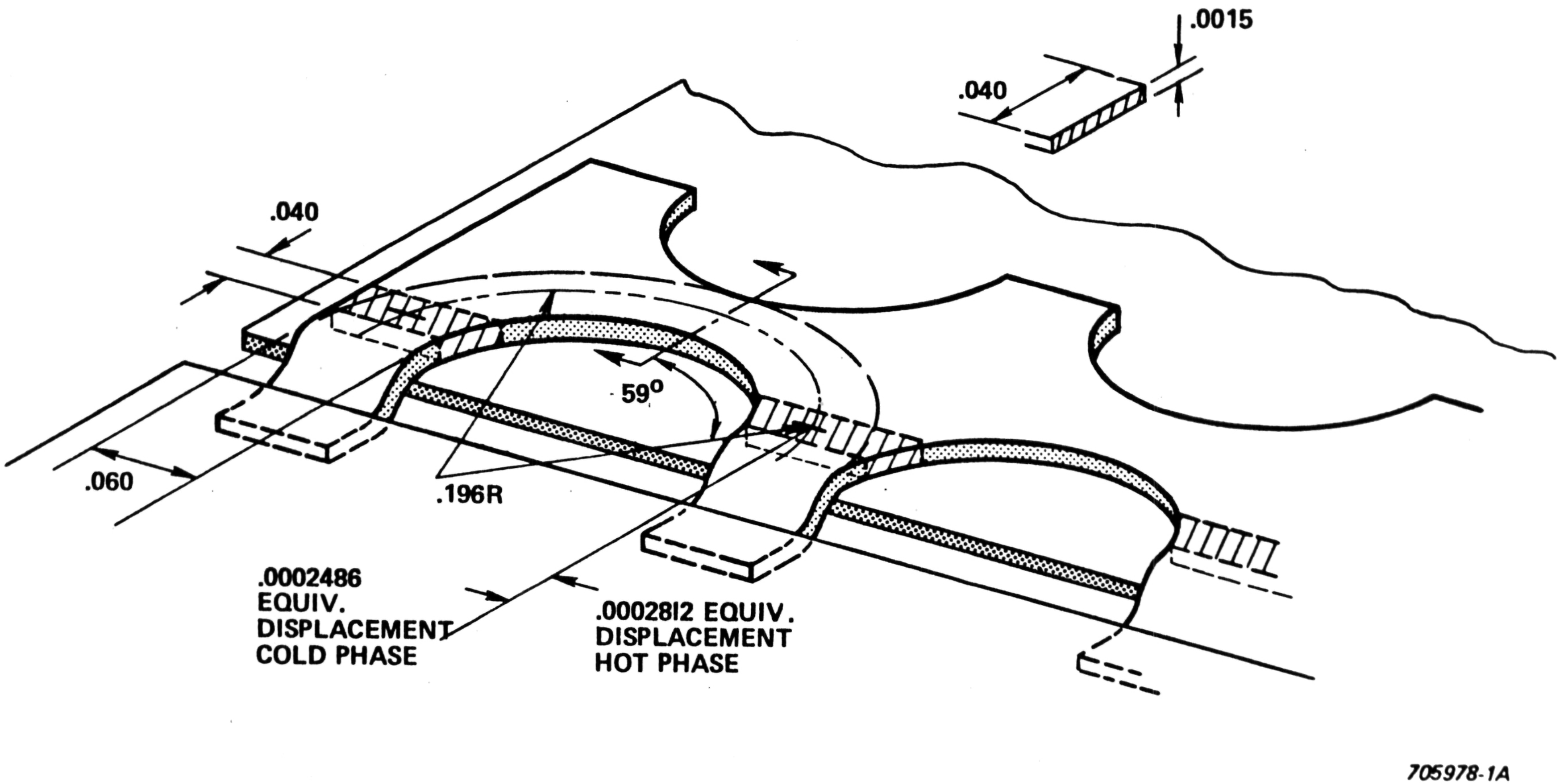

Figure 5. Geometry of Ultrasonic Bonds, Dark Side

been a concern often expressed during discussions of the Westinghouse module design. This problem has been examined; and the conclusion of the engineering analysis is that a strain relief is not necessary, and because of the cost of producing it, is not desirable. This conclusion is based upon the following logic:

- The simplified geometry of the interconnection is as shown in Figure 6.

- At some temperature below the lamination temperature of the module (150°C), the ethylene vinyl acetate (EVA) matrix "freezes," i.e., permitting no further relative movement of the unstressed components. This temperature is conservatively assumed to be 90°C, so that stress calculations can be related directly to the thermal cycling of the module between -40 and +90°C. The actual immobilization temperature is probably nearer 64°C, the softening point of EVA, which would reduce the actual thermal strains.

- The coefficients of thermal expansion of the materials involved have the following values:

  soda-lime glass - 8.46×10^{-6}/°C
  aluminum - 23.6×10^{-6}/°C
  silicon - 2.9 to 7.4×10^{-6}/°C; the value 7.4×10^{-6} was used in this analysis because it is the less optimistic assumption

- For a cell in a series string with neighbors on both sides, it is assumed that the center of the cell is fixed with respect to the glass superstrate and that differential thermal expansion is permitted by shear deflection of the low-modulus EVA.

- The relative motion of the edges of the ultrasonic welds in the aluminum interconnection during the 130°C temperature excursion from +90°C to -40°C is calculated to be:

131

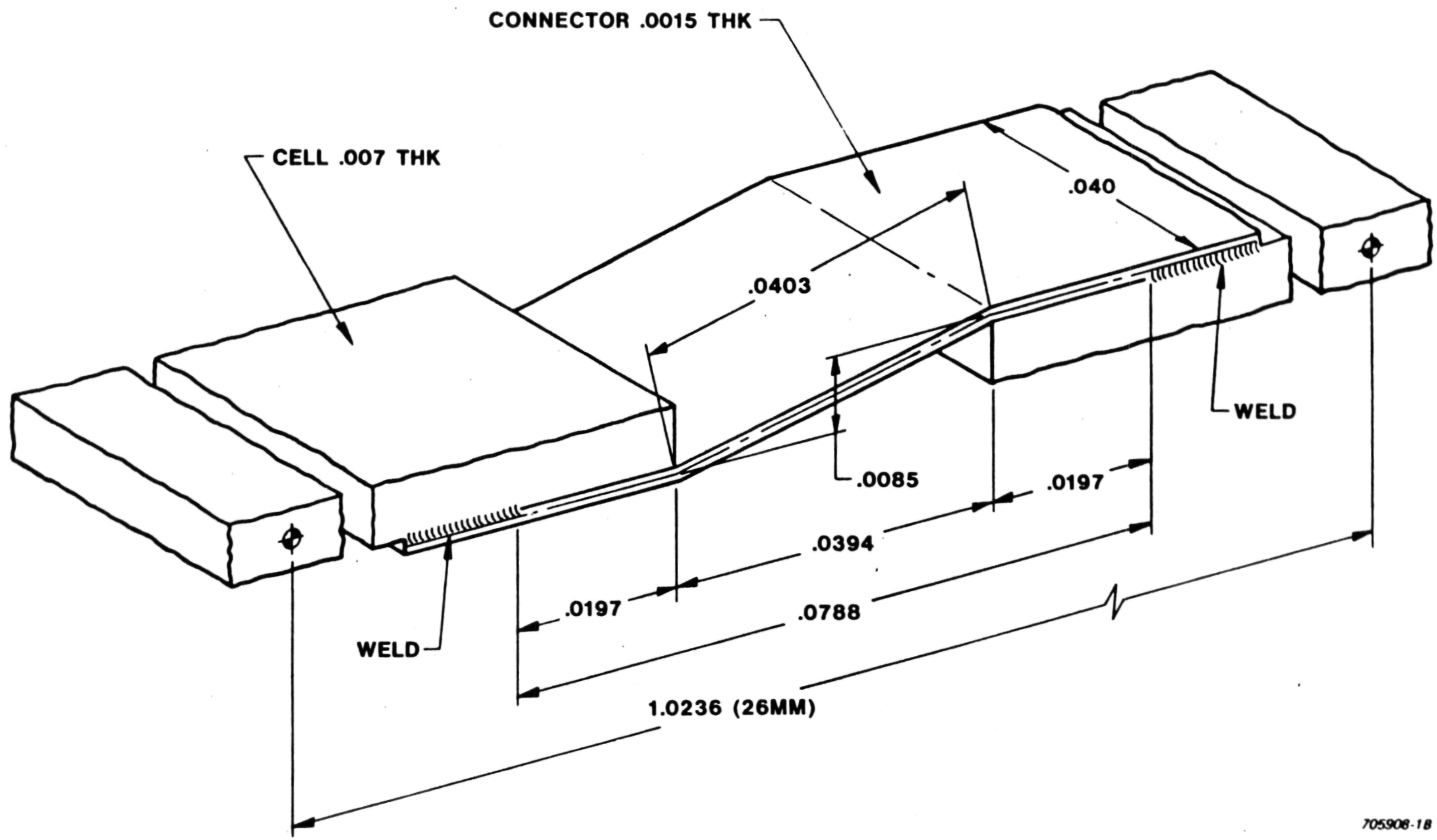

Figure 6. Cell Interconnection Geometry

contraction of the glass between centers: 0.00113 inch
contraction of silicon between centers: 0.000910 inch
differential motion: .000217 inch

- The calculated contraction of the aluminum between the edges of the welds is 0.000245 inch.

- The extension from its free state of the aluminum between welds is calculated to be 0.0000276 inch. This requires a strain of 0.0346%, which in aluminum results in a tensile stress of 3462 psi. The endurance limit of aluminum alloys 1060-H14 and 1100-0 is ±5000 psi.

- The calculated tensile force in the interconnect tab is 0.208 lbs. The shear stress in the ultrasonic weld, if it is a full area weld, is only 129.8 psi, which is negligible. Tear tests of these welds show approximately full coverage welds, whereas calculations show that as little as 10% coverage would be adequate both electrically and mechanically.

A similar type of analysis was performed to study a second interconnect or bond failure mechanism associated with stresses resulting from differential thermal expansion of the cells and interconnects in the parallel direction (ref. Figure 4). The failure mechanism postulated is successive bond failure during the cold phase of the thermal cycles, beginning at the ends of the cell interconnections and proceeding toward the center of the cell as each bond failure causes its inboard neighbor to become the outboard bond, i.e., the bond acted upon by unbalanced forces. This problem has been examined with the conclusion being that this "domino" failure will not occur and the multiple redundant interconnections will survive thermal cycling. This conclusion is based upon the following logic:

- The ultrasonic bonds between the aluminum interconnections and the silicon cells are made with the spans between bonds at room temperature (21°C); thermal cycling between -40°C and +90°C

133

causes a negative temperature excursion of 61°C and a positive excursion of 69°C.

- The coefficients of thermal expansion of the materials involved have the following values:

  aluminum - $23.6 \times 10^{-6}/°C$

  silicon - 2.9 to $7.4 \times 10^{-6}/°C$; the value $2.9 \times 10^{-6}/°C$ used in this analysis because it is the less optimistic assumption

- During the negative temperature excursion, a thermal strain of $61 \times (23.6-2.9) \times 10^{-6} = 0.001263$ in/in is imposed on the system. It is conservatively assumed that the total strain is imposed on the thin (0.0015") aluminum rather than on the thicker (0.007") and stiffer silicon and that the aluminum provides a direct (straight line) load path between bonds. The calculated equivalent stress for this strain is 16,500 psi tension, greater than the 13,000 psi yield strength reported for aluminum alloy 1060-H14, and much greater than the 5,000 psi reported for 1100-0; the aluminum would therefore yield. During the positive temperature excursion, the aluminum, because of its higher coefficient of thermal expansion, would expand more rapidly than the underlying silicon, so that the tensile load would drop to zero. Compressive loading of the aluminum foil will be very slight because the low elastic modulus of the ethylene vinyl acetate clamping the aluminum to the silicon will permit rippling of the aluminum; but upon recooling, the aluminum will again be stressed to its yield strength. An in-line load path in the aluminum between ultrasonic bond pads must therefore be avoided.

- The actual geometry of the aluminum interconnection and the silicon cell is shown in Figure 5.

- Differential strain of the aluminum and silicon can be accommodated by flexure of the aluminum "arch" at its minimum section height. Flexure would occur during both the positive and negative temperature excursions. The greater differential strain occurs during the 69°C positive excursion and is 0.00143 in/in. If each half-arch is considered to be a fixed end beam with a tip load sufficient to produce a deflection equivalent to the restraint, the equivalent deflection is .00714 mm or 0.00028 inches. The stress produced by this deflection of the tip of an equivalent cantilever beam at its point of zero deflection (the peak of the arch) is 4106 psi. The corresponding stress during the negative temperature excursion is 3630 psi. Both of these values are less than 5000 psi, the endurance limit (the stress at which an unlimited number of stress reversals can be survived) of aluminum alloys 1060-H14 and 1100-0. Either of these alloys is satisfactory - the selection to be based on mechanical handling of the interconnections during processing. To produce this stress in the interconnections, the shear stress in the end bonds, if these are 0.040" x 0.040", is only 5.06 psi.

B. Module Performance Evaluation

Performance evaluation of the prototype MEPSDU module was completed prior to fabrication and testing of a prototype module. Calculations were based on a cell of the dimensions specified in the module drawing package (2.5 cm x 9.83 cm x 0.015 cm) and having the following performance characteristics at AM1, 100 mW/cm^2 and 25°C:

Short circuit current density = 0.031 A/cm^2
Open circuit voltage = 0.580 V
Fill Factor = 78 percent
Efficiency = 14.0 percent

Dendritic web cells which have been manufactured on the Westinghouse Pre-Pilot Facility using the MEPSDU process sequence have routinely displayed these performance characteristics.

135

Encapsulation thicknesses and materials in the Westinghouse prototype MEPSDU module are as shown in Figure 7. The calculations were performed using a cell-to-still-air thermal impedance of 300°Ccm^2/W. This thermal impedance was determined experimentally using a small (5" by 8") encapsulated "minimodule" having the MEPSDU module layup configuration. An optical transmission factor of .96 (taken from "Sunadex" glass literature) and an electrical mismatch factor of .98 were assumed for the calculations. A packing factor of .92 was used in the calculations as determined from cell and module dimensions contained in the module drawing package.

Figures 8 and 9 present four significant calculated module parameters: open circuit voltage (V_{oc}), short circuit current (I_{sc}), efficiency, and power output, all plotted as functions of ambient air temperature for operation at AM1, 100 mW/cm^2. Note that the open circuit voltage and short circuit currents of the MEPSDU module have nearly the same absolute value (approximately 8.5 volts and 8.5 amps). This is a result of the specific series/parallel circuit configuration chosen for the module.

Table 5 summarizes the calculated performance parameters for the Westinghouse MEPSDU module at both standard operating conditions (80 mW/cm^2 insolation and 20°C ambient temperature) and at standard test conditions (25°C cell operating temperature and 100 mW/cm^2 insolation level). The latter case defines operating conditions under which the 1986 LSA cost objectives have been defined. The calculated efficiency level of 12.3% exceeds the 12.0% level assumed in the economic analysis presented in a later section of this report.

Figure 10 presents an actual I-V test curve for a recent prototype MEPSDU module fabricated on the Westinghouse Pre-Pilot Facility using cells produced by the baseline MEPSDU process sequence. This module, Model #AESD-1, S/N-18, differs from the prototype MEPSDU module in that the cells used in the module were 2.0 cm x 9.8 cm as opposed to the MEPSDU design of 2.5 cm x 9.83 cm. As a result, the S/N-18 module has 12 parallel strings of cell, each string containing 18 rather than 15 cells. The overall module area of the S/N-18 module is 4560 cm^2 rather than 4760 cm^2. This change modifies the I-V characteristic

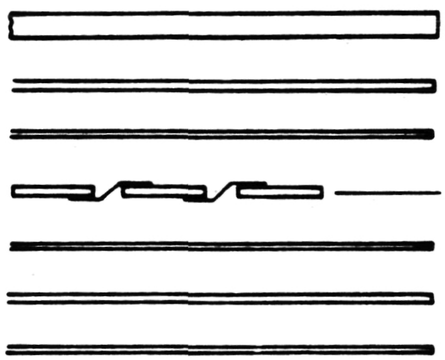

	Thickness	
	cm.	in.
Tempered Glass	.318	.125
Craneglas	.013	.005
EVA	.050	.020
Solar Cells	.015	.006
EVA	.050	.020
Craneglas	.013	.005
Mylar (Korad)	.007	.003

Figure 7. Layup Materials and Dimensions of the Westinghouse MEPSDU Module

137

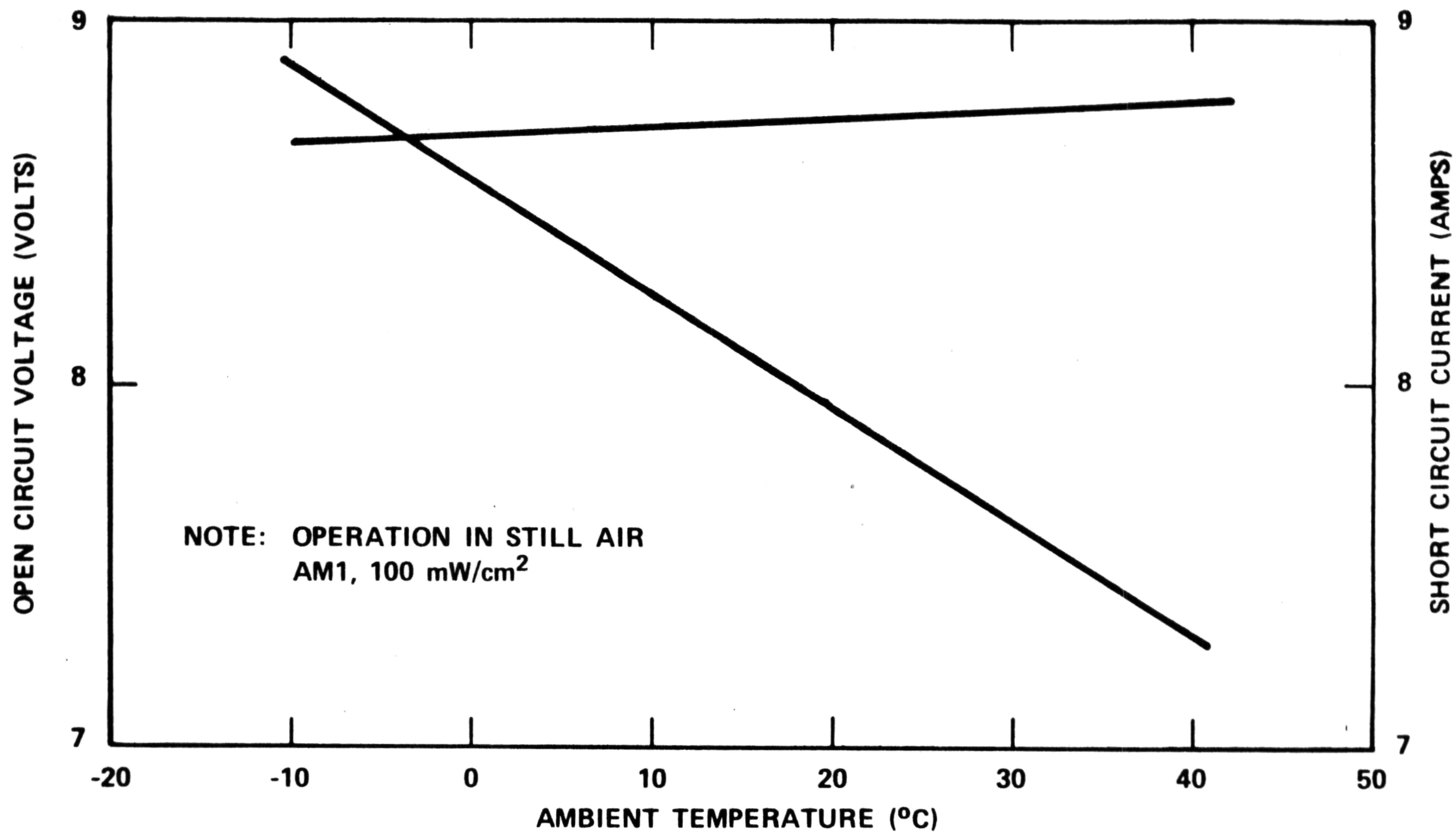

706511-3A

Figure 8. Calculated MEPSDU Module V_{OC} and I_{SC} as Functions of Ambient Temperature

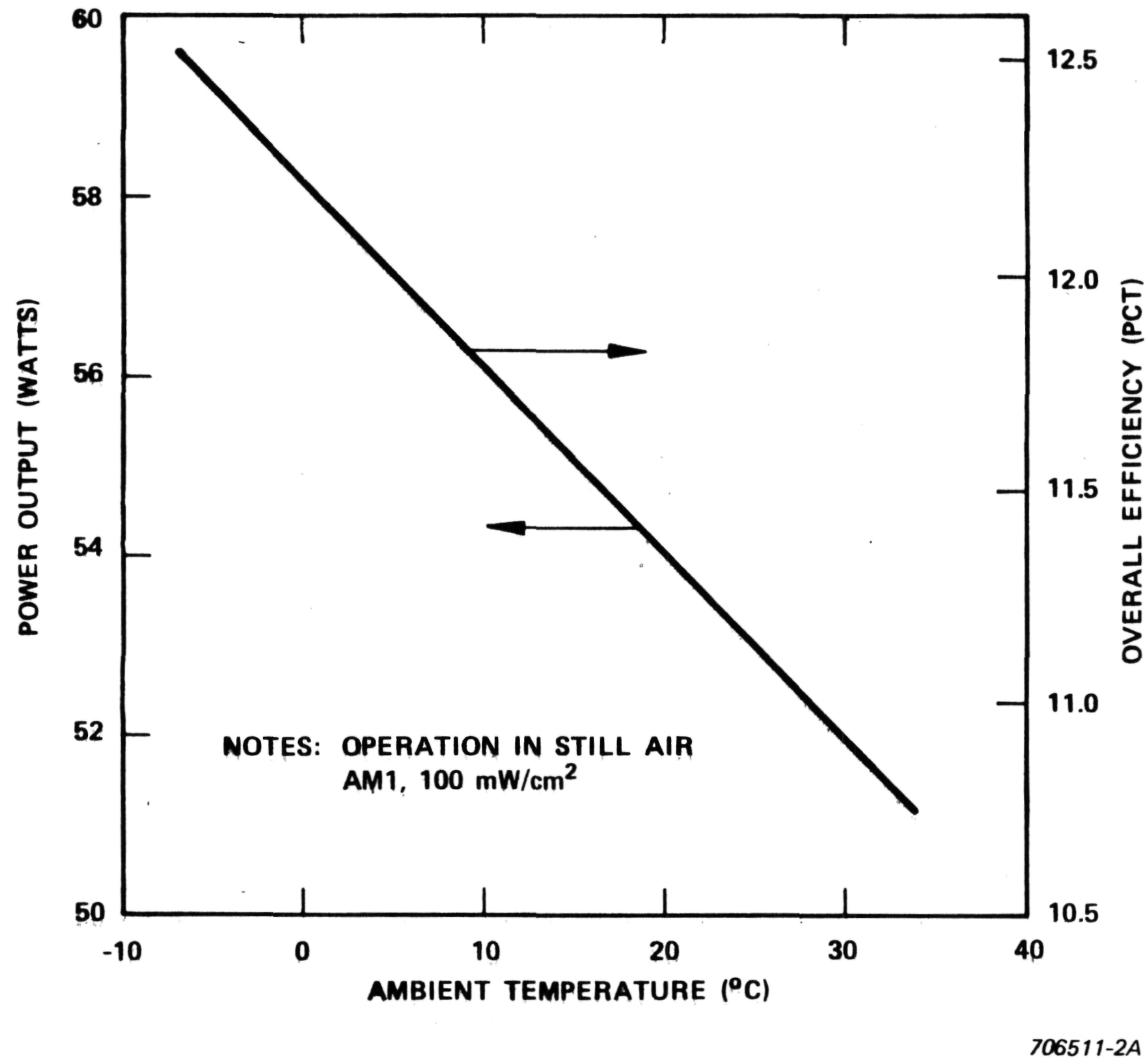

Figure 9. Calculated MEPSDU Module Power and Efficiency as Functions of Ambient Temperature

139

TABLE 5

CALCULATED MEPSDU MODULE PERFORMANCE PARAMETERS

Parameter	Standard Operating Condition(1)	Standard Test Condition(2)
Open Circuit Voltage	8.08 volts	8.61 volts
Nominal Operating Voltage	6.57 volts	7.00 volts
Short Circuit Current	6.98 amps	8.69 amps
Nominal Operating Current	6.70 amps	8.35 amps
Peak Power	44.0 watts	58.4 watts
Efficiency at Peak Power	11.6 pct	12.3 pct

(1)Standard Operating Conditions: 20°C ambient air temp, insolation = 80 mW/cm^2

(2)Standard Test Conditions: 25°C cell temperature, insolation = 100 mW/cm^2

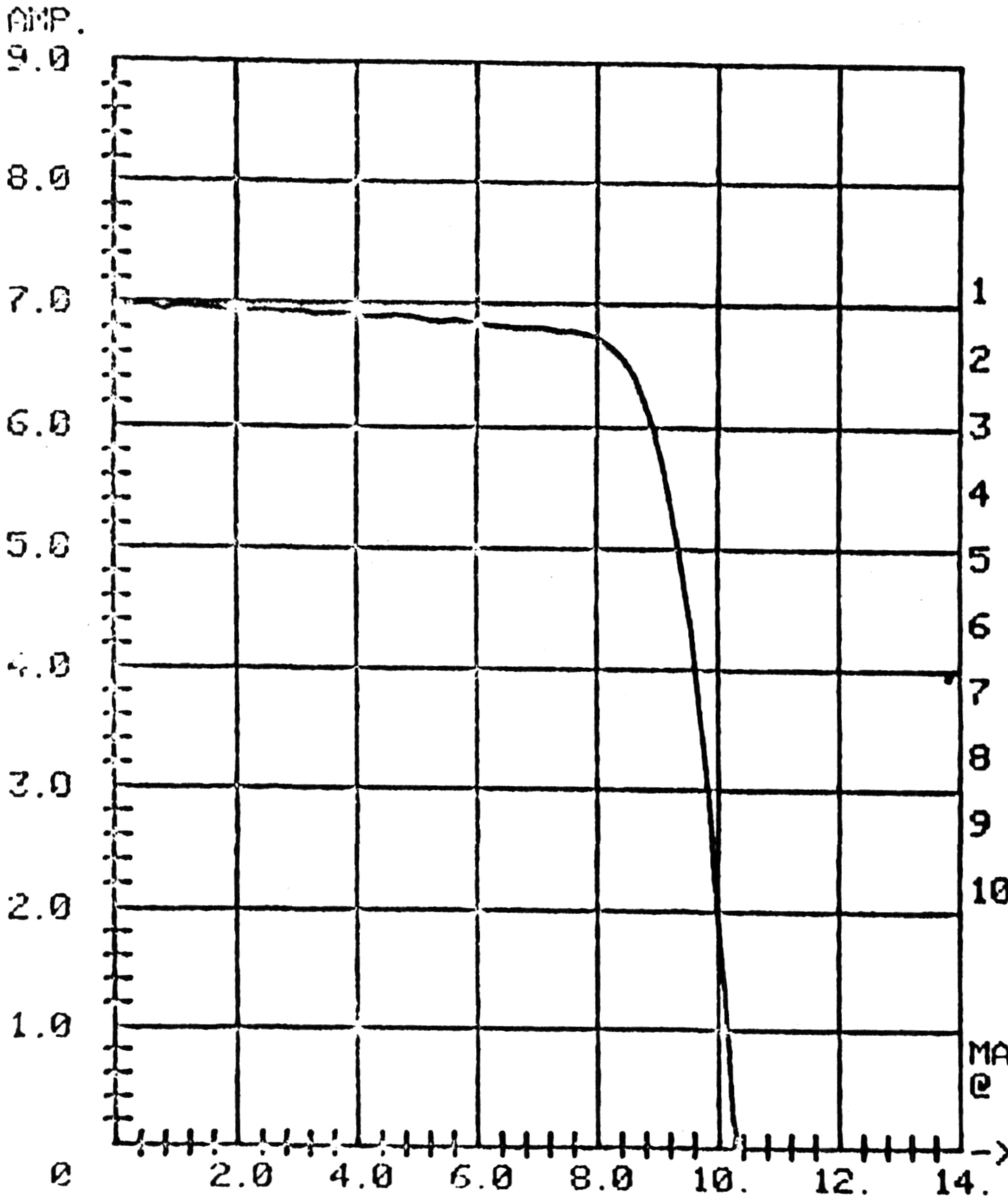

SPECTROLAB

MODEL # AESD-1
SERIAL # 0018
DATE 5/4/82

1 CELL AREA (SQ MM)
1960
2 # OF CELLS IN PARALLEL
12
3 # OF CELLS IN SERIES
18
4 AMBIENT TEMP (DEG C)
21
5 STANDARD TEMP (DEG C)
25
6 I TEMP COR(UA/SQ CM/DEG C)
25
7 V TEMP COR(UV/DEG C/CELL)
-2200
8 AM1 CAL CURRENT (0.1'S MA)
1093
9 TEST VOLTAGE (0.01'S V)
45
10 MIN I(TEST) (0.01'S A)
5

I(TEST) = 7009000 UA
ISC = 6972000 UA
VOC = 10298000 UV
MAX POWER 55338927 UW
@ 8628000 UV /A

$\eta = \frac{55.34}{456} = 12.14\%$

Figure 10. I-V Test Curve of Prototype MEPSDU Module

181

of the module and reduces the expected output power by 4.2 percent - the ratio of the module areas; but the efficiency and temperature characteristics are essentially identical to those of the MEPSDU module. Note that efficiency of the S/N-18 test module, 12.1 percent, also exceeds the 12 percent level assumed in the economic analysis presented in a later section of this report.

C. Environmental Testing

1. Hailstone Impact Tests

Two full-size simulated modules, laminated and bonded to test frames* using the adhesive configuration specified by the Westinghouse MEPSDU module interface drawing, were delivered to JPL in November 1981 for high velocity iceball impact tests as specified by JPL Document 5101-138. Preliminary testing conducted at Westinghouse indicated that the 1/8" thick tempered glass module superstrate can survive the hailstone impact tests.

Testing was completed by JPL personnel in December 1981, and both modules passed all phases of the test. It should be noted that, in addition to the 1" diameter hailstones specified by 5101-138, both modules also passed the 1 1/4" and 1 1/2" diameter hailstone tests. All of the tests were conducted using terminal velocities associated with each size hailstone. Thus the 1 1/2" diameter hailstone impacted the glass superstrate with an energy content five times that of the JPL 5101-138 requirement.

2. Wind Load Testing

Tests were conducted by Westinghouse to demonstrate that the 1/8 inch tempered glass superstrate and encapsulated cells of the prototype MEPSDU module can survive both positive and negative wind loading conditions specified by JPL Document 5101-138.

*This test frame supports the module and takes the place of the support structure in the deployed array. The frame does not protect the edges of the module.

For the positive wind loading test, the module edge support load equivalent to 125% of the design wind load was transmitted through elastomeric material overlapping the ends of the cells varying amounts, up to 3/8 inch. No damage to the superstrate or any of the cells was observed.

The simulated negative wind loading test, designed to simulate wind loads which would tend to lift the module off its edge support (thus placing the structural adhesive attachment in tension), was also successfully performed. The test was conducted on a frameless minimodule that was attached to a support by the double-faced polyurethane tape and silicone structural adhesive with which the modules will be mounted in test and service installations. The back face of the minimodule was loaded by a uniformly distributed layer of fine tungsten powder (enclosed in a thin plastic bag and restrained laterally by vertical plastic dams). The depth of the tungsten powder, 9 inches, was sufficient to develop a restraining tensile force of 25 lbs per linear foot of the module edge, applied to the module through the structural adhesive bond to the back face of the module encapsulation. This tensile force is the same as a 50 lb/ft^2 wind load will develop on a full-size module. The load was sustained for fifteen minutes, rather than for one minute as the specified gust loading, with no indications of tearing, separation, or creep in the support attachment.

3. Thermal and Humidity Cyclic Tests

Twelve small modules were assembled for environmental testing. These modules were made to evaluate several different layups, substitutes for Korad-KLEAR as the back surface weather seal, and Tedlar tape as an edge seal. Cells with efficiency levels unacceptably low for incorporation into modules were selected for use in these tests. Cut window glass was used on all the test modules rather than tempered float glass which will be used on the MEPSDU modules. The layup of each of these modules is shown in Table 6.

The following comments are made in regard to the appearance of the as-laminated modules. The sun side of module G-2 was clearer than the modules that had a layer of Craneglas between EVA and the window glass. The back surfaces of modules with Korad back covers (G-1, G-2, G-3, G-10, G-11, and G-12) were

143

TABLE 6

LAYUP OF SMALL MODULES USED FOR ENVIRONMENTAL TESTING

G-1	G-2	G-3	G-4	G-5	G-6
(1.6 x 9.4 cm cells)	(1.6 x 9.4 cm cells)	(1.6 x 9.4 cm cells)	(1.6 x 9.4 cm cells)	(1.6 x 9.4 cm cells)	(1.6 x 9.4 cm cells)
Window Glass	Window Glass	Window Glass	Window Glass	Window Glass	Window Glass
Craneglas	EVA	Craneglas	Craneglas	Craneglas	Craneglas
EVA	5 Cell String	EVA	EVA	EVA	EVA
5 Cell String	Craneglas	5 Cell Stirng	5 Cell String	5 Cell String	5 Cell String
Craneglas	EVA	Craneglas	Craneglas	Craneglas	Craneglas
EVA	Craneglas	EVA	EVA	EVA	EVA
Craneglas	Korad-KLEAR	Craneglas	Craneglas	Craneglas	Craneglas
Korad-KLEAR	Tedlar Edge Tape	White Korad	Clear Tedlar (2 mil)	Clear Tedlar (4 mil)	White Tedlar (2 mil)
			Tedlar Edge Tape		

G-7	G-8	G-9	G-10	G-11	G-12
(1.6 x 9.4 cm cells)	(1.6 x 9.4 cm cells)	(1.6 x 9.4 cm cells)	(1.2 x 10 cm cells)	(1.2 x 10 cm cells)	(1.2 x 10 cm cells)
Window Glass	Window Glass	Window Glass	Window Glass	Window Glass	Window Glass
Craneglas	Craneglas	Craneglas	Craneglas	Craneglas	Craneglas
EVA	EVA	EVA	EVA	Elvax	EVA
5 Cell String	5 Cell String	5 Cell String	5 Cell String	5 Cell String	7 Cell String*
Craneglas	Craneglas	Craneglas	EVA	Elvax	EVA
{EVA Primed Clear}	{EVA Primed White}	EVA	Craneglas	Craneglas	Craneglas
{Tedlar (2 mil)}	{Tedlar (2 mil)}	Craneglas	White Korad	White Korad	Korad-KLEAR
		Acrylar X-22417			
		Tedlar Edge Tape			

*K&S bonded

9950-892

-4

wrinkled transverse to the long direction of the cells. The back surfaces of modules made with .002 inch thick Tedlar back covers (G-4, G-6, G-7, and G-8) were fairly smooth. The .004 inch thick Tedlar back cover of module G-5 was extremely smooth. The use of EVA primed Tedlar (G-7 and G-8) simplified the layup. The Acrylar back cover of module G-9 was extremely wrinkled with a random orientation. The use of Elvax* (non-blocking EVA) in module G-11 produced no noticeable difference in lamination or module performance. Because it is non-blocking, it is much easier to handle. The elimination of Craneglas behind the cell string in modules G-10, G-11, and G-12 also had no adverse effect on either appearance or performance. The white back covers made it possible to observe shrinkage/wrinkling effects that suggest that all back cover materials should be cut slightly oversize prior to lamination. The shrinkage/wrinkling effects were not easily detected with clear back covers because of the transparency of all of the films used in the layups. The cut window glass did not have an edge of the quality of manufactured tempered float glass; therefore, the Tedlar tape edge seal did not "corner" well on all sides of modules G-2, G-4, and G-9.

A typical test module is shown in Figure 11, and the twelve test modules are shown loaded in a test fixture in Figure 12.

Because of a malfunction of the test equipment, pre-lamination measurements made on cell strings for modules G-1 through G-9 were not valid. However, pre- and post-lamination measurements were obtained on the cell strings in modules G-10, G-11, and G-12; and these data are shown in Table 7. The differences seen in the data are within the measurement error of our equipment; and the effect, if any, of the laminating materials or process upon cell or module characteristics is minimal.

All twelve modules were placed in an environmental test chamber and subjected to the thermal cycles specified in JPL 5101-138, Figure 5.1. (Due to equipment

---

*DuPont Trade Name

145

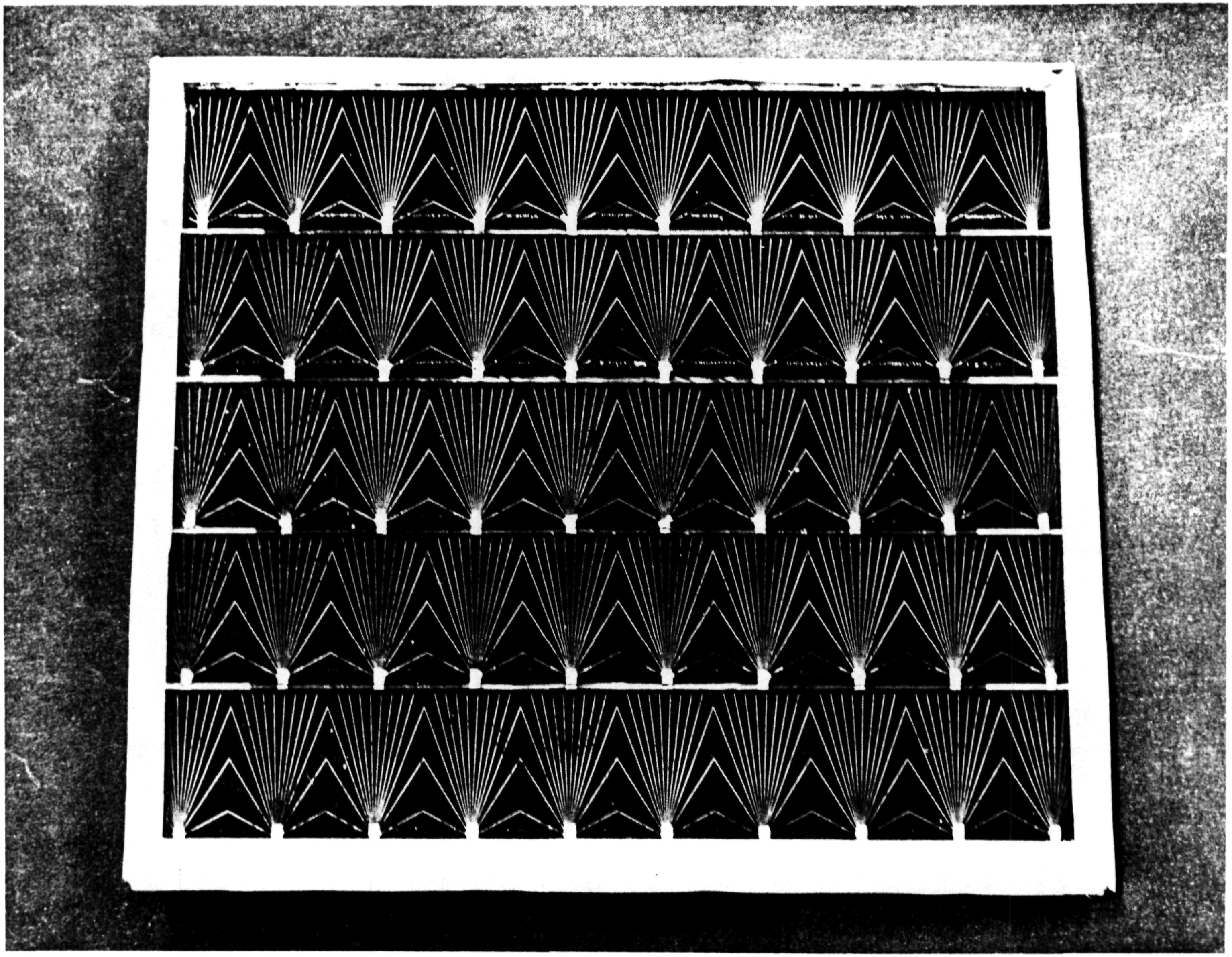

Figure 11. Environmental Test Module G-2 (10 cm x 9 cm)

9950-892

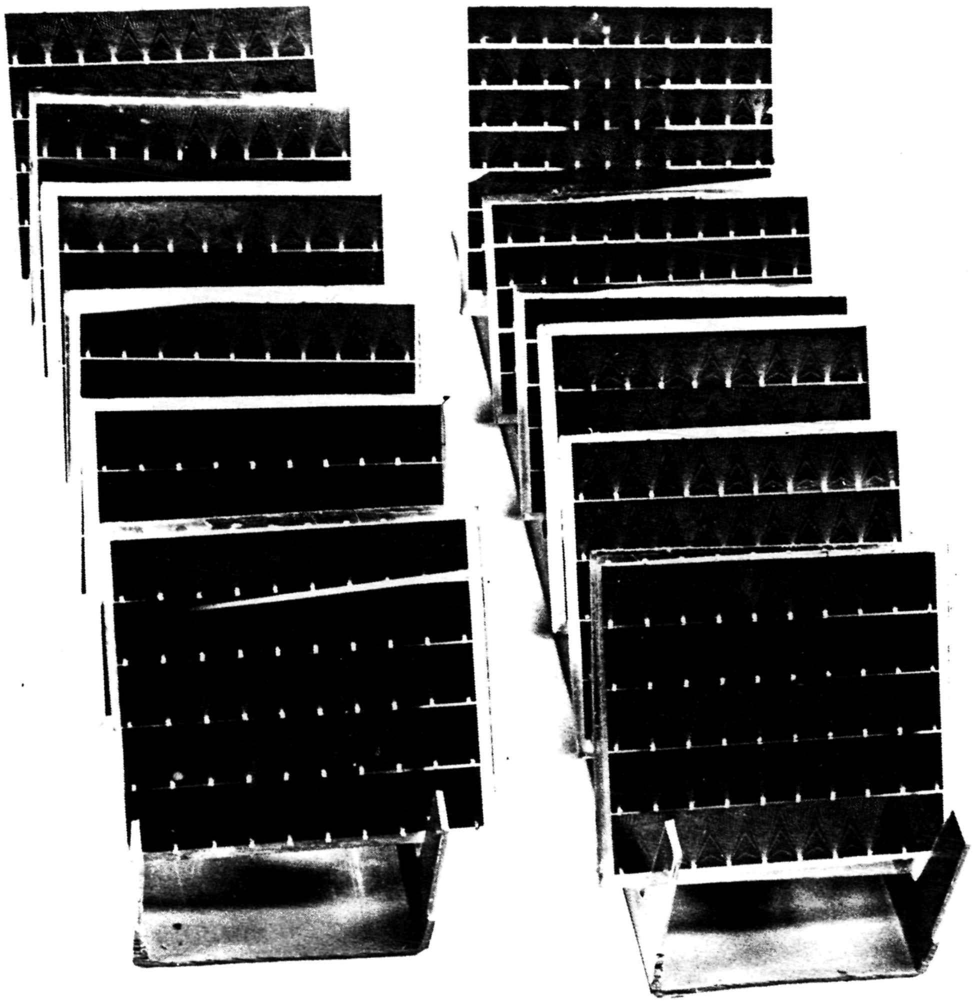

Figure 12. Environmental Test Modules in Humidity Test Fixture

TABLE 7

PRE- AND POST-LAMINATION MEASUREMENTS OF CELL STRING CHARACTERISTICS

Module No.	Pre-Lamination Cell String Characteristics				Laminated Module Characteristics			
	V_{oc} (V)	I_{sc} (A)	FF	η (%)	V_{oc} (V)	I_{sc} (A)	FF	η (%)
G-10	2.60	.298	.77	9.92	2.66	.283	.77	9.69
G-11	2.52	.309	.74	9.60	2.69	.295	.75	9.92
G-12	3.58	.297	.73	9.24	3.75	.273	.75	9.04

NOTE: All cells used in the assembly of these test articles were produced during early checkout operations on the Westinghouse pre-pilot facility. These efficiency levels are not representative of the pilot line or the MEPSDU process sequence.

limitations, the minimum temperature achievable in these tests is -35°C as opposed to the specified level of -40°C). Open circuit voltage and short circuit current measurements were made on each of the modules after lamination, after completion of 25 cycles, and again after completion of 50 cycles. These data are given in Table 8. As before, the differences seen in the data are within the measurement error of the equipment. The effect, if any, of the thermal cycling test upon cell or module characteristics is not measurable.

Each of the modules was examined after the thermal cycling test. There was some separation of the lamination from the glass on modules G-1, G-3, and G-5 and some debonding of the edge tape from the glass on module G-2. These were random effects and could not be correlated to materials or processes. They were noted, however, because it was felt that the separation may permit ingress of moisture by a route other than permeation through the lamination films during subsequent humidity tests.

All twelve small modules were then placed in an environmental test chamber and subjected to the humidity test conditions defined by JPL 5101-138, Figure 5.2. The modules were inclined at 45° during the test. The modules and the holding fixture were shown previously in Figure 12.

Open circuit voltage and short circuit current measurements were made on each of the modules within one-half hour after the completion of the humidity test. These data are compared to data obtained as-laminated and after 50 thermal cycles in Table 9. Differences seen in the data are within the measurement error of the equipment. The differences, if any, on the performance characteristics of the small modules subjected to the environmental tests specified in JPL 5101-138 are not measurably significant.

A re-examination of each of the modules after the humidity test indicated that, except for a slight darkening of the external copper leads, there was no noticeable change in the appearance of the modules as a result of the humidity test.

149

TABLE 8

MEASUREMENTS MADE ON THERMALLY CYCLED TEST MODULES

Module No.	Open Circuit Voltage: As Laminated	Open Circuit Voltage: After 25 Cycles	Open Circuit Voltage: After 50 Cycles	Short Circuit Current: As Laminated	Short Circuit Current: After 25 Cycles	Short Circuit Current: After 50 Cycles
G-1	2.58	2.61	2.52	.318	.340	.337
G-2	2.58	2.62	2.60	.278	.295	.285
G-3	2.57	2.63	2.61	.326	.351	.345
G-4	2.46	2.61	2.60	.330	.339	.330
G-5	2.48	2.53	2.52	.246	.266	.256
G-6	2.52	2.58	2.57	.262	.281	.272
G-7	2.51	2.55	2.57	.265	.280	.271
G-8	2.54	2.59	2.60	.267	.288	.283
G-9	2.58	2.63	2.64	.330	.346	.335
G-10	2.66	2.68	2.69	.283	.303	.294
G-11	2.69	2.71	2.71	.295	.309	.299
G-12	3.75	3.77	3.75	.273	.283	.272

TABLE 9

MEASUREMENTS MADE ON ENVIRONMENTAL TEST MODULES

Module No.	Open Circuit Voltage As Laminated	Open Circuit Voltage After 50 Thermal Cycles	Open Circuit Voltage After Humidity Test	Short Circuit Current As Laminated	Short Circuit Current After 50 Thermal Cycles	Short Circuit Current After Humidity Test
G-1	2.58	2.52	2.56	.318	.337	.338
G-2	2.58	2.60	2.60	.278	.285	.301
G-3	2.57	2.61	2.62	.326	.345	.338
G-4	2.46	2.60	2.60	.330	.330	.335
G-5	2.48	2.52	2.53	.246	.256	.258
G-6	2.52	2.57	2.58	.262	.272	.277
G-7	2.51	2.57	2.56	.265	.271	.272
G-8	2.54	2.60	2.60	.267	.283	.277
G-9	2.58	2.64	2.64	.330	.335	.333
G-10	2.66	2.69	2.70	.283	.294	.292
G-11	2.69	2.71	2.72	.295	.299	.294
G-12	3.75	3.75	3.80	.273	.272	.272

After completion of the humidity tests, the thermal cycle tests were repeated in three sets of 50 cycles, with data being recorded after completion of each set.

Figure 13 shows the measurement of the performance characteristics before and after the series of events occurring from lamination through the completion of 200 thermal cycles for minimodule G-2. This module, with the exception of an added layer of Craneglas over the cells that was found to be unnecessary, is representative of the MEPSDU module layup. The data shown in Figure 13 is typical of the data obtained on the other minimodules in that the modules have exhibited no performance or visual sensitivity to sustained environmental testing.

4. Loss of Cell Contact Pad Electrical Connection

Front surface (sun side) current collection from cells incorporated in the Westinghouse MEPSDU module design is achieved with a series of very fine (1 mil wide) straight conductors emanating from contact pads along one edge of each cell. Cell-to-cell electrical interconnection is achieved by bonding aluminum conductors to each of the contact pads. The fine lines are parallel connected on the surface of the cell so that if the electrical connection to a pad fails, the photocurrent can be collected by neighboring pads albeit with a somewhat higher resistance. This redundancy of contacts leads to a high tolerance for interconnect failure.

To quantify the effect of interconnect failure, several tests were made where the change in the cell output power was determined as a function of the number of pads contacted. At the time these tests were conducted, each cell contained ten interconnect pads located near the long edge of one side of the front surface of the cell.

To carry out the test, cell parameters were first measured with all 10 interconnect pads contacted. The test was then repeated 7 times with the number of pads contacted being reduced by 1 in each test. Table 10 shows the cell design and the results of this experiment. The first three columns of Table 10 show which pads were contacted during each test: the last column shows the output power of the cell at the test conditions.

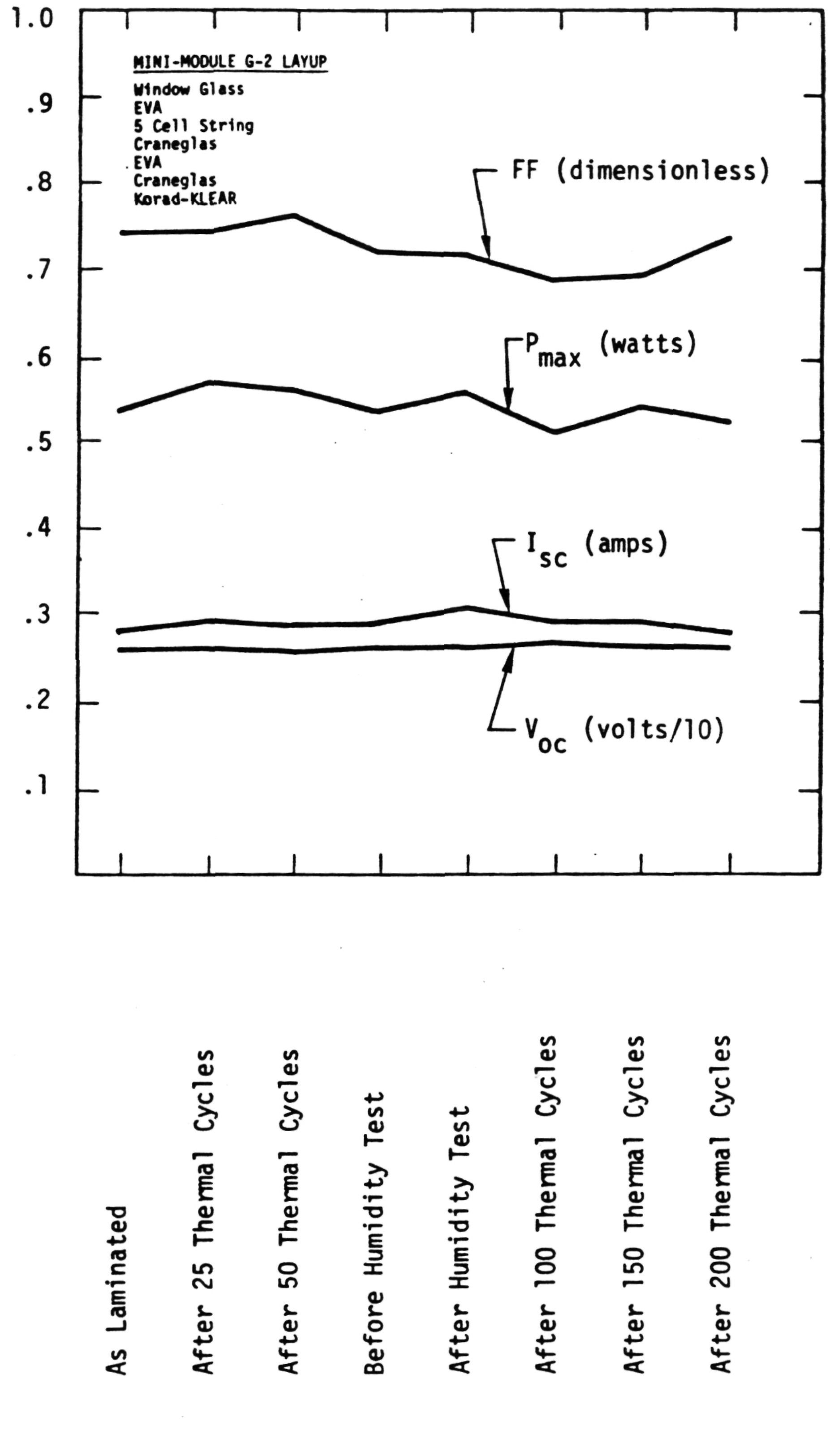

Figure 13. Environmental Test Data from Minimodule G-2

TABLE 10

OUTPUT POWER FROM SOLAR CELL AS FUNCTION
OF INTERCONNECT PADS CONTACTED

Test #	No. of Pads Contacted	Pad No. Contacted*	Cell Power - Out (watts)
1	10	1,2,3,4,5,6,7,8,9,10	0.162
2	9	1,2,3,4,5,6,7,8,9	0.158
3	8	2,3,4,5,6,7,8,9	0.152
4	7	2,3,4,5,6,7,9	0.152
5	6	2,4,5,6,7,9	0.146
6	5	2,4,5,7,9	0.145
7	4	4,5,7,9	0.117
8	3	4,5,7	0.087

*Pad No. Definition

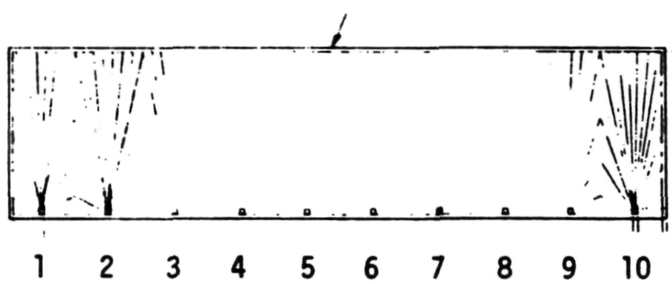

The power decreased by only 3% when nine pads were contacted and by 7% with only seven pads contacted. With only three pads connected, the power decreased by less than 50%. The major causes of the power loss were the decrease in the fill factor and short circuit current due to the added series resistance of the cell. The thin grid lines in this experiment were conducting the photocurrent over several centimeters, thereby increasing the resistance.

The results given would change if different sequences of pad numbers were contacted. For example, the power output when pads 4, 5, and 6 were contacted would be greater than if pads 1, 2, and 3 were contacted.

These data, however, do show that several interconnection contacts can be lost in a cell without significantly decreasing the power; and thus the cell design does show a high tolerance for interconnect failure. The results of these tests indicated that the ten pad configuration contained an over-redundancy, and the cell number of interconnect pads on each cell was reduced from ten to eight. This reduction reduces the time required to complete the interconnect bonding operation.

5. Cell Shading Tests

The ability of the prototype MEPSDU solar cell string to survive the short circuit/shaded cell tests specified in JPL Document 5101-138 was questioned by JPL personnel at the Module Design Review. Subsequently, cell shading tests were performed using the 5 cell modules (1.6 cm cells) that were prepared for environmental testing. Three of these modules were connected in series to simulate the 15 cell string of the MEPSDU module. Each cell was then shaded, one at a time, with the modules operating in normal sunlight conditions. Figure 14 shows the test system used for the shading tests. Figure 15 shows the change in temperature (measured on the back cover behind each of the cells) with time and incident power for a test in which the center cell of each 5 cell module of the 15 series connected cells was monitored. Both the shadowed and unshadowed cells responded to changes in incident power, and progressive overheading of the shadowed cell did not occur. In fact, in some tests the shadowed cell ran slightly cooler for corresponding insolation values than it did in the unshaded condition.

155

ORIGINAL PAGE
BLACK AND WHITE PHOTOGRAPH

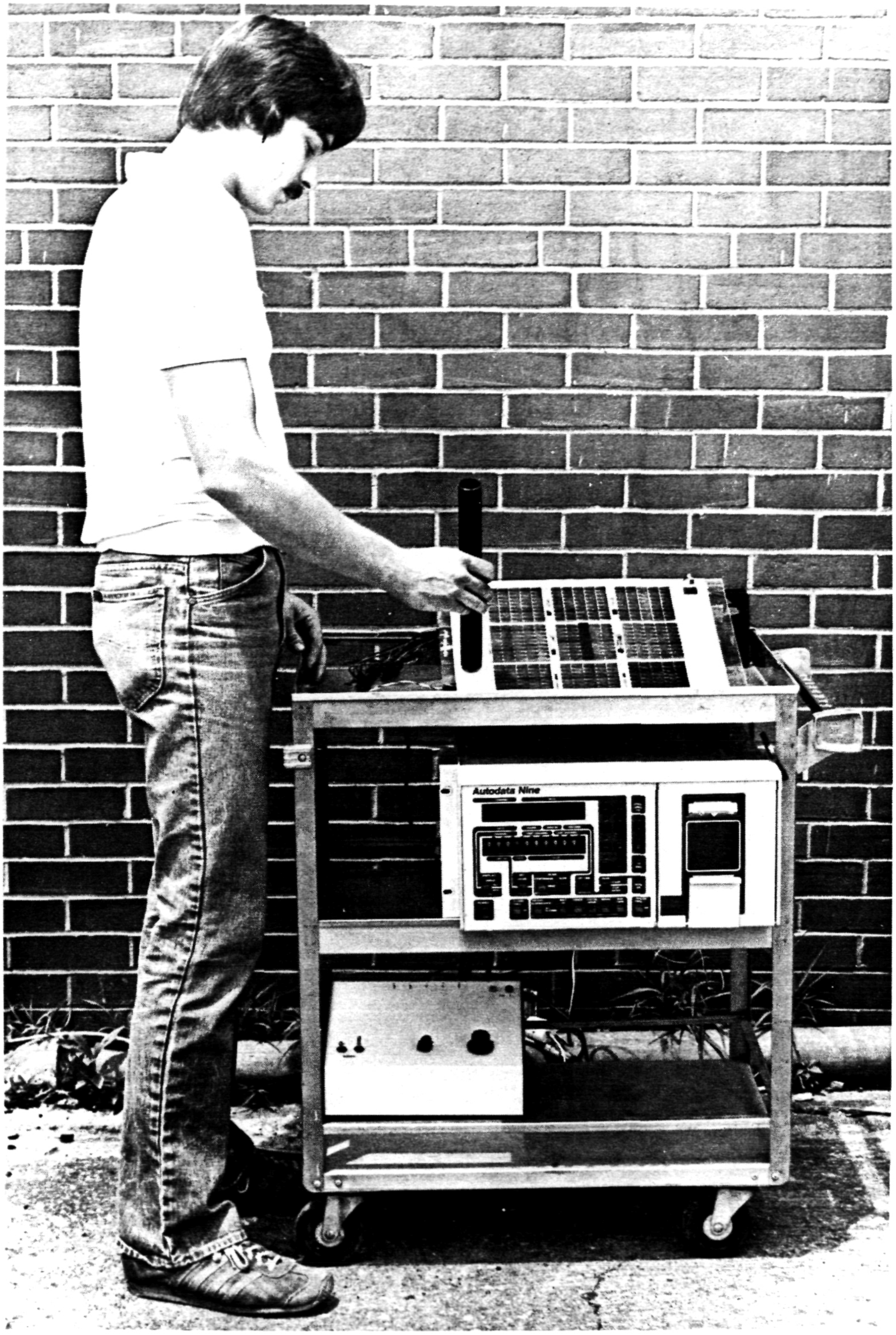

Figure 14. Test System Used for Cell Shading Tests

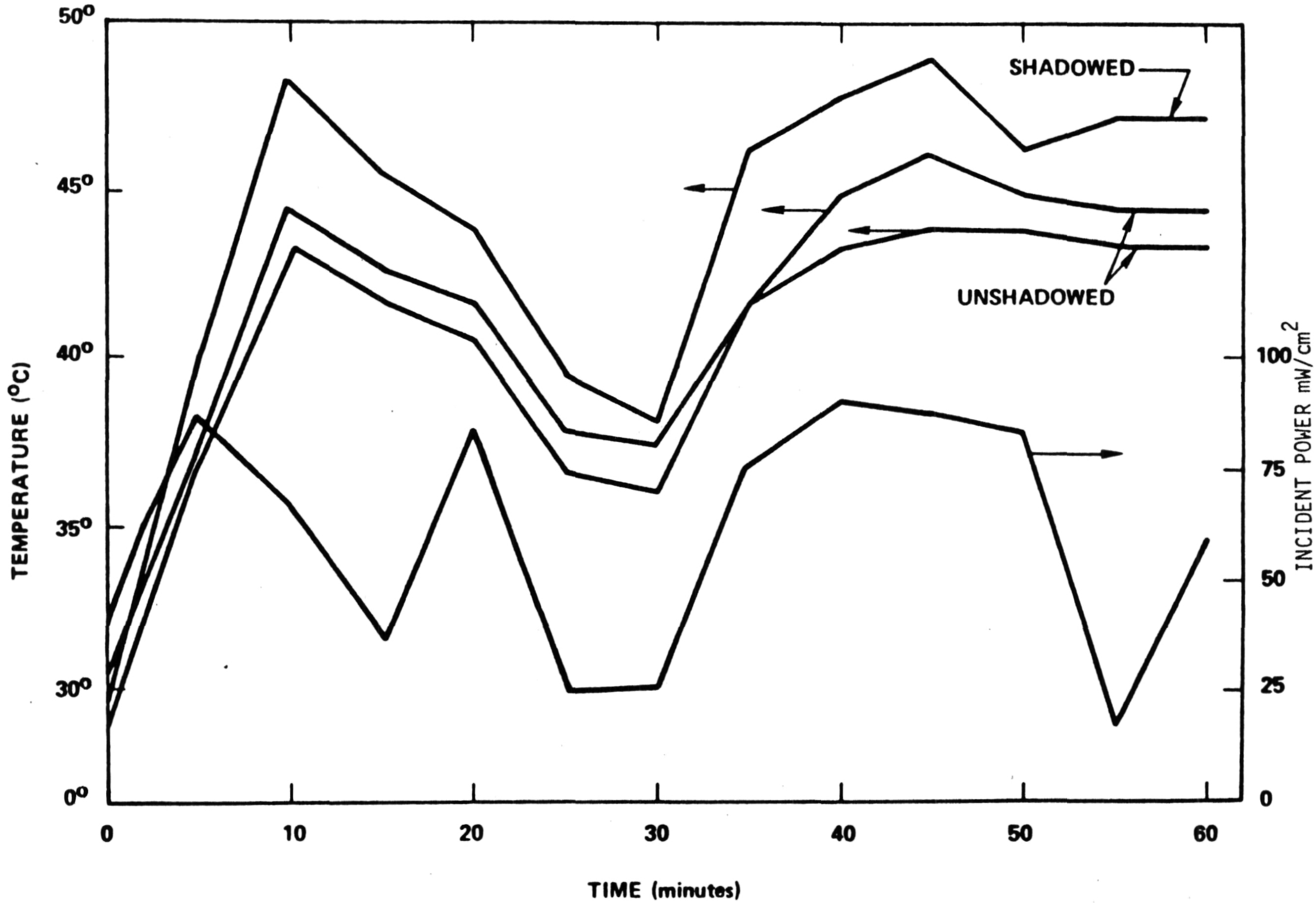

Figure 15. Shadowed Cell Heating Effects under Module Short Circuit Conditions

157

Further tests were then performed using a continuous 15 cell string of 2.5 cm cells in a layup precisely duplicating the electrical circuit of the MEPSDU module. In these tests, cells were fully shaded and also partially shaded. The results were essentially identical, i.e., no measurable increase in temperature was observed in any shaded condition.

These data reinforce the conclusions that were presented at the Module Design Review: destructive overheating of a shaded cell during short circuit operation of a module is not a problem with the Westinghouse MEPSDU module circuit configuration containing 12 strings of 15 series connected cells. Hence, no internal blocking diodes are required in this module.

V. PROCESS SEQUENCE DESIGN

A. Baseline Process Sequence

A baseline process sequence for the fabrication of dendritic web silicon into solar cells and modules was specified during the program. Most of the process steps are based on well-known industrial semiconductor practice that have, in some cases, been modified to take advantage of the unique properties of dendritic web silicon, such as thinness, smooth surfaces, long lengths, etc. These features permit economical fabrication of solar modules.

The cost factors associated with each step of the Westinghouse baseline process sequence have been determined in an economic analysis which is discussed in detail in a later section of this report. Using SAMICS methodology, it has been determined that the specified process sequence can meet the DOE/JPL overall cost objectives of producing photovoltaic modules for 70¢/peak watt in 1986 (1980$) using large scale manufacturing techniques.

The overall Westinghouse Baseline Process Sequence is outlined in Figure 16. Whereas this figure shows each of the basic operations required to transform dendritic web sheet material into photovoltaic modules ready for shipment, subdividing the process sequence into a series of unit operations is necessary to analyze the process as required to perform economic analyses.

The Westinghouse Baseline Process Sequence flow chart, depicting unit operations, is shown in Figure 17. The sequence is as follows:

1. Pre-Diffusion Cleaning - This consists of a hydrofluoric acid dip, rinse, dry sequence followed by a CF_4/O_2 plasma etch.

2. Front and Back Surface Junction Formation and Oxide Etch - The back surface junction is formed first by applying an SiO_2 layer to the sun side of cleaned web, removing splatter traces of SiO_2 from the back surface with a hydrofluoric acid dip/rinse/dry sequence, diffusing boron into the clean silicon surface, and then removing the boron glass in a hydrofluoric acid dip/rinse/dry sequence. This process is

159

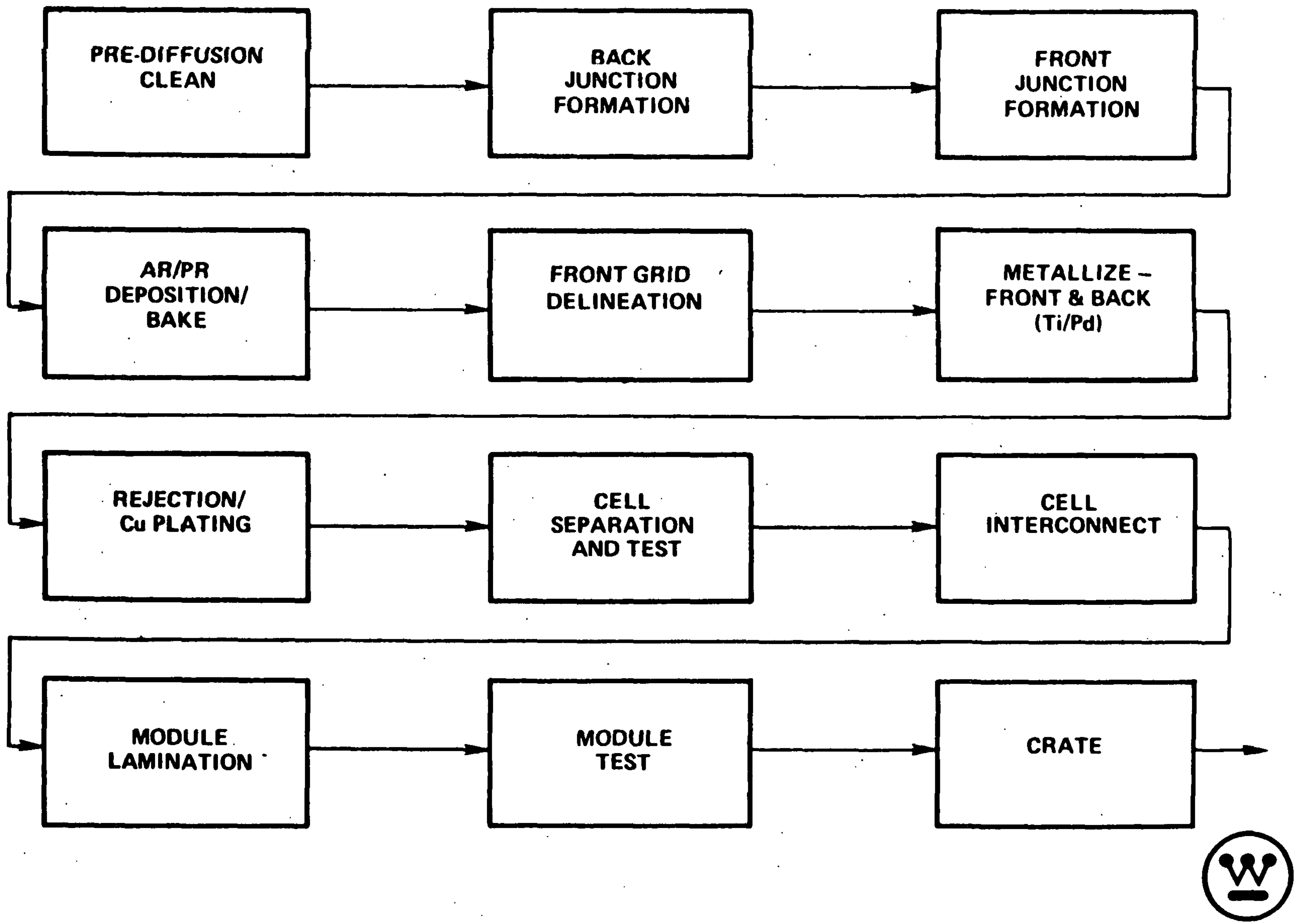

Figure 16. Westinghouse MEPSDU Overall Process Sequence

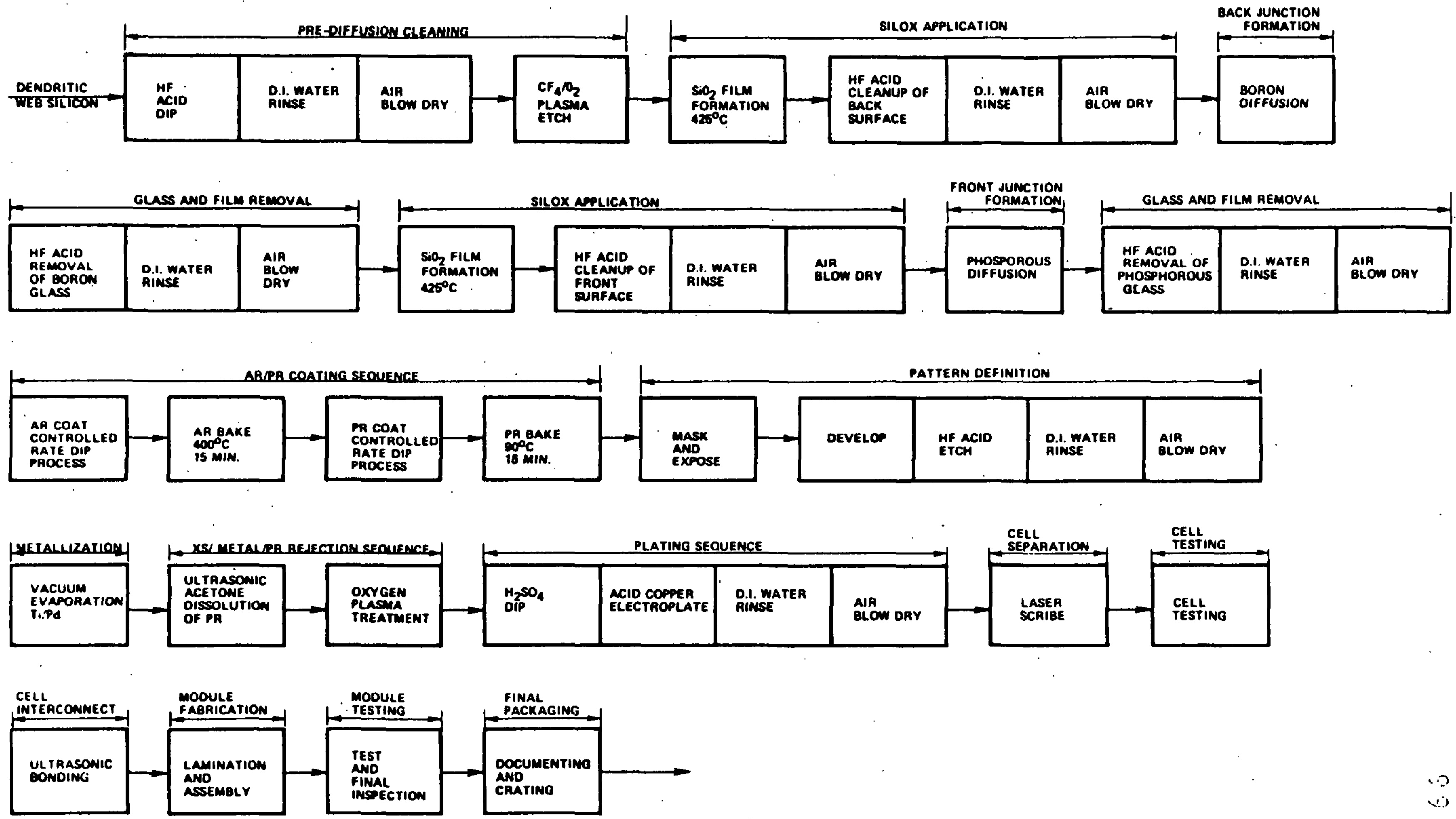

Figure 17. Westinghouse MEPSDU Baseline Process Sequence Flow Chart

9950-892

repeated for the front surface where the junction is formed by phosphorous diffusion.

3. Antireflective (AR) and Photoresist (PR) Coating Application - The AR coating is applied first by controlled rate withdrawal from an organometallic solution to give a liquid film that is converted to TiO_2/SiO_2 after baking. The PR coating is then applied, and its thickness is controlled in a similar manner.

4. Grid Pattern Definition - Standard photolithographic techniques of masking, exposing, developing, and pattern etching are employed.

5. Metallization - Successive layers of Ti and Pd and deposited on the web by vacuum deposition.

6. Metal Rejection and Plating - Excess metal and photoresist are removed by ultrasonic dissolution of the PR in acetone. Residual PR is removed by plasma stripping. Copper is electroplated over the vacuum deposited metal film.

7. Cell Separation - Four cells are separated from the 42 cm web strip using a laser scribe followed by a mechanical breakout.

8. Cell Test - The I-V characteristic of each cell is measured at AM1, 100 mW/cm^2 and 25°C.

9. Cell Interconnection - Strings of 15 cells are electrically joined in series with aluminum interconnects by ultrasonic bonding.

10. Module Lamination - Modules are built from 12 parallel connected strings of cells using a layup process of glass and polymeric materials that are laminated into a module.

11. Module Test - The I-V characteristic of each module is measured at AM1, 100 mW/cm^2 and 25°C cell temperature.

12. Module Package - Acceptable modules are crated for shipping.

The detailed steps required for Items 10, 11, and 12 are shown in Figure 18. This figure is a manufacturing flow chart of the module assembly operations. The sequence is as follows:

1. Superstrate Preparation - Low iron, tempered drawn glass of the proper size is cleaned with a commercial glass cleaner and positioned with the fine matte surface down. (The fine matte surface will be the sun side of the module.) The coarse matte surface of the opposite side is primed with a dilute solution of an organofunctional silane and dried with warm air.

2. Layup Installation - A spacer of Craneglas is placed on the primed glass surface. Ethylene vinyl acetate (EVA), used as a lamination pottant, is placed on the Craneglas. The sunside layup is then transferred to the string layup position of the automatic interconnect station.

3. Positioning of Cell Subassemblies - The cell stringing and tabbing machine uses an ultrasonic rolling spot bonder to form a series string of 15 interconnected cells. Twelve of these series strings are sequentially and automatically positioned by the automated tabbing and stringing machine on the EVA of the sunside layup. This subassembly is then moved to a finish layup station.

4. Installation of Longitudinal Conductors - The end interconnect tabs from each of the twelve series strings are ultrasonically seam welded to longitudinal copper conductors. Three rows of cells on each edge of the strings are covered with EVA/Craneglas to insulate the cells from the longitudinal conductors as they are folded back over the cells and brought into a position where the ends of the conductors can be brought through the dark side layup.

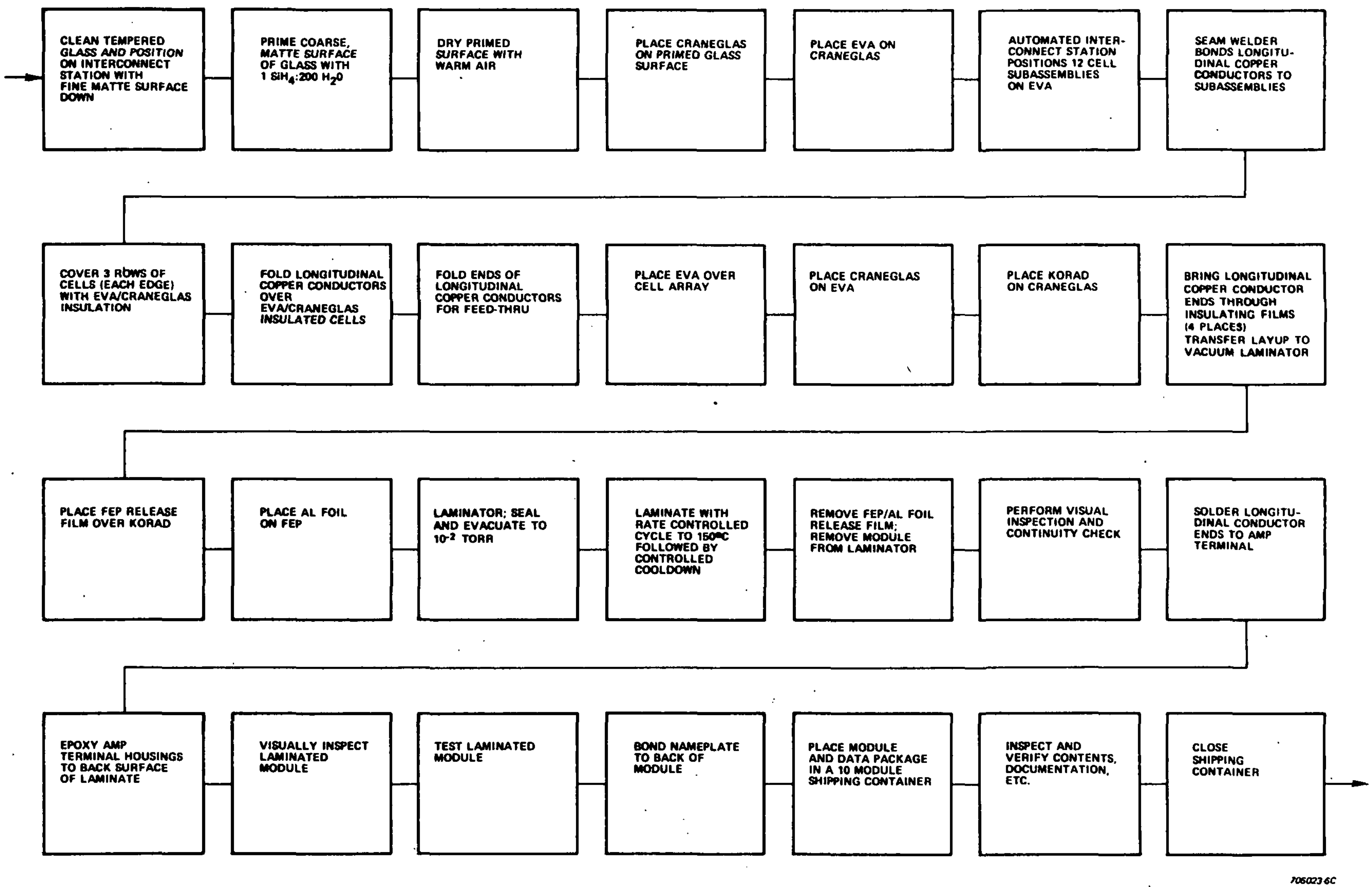

Figure 18. Westinghouse MEPSDU Module Assembly Flow Chart

5. Dark Side Layup Installation - A layer of EVA pottant is placed over the cell array. This is followed by the positioning of a layer of Craneglas and installation of the back cover film of Korad. The ends of the copper longitudinal conductors are brought through each of these insulating films as they are placed in position. The final layup is transferred (sunside down) to the vacuum laminator.

6. Lamination - Release films of aluminum foil and fluorinated ethylene propylene copolymer (FEP) are placed over the module layup, and the module is moved to the vacuum bag laminator. This laminator consists of two separate compartments which can be individually evacuated or pressurized. These compartments are separated by a flexible rubber diaphram. With the module in the lower compartment, the laminator is sealed, both compartments are evacuated to 10^{-2} torr, and the temperature raised to 110°C in less than 30 minutes. At this point, the upper compartment of the laminator is vented to atmospheric pressure which forces the rubber diaphram over the module producing a uniform pressure. The temperature is raised to 150°C, and then the system is cooled to room temperature. The FEP/Al foil release films are removed, and a visual inspection and electrical continuity check performed.

7. Electrical Terminal Installation - Pre-tinned electrical terminal end conductors are soldered to the two bus bars. The back cover/end conductor penetrations are enclosed by a conductor housing that is attached to the back surface of the laminate using an epoxy adhesive formulated for this service.

8. Inspect and Test - A visual inspection of the assembled module is performed, and the current-voltage characteristics of each module are measured at AM1, 100 mW/cm^2 and 25°C.

9. Nameplate Installation - A nameplate containing identification and electrical characteristics is attached to the back of the module.

10. Module Packaging - Acceptable modules are crated for shipping. Each shipping container holds ten modules and their respective data packages. The contents of each shipping container are verified, and the container is closed.

Verification of the adequacy of the Baseline Process Sequence was established during the course of the MEPSDU contract. This verification was achieved by:

1. Calculating all cost factors associated with each step of the process sequence and, using SAMICS methodology, determining that an overall production cost of 70¢/peak watt (1980$ in 1986) was achievable in a large scale, fully automated production facility (see Section VII).

2. Fabricating mockups or full sized modules using the Baseline Process Sequence and testing to ensure compliance with environmental specifications contained in JPL Document 5101-138 (see Section III).

3. Fabricating a full size prototype module using the Baseline Process Sequence and testing to ensure that the 12 percent overall efficiency level used in the economic analysis could be achieved (see Section III).

B. Alternate Process Sequence Steps

During the course of the MEPSDU contract, several alternates to steps defined in the Baseline Process Sequence were evaluated in an attempt to demonstrate the potential for reducing processing or production costs below the level evaluated for the baseline sequence.

1. Alternate Metallization Procedures

1.1 Evaporated Systems

The initial baseline Westinghouse MESPDU process sequence specified a metallization system comprised of evaporated layers of Ti, Pd, and Ag followed by an electroplated layer of Cu. An in-house effort was directed toward the study of alternate metallization schemes which could improve the cost effectiveness of the baseline metallization system by reducing costs of the metals used or identifying less expensive equipment for applying the metals.

The first modification studied was the replacement of the evaporated layer of silver with copper. An evaporated Ti/Pd/Cu plus electroplated Cu metallization system was presented as part of the initial baseline process sequence at the Preliminary Design Review. At that time, the possibility of etching the evaporated copper to provide a fresh surface for electroplated copper (with the intent of eliminating the need for plasma ashing equipment) was under consideration. In reviewing the evaporated Ti/Pd/Cu process, it was noted that contamination of the titanium and palladium targets could occur duirng the vacuum evaporation of copper and that eliminating this posisbility by depositing copper in a separate chamber was not cost effective. Therefore, a test was made to change the baseline metallization system to evaporated Ti/Pd, plasma ashing, electroplated copper. Experiments verified that this system, comprised of 500 Å Ti, 500 Å Pd, and about 8 microns of copper had excellent adherence on both the front (grid) and back surfaces and was incorporated into the MEPSDU baseline metallization system.

1.2 Non-Evaporative Metallization Systems

Scoping work on several significantly modified metallization systems to the baseline evaporated Ti/Pd/Plated Cu process was also performed on the MEPSDU contract. This scoping work narrowed the number of systems that were given experimental follow-up to two: (1) electroless nickel deposition on evaporated titanium, and (2) electroless nickel deposition on silicon after proper activation of the surface. In the Westinghouse MEPSDU sequence, particular attention must be given to the effect of aggressive etching or activating solutions upon not only the shallow junctions but also upon the AR and PR coatings which are applied before metallization. This is of greatest concern in the deposition of electroless nickel directly on silicon. Two vendors assisted in these follow-up experiments.

In the first case, that of electroless nickel deposition on evaporated titanium, the etchants employed by the vendor were too aggressive and etched through the evaporated titanium film. This approach was abandoned. In the second case, that of electroless nickel deposition on silicon in the presence of AR and PR

167

coatings, both vendors cited attack of the PR coating in the heated (approximately 90°C) electroless nickel baths. (Both vendors were working with silicon web that was supplied to them by Westinghouse after AR/PR coating, pattern exposure, development, and oxide etching. The PR coating had received the standard soft bake for 15-20 minutes at 90°C.)

Subsequent work continued with one of the vendors on the deposition of electroless nickel on silicon. Investigations included: (1) deposition of electroless nickel on a patterned sample given a post-bake treatment to improve the chemical and heat resistance of the PR coating, and (2) deposition of electroless nickel on silicon followed by the use of a negative resist.

A proprietary, highly alkaline nickel activating solution that showed promise on bare silicon was found to be too sensitive to deposition conditions to be used as a production process. Because the solution was highly alkaline, it also attacked the post-baked positive PR coating and, therefore, could not be used on partially processed samples. Additional work by the vendor yielded a new process that was claimed to be very reproducible with very few voids and with improved adhesion to silicon.

Using this process, numerous in-house experiments were conducted. In all cases, the inability to deposit a continuous, adherent nickel film on the web in a minimum number of process steps has made this approach less attractive than the reliable evaporation process identified in the baseline sequence. These results, in conjunction with results of a separate DOE/JPL sponsored program (Contract No. 955624) conducted recently at the Westinghouse R&D Center which suggest that nickel is not an effective long-term diffusion barrier for copper, led to abandoning the use of electroless nickel on the Westinghouse MEPSDU.

2. Dry Processing Experiments

An investigation into the use of dry plasma processing was carried out to replace many of the wet chemistry steps identified in the baseline process sequence. These steps include oxide removal from as-grown web, pre-diffusion

cleaning, and surface clean up prior to metallization and plating. In the plasma etch operation, the active species formed by an rf glow discharge react with impurities on the silicon surface and are removed as volatile products that are pumped from the system. The as-grown web has a coating of both a loose and an adherent oxide which must be removed before the first pre-diffusion cleaning. Therefore, these studies were concerned with both the standard pre-diffusion cleaning and oxide removal plus pre-diffusion cleaning.

Scoping experiments using raw web indicated that an agitated HF dip is inadequate in removing both loose and adherent oxide. However, both types of oxides are removed by lightly rubbing the surface with an HF saturated swab prior to plasma etching. Samples which had the best plasma etched appearance were processed in standard 96% CF_4:4% O_2 etching gas for 2 min. at 300 watts or 10 min. at 100 watts. Those processed for longer times or at higher powers exhibited roughening of the surface.

A test was made in which three sets of samples were pre-diffusion cleaned as follows:

Group I - Web wiped with cotton swab and plasma etched.
Group II - Web wiped with HF/H_2O and plasma etched.
Group III - Web given standard semiconductor pre-diffusion cleaning.

These groups, containing a total of 32 cells, were then processed together through the Westinghouse Pre-Pilot Facility. The standard baseline process was used for all other operations.

Web from Group I (dry wiped with a cotton swab to remove loose oxide) had, in many cases, a post-plating copper haze and yielded cells of poorer quality than did web swabbed with the acid solution. In general, cells produced from web given an acid swab and a plasma etch were equal to those produced from web given the standard semiconductor pre-diffusion cleaning process, which verifies the selection of the plasma technique in the Baseline Process Sequence.

169

Screening tests were performed by a vendor to establish conditions for cleaning raw web by plasma processing. Their findings were similar in that using the standard 96/4:CF_4/O_2 etching gas without prior oxide removal, the silicon surface is not uniformly etched. Table 11 summarizes their results.

After 50 min. of etching with a 30/70:CF_4/O_2 plasma at 85 watts R.F. power, there was no SiO_2 powder present; and, although there was a suggestion of a nonuniform adherent oxide, the surface had a reflectivity similar to web cleaned by standard wet chemical techniques. However, the time is considered excessive for cost effective processing; and, therefore, a combination of wet chemical/plasma etch processing was pursued.

Work on this task was then focused on developing a non-contact cleaning method to replace web scrubbing operations. Samples were sent out for vendor trials of cleaning in a "Megasonic" unit to determine if it will effectively remove oxide particles from the web surface in preparation for plasma etching. In these trials, a Megasonic cleaner modified (a vitreous carbon faceplate was substituted for the standard tantalum faceplate) for use with HF was filled with a solution of 1 part of HF in 10 parts of water and agitated. Samples of dendritic web with growth oxide on their surfaces were placed in the solution (equilibrium temperature of 45°C) for times up to 9 minutes. Samples processed in this manner were not completely free of loose oxide; however, there was an improvement with time. Thus, the need for longer immersion times, stronger solutions, or other solutions was indicated.

While arrangements were being made for follow-up trials, the vitreous carbon faceplate in the transducer array panel failed; and the vendor's original customer switched to an acid other than HF for his etching and, therefore, could use a standard Megasonic unit. Because of the high cost of preparing a new faceplate, the vendor decided not to repair the equipment without customer support. The cost of this repair to run additional trials without assured success was beyond the means of the MEPSDU contract; and, therefore, a new approach using a standard Megasonic cleaner and an altered sequence was currently under consideration at the time work was stopped on the MEPSDU contract.

170

TABLE 11

PLASMA ETCHING OF RAW WEB

Plasma	Pressure (torr)	R. F. Power (watts)	Time (min.)	Comments
Argon	.4-.6	300-500	2-15	No reaction.
96/4:CF_4/O_2	.3	300	2-6	Non-uniform surface attack.
30/70:CF_4/O_2	.1-.3	85-400	1-50	Best results obtained at 85W and times in excess of 5 min.
5/95:CF_4/O_2	.3-.4	250-350	5-10	Surface clouding due to excess oxidation.

171

At the present time, the baseline sequence incorporates an HF scrub for oxide removal before proceeding to the first pre-diffusion cleaning. Automated equipment is available for this scrubbing operation, and this equipment is being considered for the Westinghouse semi-automated production line. The experiments discussed previously, however, showed that an acid dip and plasma etch is a suitable, cost effective step for pre-diffusion cleaning.

3. Liquid Precursor Films for Diffusion Masks

The baseline process sequence specifies a chemical vapor deposited SiO_2 film to be used as a diffusion mask prior to the two junction diffusion processes. This mask is required to allow diffusion in only one surface of the web (front or back) at a time. Although the formation of an SiO_2 film from silane oxidation produces an effective diffusion mask on one side of the web, there is always some spotty deposition on the reverse side; and a quick acid dip is required to provide a clean surface for diffusion. A film from a liquid precursor, however, can be applied to one surface and, thus, eliminate the acid clean up.

In the initial experiment, the Westinghouse antireflective (AR) coating (a TiO_2-SiO_2 solution in alcohol) was used as a diffusion barrier. There were two groups of web used in the experiment with the antireflective coating: Group No. 1 used the standard SiO_2 (Silox) masking before boron and phosphorous diffusion, and Group No. 2 had the Westinghouse antireflective coating solution painted on one side of the web before diffusion.

It was difficult to etch the antireflective coating from the web after diffusion, particularly after phosphorous diffusion. In order to process this group into cells, it was necessary to acid scrub to remove the coating; and this procedure gave cells that were slightly discolored.

Test data from the cells indicated that the antireflective coating does act as a diffusion mask in that the measured cell parameters from the two groups were the same. However, the etching behavior of the coating precludes its use in a production facility.

A second diffusion barrier experiment was then performed in which a modified Westinghouse AR coating was used as a diffusion barrier. This solution contained only an SiO_2 precursor, and the film formed from this solution did not completely oxidize in the diffusion furnace. Therefore, in contrast to cells masked using the standard Silox process, the cells were contaminated with carbon and gave very poor results in the subsequent gaseous diffusion processing steps. This diffusion masking method shows promise, but more control over the initial coating material and application is required.

4. Liquid Dopant Diffusant Studies

Gaseous diffusion of boron and phosphorous to form the solar cell back and front junctions respectively is specified for the MEPSDU Baseline Process Sequence. Since these diffusions must be done at significantly different temperatures (960°C for boron, 850°C for phosphorous), the diffusion processes require separate furnaces, significant web handling, etc. Although gaseous diffusion produces high efficiency cells and has been shown to meet the JPL/DOE cost goals, an alternative technique using doped liquid precursors as diffusion sources was investigated.

Initial experiments were conducted using several commercial grade dopants having different concentrations. Web coated with these dopants was processed at different temperatures to determine if suitable sheet resistivities for the n+ and p+ surfaces could be obtained. The main emphasis in the initial phase of the study was placed on finding materials and concentrations which would yield the proper sheet resistivities* when diffused at the same temperature for the same time period. This would allow simultaneous diffusion of the p-type and n-type dopant source in a single furnace. Based on results of these experiments, more extensive tests were made using a commercial liquid dopant which in the early experiment showed promise.

The tests were carried out as follows:

a. Boron dopant applied to one side of web strip and baked at 200°C.
b. Phosphorous dopant applied to opposite side of web strip and baked at 200°C.

---

*The MEPSDU specifications for sheet resistivity are:

Boron doped p+: 40 ±10 Ω/□
Phosphorous doped n+: 60 ±10 Ω/□

173

c. Web strip heated in an 80% N_2 - 20% O_2 ambient at 900-960°C and then slow cooled to 700°C.

d. Baseline Process Sequence used to finish processing strip into cells.

The first group of cells processed in this experiment had sheet resistivities which fell out of the given specification, with the p+ resistivity being 70-150 Ω/□ while the n+ resistivity was 25-35 Ω/□.

The efficiency of the cells processed from these diffusion experiments was 10.4 ±0.6% with a maximum efficiency of 11.3%. The efficiency was generally inversely proportional to the p+ sheet resistivity.

Several subsequent tests were made using liquid dopants from different suppliers and having different dopant concentrations. Table 12 gives the results from several of these tests. The table shows that cells fabricated from the same web growth run using liquid dopants have consistently lower efficiencies as compared to those fabricated using the gaseous diffusion process of the Baseline MEPSDU Process Sequence. This lower efficiency is due in part to non-optimum n and p sheet resistivities (p+ sheet resistivity is high by 25-50% while n+ is low by 25%).

Another factor which became more obvious during these tests is the poor surface quality of many of the cells after diffusion. This surface problem leads to irregular coverage of the AR coating and poor Cu plating in subsequent processing steps. This surface effect is believed due to the technique used for applying the liquid doapnt. In tests conducted to date, the dopant has been applied using a sponge-squeegee method. After diffusion and diffusion glass removal, streaky surface color irregularities are noted which are apparently related to the dopant application. These same irregularities are then noted after the AR coating and electroplating step.

To eliminate this surface condition, alternate techniques for liquid application to dendritic web were investigated. Both paint-on and spin application techniques were pursued. The results were again unsuccessful due to nonuniform coverage of the liquid. Finally, experiments were initiated in which the liquid precursor was applied using a meniscus coating* application technique.

*Commercial equipment using this coating method has been developed by Integrated Technologies, Acushnet, MA.

.17

9950-892

TABLE 12

COMPARISON OF CELLS PRODUCED USING THE BASELINE PROCESS
(GASEOUS DIFFUSION) AND LIQUID DOPANTS

Web Growth Run		Web Quality (Efficiency - %)		
No.	Designation	Baseline Process η_o	Liquid Dopant η_1	η_1/η_o
1	6·100	---	12.1	---
2	4·81	12.6	8.2	.65
3	1·120	12.9	10.6	.82
4	4·82	13.8	7.1	.51
5	7·47	11.3	10.6	.94
6	5·102	13.9	10.9	.78

NOTES: 1. All cells - 2.0 cm x 9.8 cm.
2. Tested at AM-1; 100 mW/cm^2.

Figure 19 is a schematic drawing of the meniscus fluid coater. The fluid is applied to a porous applicator. The substrate (web) is drawn across the top of the fluid meniscus which forms at the top of the applicator. The thickness of the meniscus (dimension t in Figure 19) is greater than the radius of web dendrities, and the fluid is applied evenly on the surface of the web. The application experiments were performed by the meniscus coating equipment vendor. It is anticipated that this application technique can be used for liquid dopants, antireflective coatings, and photoresist coatings as well as diffusion masks.

Due to the potential high payoff advantages associated with liquid junction formation and liquid application techniques, this research work was selected by JPL for continuation beyond the stop work date of February 10, 1982. Thus, this report does not finalize efforts in this area.

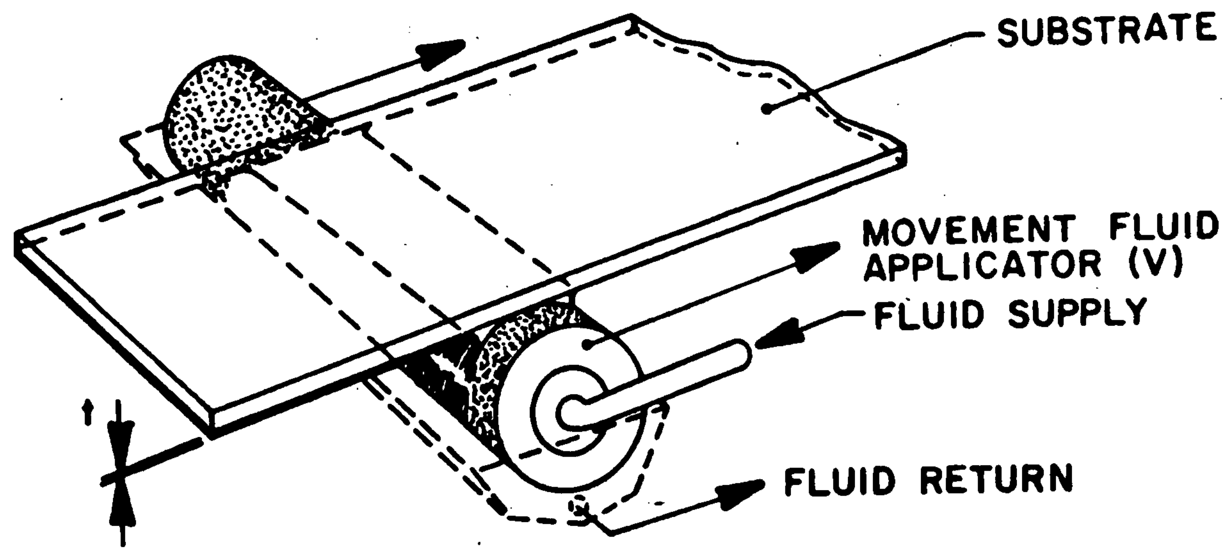

Figure 19. Meniscus Coating of Precursor Fluids to Dendritic Web Silicon

VI. MEPSDU DESIGN

A. General

As specified by the MEPSDU contract, demonstration of technical readiness of the Westinghouse photovoltaic module production process was to be achieved by designing or specifying and procuring all equipment required to fabricate modules using the specified process sequence. Primary engineering effort was focused on this phase (design and specification) at the time the stop work order was received from JPL on February 10, 1982. This section of the report summarizes the status of each Westinghouse MEPSDU process station as of that date.

In the case of equipment to be procured outside Westinghouse, purchasing specifications were prepared in accordance with Westinghouse Equipment Specification (E-Spec) procedures. The E-Specs are formal Westinghouse documents signed by appropriate Westinghouse management personnel, and the document follows rigorous configuration control procedures. Each E-Spec contains the following information:

1. Throughput of web required (200 cm^2/minute)
2. Process requirements
3. Control requirements
4. Reproducibility requirements
5. Operation and maintenance manuals requirements
6. Preventative maintenance schedule
7. Recommended spare parts inventory
8. Installation and training requirements

B. Pre-Diffusion Cleaning

The Baseline Westinghouse Process Sequence specifies a simple, efficient and cost effective process for pre-diffusion cleaning of dendritic web silicon. This two-step process consists of an acid dip followed by a plasma etch.

The etching station consists of a series of commercially available plastic tanks into which the dendritic web strips, mounted in plastic racks, are

immersed in HF and DI water for initial cleaning. After etching, the strips of web are unloaded from the plastic racks and placed in quartz boats for plasma cleaning.

As described in Section V of this report, substantial investigative work was underway to replace wet chemical cleaning operations of the baseline process sequence with dry processing operations at the time of the stop work order. Because of this effort, preparation of equipment specifications for this operation had not been initiated.

C. Junction Formation Station

Gaseous diffusion of boron and phosphorous is used to form the back and front junctions respectively of the Westinghouse solar cells as specified in the MEPSDU baseline process sequence. The diffusions are carried out in a standard 5" diffusion tube furnace commercially available from numerous vendors.

An equipment specification was prepared for the diffusion furnace system required to perform front and back junction formations, as included in the baseline process sequence. Firm fixed price quotations were received from four vendors prior to receipt of the JPL stop work order.

In addition to the diffusion furnaces, a preliminary E-Spec was prepared for the CVD SiO_2 (Silox) reactor, which is required to deposit an SiO_2 diffusion barrier on the web strips prior to the diffusion step to prevent simultaneous front and back side diffusion. However, as discussed earlier in this report, it was hoped that this equipment would be replaced by a liquid meniscus coating apparatus; and vendor quotations to the E-Spec were not solicited.

After diffusion, an oxide etch is used to remove the phosphorous glass coating on the surface of the dendritic web strip. The web strips are removed from the quartz boats and placed in plastic racks similar to those used in the pre-diffusion cleaning operation. This station is the same as the first station in the pre-diffusion cleaning process and has the same throughput. Immersion of the diffused web into plastic tanks containing dilute HF and DI water

removes the boron or phosphorus glass that is formed on the web during diffusion. After the water rinse, the web is dried in a warm air stream.

D. Antireflective (AR) and Photoresist (PR) Application Stations

The Westinghouse MEPSDU baseline process sequence requires sequential application of two coatings to the surface of the dendritic web sqrips immediately after junction formation and removal of the diffusion oxides.

During the course of the program, an unsolicited proposal was received from a vendor for the design and fabrication of a device which will automatically dip a batch of web strips into the AR solution, withdraw the strips, hard bake the AR coatings, dip the batch of strips into the PR solution, and bake the PR coatings. The equipment would have the throughput capacity of the Westinghouse MEPSDU line and would require a single load and a single unload operation.

In the proposed system, two dipping tanks and two baking ovens would be used following techniques proven on the Westinghouse 50 kW Pre-Pilot Line facility. The four pieces of equipment (two tanks and two furnaces) are placed in a row with a support track overhead. The tanks are plastic, and the bake furnaces are commercially available, upright, open top furnaces.

The rate of withdrawal from the solution is controlled using a motor-driven screw mounted above the track which is moved along the tank. The motor has a reversible, wide range speed control for rapid motion or slower precision operation. Attached to the screw drive is a fixture, holding web lengths in a vertical position, much as a candle dipping procedure. The fixture will hold 60 pieces of web in a 10 x 6 matrix.

In operation, the web strips are fastened to the fixture, placed on the movable screw drive, and moved into position above the antireflection coating solution tank. A simple program logic controller processes the web through the four stations in the following sequence.

1. Rapidly dip dendritic web into the antireflection coating and remove at a controlled rate (≈ 2 cm/min)

2. Horizontal translation of fixture above antireflection coating bake furnace

3. Rapidly lower web into bake furnace and hold (10 min)

4. Rapidly withdraw web from bake furnace

5. Horizontal translation of holding fixture to above photoresist tank

6. Rapidly lower web into photoresist coating and remove at a controlled rate (2 min)

7. Horizontal translation of fixture above photoresist bake furnace

8. Rapidly lower web into bake furnace and hold (14 min)

9. Remove from bake furnace and translate to end of line

The total processing time will be 28 minutes per fixture including translations, and the throughput rate exceeds the 2 web strip/minute (8 cells/min) throughput required for 1 MW/yr.

A second vendor initiated efforts to establish process parameters for applying AR and PR coatings in a meniscus coating system as described in Section V of this report. Conversations with the vendor indicate that progress was being made toward uniform coatings of the required thicknesses and that samples of coated material would soon be returned for evaluation. This coating technique is of interest because it can apply coating to only one side of the web and can be easily adapted to form part of an in-line processing system in the MEPSDU coat, bake, expose, develop, and etch sequence.

E. Expose/Develop/Etch Station

Standard photolithographic techniques of masking, exposing, developing, and etching are used to define the electrical contact grid pattern on the front surface of the Westinghouse solar cell.

The station consists of exposure of the photoresist (PR) applied in the previous station, development of the exposed PR, and etching of the exposed antireflective (AR) coating. The process produces a grid pattern on the n+ silicon of the front web surface and a clean p+ back surface.

Since the baseline process for applying both the PR and AR is by dipping which coats both sides of the web strip, both sides of the web must be exposed, developed, and etched.

On the n+ front surface, the PR is exposed through a contact mask which is a positive print of the grid structure. The p+ back surface is totally exposed. During the development, the exposed PR is removed; and a grid pattern (down to the AR layer) is obtained on the front surface, and the AR on the back surface is exposed. The final step in the process is a mild HF etch which removes the AR from the back surface and from the grid pattern on the front surface. After rinsing and drying, the web strip is ready for metallization.

In the Westinghouse MEPSDU, a concept for the exposure system is being discussed with a vendor. In this preliminary design, 4-8 strips of 42 cm long web are loaded onto a fixture and held in place by vacuum. A hinged lid, containing the proper masks, is lowered over the web strips with the masks mating to the proper place on the web. An exposure lamp then traverses the web strips exposing the grid pattern. To expose the back, the strips are turned over and exposed without the masks.*

---

*As discussed in the previous section, application methods are presently being investigated where the PR and AR are applied only to the front surface. If this technique is satisfactory, exposure on the back will not be required.

The second piece of equipment for this station is a development and etching apparatus. For this process, a standard semiconductor processing station, modified to accept the long web lengths, will be used.

The web will be loaded into baskets and cycled through 5 substations: (1) developing solution, (2) DI H_2O rinse, (3) etching solution, (4) DI H_2O rinse, and (5) hot air drying station. The length of time at each substation will be controlled and programmed.

Several vendors of automated equipment performing all operations of the five identified substations have been contacted. In each, modifications would be required to accommodate the dimensions of the Westinghouse dendritic web strips. However, no problems are anticipated in engineering the machine to these specific requirements. In point of fact, nearly all units sold by the various vendors are modified to some extent.

E-Specs for the two pieces of equipment associated with the expose/develop/etch station were being prepared at the time of the JPL stop work order.

F. Metallization Box Coater

An E-Spec was prepared for the electron beam evaporation system required to perform base metal applications (Ti/Pd) as included in the baseline process sequence. The system would deposit these layers on both the front and back sides of the web. The machine needed for this station would be built from standard components (EB guns and power supplies, valves, pumps, thickness controllers, etc.) and engineered to the requirements of the E-Spec.

Highlights of the equipment requirements are summarized in Table 13. These requirements are well within commercial practice of large area, high throughput metallization system manufacturers. Commercial operating systems using electron beam evaporation have the capability of coating several hundred square meters per hour with a machine up time of greater than 90%.

TABLE 13

METALLIZATION BOX COATER SPECIFICATION HIGHLIGHTS

- Automatic operation
- Compartment deposition chamber with three evaporation stations (Temescal or equivalent SFIH-270-3 electron beam guns, 156 cc crucible capacity, single jacket)
- Diffusion pumped system (2-3 diffusion pump stations) with LN_2 traps or cryopumped system
- Process chamber at 1×10^{-6} torr or less during evaporation
- Film thickness control by EB gun power level and line speed (with quartz crystal monitors for initial set up and periodic checks)
- Full automation by relay logic or solid state (to be evaluated)
- Recommended spare parts inventory
- Vendor conducted training program on equipment operation and maintenance
- Detailed operating and maintenance manuals
- Optional conversion to planar magnetron sputtering by installing sputtering cathode, power supplies and argon backfill hardware

184

Firm fixed price quotations for the metallization box coater system had been received from five vendors prior to the JPL stop work order. Each of the proposed systems was responsive to the specification.

G. Metal Rejection/Plating Station

To insure minimum cost, the Westinghouse MEPSDU will carry out the rejection of the excess base metals applied to the front surface of the cells and the addition of copper plating to the grid lines and back side surface in a single unitized process station.

The rejection process uses acetone or other suitable solvent to dissolve the unexposed photoresist on the cell front surface, flushing away excess metal and leaving the grid delineated.

The use of such a plating station is well esbablished. A similar (although larger) station is used by Westinghouse for plating battery grids. Its reliability has been established in over 10 years of routine, successful operation.

As noted in the cycle specification below, the MEPSDU rejection and plating station will consist of a series of 12 operations as shown in Table 14. Similar to the process station for antireflection coating and photoresist coating and baking, an overhead conveyor system will carry the web, loaded in racks, through the various tanks where a specific process will be performed.

A program logic controller will control the rate of progress of the web through the various tank stations with the program alterable at any time in the process. Thus, after the web is located on the fixture and the fixture enters the line, it will automatically progress to the end of the process step.

The dendritic web holding fixture will consist of a matrix of individual plastic holders with electrical connections to the web. Due to the high conductivity of the n+ diffused layer, contact can be made to any portion of the web where there is evaporated metal, e.g., on the dendrite outside the mask area. This eliminates tedious hand positioning of the electrical connection clips.

155

TABLE 14

REJECTION/PLATING STATION TREATMENT CYCLE

Operation Number	Description	Approximate Time
1	Load/Unload	7 Minutes
2	Acetone Bath	3 Minutes
3	Acetone Spray	1 Minute
4	Alcohol Spray	1 Minute
5 & 6	Deionized Water Rinse	Dip
7 & 8	Copper Plate	15-1/2 Minutes
9-10 & 11	Deionized Water Rinse	Dip
12	Hot Air Dry	7-1/2 Minutes

9950-892

H. Cell Separation Station

In the Westinghouse MEPSDU process sequence, the separation of the four discrete solar cells from each dendrite-web matrix is accomplished by scribing the cell outline on the back of the web strip and fracturing out the individual cells. This scribing is accomplished using a Nd-YAG laser to penetrate into the back surface of the web strip about one third of its thickness.

An equipment specification for a laser scribe suitable for the MEPSDU throughput was prepared. Quotations were received from three vendors. A formal vendor selection was made, and a contract for this station was placed with Quantronix Corporation.

The laser scribe system described in the equipment specification consists of the following elements:

1. Nd-YAG laser powered by krypton arc lamps

2. Positioning fixture such that the web can be aligned to assure proper scribing directions and distances. This alignment is specified to be automatic - the operation constrained only to placing the web strip in a defined area. (This item is of prime importance in meeting the MEPSDU throughput requirement.)

3. A control unit which can be programmed to drive the fixture (or move the laser beam) through the required scribing path.

Figure 20 shows the layout of the automated laser scribe to be incorporated into the Westinghouse MEPSDU cell separation station. The system consists of a control unit, a power supply, and an opto-mechanical unit.

Table 15 lists the novel features of the Quantronix laser scribe. The most significant item in meeting the MEPSDU throughput requirements is the automatic alignment system, the key features of which are itemized in Table 16.

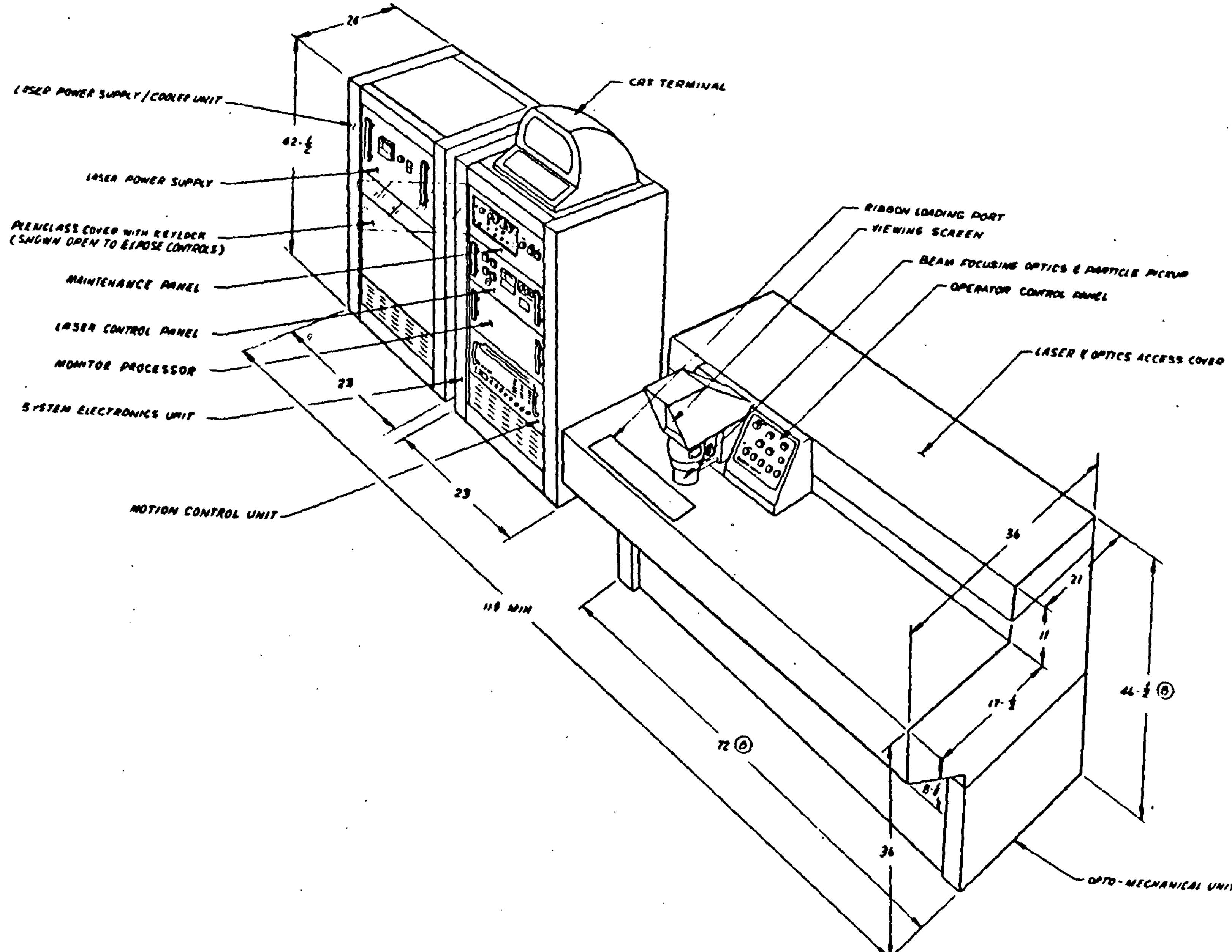

Figure 20. Automated Laser Scribe

TABLE 15

NOVEL FEATURES OF THE WESTINGHOUSE MEPSDU FACILITY LASER SCRIBE

* AUTOMATIC ALIGNMENT DETERMINATION INVOLVING STRIP POSITION MEASUREMENT AND SCRIBE PATTERN TRANSFORMATION RATHER THAN PHYSICAL MOTION OF THE STRIP ("INERTIALESS CORRECTION").

* A LARGE X-Y MOTION SYSTEM CAPABLE OF MOVING AN ENTIRE FIELD OF POSSIBLE STRIPS UNDER THE LASER BEAM.

* A VERSATILE TERMINAL DATA INPUT SYSTEM TO ALLOW FLEXIBILITY.

* SIMPLIFIED OPERATOR CONTROL AND EASY LOAD/UNLOAD ACCESS.

* NO EXTERNAL FIXTURES OR STRIP PREPARATION REQUIRED DURING LOAD/UNLOAD CYCLE.

189

TABLE 16

MEPSDU LASER SCRIBE AUTOMATIC ALIGNMENT SYSTEM FEATURES

* HIGH SPEED ACQUISITION OF COORDINATES OF FIDUCIAL MARKS ON CELL BY MEANS OF TABLE MOTION SCAN IN CONJUNCTION WITH CCD LINE SCAN CAMERA.

* HARDWARE PATTERN RECOGNITION OF CENTROID OF FIDUCIAL MARKS IN CROSS-SCAN AXIS BY DIGITAL TEMPLATE MATCHING.

* ACQUISITION OF CENTROID OF FIDUCIAL MARKS IN ALONG-SCAN AXIS BY MICROPROCESSOR CONTROL.

* RELATIVE IMMUNITY TO SPURIOUS SIGNALS DUE TO SPATIAL DISCRIMINATION ALONG TWO AXES.

* DISCRIMINATORS DESIGNED TO TOLERATE ELECTRONIC DROPOUTS DURING DATA ACQUISITION.

190

Table 17 presents time budgets for each phase of the laser scribe operation. With these time budgets, each strip of web material will be scribed into 4 cells in only 25 seconds. Thus, operating the system 22 hours per day, 340 days per year will produce the required cells for 1 MW production each year.

A Preliminary Design Review of the automated laser scribe was presented by the vendor, Quantronix, during December 1981. The design review was held at Westinghouse AESD and required a full day. Items presented and discussed were: the mechanical system description, arrangement (floor layout) drawings, motion system drive, microprocessor control, alignment pattern, utilities and installation requirements, control software, system flow charts, and operating sequence. Delivery of the unit is scheduled for September 1982.

I. Cell/Module Test Stations

Both the solar cell and module test stations for the Westinghouse MEPSDU were placed on order. The order consists of a M.A.P.S.S. solar simulator (medium area light source) and a semi-automatic cell test system with a digital electronic load to be interfaced with the M.A.P.S.S. data system. Both units are commercially available items manufactured by Spectrolab. Since the MEPSDU line will require testing a cell every five seconds and a module every half hour, it has been rationalized that a single data acquisition system can be utilized to interface with both a small area and large area light source and their associated data channels.

The Spectrolab M.A.P.S.S. module test station was delivered in early January 1982. Installation of the light source and module test fixture has been completed. Initial problems in both the computer test program and the printer have been rectified by the vendor, and final checkout of the unit was completed in February.

TABLE 17

LASER SCRIBE TIME BUDGETS

MANUAL LOAD	3 SEC.	MAXIMUM
AUTO ALIGNMENT	5 SEC.	MAXIMUM
SCRIBING (NOMINAL PATTERN)	14 SEC.	MAXIMUM
MANUAL UNLOAD	3 SEC.	MAXIMUM
	25 SEC.	MAXIMUM, WORST CASE

VII. KULICKE AND SOFFA SUBCONTRACT

A. General

Westinghouse selected Kulicke and Soffa (K&S) Industries, Inc., as its subcontractor for the design and development of MEPSDU equipment dealing with the automation of interconnection and assembly of its dendritic web silicon solar cells into modules. This subcontract deals with design, development, testing, and operation of equipment, and preparation of instruction manuals for the automated interconnect station.

The solar cell electrical interconnect configuration to be utilized by the interconnect station will be thin (.0015") aluminum tabs connecting metallized pads located on the front surfaces of each cell with the metallized rear surface of the adjacent cell. A major innovation in the Westinghouse cell interconnect station is the ultrasonic bonding technology to be used to join aluminum tabs to metallized cell surfaces. A rolling spot bonding technique has been developed by K&S specifically for this application.

As described in Section III of this report, the Westinghouse module will incorporate 12 separate cell string assemblies. Each cell string assembly will contain 15 individual cells electrically connected in series. The 12-cell string assemblies will be positioned by the automated cell interconnect station equipment to form an array of 12 rows of 15 cells each, with nominal dimensions of 16 x 48 inches. The target machine cycle is 5 seconds/cell with a yield of 95% or better. The machine will also include substations for making subsequent parallel or bus bar electrical interconnections of the 12 individual cell string assemblies.

Figure 21 is a schematic of the automated cell interconnect station showing the individual mechanical subsystems. Details and status of the subsystems at the time of the stop work order are described in the following sections.

193

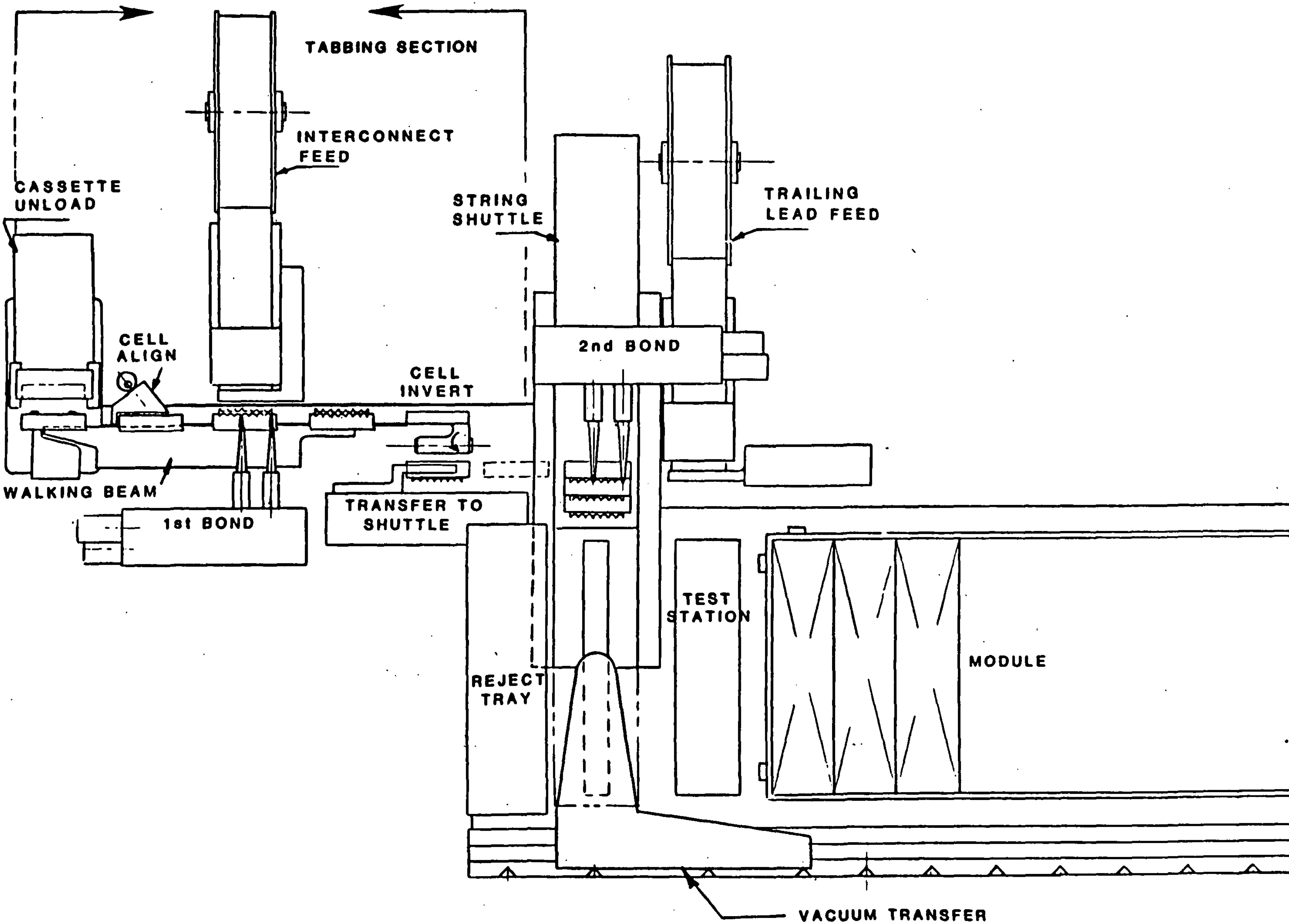

Figure 21. Westinghouse MEPSDU Automated Cell Interconnect Station.

B. Bonder

The heart of the automated cell interconnect station is the bonder. Ultrasonic joining techniques were selected to replace conventional reflow soldering for two primary reasons: first, the ultrasonic bond is performed more quickly allowing increased redundancy of interconnects (8 interconnect bonds are made on each cell), and second, no fluxes are required for the ultrasonic joining process eliminating the need for a post-bond cleanup operation.

During the initial phase of the Kulicke and Soffa subcontract, two ultrasonic bonding techniques were evaluated: rotary seam and rolling spot bonding. Actions of two types of ultrasonic bonders are shown in Figures 22 and 23. Satisfactory aluminum-to-cell bonds were achieved using both methods based on pull test strength and electrical resistance measurements. However, the rolling spot bonding technique was selected for use in the MEPSDU solar cell tabbing and stringing machine for the following reasons:

- Bond Cycle Time - To achieve the minimum throughput rate required with the seam bonding system, the seam roller would have to move from bond to bond at high speed. However, the relatively high mass of the seam roller, as compared to the spot bonding head, makes this high speed movement more difficult.

- Cell Efficiency - Basically, the seam bonding technique accomplishes bonding by a continual rolling motion of the bonding tool. Consequently, additional steps must be taken to prevent the tool from engaging the cell between bonds since this has a negative effect on cell efficiency. To ensure proper operation at the high speeds necessary to meet throughput requirements, this additional action would have to be accomplished in a manner that would also avoid excessive tool impact on the cell. The spot bonding tooling engages the cell only at the bond locations and, therefore, should not cause any decrease in cell efficiency.

- Multiple Heads - To achieve the required throughput with present equipment, it was found necessary to use two bonding heads. The

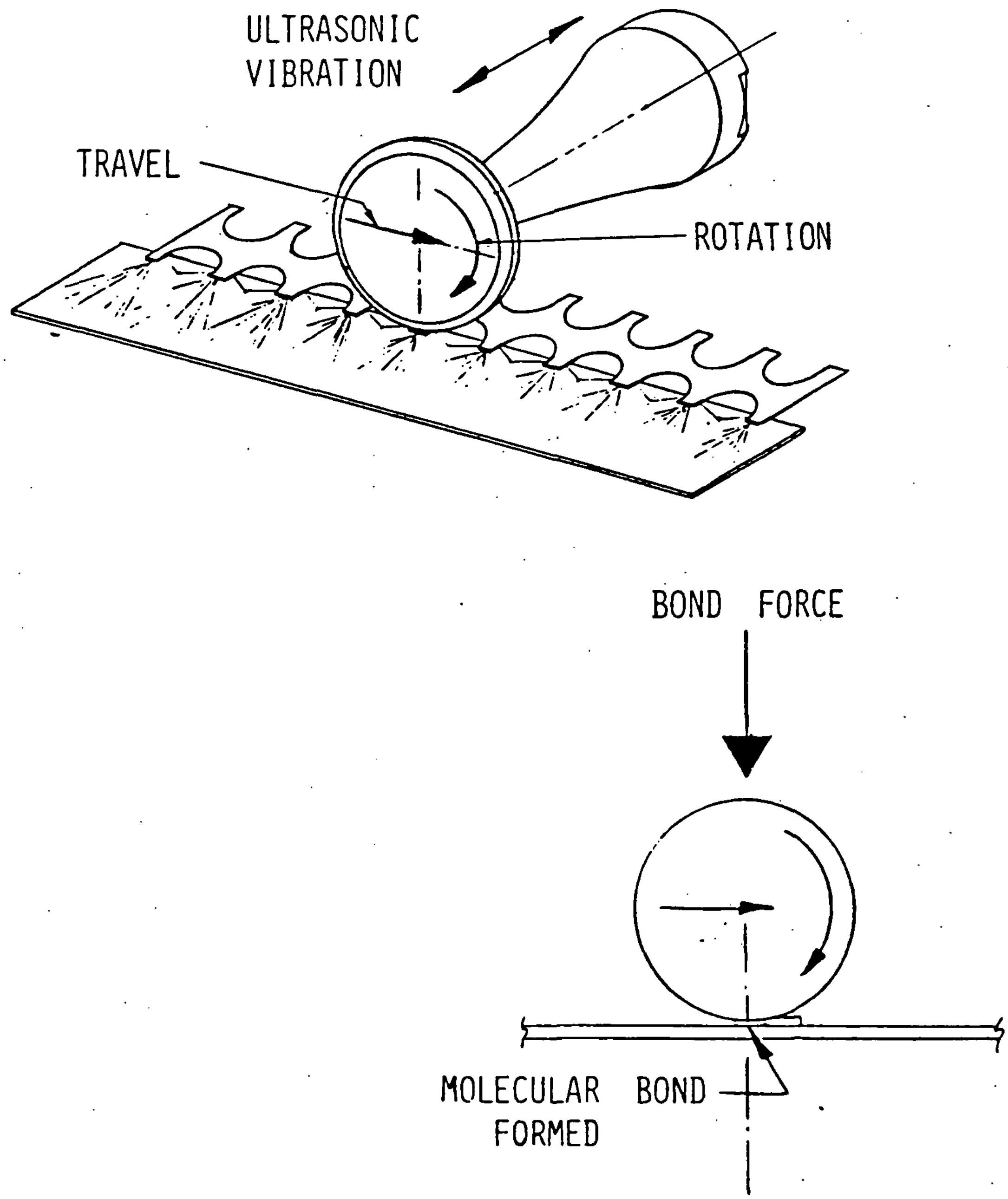

Figure 22. Rotary Ultrasonic Seam Bonding

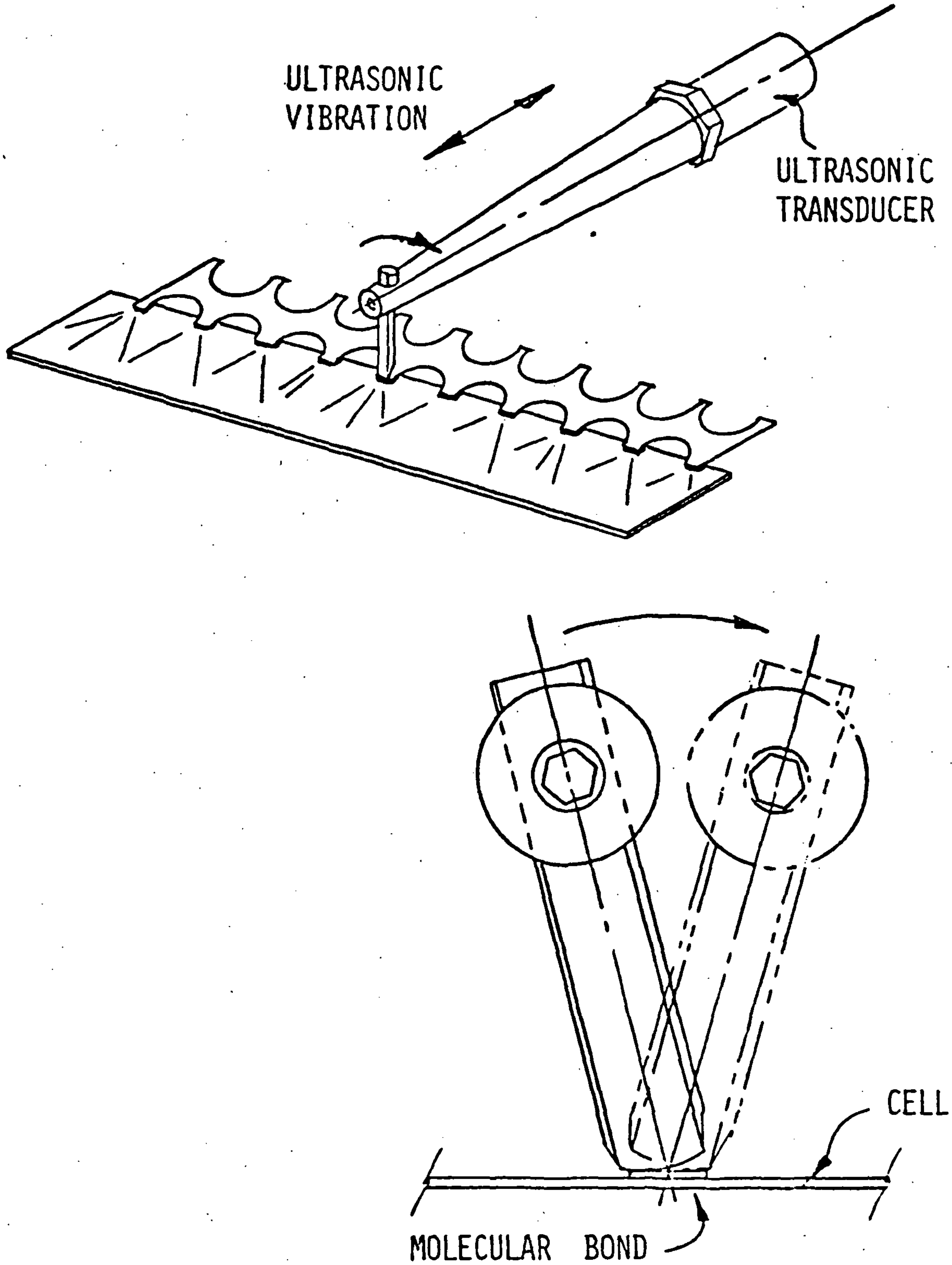

Figure 23. Rolling Spot Ultrasonic Bonding

lower mass of the spot bonding head permits the use of two parallel heads in the same bonding station. This would prove difficult with rotary seam bond tooling.

- Power Range - Present seam bonding equipment operates at the very low end of its capability which mades adjustment both more difficult and more critical. On the other hand, the spot bonding equipment operates at mid-range which is more stable.

- Bond Force - Spot bonding can be accomplished with less bond force than seam bonding. As a result, spot bonding subjects the solar cell to less localized stress which should result in less damage to cells.

- Tooling Flexibility - Tooling changes with the seam roller are limited and expensive since the entire horn must be changed. The spot bonding tools are simple carbide wedges which are inserted into the horn and may be changed easily. In addition, the carbide wedge wears longer than the hardened steel seam roller.

- Cost - The ultrasonic system and tooling required for the seam roller cost approximately ten times more than the ultrasonic generator, transducer, and wedge used for spot bonding.

After completing experimental work leading to the selection of the basic bonding configuration to be used on the machine, work was directed toward the design and fabrication of the actual bonding mechanism to be used for the first bond station. This mechanism is shown in Figure 24. As can be seen, the unit contains two heads: the first performs the bonds on cell pads 1 through 4 while the second head simultaneously bonds pads 5 through 8. Testing of this unit has demonstrated that electrical and mechanical bonds are satisfactory and that bond cycle time is under 2 seconds, which is approximately 30% lower than the budgeted time for this operation.

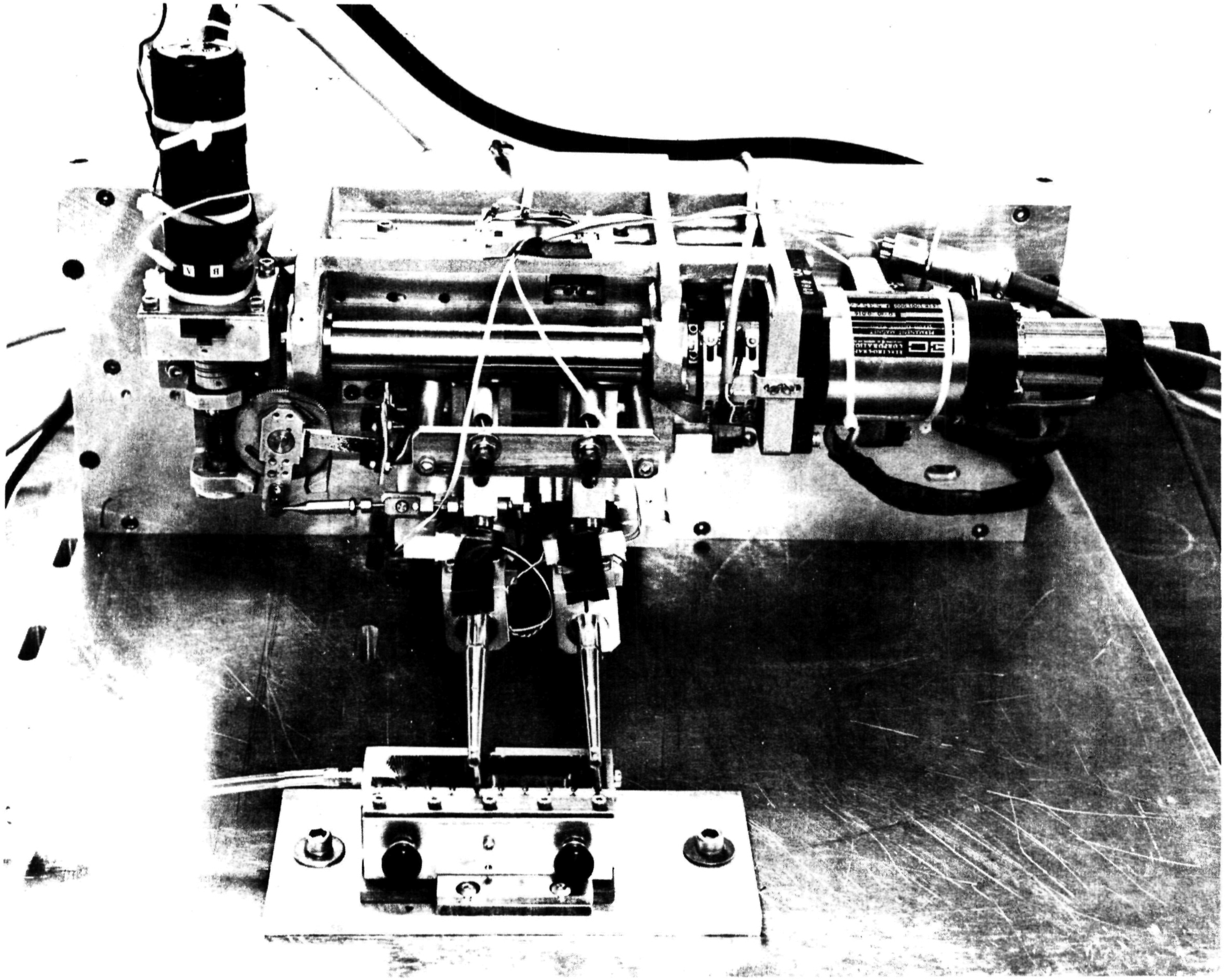

Figure 24. Bonding Mechanism for First Bond Station

C. Cassette Unload Station

Operation of the automated cell interconnect station is initiated with the removal of a single cell from a preloaded cassetee. The cassette is a "coin stack" configuration in which 25 individual cells are stacked one on top of another. The cassette is designed to prevent relative lateral motion of individual cells in order to eliminate potential surface damage.

Figure 25 is a photograph of a mockup cassette unload station built to test the concept. Cells are removed from the cassette using a dual vacuum cup pickup. An air jet is directed laterally on the stack of cells in the cassette to prevent them from sticking together during pickup operations. The cells are transported by the unload pickup device to the walking beam portion of the automated cell interconnect station (see Figure 21).

After the cell is delivered to the walking beam, it is indexed to the alignment station and then to the first bond station.

D. Bond Stations

In the first bond station, the aluminum interconnect is bonded to the pads on the front (sun) side of the cells. The interconnect is fed from a prepunched continuous roll of aluminum foil, sheared, and transferred into position over the cell, and bonded to the cell using the rolling spot bonding device discussed previously.

Figure 26 shows the interconnect feed mechanism loaded with the roll of .0015 inch thick prepunched aluminum foil. The shearing mechanism is shown in the photograph, but the interconnect transfer mechanism is not.

The walking beam conveyor then indexes the cell to an inverter system (refer to Figure 21) which inverts the cell along with its attached interconnect and places it on the string conveyor in position for the extended interconnect to be bonded to the back of the previous cell. This bonding operation is performed with a two-head rolling spot bond device which is essentially identical to the

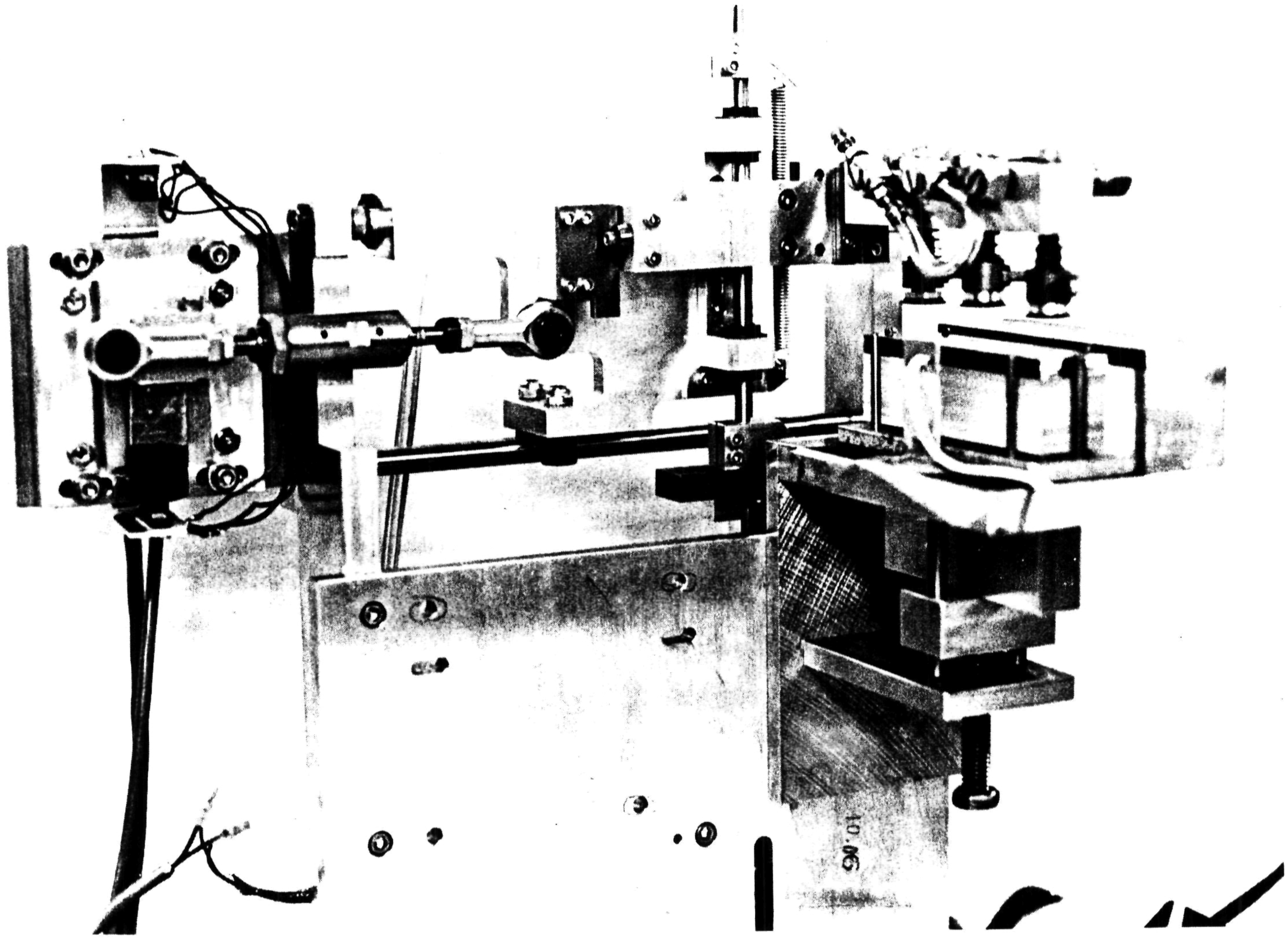

Figure 25. Mockup of Cassette Unload Station

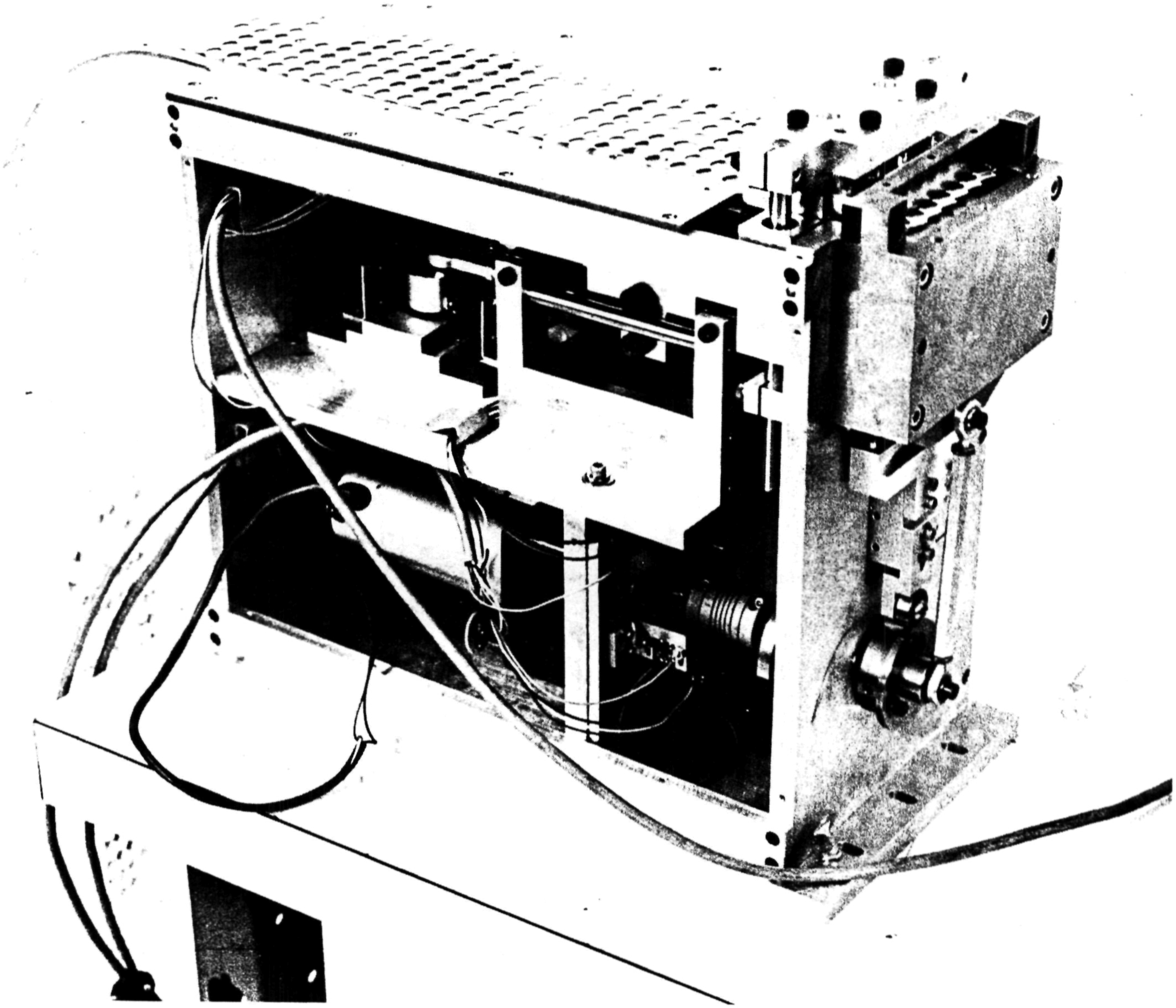

Figure 26. Interconnect Feed Station (Minus Ribbon Transfer Mechanism)

bonder used to make the front bonds. All bond parameters (i.e., force, speed, and excitation energy) are identical for the front and back bonds.

E. String Conveyor

A string conveyor is used to index cells as they are joined together into strings of fifteen cells approximately 16 inches in length (refer again to Figure 21).

A steel belt conveyor and a shuttle system were evaluated to determine the mechanism best suited for use as the cell string conveyor. The belt conveyor uses two parallel steel belts driven by sprocketed pulleys. The belts index continuously. Cells are transferred to the conveyor onto precise "pockets" defined by registration/retaining hardware on the belts. The pockets maintain the accuracy of intercell pitch (distance between cells).

The shuttle uses a reciprocating table, or plate, driven by a lead screw. The length of the plate corresponds to the length of the cell string to be made. The plate begins in a reset position at the cell transfer area and indexes (advances) one intercell pitch as each cell is deposited on the plate. After the complete string is formed, the plate indexes to the string pickup area, where the string is transferred to the module array area. The shuttle then returns to its reset position. The return to reset is an additional motion not required by the belt conveyor. However, the shuttle recovers this lost time by requiring less time for each index cycle. Cells can also be transferred to the shuttle faster because it uses no pockets, eliminating the additional care and time required to transfer a cell to such precise locations. The shuttle's reliability depends on the accuracy of cell transfer and elimination of any movement of the plate in relation to the cells during index cycles.

Based on the following factors, the shuttle was chosen as the system to be used for the string conveyor.

1. Handling and transfer of the cell to the shuttle presents fewer problems, minimizing the chance for cell breakage.

2. The shuttle's design allows optimizing intercell pitch to accommodate manufacturing tolerances. Index pitch is a programmable function and may be changed with minimal changing of parts.

3. The shuttle is a relatively simple mechanism, containing few parts, and should be less expensive.

When each string is completed, it is automatically picked up using a track-mounted vacuum lance and moved to a test station where the string will be electrically tested prior to being placed in the module array area in the format specified by the MEPSDU module assembly drawing. The vacuum lance maintains the intercell mechanical spacing, and a track will be provided with detents to locate the strings for correct interstring spacing. A reject station is provided in the discharge area in case it is determined that the cell string should not be delivered to the module array area.

F. Control System

An extensive survey was conducted to identify the optimum machine control system to be used for the automated cell interconnect station. The control system to be utilized is a programmable controller that is compatible with, and can be enhanced by, microprocessor and servo circuitry. A programmable controller is required to provide the flexibility desired in such equipment along with relative simplicity in programming, operation, and maintenance.

The following factors were considered in the evaluation of commercially available programmable controllers:

- Memory - Type and back-up
- Scan time (per 1K of memory)
- Types of input/output (I/O) interface available
- Programming features
- Service availability
- Manufacturer experience
- Price - based on:
  - Basic processor
  - Minimum memory
  - 150 I/O capability

54

This evaluation resulted in the selection of a GE Model 600 unit which has the high technical specifications required for this application. The unit's high scan speed (1 msec/1 K) eliminates the additional software and associated hardware development that would be required to adapt previously available controllers. The PC works in conjunction with a programming terminal capable of providing ladder diagrams, simulation data, and diagnostic data on the terminal's CRT screen for development and troubleshooting purposes, which makes the unit more desirable from a user standpoint.

At the time of the JPL stop work order, work was proceeding on determining the complete machine sequence of events and developing timing diagrams to aid the programming effort. A block diagram of the control structure for first and second bond stations, including the PC and some microprocessor controls, is shown in Figure 27.

G. Design Review

A design review of the automated cell interconnect station was conducted at the K&S facility at Horsham, Pennsylvania, in November 1981. The Westinghouse design review team consisted of the MEPSDU Program Manager and two senior engineering personnel (one electrical and one mechanical) who are not directly related to the MEPSDU project. The primary purpose of the review was to establish that the equipment proposed by K&S could meet the requirements of the automated cell interconnect station equipment specification (E-Spec). This evaluation is necessary prior to placing the order for the Westinghouse funded equipment.

The evaluation team report was completed and indicated that K&S proposed equipment should meet the E-Spec requirements both electrically and mechanically. Accordingly, the Westinghouse capital equipment order was placed with K&S in January 1982. The design and fabrication effort continued under Westinghouse funding after receipt of the JPL stop work order received in February 1982.

205

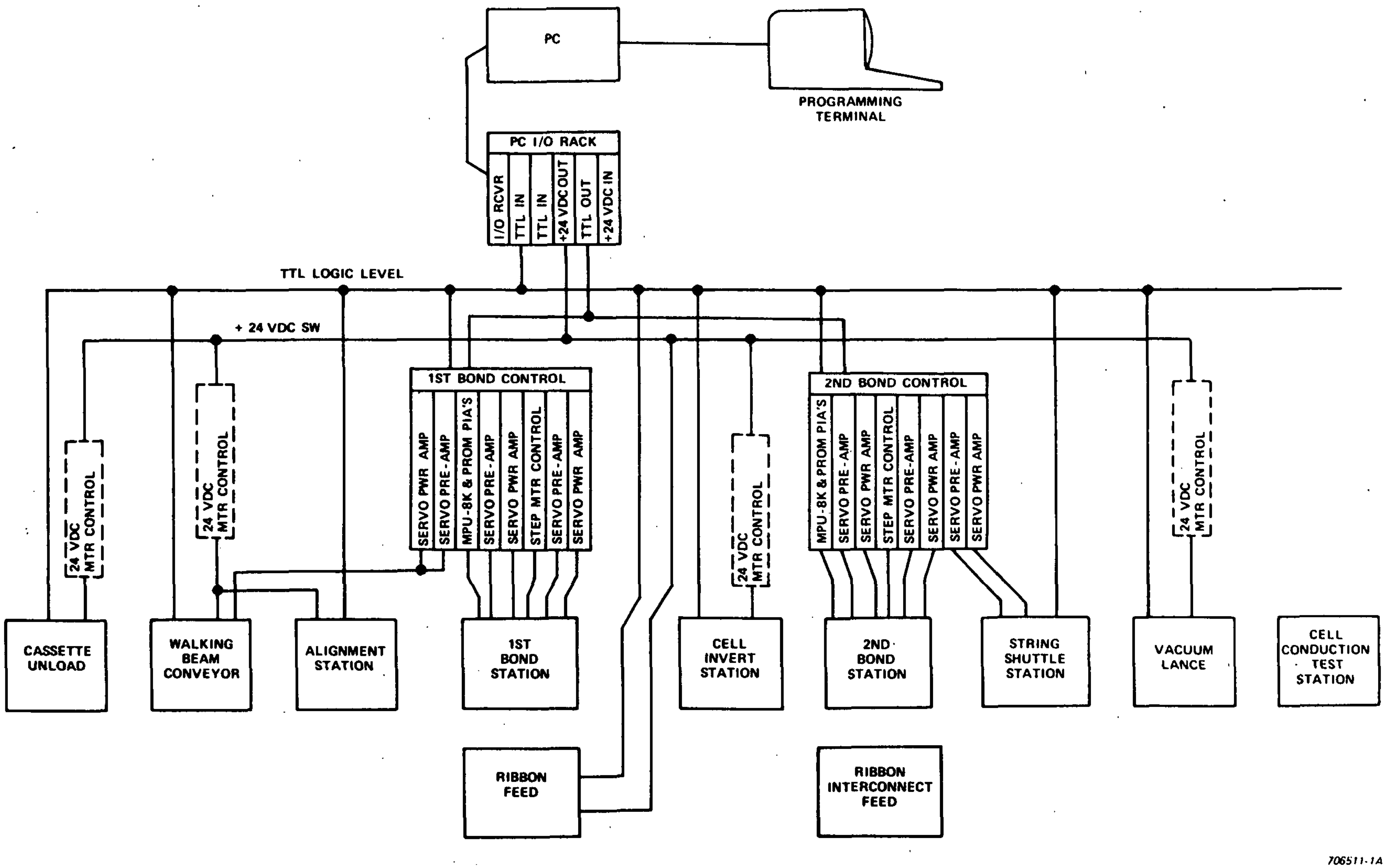

Figure 27. Interconnect Station Control Structure

9950-392

VIII. ECONOMIC ANALYSES

A. Background

During the course of the Westinghouse MEPSDU contract, a significant effort was completed to evaluate the cost of fabricating solar modules from dendritic web silicon using the Baseline Westinghouse Process Sequence. This economic analysis was conducted in iterative fashion in parallel with technical work on the contract. That is, as changes were made (or considered) to the baseline process sequence, the economic impact of these changes were evaluated.

To establish the capability for performing detailed in-house economic analyses, a computer terminal, including a CRT and Modem, was leased by Westinghouse and used exclusively for MEPSDU cost analysis (SAMICS). A Westinghouse engineer and a technician attended an introductory terminal usage seminar given by the computer leasing service personnel in Pittsburgh.

All economic analysis work required by the MEPSDU contract was performed. In all cost analysis SAMICS simulations, two separate production rates were assumed. The first production rate, 1 MW/yr, corresponds directly to the capacity of the Westinghouse MEPSDU facility. Then, to project high volume production costs, a similar analysis was made for an automated production facility having a 25 MW/yr production rate using the same process sequence. Throughout this report, these two simulations are referred to as the M-Process (1 MW/yr) and the P-Process (25 MW/yr).

To allow a direct comparison of costs of the individual steps within the process sequences, the 1 MW/yr and 25 MW/yr simulations follow the same sequence steps and use the same step referents.

Table 18 is a listing of the process steps and referents used for these two simulations. The eleven individual steps follow a natural grouping of subtasks within the process sequence.

The data used in the Format A's for the two processes were based on recent vendor quotes for capital equipment and materials. The material usage was based on calculated requirements and pre-pilot facility experience.

207

TABLE 18

PROCESSES AND REFERENTS USED IN SAMICS COST ANALYSES

Process #	Referent	Process Name
M1/P1	CLENWEB	Pre-Diffusion Cleaning
M2/P2	DIFFWEB	Boron Diffusion
M3/P3	BSF	Phosphorous Diffusion
M4/P4	ARPR	Application of Antireflective Coating and Photoresist
M5/P5	GRIDDE	Expose, Develop, Etch
M6/P6	METWEB	Metallize
M7/P7	REJPL	Reject/Plating
M8/P8	TESCEL	Cell Separation and Test
M9/P9	INTCON	Cell Interconnection
M10/P10	LAMMOD	Module Lamination and Test
M11/P11	CRAMOD	Crating

208

B. Assumptions Used in SAMICS Cost Analyses

- 3 shift, 345 days per year operation (4.97×10^5 operating minutes per year)

- The modules fabricated in both the 1 MW/yr M-Process and the 25 MW/yr P-Process facilities have nominal dimensions of 40 cm x 120 cm (16" x 48").

- These modules are assumed to produce 60 watts at 25°C and 100 mW/cm^2 insolation. This is based on module performance calculations presented in Section IV of this report.

- The M-Process assumes a throughput rate of 200 cm^2/min of usable web (99.4×10^2 m^2/yr).

- The P-Process assumes a throughput rate of 5000 cm^2/min of usable web (2.485×10^5 m^2/yr).

- The strips of dendritic web input into both processes are 42 cm long by 2.7 cm wide. From these strips four 2.5 cm x 10 cm (nominal) cells will be fabricated. The cost for the silicon used in the Format A input includes all losses due to non-utilization, e.g., dendrites and strip end losses.

- Yields for the process are taken into account in each step of the sequence. The assumed yields are based on projections from current yield data being observed in the Westinghouse Pre-Pilot Facility which operates using the Baseline Process Sequence.

- Machine up-time (A8 on Format A) assumed for each station is based on best industry experience.

- The maintenance and quality control personnel are included in costs associated with the specific process steps where they are required.

- Waste materials (organics, acids, oils, etc.) are disposed of by a local contractor. The Format A inputs for this disposal are derived from a vendor quote.

- Commodity and capital equipment costs are based on vendor estimates.

- In extrapolating from the 1 MW/yr M-Process to a 25 MW/yr P-Process, a highly automated factory was assumed. This automated factory concept increases capital cost but greatly decreases labor input. In general, the material usage was scaled very nearly proportional to the production rate with very small savings in usage assumed. This is a realistic assumption since most of the expensive materials (e.g., glass, laminating material, etc.) are area related and are absolutely proportional to production rate.

C. Results and Conclusions

The first complete analysis was presented to JPL in topical report, which included SAMICS Format A's and a detailed description of the input data. This report was submitted to JPL in July 1981.

Subsequently, a workshop was held with JPL personnel to discuss the inputs and results of the first analysis and to identify modifications mutually agreed upon. The P-Process and M-Process analyses were then repeated, and results reported herein represent the final calculations.

Table 19 presents results of the SAMICS analysis of a 1 MW/yr (MEPSDU sized) production facility. Results are presented as the value added for each step in the Baseline Process Sequence. Also shown is the fraction of the total

TABLE 19

SAMICS COST ANALYSIS

Value Added for Process Steps

1 MW/yr Production Facility

Process Step	Process	Value Added (1980$/peak watt)	Percent of Total
1	Prepare Input Web	0.615	18.9
2	Boron Diffusion	0.192	5.9
3	Phosphorous Diffusion	0.181	5.6
4	Application of AR/PR	0.182	5.6
5	Define Grid Pattern	0.193	5.9
6	Metallize Web	0.357	10.9
7	Rejection and Plating	0.307	9.4
8	Cell Separation and Test	0.576	17.7
9	Cell Interconnection	0.254	7.8
10	Lamination	0.345	10.6
11	Crating	0.061	1.9

Total for Process - 3.27 $\frac{\text{1980\$}}{\text{Peak Watt}}$

211

cost represented by each step. Note that, in accordance with the JPL cost goals, the costs are determined using 1980 dollars.

The largest cost contribution comes from the first step: Preparation of input web. This step includes the cost of polycrystal silicon ($14/kg), growth of the dendritic web, and cleaning operations required prior to diffusion of junctions.

Table 20 presents similar results for the fully automated 25 MW/yr production facility. Note here that almost 50% of the total cost is associated with the raw materials and growth of the dendritic web material. The other major cost driving step in the process is the module lamination step. The most significant portion of the cost of this step is the raw material cost for glass, EVA, and Mylar backing material.

Table 21 presents a breakdown of cost categories for the two production facilities. This is presented to show how the costs are driven by labor, materials, utilities, capital expenses, and taxes.

The simulation data indicates that extrapolation of the 1 MW/yr MEPSDU process to a 25 MW/yr production facility leads to a cost effective manufacturing sequence which essentially meets the DOE/JPL cost goals of 70¢/watt (1980 dollars) in 1986. The scaling was based on the assumption of a highly automated process, both within a given step and between process steps. This assumption reduces the labor content of the product cost. The material costs were scaled at a ratio of 19:1 usage factor for a 25:1 production ratio. Therefore, only minimal savings are assumed for material costs in the scale up.

212

9950-89?

TABLE 20

SAMICS COST ANALYSIS

Value Added for Process Step

25 MW/yr Production Facility

Process Step	Process	Value Added (1980$/peak watt)	Percent of Total
1	Prepare Input Web	0.340	49.5
2	Boron Diffusion	0.033	4.5
3	Phosphorous Diffusion	0.024	3.3
4	Application of AR/PR	0.016	2.2
5	Define Grid Pattern	0.017	2.4
6	Metallize Web	0.037	5.1
7	Rejection and Plating	0.046	6.3
8	Cell Separation and Test	0.029	4.0
9	Cell Interconnection	0.026	3.6
10	Lamination	0.121	16.6
11	Crating	0.019	2.5

Total for Process - 0.709 $\frac{\text{1980\$}}{\text{Peak Watt}}$

213

9950-802

TABLE 21

SAMICS COST ANALYSIS

Value Added per Watt Cost Factors for
the 1 MW/yr and 25 MW/yr Simulations

(All Costs in 1980$)

	1 MW/yr	25 MW/yr
Direct Labor	0.820	0.060
Direct Materials	0.539	0.388
Direct Utilities	0.033	0.008
Indirect Labor	0.469	0.038
Indirect Materials	0.060	0.004
Indirect Utilities	0.044	0.005
Capital Expenses	0.770	0.111
Taxes/Misc.	0.521	0.095

215

IX. DOCUMENTATION

All contractual documentation requirements associated with the MEPSDU contract were met during the course of the program. These documents and their submittal dates are summarized in Table 22.

215

TABLE 22

MEPSDU PROGRAMMABLE DOCUMENTATION SUBMITTAL STATUS

ITEM	SUBMITTAL DATE(S)
1. COST ESTIMATES	
a. Baseline	December 17, 1980
b. Revision 1	May 22, 1981
c. Revision 2	January 8, 1982
2. SCHEDULE ACCOMPLISHMENT REPORT/FINANCIAL REPORT	December 17, 1980 January 14, 1981 February 16, 1981 March 16, 1981 April 16, 1981 May 16, 1981 June 16, 1981 July 16, 1981 August 17, 1981 October 15, 1981 November 16, 1981 January 15, 1982 February 16, 1982
3. PROGRAM PLAN AND WBS	
a. Original	December 17, 1980
b. Revision 1	May 22, 1981
c. Revision 2	January 8, 1982
4. MONTHLY TECHNICAL PROGRESS REPORT	January 15, 1981 February 15, 1981 March 15, 1981 April 15, 1981 May 15, 1981 June 4, 1981 July 6, 1981 August 6, 1981 September 8, 1981 October 8, 1981 November 5, 1981 December 11, 1981 January 12, 1982
5. PRELIMINARY DESIGN REVIEW PACKAGE	February 19, 1981
6. MODULE DESIGN REVIEW PACKAGE	June 30, 1981
7. QUARTERLY TECHNICAL PROGRESS REPORT	March 15, 1981 June 15, 1981 September 15, 1981 December 15, 1981

216

APPENDIX B

LIQUID JUNCTION TECHNICAL FEASIBILITY AND TEST MATRIX

TME 3171

LIQUID JUNCTION TECHNICAL FEASIBILITY AND TEST MATRIX

Contract No. 955909

R. B. Campbell

January 10, 1983

This work was performed for the Jet Propulsion Laboratory, California Institute of Technology, under NASA contract for the U. S. Department of Energy.

Advanced Energy Systems Division
WESTINGHOUSE ELECTRIC CORPORATION
P. O. Box 10864
Pittsburgh, Pennsylvania 15236

412-892-5600

218

1. INTRODUCTION AND SUMMARY

One of the major objectives of JPL Contract 955909 is to determine the technical feasibility of forming front and back junctions in dendritic web silicon using liquid dopant techniques. This report presents a test matrix currently being used by Westinghouse to establish that feasibility and is submitted to JPL as the second technical milestone of the current contract.

Individual steps required to establish the technical feasibility of liquid junction formation are as follows:

- Determination of Method of Liquid Dopant Application to Web Surface
- Establishment of Time and Temperature Matrix to Obtain Required Sheet Resistivity and Junction Profile
- Optimization of Gas Flows and Concentrations to Minimize Web Surface Staining
- Evaluation of Liquid Dopant Process Step Compatibility with Baseline Process Sequence
- Completion of Initial Test Runs
- Verification of Process through Generation of Sufficient Data Base
- Evaluation of Various Vendors' Liquid Dopants
- Determination of Equipment Required

Each of these steps are discussed in this report.

219

2. LIQUID BORON DOPANT

2.1 Application Methods

Table 1 shows application methods tested in this program. Based on results of initial experiments, present work is being done using the sponge-squeegee application technique. However, a meniscus coater has been ordered to study automated application techniques.

2.2 Time-Temperature Conditions to Obtain Required Sheet Resistivity and Junction Profile

Table 2 shows results of a series of tests made on dendritic web silicon using a liquid boron dopant solution. The sheet resistivity data presented here suggests diffusion for 45 minutes at 980°C.

Figure 1 shows a comparison of the P^+P junction profiles obtained using a liquid boron dopant and gaseous BBr_3 dopant. There is no significant difference. Of special importance is the equal surface concentration (C_o).

2.3 Gas Flows and Concentrations to Minimize Staining

Table 3 shows the relationship of the ambient gas during diffusion to the resultant web surface and the sheet resistivity. This data is for one vendor's grade of liquid boron dopant only. It will be necessary to optimize the gas composition and flow rate for each supplier's product.

3. LIQUID PHOSPHORUS DOPANT

Since on a P-type base web material the liquid phosphorus is used to prepare the N^+P junction (sun side), the quality of the web surface is more critical.

The same techniques discussed in Table 1 for the application of liquid boron were used for the liquid phosphorus solution.

None of the first four methods worked satisfactorily in that they left the front surface badly stained. Due to this staining, the antireflective coating

220

TABLE 1

APPLICATION METHODS FOR LIQUID BORON

Method	Comments
Spraying	Non-uniform coverage; formation of droplets.
Dipping	Non-uniform coverage; undesirable due to coating of both sides.
Spinning	Non-uniform coating; difficult experimentally due to web geometry.
Sponge-Squeegee	Satisfactory for tests and low production rates. Control of pressure required.
Meniscus Type Coater	Applicability verified; uniform coatings obtained.

TABLE 2

LIQUID BORON DIFFUSION - TIME/TEMPERATURE STUDY

Diffusion Temperature (°C)	Diffusion Time (min)	Sheet Resistivity (Ω/□)
925	20	90
925	30	80
960	20	65
960	30	50
960	40	48
980	15	75
980	30	55
980	45	45
980	60	30

NOTES:
1. Baseline BBr_3 gaseous diffusion carried out at 960°C for 20 minutes.
2. Baseline process specification for boron doped P^+P junction = 40Ω/□ ±10Ω/□.

222

LIQUID VS GASEOUS DIFFUSED JUNCTION PROFILES

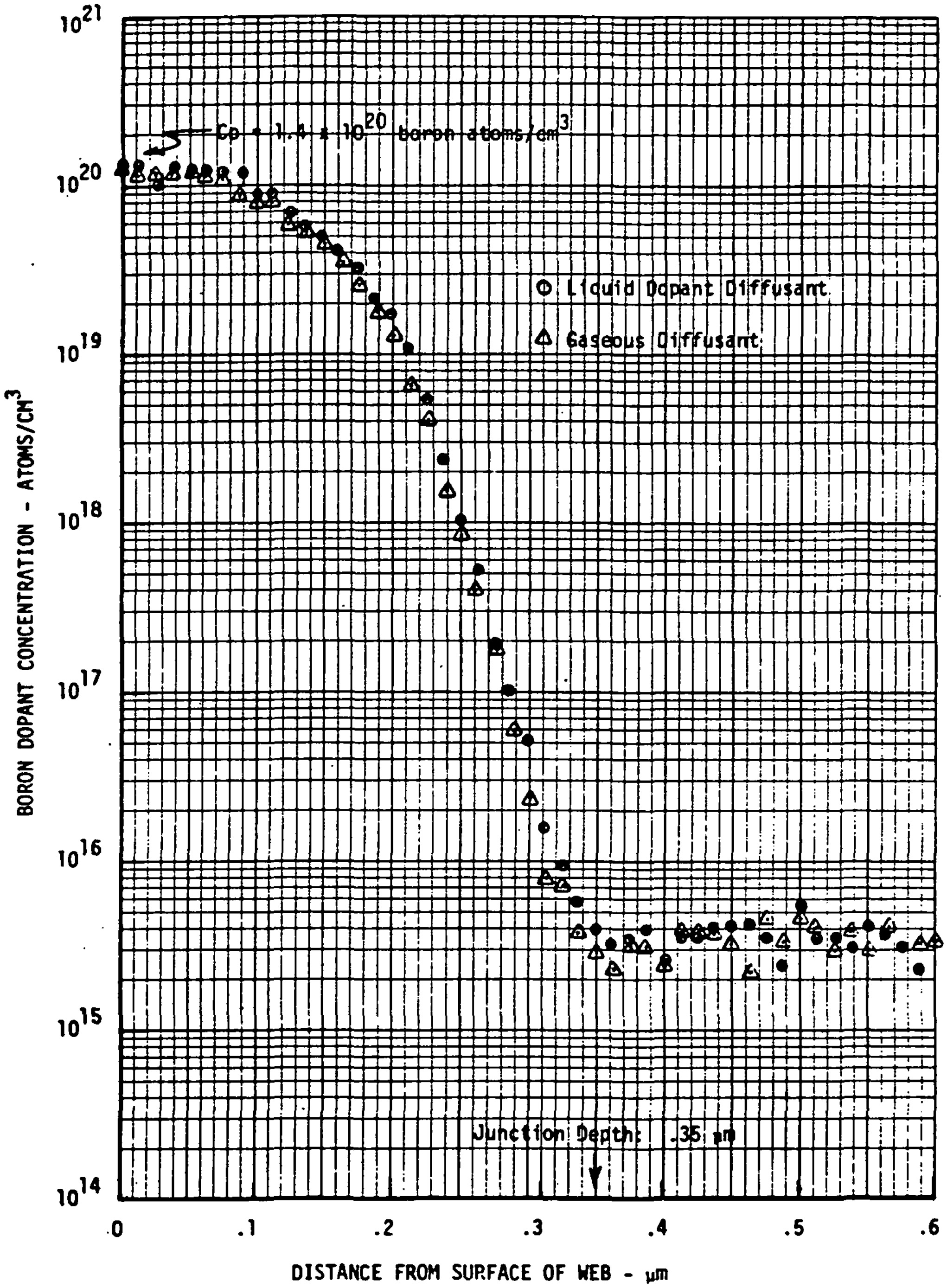

Figure 1. P^+P Junction Profiles in a Liquid Diffused Cell and a Standard Gaseous BBr_3 Diffused Cell

223

TABLE 3

RELATIONSHIP OF GAS COMPOSITION TO SURFACE STAINS AND SHEET RESISTIVITY

Gases	Composition and Flows	Comments
N_2/O_2	1000 cc/min - N_2 90 cc/min - O_2	Stained surface after glass removal, high sheet resistivity.
O_2	90 cc/min - O_2	Essentially no surface staining, lower sheet resistivity.

224

was non-uniform; and the cell efficiencies generally low. Obviously, a technique for applying this phosphorus dopant more uniformly is required.

A meniscus coater ("CAVEX") has been developed by Integrated Technologies for uniform coating of various substrates. In conjunction with the vendor, initial tests have been conducted where the antireflective (AR) coating was applied using this equipment. Since uniform thicknesses of the AR coating were obtained in these tests, this equipment was tested for the application of the liquid phosphorus dopant.

A total of 72 strips, each 14 cm long, were coated on the sun side with a liquid phosphorus dopant after an initial $P^{+}P$ junction had been formed on the back side.

After coating, baking, diffusing, and removing the phosphorus glass, the surfaces were clean with no staining. A uniform antireflective coating could be applied.

Although cell quality was variable due to contamination of the liquid phosphorus in the unit, the feasibility of the application method was shown.

Based on these results, a meniscus coater has been ordered. Further work in the liquid phosphorus dopant area is required, especially to establish the time-temperature relationship to obtain the optimum sheet resistance and junction depth. This work will be performed after the meniscus coater is installed.

4. COMPATIBILITY OF THE LIQUID DOPANT PROCESS STEP WITH THE BASELINE PROCESS SEQUENCE

Table 4 (Steps 1 through 9) shows the individual operations associated with the liquid boron diffusion step incorporated into the baseline process sequence. The remainder of the table (Steps 10 through 15) shows the completion of the diffusion step with gaseous $POCl_3$.

225

9350-822

TABLE 4

PROCESS SEQUENCE FOR FABRICATION OF SOLAR CELLS USING LIQUID BORON DOPANTS

1. Raw web cleaning (including the hot H_2SO_4 treatment).
2. Pre-diffusion cleaning (standard chelating).
3. Apply CVD SiO_2 on designated N^+ side.
4. Paint on liquid boron dopant on designated P^+ side using a sponge-squeegee.
5. Dry under heat lamp for 5 minutes (about 80°C).
6. Load strips in boat with SiO_2 side facing SiO_2 side and P^+ side facing P^+ side. Pre-bake in oven for 15 minutes at 200°C.
7. Place loaded boat in front end of diffusion furnace and bake strips for 10 minutes at approximately 300°C.
8. Move boat into furnace and diffuse for 40 minutes at 980°C. Slow cool furnace to 700°C at 3°C/minute.
9. Strip oxides in 10:1 H_2O:HF.
10. Repeat Step 2.
11. Apply CVD SiO_2 on boron diffused side.
12. Load strips into boat with SiO_2 side facing SiO_2 side.
13. Place boat into front end of $POCl_3$ diffusion tube and bake strips for 10 min. at approximately 300°C.
14. Move boat into furnace and diffuse in gaseous $POCl_3$ for 20 minutes at 850°C (baseline conditions). Slow cool furnace to 700°C at 3°C/minute.
15. Strip oxides and complete baseline process.

226

Table 5 shows a comparison of individual steps required for various liquid and gaseous dopant processes.

Solar cells have been fabricated using this process sequence. The results (discussed in the following sections) show that the liquid dopant process is compatible with our baseline sequence.

5. INITIAL TEST RUNS

To further evaluate liquid boron as a diffusant source, comparison runs were made where the BBr_3 was replaced with liquid boron and a standard CVD SiO_2 coating was used as a diffusion mask. Time, temperature, and ambient gas conditions for this evaluation were as given in earlier sections; and the process step fitted into the overall process sequence.

Representative results for an entire run are shown in Table 6. Table 7 compares data from cells which were prepared from the same web crystal.

Table 8 shows the results of dark I-V measurements on one cell produced in this way compared to a baseline cell. The low values of J_{02} (the junction current) indicate a high quality junction while the bulk lifetime is nearly that measured on high quality float zone silicon.

These data indicate that the liquid boron process is feasible.

6. VERIFICATION RUNS

After establishing feasibilities of the liquid boron junction formation process, a large number of sequential runs were made to obtain a data base. A total of 21 consecutive runs were made using the liquid boron process. Each run contained 24 web strips with the potential of yielding 72 cells. In these runs, the CVD SiO_2 mask was replaced with a liquid SiO_2 mask. The remainder of the baseline process sequence was followed.

TABLE 5

SOLAR CELL JUNCTION FORMATION PROCESS STEPS:
BASELINE VS VARIOUS LIQUID DOPANT SEQUENCES

Step No.	Process	Baseline	Liquid Boron + CVD SiO_2 Mask	Liquid Boron + Liquid Mask	Liquid Boron + Liquid Phosphorous (using CVD SiO_2)	Liquid Boron + Liquid Phosphorous +Liquid Mask	Simultaneous Drive of Boron and Phosphorous
1	CVD SiO_2 N+ Side	•	•		•		
1A	Apply Liquid Boron and Bake		•	•	•	•	•
1B	Apply Liquid Mask and Bake			•		•	
2	HF Etch	•	•		•		
3	Pre-Diffusion Clean	•					
4	Diffuse P+	•	•	•	•	•	
5	Oxide Etch	•	•	•	•	•	
5A	Apply Liquid Phos-phorous and Bake				•	•	•
6	CVD SiO_2 P+ Side	•	•		•		
6A	Apply Liquid Mask and Bake			•		•	
7	HF Etch	•	•				
8	Pre-Diffusion Clean	•	•	•			
9	Diffuse N+	•	•	•	•	•	
9A	Drive Boron and Phosphorous						•
10	Oxide Etch	•	•	•	•	•	•

NOTE: Starting Point - All web pre-diffusion cleaned.

TABLE 6

EFFICIENCIES MEASURED ON CELLS PROCESSED IN GASEOUS BBr_3 AND IN LIQUID BORON (STANDARD CVD SiO_2)

Cell Efficiency (pct); Measured with AR Coating

	CVD SiO_2/ Standard Boron	CVD SiO_2 Liquid Boron
	12.19	13.52
	12.34	14.23
	10.81	11.38
	10.71	10.26
	11.27	12.81
	12.50	12.35
	12.60	12.70
	12.29	13.72
	12.60	14.28
	12.70	14.85
	12.85	15.56
	12.60	
	13.82	
	14.03	
Average	12.38 ±0.92	13.24 ±1.48

TABLE 7

COMPARISONS OF EFFICIENCIES OF CELLS PRODUCED FROM A SINGLE WEB CRYSTAL PRODUCED USING LIQUID BORON VS BBr_3 (STANDARD CVD SIO_2 MASK)

Crystal No.	Diffusion Drive	Cell No.	Cell Efficiency (%)
4-122-18	Liquid Boron	6A	11.38
4-122-18	Liquid Boron	6B	10.26
4-122-18	BBr_3	7A	12.50
4-122-18	BBr_3	7B	12.60
4-122-18	BBr_3	7C	12.29
4-122-16	Liquid Boron	11A	12.81
4-122-16	Liquid Boron	11B	12.35
4-122-16	Liquid Boron	11C	12.70
4-122-16	BBr_3	10A	12.6
1-157-1	Liquid Boron	15A	14.28
1-157-1	Liquid Boron	15B	14.85
1-157-1	Liquid Boron	15C	15.56
1-157-1	BBr_3	16A	13.82
1-157-1	BBr_3	16B	14.03

230.

TABLE 8

DARK I-V MEASUREMENTS

Cell ID	Cell Area cm^2	τ Bulk µsec	J_{sc} ma/cm^2	V_{oc} Volts	Fill Factor	η %	R_S Series Resistance Ω-cm	R_{SH} Shunt Resistance kΩ-cm^2	J_{02} A/cm^2	Remarks
2102-15C	19.6	434	33.8	0.578	0.798	15.6	0.31	68	3.2×10^{-7}	Liq.Boron/$POCl_3$ Process
2090-36C	19.6	339	32.5	0.578	0.802	15.1	0.44	31	6.2×10^{-8}	Std BBr_3/$POCl_3$ Process

(The bulk lifetime calculated from the dark I-V measurements cannot be directly compared to the OCD lifetime. It is, however, a good relative measure of cell quality.)

Table 9 shows overall data for these verification runs while Figures 2 and 3 show efficiency histograms of the two sizes of cells produced.

These results indicate the liquid process produces cells essentially of the same quality as the baseline process.

7. VENDOR EVALUATION

The work reported thus far has shown that the liquid boron process is feasible and can, under the proper conditions, produce cells equal to the baseline gaseous diffusion process.

The work described was carried out using one vendor's[1] grade of liquid boron dopant solution. An experimental program is now underway to investigate this type of material from three other suppliers[2].

These tests are to be carried out as follows:

A. Determination of time and temperature for diffusion to obtain the proper sheet resistivity[3].

B. Gas flow and composition to obtain clean unstained surfaces[3].

C. Initial test runs to produce cells for detailed analysis of junction properties.

D. Verification runs (generally 20-30 runs in sequence) to obtain a data base.

---

(1) Filmtronics Corp.

(2) Emulsitone, Inc.
Allied Chemical Co.
Diffusion Technology Co.

(3) Generalized data of this type is provided by the vendor.

TABLE 9

LIQUID DOPANT/LIQUID MASK VERIFICATION RESULTS

Run #	# Cells	Avg. Efficiency	Max/Min. Efficiency
1*	32	11.9	14.2/10.7
2*	35	12.4	13.9/10.3
3	52	12.7	13.9/9.6
4	43	11.9	13.3/10.6
5	43	12.3	13.6/10.8
6	39	12.0	13.8/10.3
7	51	12.3	13.7/10.6
8*	47	12.2	14.2/10.0
9*	46	12.4	14.5/10.8
10	42	13.1	14.1/11.0
11*	56	13.1	14.7/11.8
12*	56	12.7	13.6/11.3
13	41	12.5	14.1/10.1
14*	48	13.0	14.2/11.8
15	23	12.1	13.4/10.0 (process problem)
16	43	11.0	12.6/8.7 (process problem)
17*	39	12.6	13.9/11.0
18	47	13.6	14.9/12.2
19	36	12.7	14.6/10.9
20*	51	12.5	14.5/11.3
21*	48	12.5	14.4/10.8

*1.6 x 9.4 cm cells (all other cells 2.0 x 9.8 cm)

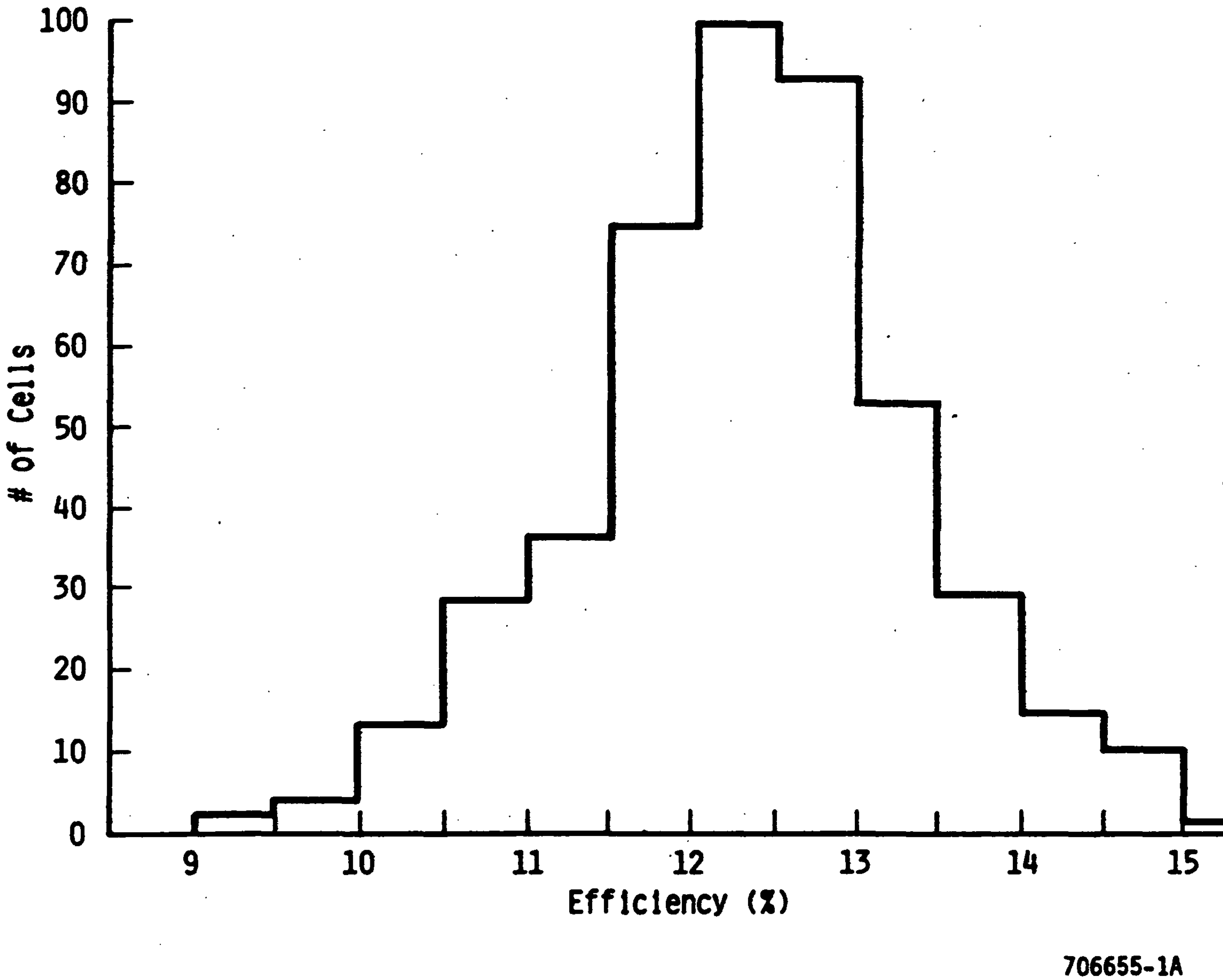

Figure 2. Efficiency Histogram of 2.0 cm x 9.8 cm Cells Fabricated in Liquid Boron/Liquid SiO_2 Verification Runs

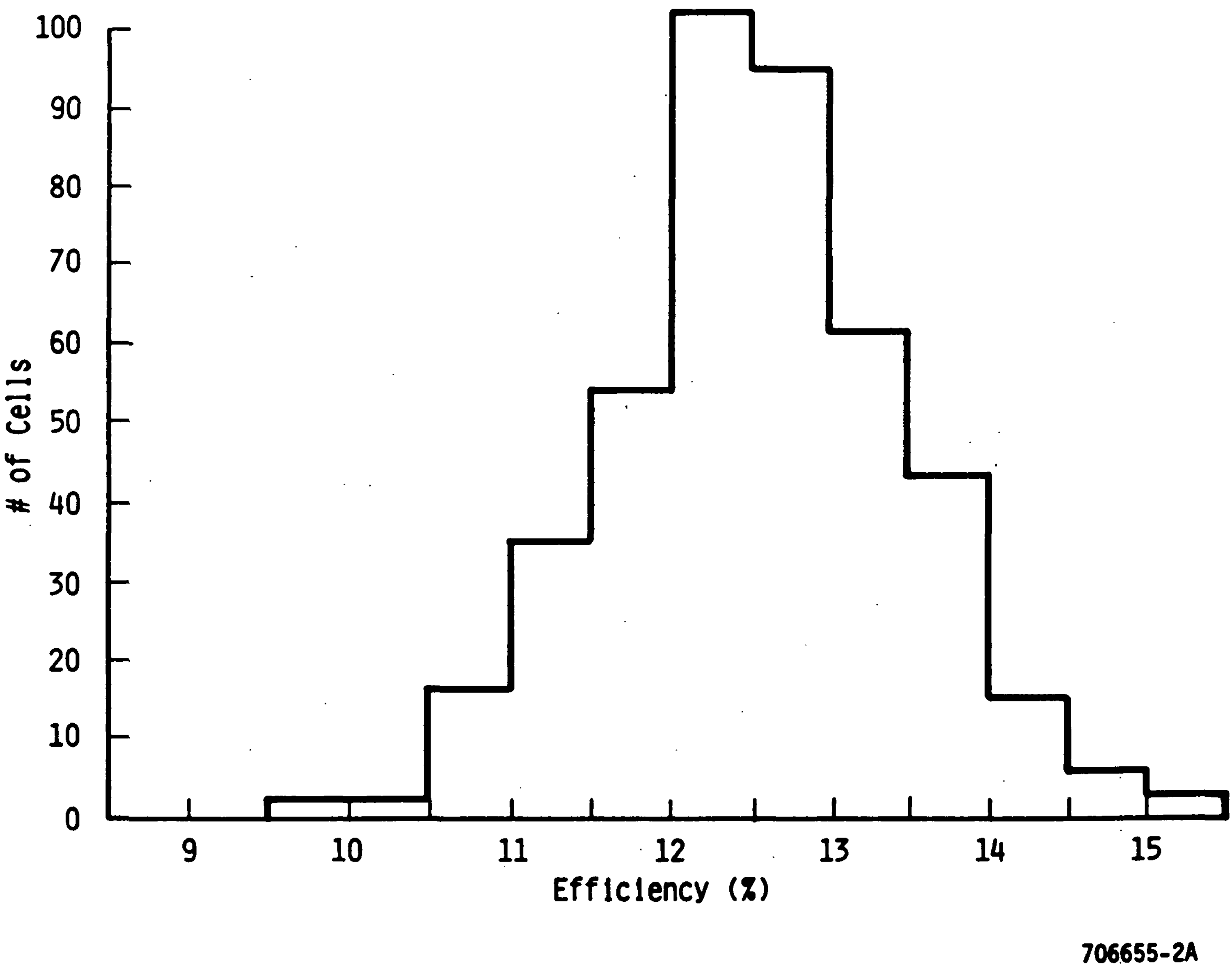

Figure 3. Efficiency Histogram of 1.6 cm x 9.4 cm Cells Fabricated in Liquid Boron/Liquid SiO_2 Verification Runs

235

8. EQUIPMENT

An important experiment was conducted to determine the feasibility of using a belt furnace to diffuse junctions in dendritic web strips with liquid dopants applied. A belt furnace of a given capacity is substantially less expensive than the tube-type diffusion furnace specified by the Westinghouse baseline process sequence. In addition, belt furnace operations are inherently more continuous, hence, more automatable and cost effective than diffusion furnace operations. Development of a high quality belt furnace junction formation process using liquid dopants could be a benefit to processing of virtually all ribbon sheet materials.

For this experiment, which was conducted at the facilities of Radiant Technologies, Inc., at Cerritos, California, a total of 96 strips of silicon web were processed. The JPL contract monitor for the Westinghouse program was present for the diffusion runs made at Radiant Technologies.

Half of the strips were taken to Radiant Technologies, coated with liquid SiO_2/liquid boron, and processed through their belt furnace in four separate runs. The ambients used in these runs were 100% O_2, 50% O_2 and 50% N_2, and pure dry air. The diffusion temperatures were 950°C and 980°C. All diffusions were for 30 minutes with a slow furnace cool to 750°C at 4°C/min. The remaining half of these strips were diffused in the Westinghouse pre-pilot tube type diffusion facility using the liquid SiO_2/liquid boron. These strips were generally crystal pairs of the samples diffused in the belt furnace. Results of the experiment are tabulated in Table 10.

Cells diffused in the belt furnace using the various atmospheres described above yielded similar electrical results; however, cells diffused in a pure O_2 ambient produced the most acceptable appearances in that post-diffusion surface stains were minimized.

Although optimum conditions were not determined from these tests, the feasibility of substituting a belt furnace for the standard tube-type diffusion furnace has been established.

236

TABLE 10

DATA FROM BELT FURNACE JUNCTION FORMATION EXPERIMENT

1. Overall Results

	Belt Furnace Junction Formation (Liq B/Liq SiO_2)		Tube Diffusion Furnace Junction Formation (Liq B/Liq SiO_2)	
Cell Run #*	No. of Cells	Av. Eff.**	No. of Cells	Av. Eff.**
924-1W	36	12.4	18	12.3
924-24W	18	12.9	25	12.4
924-49W	25	12.8	28	12.5
924-72W	17	12.9	15	12.6

*This cell run number defines the original group of web strips selected for test. Portions of each run were diffused at AESD and at Radiant Technologies, Inc.

**Four cells with efficiencies less than 11% not included in average.

2. Details of V_{oc}, I_{sc}, and FF measurements (averages for all cells)

	V_{oc} (V)	I_{sc} (A)	FF
Processed in Belt Furnace	0.544 ±.010	.578 ±.027	0.780 ±.023
Processed in Tube Diffusion Furnace	0.542 ±.008	.578 ±.028	0.778 ±.029

APPENDIX C

LIQUID DIFFUSION MASK - TECHNICAL FEASIBILITY AND TEST MATRIX

238

WAESD-TR-83-1004

LIQUID DIFFUSION MASK - TECHNICAL FEASIBILITY AND TEST MATRIX

Contract No. 955909

R. B. Campbell

May 13, 1983

This work was performed for the Jet Propulsion Laboratory, California Institute of Technology, under NASA contract for the U. S. Department of Energy

Advanced Energy Systems Division
WESTINGHOUSE ELECTRIC CORPORATION
P. O. Box 10864
Pittsburgh, Pennsylvania 15236

412-892-5600

239

1. INTRODUCTION AND SUMMARY

A primary objective of JPL Contract 955909 is to determine the technical feasibility of using an SiO_2 containing liquid as a diffusion mask. (In this report, this liquid will be referred to as a "liquid mask.")

The purpose of the mask is to protect one side of a solar cell while the other side is undergoing a junction forming diffusion process. In this way, dopants can be diffused into silicon sheet material (dendritic web silicon), one side at a time. Such a process is required to form the N^+PP^+ cell structure specified in the Westinghouse baseline process sequence.

The liquid mask material, available from a number of vendors*, is a metallo-organic containing 1-3% SiO_2 in an alcohol base. During processing, the liquid is applied to the sheet (ribbon) surface to be protected and then baked to remove the solvent, forming a glassy oxide. The optimum oxide layer should be free of pinholes and cracks with a thickness of 0.3-0.7 μm.

This report presents the results of a test matrix used to establish the feasibility of using this liquid mask in the Westinghouse diffusion process sequence using either a liquid boron solution or BBr_3 as a diffusant. It is submitted to JPL as the third technical milestone of the current contract.

Individual steps required to establish the technical feasibility of liquid mask usage are as follows:

- Determination of Method of Liquid Mask Application to Web Surface
- Establishment of Time and Temperature to Obtain Required Oxide Film Properties
- Evaluation of Liquid Mask Process Step Compatibility with Baseline Process Sequence
- Completion of Initial Test Runs

---

*Allied Chemical Co.
Diffusion Technology Co.
Emulsitone, Inc.
Filmtronics Corp.

240

- Verification of Process through Generation of Sufficient Data Base
- Evaluation of Various Vendors' Liquid Dopants

Each of these steps are discussed in this report.

2. LIQUID MASK STUDIES

2.1 Application Methods

Table 1 shows application methods tested in this program. Based on results of initial experiments, present work is being done using the sponge-squeegee application technique. However, a meniscus coater has been ordered to study automated application techniques.

2.2 Time and Temperature Conditions

After the liquid mask material was applied to the web, the strips were baked under a heat lamp at approximately 80°C for 5 min. to remove most of the solvent carrier. This was followed by a 15 minute bake in air at 200°C. After these heat treatments, which were recommended by the various vendors, the coated surface of the strip showed a colored oxide pattern with the colors ranging from light blue to red. The film thickness, measured using an "Alpha Step" varied from 0.3 to 0.6 μm. If the films were over 1.0 μm in thickness, they were dull and colorless; and in many cases, showed a cracked and frosty appearance. Films of this type did not prevent diffusion into the protected side.

2.3 Initial Experiments and Results

To evaluate liquid SiO_2 as a diffusion mask, detailed experiments were run comparing the liquid SiO_2 mask and the CVD SiO_2* mask using both liquid boron solutions and BBr_3 as diffusants.

The process sequence used for these tests is given in Table 2. These sequences shows that the liquid mask technique is compatible with the overall baseline sequence.

*An SiO_2 film deposited by chemical vapor deposition is specified in the Westinghouse baseline sequence.

241

TABLE 1

APPLICATION METHODS FOR LIQUID MASK

Method	Comments
Spraying	Non-uniform coverage; formation of droplets.
Dipping	Non-uniform coverage; undesirable due to coating of both sides.
Spinning	Non-uniform coating; difficult experimentally due to web geometry.
Sponge-Squeegee	Satisfactory for tests and low production rates. Control of pressure required.
Meniscus Type Coater	Applicability verified; uniform coatings obtained.

.242

TABLE 2

SOLAR CELL JUNCTION FORMATION PROCESS STEPS:
BASELINE VS LIQUID MASK-LIQUID DOPANT SEQUENCES

Step No.		BBr_3 + CVD SiO_2 Mask	Liq. Boron + CVD SiO_2 Mask	Liquid Boron + Liq. Mask	BBr_3 + Liquid Mask
1	CVD SiO_2 N^+ Side	•	•		
2	HF Etch	•	•		
3A	Apply Liquid Mask and Bake			•	•
3B	Apply Liquid Boron and Bake		•	•	
4	Pre-Diffusion Clean	•			
5	Diffuse P^+	•	•	•	•
6	Oxide Etch	•	•	•	•
7	CVD SiO_2 P^+ Side	•	•		
8	HF Etch	•	•		
9	Apply Liquid Mask and Bake			•	•
10	Pre-Diffusion Clean	•	•		
11	Diffuse N^+	•	•	•	•
12	Oxide Etch	•	•	•	•

NOTE: Starting Point - All web pre-diffusion cleaned.

Four sets of diffusion conditions, as given below, were used.

	1	2	3	4
Diffusion Mask	CVD SiO_2	CVD SiO_2	Liquid SiO_2	Liquid SiO_2
Diffusant	BBr_3	Liquid Boron	BBr_3	Liquid Boron

After these diffusions, which formed the P^+P back junction, the cells were finished processed using the baseline sequence.

The overall results of this first test matrix are summarized in Table 3. Comparisons of cells produced from a single web crystal are given in Table 4. These results indicated that the CVD SiO_2 mask with liquid boron diffusant yielded cells with the highest efficiency. However, in this experiment, difficulties were encountered in removing the liquid mask after the diffusion process. When the mask is incompletely removed, the following $POCl_3$ diffusion will be ineffective; and the cells will show a low efficiency. For this reason, these data are suspect. An improved etching solution of 10:1 DI H_2O + HF at 70°C was developed for later tests.

The reason for the low efficiency of several cells processed using the liquid SiO_2 mask and BBr_3 diffusant will be discussed later.

Data from a similar experiment are shown in Table 5. In this test, the CVD SiO_2 was compared to two liquid SiO_2 solutions, designated 700A* and 700B*. The major difference being the higher viscosity of 700B. In one run of 24 web strips chosen for this experiment, 8 strips were coated with CVD SiO_2, 8 strips with 700A, and 8 strips with 700B. The diffusant in all cases was a liquid boron solution.

There is no significant difference in the efficiencies measured for cells produced from these three processes. However, the thicker 700B is more difficult to apply and to strip after diffusion; and all further tests with this specific

*Filmtronics Corporation designations

244

TABLE 3

EFFICIENCIES MEASURED ON CELLS PROCESSED IN MATRIX EXPERIMENT

	Percent Efficiency (Measured with AR Coating)			
Cell No.	Standard CVD SiO_2/ Standard Boron	Liquid SiO_2/ Standard Boron	Standard Silox/ Liquid Boron	Liquid SiO_2/ Liquid Boron
1	12.19	12.29	13.52	12.29
2	12.34	.2.24	14.23	12.39
3	10.81	11.83	11.38	8.41
4	10.71	11.83	10.26	7.95
5	11.27	7.65	12.81	12.04
6	12.50	7.34	12.35	12.04
7	12.60	12.34	12.70	10.96
8	12.29	12.55	13.72	11.42
9	12.60	11.27	14.28	12.34
10	12.70	12.39	14.85	12.39
11	12.85	11.78	15.56	10.86
12	12.60	11.88		11.17
13	13.82	11.98		11.53
14	14.03	8.57		11.68
15				10.96
16				12.14
17				13.01
18				13.06
Average	12.38 ±0.92	11.04 ±1.74	13.24 ±1.48	11.48 ±1.33

TABLE 4

COMPARISONS OF EFFICIENCIES OF CELLS PRODUCED FROM A SINGLE WEB CRYSTAL PRODUCED USING VARIOUS DIFFUSION DRIVE ANS MAS PROCESS

1. Standard SiO_2 Diffusion Mask

Crystal No.	Diffusant	Cell No.	Cell Efficiency (%)
4-122-18	Liquid Boron	6A	11.38
4-122-18	Liquid Boron	6B	10.26
4-122-18	BBr_3	7A	12.50
4-122-18	BBr_3	7B	12.60
4-122-18	BBr_3	7C	12.29
4-122-16	Liquid Boron	11A	12.81
4-122-16	Liquid Boron	11B	12.35
4-122-16	Liquid Boron	11C	12.70
4-122-16	BBr_3	10A	12.6
1-157-1	Liquid Boron	15A	14.28
1-157-1	Liquid Boron	15B	14.85
1-157-1	Liquid Boron	15C	15.56
1-157-1	BBr_3	16A	13.82
1-157-1	BBr_3	16B	14.03

2. Liquid SiO_2 Diffusion Mask

Crystal No.	Diffusant	Cell No.	Cell Efficiency (%)
4-122-13	Liquid Boron	54A	12.34
4-122-13	Liquid Boron	54B	12.39
4-122-13	BBr_3	55AX	12.29
4-122-13	BBr_3	55BX	12.24
1-156-23	Liquid Boron	66A	11.68
1-156-23	Liquid Boron	66B	10.96
1-156-23	BBr_3	65AX	12.34
1-156-23	BBr_3	65BX	12.55
7-131-3	Liquid Boron	68A	12.14
7-131-3	Liquid Boron	68B	13.01
7-131-3	Liquid Boron	68C	13.06
7-131-3	BBr_3	69AX	11.27
7-131-3	BBr_3	69BX	12.55
7-131-3	BBr_3	69CX	12.39

246

TABLE 5

RESULTS OF DIFFUSION MASK COMPARISON EXPERIMENT: CVD SIO_2 VS LIQUID SIO_2

- Total Cells

	CVD SiO_2	Liquid SiO_2 700A*	Liquid SiO_2 700B*
No. of Cells	15	14	19
Average Efficiency	12.18%	11.99%	12.29%
Maximum Efficiency	13.0%	13.87%	14.74%
Minimum Efficiency	11.68%	11.12%	11.27%

NOTE: Liquid boron diffusant used on all cells.

*Filmtronics Corporation designations

277

vendor's products were made with 700A. This test established that a liquid SiO_2 can be used as an effective diffusion mask.

The next series of tests were made to directly compare the baseline CVD SiO_2 + BBr_3 to the liquid mask + liquid boron process. As before, after this back junction diffusion, the cell junction formation process was finished using the baseline $POCl_3$ diffusion.

The procedure followed in these runs is outlined in Table 6. Results of three such tests are shown in Table 7. These data indicate that there is no significant difference in the average efficiencies of cells produced by the two techniques. The direct comparison of cells from the same web crystal is shown in Section 2 of Table 7 and bears out this same conclusion.

From these initial tests, we concluded that a liquid mask + liquid boron diffusion cycle is feasible. The next step was to carry out a series of verification runs.

3. VERIFICATION RUNS

After establishing the feasibility of using a liquid mask as a diffusion barrier in the junction formation process, a large number of sequential runs were made to obtain a meaningful data base. A total of 21 processing runs were made with each run having a potential of 72 cells.

The liquid mask-liquid boron procedure was used for the P^+ diffusion, and the remainder of the process followed the baseline sequence.

Table 8 shows overall data for these verification runs while Figures 1 and 2 show efficiency histograms of the two sizes of cells produced.

These results indicate the liquid process produces cells essentially of the same quality as the baseline process.

TABLE 6

PROCEDURE FOR DIFFUSION PROCESS STEP DIRECT COMPARISON EXPERIMENT

1. Obtain sufficient strips of web for two processing runs (48 strips).

2. Within these 48 strips, choose pairs of strips from the same web crystal.

3. Separate these 48 strips into two separate processing runs of 24 web strips each - each run containing one of the pairs chosen in #1.

4. Process one 24 strip run through the baseline gaseous diffusion process - the other 24 strip run through the liquid SiO_2-liquid boron process.

5. Finish processing all strips through remainder of baseline process.

TABLE 7

LIQUID SiO_2-LIQUID BORON VS BASELINE GASEOUS BBr_3 PROCESS

1. Overall Results

Process	Experiment Number		
BBr_3 Basline Process	1	2	3
No. of Cells	20	12	20
Average Efficiency	12.01%	12.55%	13.20%
Maximum Efficiency	14.33%	14.43%	14.03%
Minimum Efficiency	10.77%	11.02%	12.09%
Liquid Process			
No. of Cells	16	18	8
Average Efficiency	12.68%	12.30%	13.60%
Maximum Efficiency	14.44%	13.0%	14.69%
Minimum Efficiency	11.37%	11.33%	12.90%

2. Direct Comparison of Cells from the Same Web Crystal or Furnace Run

	Web Crystal No.	Avg. Efficiency Liq. Boron	Avg. Efficiency BBr_3
Pair #1	7.124-8.2	12.37 ±.07%	
	7.124-8.3		12.1 ±0.35%
Pair #2	6.138-7.2	12.5%	
	6.138-7.3		11.51 ±.38%
Pair #3	6.134-12.7	12.08 ±.32%	
	6.134-12.6		12.09 ±.05%
Pair #4	6.134-7.4	12.57 ±0.17%	
	6.134-8.5		12.80 ±0.34%
Pair #5	1.150-16.2	12.65 ±.25%	
	1.150-17.2		13.48 ±0.57%
Pair #6	4.112-8.3	13.13 ±.03%	
	4.112-5.2		13.66 ±0.15%

250

9950-973

TABLE 8

LIQUID DOPANT/LIQUID MASK VERIFICATION RESULTS

Run No.	No. of Cells	Avg. Efficiency	Max./Min. Efficiency
1*	32	11.9	14.2/10.7
2*	35	12.4	13.9/10.3
3	52	12.7	13.9/9.6
4	43	11.9	13.3/10.6
5	43	12.3	13.6/10.8
6	39	12.0	13.8/10.3
7	51	12.3	13.7/10.6
8*	47	12.2	14.2/10.0
9*	46	12.4	14.5/10.8
10	42	13.1	14.1/11.0
11*	56	13.1	14.7/11.8
12*	56	12.7	13.6/11.3
13	41	12.5	14.1/10.1
14*	48	13.0	14.2/11.8
15	23	12.1	13.4/10.0 (process problem)
16	43	11.0	12.6/8.7 (process problem)
17*	39	12.6	13.9/11.0
18	47	13.6	14.9/12.2
19	36	12.7	14.6/10.9
20*	51	12.5	14.5/11.3
21*	48	12.5	14.4/10.8

*1.6 x 9.4 cm cells (all other cells 2.0 x 9.8 cm)

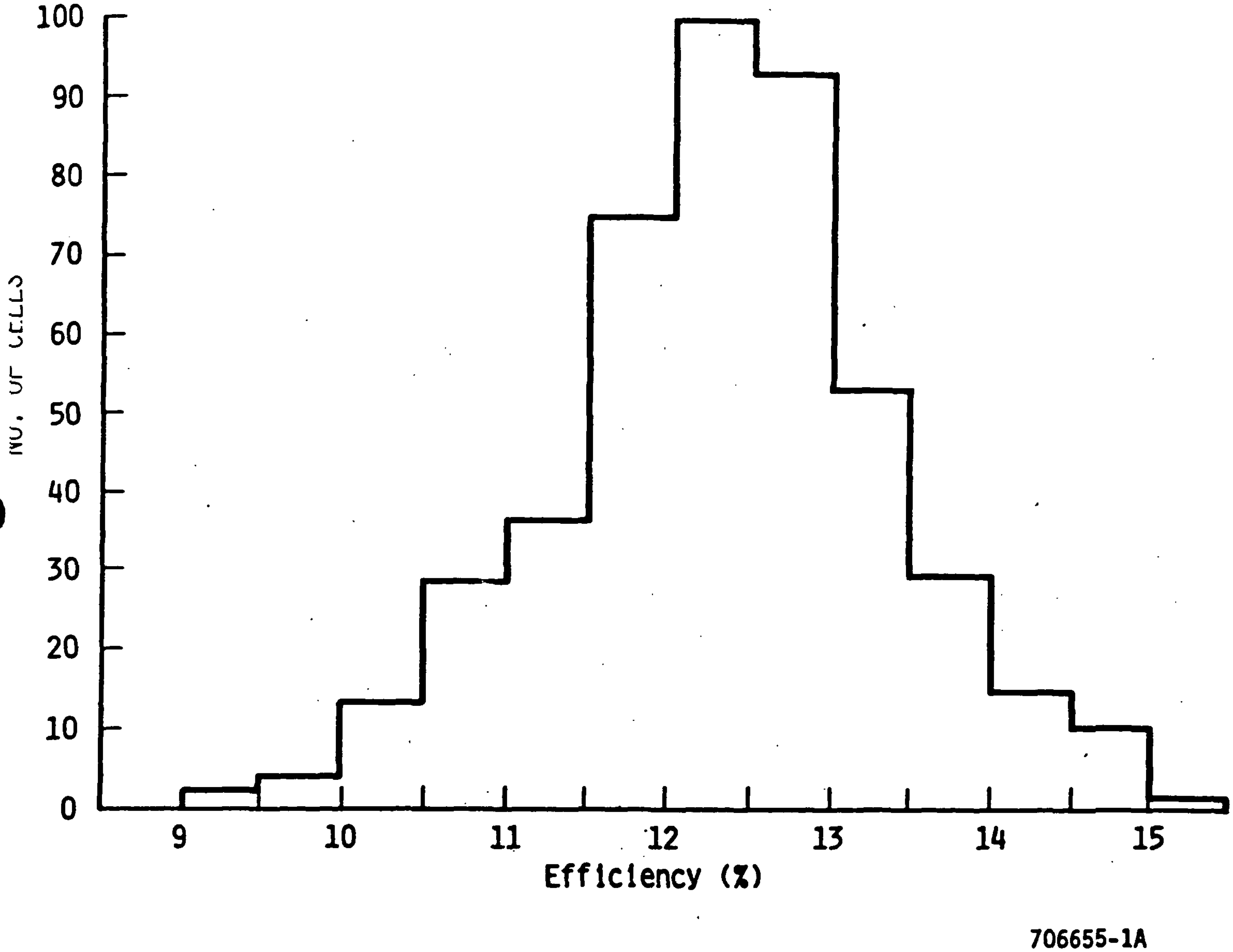

Figure 1. Efficiency Histogram of 2.0 cm x 9.8 cm Cells Fabricated in Liquid Boron/Liquid SiO_2 Verification Runs

252

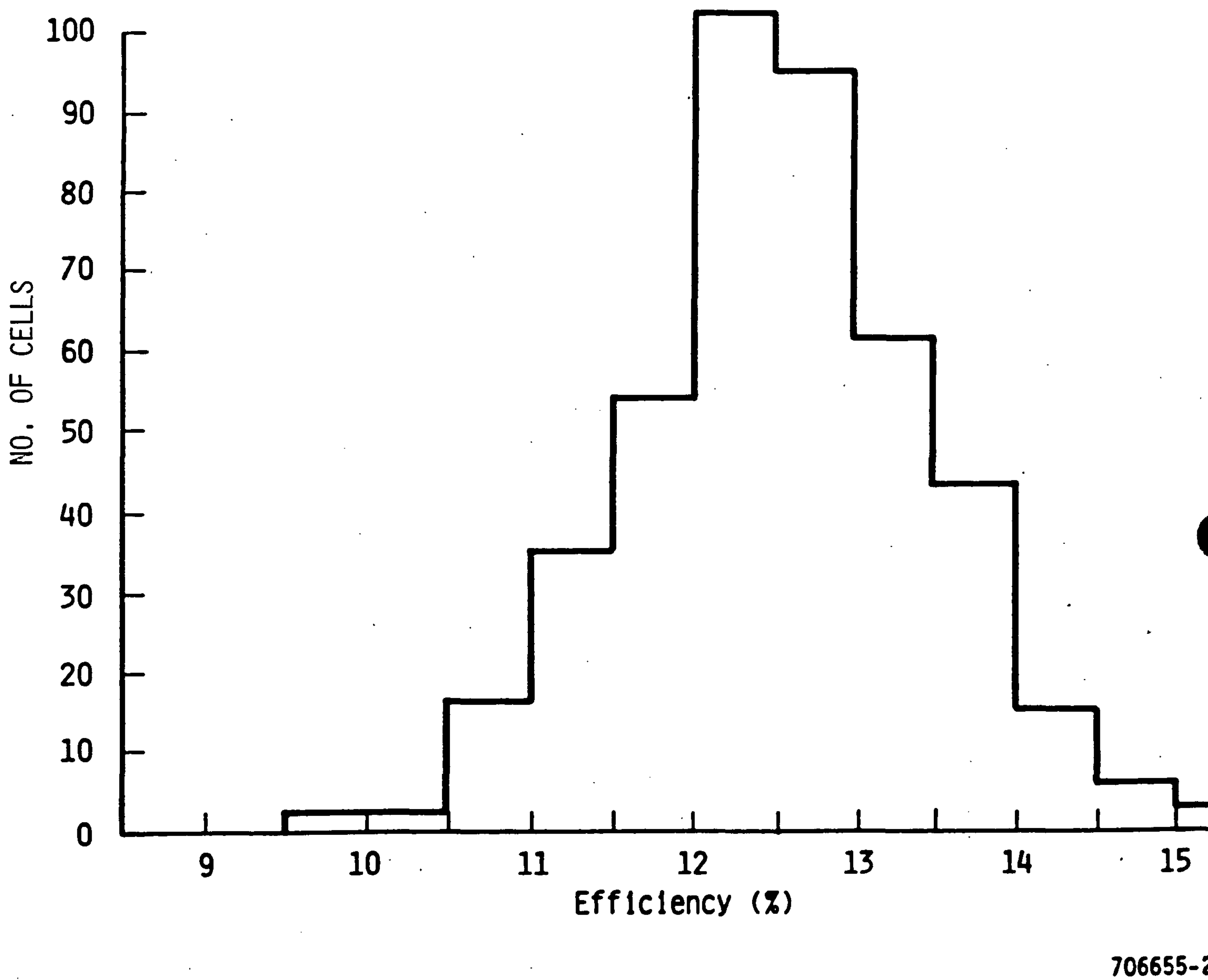

Figure 2. Efficiency Histogram of 1.6 cm x 9.4 cm Cells Fabricated in Liquid Boron/Liquid SiO_2 Verification Runs

An even larger data base is shown in Table 9 where data is given on cells produced in a 5 month period in 1982. These data again show there is no significant difference between the two processes and that feasibility is established.

4. EFFECTS OF PINHOLES IN LIQUID MASK

During the period the liquid mask and liquid dopant processes were being studied, a number of cells with very low efficiencies (1-6%) were fabricated. A selected group of these reject cells were analyzed to determine the cause of the low efficiency.

Approximately 20% of these cells showed obvious processing problems such as poor copper plating, non-adherent grid fingers, low shunt resistance, high series resistance, etc. These are problems which are not necessarily due to the liquid processing. However, about 80% of the cells showed no obvious processing defects and had lighted IV properties as shown below.

$V_{oc} < 0.4V$
$J_{sc} < 20\ mA/cm^2$
$FF < 0.6$
Efficiency - 1-6%

Dark IV measurements showed normal series resistance with a low shunt resistance. The bulk lifetime was less than 1 microsecond, and the junction current density exceeded $10^{-4}\ A/cm^2$.

Eight cells were selected from this group, and the contact metals and antireflective coatings were removed. The sheet resistivity and conductivity type were then measured on these bare cells. This data, shown in Table 10, indicates the back (P^+) surface is not at fault. The sheet resistivity is within specification, and the conductivity is strongly P-type. Analysis of the front surface, however, indicated considerable problems. The sheet resistivities are quite variable, and the conductivity varies from N to P over the surface.

TABLE 9

COMPARISON OF BASELINE PROCESS WITH
LIQUID SIO_2/LIQUID BORON PROCESS

Baseline Process		Liquid SiO_2/Liquid Boron Process	
No. of Cells	Av. Eff. (%)	No. of Cells	Av. Eff. (%)
6161	12.6	9265	12.7

NOTES:

1. Period Covered - July 1, 1982 through November 24, 1982
2. Baseline Process - CVD SiO_2 + BBr_3
   CVD SiO_2 + $POCl_3$
3. Liquid Process - Liquid SiO_2 + Liquid Boron
   Liquid SiO_2 + $POCl_3$
4. Data includes cells of different sizes (15.7 cm^2; 19.6 cm^2; and 24.5 cm^2) and using various vendors' liquid dopants.

255

5950-822

SOLAR ARRAY MANUFACTURING INDUSTRY COSTING STANDARDS
NEW EXPENSE ITEM SHEET

JET PROPULSION LABORATORY
California Institute of Technology
4800 Oak Grove Dr. Pasadena, CA 91109

EXPENSE ITEM ☒ NEW ☐ REVISED

E B B 3 D — Referent used on Format A, A-20 or A-16
B B R 3 D I F F U S A N T — Name and Specifications
Specifications Continued

G M — Units in which quantities are expressed
Quantity: 1
Price of this quantity: 0.85
Price/Unit:

1 9 8 0 — Price Year
Inflation Rate (or code) ______ %/Year

In storage, 100 units take 5 square feet of warehouse space. (Multiply number of units by 26 before entering as RQT for A2272I).

Other indirect requirements:
____ units require ____ amount ____ units of ____ Catalog Number ____ description
____ units require ____ amount ____ units of ____ Catalog Number ____ description

Supplier: TBD
Address:
Supplier's Part Number(s):
Supplier's Catalog and Page Number(s):
Supplier's Salesperson and Phone Number:

EXPENSE ITEM: ☐ NEW ☐ REVISED

Referent used on Format A, A-20 or A-16
Name and Specifications
Specifications Continued
Units in which quantities are expressed
Quantity:
Price of this quantity:
Price/Unit:
1 9 — Price Year
Inflation Rate (or code) ______ %/Year
In storage, ____ units take ____ square feet of warehouse space. (Multiply number of units by 26 before entering as RQT for A2272I).
Other indirect requirements:
____ units require ____ amount ____ units of ____ Catalog Number ____ description
____ units require ____ amount ____ units of ____ Catalog Number ____ description
Supplier:
Address:
Supplier's Part Number(s):
Supplier's Catalog and Page Number(s):
Supplier's Salesperson and Phone Number:

EXPENSE ITEM: ☐ NEW ☐ REVISED

Referent used on Format A, A-20 or A-16
Name and Specifications
Specifications Continued
Units in which quantities are expressed
Quantity:
Price of this quantity:
Price/Unit:
1 9 — Price Year
Inflation Rate (or code) ______ %/Year
In storage, ____ units take ____ square feet of warehouse space. (Multiply number of units by 26 before entering as RQT for A2272I).
Other indirect requirements:
____ units require ____ amount ____ units of ____ Catalog Number ____ description
____ units require ____ amount ____ units of ____ Catalog Number ____ description
Supplier:
Address:
Supplier's Part Number(s):
Supplier's Catalog and Page Number(s):
Supplier's Salesperson and Phone Number:

PREPARED BY	COMPANY	DATE	JPL USE ONLY
CHECKED BY	COMPANY	DATE	☐

JPL 3037-1-S R 6/81

17.4

TABLE 10

ANALYSIS OF REJECT CELLS

Cell No.	Avg. Sheet Resistivity (Ω/□) Front	Back	Conductivity Type Front	Back
4A	55	45	Spotty N & P	Strong P
77C	100	44	Spotty N & P	Strong P
59A	95	40	Spotty N & P	Strong P
79C	90	35	N	Strong P
88A	30-100	35	Heavy P in spots	Strong P
66B	65	40	P	Strong P
44C	65	40	Spotty N & P	Strong P
53A	80	40	Spotty N & P	Strong P

These results indicate that during the initial boron diffusion, the sun side of the cell (protected by the liquid SiO_2 mask) became contaminated with boron which shorted out the (later diffused) N^+P junction. These shorted regions would account for the low shunt resistance and very low bulk lifetime.

This front surface contamination may have occurred during the liquid boron application where the liquid "wicked" by capillary action to the sun side and was subsequently driven in. A second more probable cause of contamination is that the protective liquid SiO_2 mask contains small pinholes through which boron (in the furnace tube ambient) diffuses.

In either case, the integrity of the liquid mask must be questioned. In fact, several runs made in late 1982 used a liquid SiO_2 mask with a BBr_3 diffusant. These runs had a large number of rejects. Also referring back to Table 3, this same effect is noted where the liquid mask-BBr_3 diffusant was used. These results are consistent with the existence of pinholes in the SiO_2 mask.

From this analysis, it is concluded that the liquid SiO_2 mask will, on occasion, permit boron to diffuse through and thus degrade the sun side surface of the cell.

Since the liquid mask is applied using a sponge-squeegee, it is quite possible that a non-uniform thickness and coating technique can lead to pinholes. The problem may be obviated when a meniscus coater (shown to apply uniform coatings) can be used to apply the liquid SiO_2.

5. EVALUATION OF DIFFERENT VENDORS SOLUTIONS

During the period this study was underway, liquid SiO_2 solutions from various vendors were evaluated. The vendors and the solutions used were:

- Allied Chemical Co. (X-600; UDG)
- Diffusion Technologies, Inc. (U1A)
- Emulsitone Co. (100)
- Filmtronics, Inc. (700A; 700B)

237

In general, it was found that when the solutions were properly applied and dried before diffusion, all served adquately as diffusion masks.

6. CONCLUSIONS

From the data presented here, it is concluded that the use of a liquid SiO_2 mask for diffusion is feasible. This work has shown, however, that care must be taken to ensure that the oxide film is of the proper thickness and free of pinholes.

APPENDIX D

TOPICAL REPORT

This Appendix contains:

- Format A's for the M and P Processes
- Format B's for the M and P Processes
- Format C's for the M and P Processes
- New Expense Items Forms

SOLAR ARRAY MANUFACTURING INDUSTRY COSTING STANDARDS
FORMAT A - PROCESS DESCRIPTION

JET PROPULSION LABORATORY
California Institute of Technology
4800 Oak Grove Dr Pasadena, CA 91109

☐ A-1 Process [Referent] M2
Revision Number:

Note: Names given in brackets [ ] are the names of process attributes requested by the SAMIS Computer Program.

☐ A-2 [Descriptive . Name] of process BASELINE BORON DIFFUSION

PART 1 - PRODUCT DESCRIPTION

☐☐ A-3 [Product . Referent] DIFFWEB A-5 Unit of Measure [Product . Units] CM2

☐ A-4 Descriptive Name [Product . Name] WEB WITH BSF

PART 2 - PROCESS CHARACTERISTICS

☐ A-6 [Output . Rate] (Not Thruput) 224.6 Units (given on line A-5) Per Operating Minute

☐ A-7 [Inprocess . Inventory . Time] 60 Calendar Minutes

☐ A-8 [Duty . Cycle] .98 Operating Minutes Per Minute

☐ A-8a [Number . Of . Shifts . Per . Day] 3 Shifts

☐ A-8b [Personnel . Integerization . Override . Switch] Off (Off or On)

PART 3 - EQUIPMENT COST FACTORS [Machine . Description]

☐ A-9 Component [Referent]	SICXII	DIFCE	ESTA2
☐ A-9a Component [Descriptive . Name]	Silox Reactor	Diff. Furnace	Etch Station
☐ A-10 Base Year for Equipment Prices [Price . Year]	1980	1980	1980
☐ A-11 [Purchase . Cost . Vs . Quantity . Bought . Table] (Number Of and $ Per Component)	1 25,000	1 85,000	1 4,000
☐ A-12 Anticipated [Useful . Life] (Years)	7	7	7
☐ A-13 [Salvage . Value] ($ Per Component)	2,000	5,000	---
☐ A-14 [Removal . And . Installation . Cost] ($/Component)	1,000	3,000	500
[Payment . Float . Interval]	0.0	0.0	0.0
[Inflation . Rate . Table]	IRTJ	IRTJ	IRTJ
[Equipment . Tax . Depreciation . Method]	DDB	DDB	DDB
[Equipment . Book . Depreciation . Method]	SL	SL	SL

A-15 Process Referent (From Front Side Line A-1)

PART 5a - BYPRODUCTS PRODUCED PER MACHINE PER MINUTE [Byproduct]

A-20 Catalog Number (Expense Item Referent)	A-22 Amount Produced Per Machine Per Minute [Amount . Per . Cycle]	A-23 Units	A-21 Byproduct Specifications
EACDP	2.8×10^{-3}	gal	Acid Disposal

PART 4 - FLOORSPACE PER MACHINE and PERSONNEL PER MACHINE PER SHIFT [Facility . Or . Personnel Requirement]

A-16 Catalog Number (Expense Item Referent)	A-18 Amount Required [Amount . Per . Machine]	A-19 Units	A-17 Requirement Description
A2064D	250	sq ft	Space
B3672D	.75	py	Operator
B3688D	0.06	py	Mech. & Elec. Maint.
B3736D	0.06	py	Mech. & Elec. Maint.

PART 5b - DIRECT REQUIREMENTS PER MACHINE PER MINUTE [Utility . Or . Commodity Requirement]

A-20 Catalog Number (Expense Item Referent)	A-22 Amount Required Per Machine Per Minute [Amount . Per . Cycle]	A-23 Units	A-21 Requirement Specifications
C1032B	0.12	kw	Elec.
E1328D	0.010	lbs	HF
E1584D	10^{-4}	lbs	Silane
EBB3D	0.0219	gm	BBr_3
C1128D	0.67	cu ft	H_2O
C1080D	10^{-4}	cu ft	Liq N_2
C1096D	4×10^{-5}	cu ft	Liq O_2
ED100	0.033	cu ft	DI H_2O

PART 6 - INTRA-INDUSTRY PRODUCT(S) REQUIRED

A-24 [Required . Product] (Reference)	A-28 [Yield] (%)	A-26 [Ideal . Ratio] Of Units Out/Units In	A-27 Units of A-26	A-25 Product Name
CLENWEB	99	1/1	cm^2/cm^2	

PREPARED BY	COMPANY	DATE	JPL USE ONLY
R. B. Campbell	WESTINGHOUSE ELECTRIC CORPORATION		
CHECKED BY	COMPANY	DATE	

261

PROCESS M-2 (1)

Format A # and Description	Catalog #	Description	Usage/Units	Basis for Usage
A-1 — A-6				See M-1.
A-7		Oxide deposition and diffusion	60 min.	SiO_2 Coating - 20 min. Diffusion - 30 min. Clean - 10 min.
A-11		SiO_2 Reactor	$25,000	Vendor Quote } Vendor quote was 2 x these figures. Units will be used in both M-2 & M-3.
		Diffusion Furnace	$85,000	Vendor Quote
		Etching Station	$ 4,000	Engineering estimate. These costs are 1/2 estimate; other 1/2 in M-3.
A-14				Estimated costs derived from experience on the pre-pilot facility.
A-16 — A-19	A2096D	Mfg. space	250 sq. ft.	Type C space required. Amount based on vendor quote plus aisle and maintenance space.
	B3672D	Operator	.75 Operator	Based on analysis of work load. Also extrapolated from pre-pilot facility experience.

262

23-32.

263

PROCESS M-2 (2)

Format A # and Description	Catalog #	Description	Usage/Units	Basis for Usage
A-20 — A-23	C1032D	Electricity	0.12 $\frac{KwH}{min.}$	Four tube diffusion furnaces at 4 Kw/tube, 30% average drain = 4.8 Kw. Silox reactor - up 20% = 0.4 Kw Motors for fans - 2 Kw Total power = 7.2 Kw or 0.12 $\frac{Kw\#}{min.}$
	ED100	DIH_2O	0.033 $\frac{cuft}{min.}$	Major usage will be overflow from recirculating rinse tank in etching station. Overflow rate g 1 ℓ/min. = 0.033 $\frac{cuft}{min.}$
	E1328D	Hf	0.010 $\frac{lb}{min.}$	1:1 H_2O:HF etching solution in 4 gal. tank. Solution discarded every 24 hours. Usage of 14 lb/day or 0.010 lb/min.
	EBB3D	Boron Diffusant	0.0219 gm/min	Diffusent dopant tubes are emptied and refilled every 100 hours of operation. Each tube contains 25 cc dopant. With a 50% up time, every 200 hours 25 ccg BBr_3 are used. For four tubes usage is 100 cc each 200 hours. $\frac{100\ cc}{200\ hrs} \times \frac{1\ hr}{60\ min} \times \frac{2.64\ gm}{cc} = 0.0219$ gm/min.

267

9950-322

PROCESS M-2 (3)

Format A # and Description	Catalog #	Description	Usage/Units	Basis for Usage
	C1080D	Liquid N_2	10^{-4} $\frac{cuft}{min.}$	Used in blow dry apparatus, carrier gas for diffusion and CVD reactor. Carrier gas-diffusion 600 $\frac{cc}{min.}$ - 100% of time, blowing 4000 $\frac{cc}{min.}$ - 5% of time or 1100 cc/min. In terms of liquid usage this is $\frac{1100}{10^3}$ or 1.1 $\frac{cc}{min.}$ or 4×10^{-5} $\frac{cuft}{min.}$ - assume 150% waste so usage is 10^{-4} $\frac{cuft}{min.}$
	C1096D	Liquid O_2	4×10^{-5} $\frac{cuft}{min.}$	LO_2 is used as a carrier gas in the diffusion and in the CVD reactor. Diffusion furnace - 100 $\frac{cc}{min.}$ - 100% up time. CVD reactor - 600 $\frac{cc}{min.}$ - 50% up time. Usage is $\frac{400cc}{min.}$. As above, usage is 4×10^{-5} cuft/min.
	EACDP	Acid Disposal	2.8×10^{-3} gal/min	4 gal. of 1:1 HF-H_2O will be discarded every 24 hours or 2.8×10^{-3} gal/min.

PROCESS M-2 (4)

Format A # and Description	Catalog #	Description	Usage/Units	Basis for Usage
	C1128D	Cooling H_2O	.67 $\frac{cuft}{min.}$	Vendor specification for furnace and CVD reactor - 5 gal/min. or .67 cuft/min.
	E1584D	Silane	10^{-4} $\frac{lb}{min.}$	The flow rate is 100 cc/min. and operates 65% of the time or 65 cc/min. This is about 6.5×10^{-2} gm/min. or 10^{-4} lb/min.

265

JET PROPULSION LABORATORY
California Institute of Technology
4800 Oak Grove Dr. Pasadena CA 91109

SOLAR ARRAY MANUFACTURING INDUSTRY COSTING STANDARDS
FORMAT A - PROCESS DESCRIPTION

☐ A-1 Process [Referent] M3
Revision Number:

Note: Names given in brackets [ ] are the names of process attributes requested by the SAMIS Computer Program.

☐ A-2 [Descriptive . Name] of process PHOS DIFFUSION-BASELINE

PART 1 - PRODUCT DESCRIPTION

☐☐ A-3 [Product . Referent] BSF

A-5 Unit of Measure [Product . Units] CM2

☐ A-4 Descriptive Name [Product . Name] DIFFUSED WEB - BASELINE PROCESS

PART 2 - PROCESS CHARACTERISTICS

☐ A-6 [Output . Rate] (Not Thruput) 222.4 Units (given on line A-5) Per Operating Minute

☐ A-7 [Inprocess . Inventory . Time] 60 Calendar Minutes

☐ A-8 [Duty . Cycle] .98 Operating Minutes Per Minute

☐ A-8a [Number . Of . Shifts . Per . Day] 3 Shifts

☐ A-8b [Personnel . Integerization . Override . Switch] Off (Off or On)

PART 3 - EQUIPMENT COST FACTORS [Machine . Description]

☐ A-9 Component [Referent]	SILX12	DIFCE	ESTA3
☐ A-9a Component [Descriptive . Name]	Silox Reactor	Diffusion Furnace	Etch Station
☐ A-10 Base Year for Equipment Prices [Price . Year]	1980	1980	1980
☐ A-11 [Purchase . Cost . Vs . Quantity . Bought . Table] (Number Of and $ Per Component)	1 25,000	1 85,000	1 4,000
☐ A-12 Anticipated [Useful . Life] (Years)	7	7	7
☐ A-13 [Salvage . Value] ($ Per Component)	2,000	5,000	---
☐ A-14 [Removal . And . Installation . Cost] ($/Component)	1,000	3,000	500
[Payment . Float . Interval]	0.0	0.0	0.0
[Inflation . Rate . Table]	IRTJ	IRTJ	IRTJ
[Equipment . Tax . Depreciation . Method]	DDB	DDB	DDB
[Equipment . Book . Depreciation . Method]	SL	SL	SL

A-15 Process Referent (From Front Side Line A-1) M 3

PART 5a - BYPRODUCTS PRODUCED PER MACHINE PER MINUTE [Byproduct]

A-20 Catalog Number (Expense Item Referent)	A-22 Amount Produced Per Machine Per Minute [Amount . Per . Cycle]	A-23 Units	A-21 Byproduct Specifications
EACDP	10^{-3}	gal	Acid Disposal

PART 4 - FLOORSPACE PER MACHINE and PERSONNEL PER MACHINE PER SHIFT [Facility . Or . Personnel Requirement]

A-16 Catalog Number (Expense Item Referent)	A-18 Amount Required [Amount . Per . Machine]	A-19 Units	A-17 Requirement Description
A2064D	250	sq ft	Space
B3672D	.75	py	Operator
B3688D	0.06	py	Mech. & Elec. Maint.
B3736D	0.06	py	Mech. & Elec. Maint.

PART 5b - DIRECT REQUIREMENTS PER MACHINE PER MINUTE [Utility . Or . Commodity Requirement]

A-20 Catalog Number (Expense Item Referent)	A-22 Amount Required Per Machine Per Minute [Amount . Per . Cycle]	A-23 Units	A-21 Requirement Specifications
C1032D	0.12	kw	Elec.
ED100	0.033	cu ft	DI H_2O
E1328D	0.010	lb	HF
E1584D	10^{-4}	lb	Silane
EPOCL	5×10^{-5}	lb	$POCl_3$ Diffusant
C1128D	0.8	cu ft	H_2O
C1080D	10^{-4}	cu ft	Liq N_2
C1096D	5×10^{-5}	cu ft	Liq O_2
E1112D	0.022	cu ft	Argon

PART 6 - INTRA-INDUSTRY PRODUCT(S) REQUIRED

A-24 [Required . Product] (Reference)	A-28 [Yield] (%)	A-26 [Ideal . Ratio] Of Units Out/Units In	A-27 Units of A-26	A-25 Product Name
DIFFWEB	99	1	cm^2/cm^2	

PREPARED BY	COMPANY	DATE	JPL USE ONLY
R. B. Campbell	WESTINGHOUSE ELECTRIC CORPORATION		
CHECKED BY	COMPANY	DATE	

268

PROCESS M-3 (1)

Format A # and Description	Catalog #	Description	Usage/Units	Basis for Usage
A-1 — A-6				See M-1
A-7				See M-2
A-11 — A-14				See M-2
A-16 — A-19	A2064D B3672D	Space Operator	.75 PY	Same as in M-2
A-20 — A-23				Verification for C1032D, C1044D, E1128D, E1584D, A1240I, A1160I, A1176I and EACDP same as M-2.
	EPOCl	$POCl_3$ diffusion	5×10^{-5} lb/min.	Usage same as BBr_3 in M-2
	E1112D	Argon	$0.022 \frac{cuft}{min.}$	Ar is carrier gas in diffusion process. Flow rate is 600 cc/min., 100% of the time $600 \frac{cc}{min.}$ gas — $0.022 \frac{cuft}{min.}$.

JET PROPULSION LABORATORY
California Institute of Technology
4800 Oak Grove Dr Pasadena, CA 91109

SOLAR ARRAY MANUFACTURING INDUSTRY COSTING STANDARDS
FORMAT A - PROCESS DESCRIPTION

☐ A-1 Process [Referent] M12
Revision Number:

Note: Names given in brackets [ ] are the names of process attributes requested by the SAMIS Computer Program.

☐ A-2 [Descriptive . Name] of process D'LS BORON PLUS DLS MASK

PART 1 - PRODUCT DESCRIPTION

☐☐ A-3 [Product . Referent] DIFFWEB   A-5 Unit of Measure [Product . Units] CM2

☐ A-4 Descriptive Name [Product . Name] DIFFUSION OF BSF USING LIQUID SOURCE AND MASK

PART 2 - PROCESS CHARACTERISTICS

☐ A-6 [Output . Rate] (Not Thruput) 224.6 Units (given on line A-5) Per Operating Minute

☐ A-7 [Inprocess . Inventory . Time] 30 Calendar Minutes

☐ A-8 [Duty . Cycle] 0.9 Operating Minutes Per Minute

☐ A-8a [Number . Of . Shifts . Per . Day] 3 Shifts

☐ A-8b [Personnel . Integerization . Override . Switch] Off (Off or On)

PART 3 - EQUIPMENT COST FACTORS [Machine . Description]

☐ A-9 Component [Referent]	MENISCUS1	ETCHSTA1	BLTFCE
☐ A-9a Component [Descriptive . Name]	Meniscus Coater (2 each)	Etch Station	Belt Furnace
☐ A-10 Base Year for Equipment Prices [Price . Year]	1980	1980	1980
☐ A-11 [Purchase . Cost . Vs . Quantity . Bought . Table] (Number Of and $ Per Component)	2 42,000	1 4,000	1 42,000
☐ A-12 Anticipated [Useful . Life] (Years)	7	7	7
☐ A-13 [Salvage . Value] ($ Per Component)	5,000	0	4,000
☐ A-14 [Removal . And . Installation . Cost] ($/Component)	2,000	500	2,000
[Payment . Float . Interval]	0.0	0.0	0.0
[Inflation . Rate . Table]	IRTJ	IRTJ	IRTJ
[Equipment . Tax . Depreciation . Method]	DDB	DDB	DDB
[Equipment . Book . Depreciation . Method]	SL	SL	SL

JPL 3037-S R 6/81

A-15 Process Referent (From Front Side Line A-1) M 1 2

PART 5a - BYPRODUCTS PRODUCED PER MACHINE PER MINUTE [Byproduct]

A-20 Catalog Number (Expense Item Referent)	A-22 Amount Produced Per Machine Per Minute [Amount . Per . Cycle]	A-23 Units	A-21 Byproduct Specifications
EACDP	8.3×10^{-4}	gal	Acid Disposal

PART 4 - FLOORSPACE PER MACHINE and PERSONNEL PER MACHINE PER SHIFT [Facility . Or . Personnel Requirement]

A-16 Catalog Number (Expense Item Referent)	A-18 Amount Required [Amount . Per . Machine]	A-19 Units	A-17 Requirement Description
A2064D	400	sq ft	Type C Space
B3672D	0.75	py	Operator
B3688D	0.06	py	Mech. & Elec. Maint.
B3736D	0.06	py	Mech. & Elec. Maint.

PART 5b - DIRECT REQUIREMENTS PER MACHINE PER MINUTE [Utility . Or . Commodity Requirement]

A-20 Catalog Number (Expense Item Referent)	A-22 Amount Required Per Machine Per Minute [Amount . Per . Cycle]	A-23 Units	A-21 Requirement Specifications
C1032D	0.08	kw	Electricity
E1328D	.005	lb	HF
EBLIQ	0.01	mℓ	Liquid Source for Boron
ELMAS	0.01	mℓ	Liquid Source for Mask
ED100	0.033	cu ft	DI H_2O
C1080D	6.8×10^{-5}	cu ft	Liq N_2

PART 6 - INTRA-INDUSTRY PRODUCT(S) REQUIRED

A-24 [Required . Product] (Reference)	A-28 [Yield] (%)	A-26 [Ideal . Ratio] Of Units Out/Units In	A-27 Units of A-26	A-25 Product Name
CLENWEB	99	1/1 = 1	cm^2/cm^2	BSF diffused web

PREPARED BY	COMPANY	DATE	JPL USE ONLY
R. B. Campbell	WESTINGHOUSE ELECTRIC CORPORATION		
CHECKED BY	COMPANY	DATE	

SOLAR ARRAY MANUFACTURING INDUSTRY COSTING STANDARDS
FORMAT A - PROCESS DESCRIPTION

JET PROPULSION LABORATORY
California Institute of Technology
4800 Oak Grove Dr Pasadena, CA 91109

☐ A-1 Process [Referent]
M 1 2
Revision Number:

Note: Names given in brackets [ ] are the names of process attributes requested by the SAMIS Computer Program.

☐ A-2 [Descriptive . Name] of process

PART 1 - PRODUCT DESCRIPTION

☐☐ A-3 [Product . Referent]

A-5 Unit of Measure [Product . Units]

☐ A-4 Descriptive Name [Product . Name]

PART 2 - PROCESS CHARACTERISTICS

☐ A-6 [Output . Rate] (Not Thruput) ____ Units (given on line A-5) Per Operating Minute

☐ A-7 [Inprocess . Inventory . Time] ____ Calendar Minutes

☐ A-8 [Duty . Cycle] ____ Operating Minutes Per Minute

☐ A-8a [Number . Of . Shifts . Per . Day] ____ Shifts

☐ A-8b [Personnel . Integerization . Override . Switch] ____ (Off or On)

PART 3 - EQUIPMENT COST FACTORS [Machine . Description]

☐ A-9 Component [Referent]	D R Y F C E		
☐ A-9a Component [Descriptive . Name]	200°C Fce		
☐ A-10 Base Year for Equipment Prices [Price . Year]	1980		
☐ A-11 [Purchase . Cost . Vs . Quantity . Bought . Table] (Number Of and $ Per Component)	1 3,000		
☐ A-12 Anticipated [Useful . Life] (Years)	7		
☐ A-13 [Salvage . Value] ($ Per Component)	---		
☐ A-14 [Removal . And . Installation . Cost] ($/Component)	---		
[Payment . Float . Interval]	0.0	0.0	0.0
[Inflation . Rate . Table]	IRTJ	IRTJ	IRTJ
[Equipment . Tax . Depreciation . Method]	DDB	DDB	DDB
[Equipment . Book . Depreciation . Method]	SL	SL	SL

271

A-15 Process Referent (From Front Side Line A-1) ____________

PART 5a - BYPRODUCTS PRODUCED PER MACHINE PER MINUTE [Byproduct]

☐ A-20 Catalog Number (Expense Item Referent)	A-22 Amount Produced Per Machine Per Minute [Amount . Per . Cycle]	A-23 Units	A-21 Byproduct Specifications

PART 4 - FLOORSPACE PER MACHINE and PERSONNEL PER MACHINE PER SHIFT [Facility . Or . Personnel Requirement]

☐ A-16 Catalog Number (Expense Item Referent)	A-18 Amount Required [Amount . Per . Machine]	A-19 Units	A-17 Requirement Description

PART 5b - DIRECT REQUIREMENTS PER MACHINE PER MINUTE [Utility . Or . Commodity Requirement]

☐ A-20 Catalog Number (Expense Item Referent)	A-22 Amount Required Per Machine Per Minute [Amount . Per . Cycle]	A-23 Units	A-21 Requirement Specifications

PART 6 - INTRA-INDUSTRY PRODUCT(S) REQUIRED

☐ A-24 [Required . Product] (Reference)	A-28 [Yield] (%)	A-26 [Ideal . Ratio] Of Units Out/Units In	A-27 Units of A-26	A-25 Product Name

PREPARED BY	COMPANY	DATE	JPL USE ONLY
CHECKED BY	COMPANY	DATE	☐

PROCESS M12

Format A # and Description	Catalog #	Description	Usage/Units	Basis for Usage
A9		Capital Eqpt.	88K$	Meniscus Coater - cost of last unit purchased Etch Station - standard equipment Belt Furnace - RTC vendor quote Drying Furnace - catalog price (Fisher Scientific)
A20	EACDP	Acid Disposal	8.3×10^{-4} gal/min	1.2 gal of 1:1 HF:H_2O will be discarded every 24 hours or 8.3×10^{-4} gal/min
A16	B3688D B3736D	Maintenance	py	Apportioned time of machine maintenance
A20	C1032D	Electricity	kw/min	1 meniscus coater - 1 kw up 75% 1 belt furnace - 4 kw up 100% 0.08 kw/min
A20	E1328D	HF	lb/min	1:1 HF solution in 4 gal tank - solution discarded every 48 hours. Usage of 7 lb/day or 0.005 lb/min
A20	EBLIQ	Liquid Source - B	mℓ/min	Coat thickness of 0.5 μm - 200 cm^2 each min - vol coated = 100×10^{-4} cm/min
A20	ELMAS	Liquid Mask Source	mℓ/min	As above

278

PROCESS M12

Format A # and Description	Catalog #	Description	Usage/Units	Basis for Usage
A20	ED-100	DI H_2O	cu ft/min	Major usage is overflow from rinse tank. Overflow rate = 1 ℓ/min or 0.033 cu ft/min.
A20	C1080D	Liq N_2	6.8×10^{-5} cu ft/min	Use 600 cc/min as carrier gas in diffusion (100% of time). Use 6000 cc/min for drying station (10% of time). Total usage is 1200 cc/min. For liquid usage, this is $1200/10^3 = 1.2$ cc/min or 3.4×10^{-5} cu ft/min. Assume 50% waste 6.8×10^{-5} cc/min.

JET PROPULSION LABORATORY
California Institute of Technology
4800 Oak Grove Dr. Pasadena, CA 91109

SOLAR ARRAY MANUFACTURING INDUSTRY COSTING STANDARDS
FORMAT A - PROCESS DESCRIPTION

A-1 Process [Referent] M13
Revision Number:

Note: Names given in brackets [ ] are the names of process attributes requested by the SAMIS Computer Program.

A-2 [Descriptive . Name] of process DLS MASK PLUS POCL3

PART 1 - PRODUCT DESCRIPTION

A-3 [Product . Referent] BSF

A-5 Unit of Measure [Product . Units] CM2

A-4 Descriptive Name [Product . Name] DIFFUSION OF FRONT JUNCTION USING POCL3 WITH LIQUID SOURCE MASK

PART 2 - PROCESS CHARACTERISTICS

A-6 [Output . Rate] (Not Thruput) 222.4 Units (given on line A-5) Per Operating Minute

A-7 [Inprocess . Inventory . Time] 60 Calendar Minutes

A-8 [Duty . Cycle] .98 Operating Minutes Per Minute

A-8a [Number . Of . Shifts . Per . Day] 3 Shifts

A-8b [Personnel . Integerization . Override . Switch] Off (Off or On)

PART 3 - EQUIPMENT COST FACTORS [Machine . Description]

A-9 Component [Referent]	DIFCE	ESTA3	
A-9a Component [Descriptive . Name]	Diffusion Furnace	Etch Station	
A-10 Base Year for Equipment Prices [Price . Year]	1980	1980	
A-11 [Purchase . Cost . Vs . Quantity . Bought . Table] (Number Of and $ Per Component)	85,000	4,000	
A-12 Anticipated [Useful . Life] (Years)	7	7	
A-13 [Salvage . Value] ($ Per Component)	5,000	0	
A-14 [Removal . And . Installation . Cost] ($/Component)	3,000	500	
[Payment . Float . Interval]	0.0	0.0	0.0
[Inflation . Rate . Table]	IRTJ	IRTJ	IRTJ
[Equipment . Tax . Depreciation . Method]	DDB	DDB	DDB
[Equipment . Book . Depreciation . Method]	SL	SL	SL

275

A-15 Process Referent (From Front Side Line A-1) M13

PART 5a - BYPRODUCTS PRODUCED PER MACHINE PER MINUTE [Byproduct]

A-20 Catalog Number (Expense Item Referent)	A-22 Amount Produced Per Machine Per Minute [Amount . Per . Cycle]	A-23 Units	A-21 Byproduct Specifications
EACDP	8.3×10^{-4}	gal	Acid Disposal

PART 4 - FLOORSPACE PER MACHINE and PERSONNEL PER MACHINE PER SHIFT [Facility . Or . Personnel Requirement]

A-16 Catalog Number (Expense Item Referent)	A-18 Amount Required [Amount . Per . Machine]	A-19 Units	A-17 Requirement Description
A2064D	400	sq ft	Type C Space
B3672D	0.75	py	Operator
B3688D	0.06	py	Mech. & Elec. Maint.
B3736D	0.06	py	Mech. & Elec. Maint.

PART 5b - DIRECT REQUIREMENTS PER MACHINE PER MINUTE [Utility . Or . Commodity Requirement]

A-20 Catalog Number (Expense Item Referent)	A-22 Amount Required Per Machine Per Minute [Amount . Per . Cycle]	A-23 Units	A-21 Requirement Specifications
C1032D	0.12	kw	Electricity
ED100	0.033	cu ft	DI H_2O
E1328D	0.005	lbs	HF
EPOCL	5×10^{-5}	lb	$POCl_3$ Diffusant
ELMAS	0.01	mℓ	Source for Liquid Mask
C1080D	6.8×10^{-5}	cu ft	Liq N_2
E1112D	0.022	cu ft	Argon

PART 6 - INTRA-INDUSTRY PRODUCT(S) REQUIRED

A-24 [Required . Product] (Reference)	A-28 [Yield] (%)	A-26 [Ideal . Ratio] Of Units Out/Units In	A-27 Units of A-26	A-25 Product Name
DIFFWEB	99	1	cm^2/cm^2	

PREPARED BY	COMPANY	DATE	JPL USE ONLY
R. B. Campbell	WESTINGHOUSE ELECTRIC CORPORATION		
CHECKED BY	COMPANY	DATE	

277

PROCESS M13

Format A # and Description	Catalog #	Description	Usage/Units	Basis for Usage
A9		Capital Eqpt.		Diffusion Furnace - vendor quote
A20	EACDP	Acid Disposal		See M12
A16	B3688D B3736D	Maintenance	py	Apportioned time of maintenance personnel.
A20	C1032B	Electricity	kw	See M12
A20	ED100 EPOCL ELMAS C1080D E1112D	DI H_2O $POCl_3$ Diffusant Diffusant Mask Liq N_2 Argon	cu ft lb mℓ cu ft cu ft	See M12 See M3 See M12 See M12 See M3

JET PROPULSION LABORATORY
California Institute of Technology
4800 Oak Grove Dr. Pasadena CA 91109

SOLAR ARRAY MANUFACTURING INDUSTRY COSTING STANDARDS
FORMAT A - PROCESS DESCRIPTION

☐ A-1 Process [Referent] M23

Revision Number:

Note: Names given in brackets [ ] are the names of process attributes requested by the SAMIS Computer Program.

☐ A-2 [Descriptive . Name] of process DLS MASK PLUS DLS PHOS

PART 1 - PRODUCT DESCRIPTION

☐☐ A-3 [Product . Referent] BSF

A-5 Unit of Measure [Product . Units] CM2

☐ A-4 Descriptive Name [Product . Name] DIFFUSION OF FRONT JUNCTION WITH DLS MASK AND DLS PHOS

PART 2 - PROCESS CHARACTERISTICS

☐ A-6 [Output . Rate] (Not Thruput) 222.4 Units (given on line A-5) Per Operating Minute

☐ A-7 [Inprocess . Inventory . Time] 30 Calendar Minutes

☐ A-8 [Duty . Cycle] .98 Operating Minutes Per Minute

☐ A-8a [Number . Of . Shifts . Per . Day] 3 Shifts

☐ A-8b [Personnel . Integerization . Override . Switch] Off (Off or On)

PART 3 - EQUIPMENT COST FACTORS [Machine . Description]

☐ A-9 Component [Referent]	MENISCUS2	ETSTA2	
☐ A-9a Component [Descriptive . Name]	Meniscus Coater for applying liq. phos. source	Etch Station	
☐ A-10 Base Year for Equipment Prices [Price . Year]	1980	1980	
☐ A-11 [Purchase . Cost . Vs . Quantity . Bought . Table] (Number Of and $ Per Component)	42,000	4,000	
☐ A-12 Anticipated [Useful . Life] (Years)	7	7	
☐ A-13 [Salvage . Value] ($ Per Component)	4,000	0	
☐ A-14 [Removal . And . Installation . Cost] ($/Component)	2,000	500	
[Payment . Float . Interval]	0.0	0.0	0.0
[Inflation . Rate . Table]	IRTJ	IRTJ	IRTJ
[Equipment . Tax . Depreciation . Method]	DDB	DDB	DDB
[Equipment . Book . Depreciation . Method]	SL	SL	SL

278

A-15 Process Referent (From Front Side Line A-1) M 2 3

PART 5a - BYPRODUCTS PRODUCED PER MACHINE PER MINUTE [Byproduct]

A-20 Catalog Number (Expense Item Referent)	A-22 Amount Produced Per Machine Per Minute [Amount . Per : Cycle]	A-23 Units	A-21 Byproduct Specifications
E A C D P	8.3×10^{-4}	gal	Acid Disposal

PART 4 - FLOORSPACE PER MACHINE and PERSONNEL PER MACHINE PER SHIFT [Facility . Or . Personnel Requirement]

A-16 Catalog Number (Expense Item Referent)	A-18 Amount Required [Amount . Per . Machine]	A-19 Units	A-17 Requirement Description
A 2 0 6 4 D	300	sq ft	Type C Space
B 3 6 7 2 D	0.75	py	Operator
B 3 6 8 8 D	0.06	py	Mech. & Elec. Maint.
B 3 7 3 6 D	0.06	py	Mech. & Elec. Maint.

PART 5b - DIRECT REQUIREMENTS PER MACHINE PER MINUTE [Utility . Or . Commodity Requirement]

A-20 Catalog Number (Expense Item Referent)	A-22 Amount Required Per Machine Per Minute [Amount . Per . Cycle]	A-23 Units	A-21 Requirement Specifications
C 1 0 3 2 D	1.3×10^{-2}	kw	Electricity
E 1 0 0 D	0.033	cu ft	DI H_2O
E 1 3 2 8 D	0.005	lb	HF
E P L I Q	0.01	mℓ	Liquid Phosphorus Source
E L M A S	0.01	mℓ	Liquid Diffusion Mask Source
C 1 0 8 0 D	6.8×10^{-5}	cu ft	Liq N_2

PART 6 - INTRA-INDUSTRY PRODUCT(S) REQUIRED

A-24 [Required . Product] (Reference)	A-28 [Yield] (%)	A-26 [Ideal . Ratio] Of Units Out/Units In	A-27 Units of A-26	A-25 Product Name
D I F F W E B	99	1	cm^2/cm^2	

PREPARED BY	COMPANY	DATE	JPL USE ONLY
R. B. Campbell	WESTINGHOUSE ELECTRIC CORPORATION		
CHECKED BY	COMPANY	DATE	

PROCESS M23

Format A # and Description	Catalog #	Description	Usage/Units	Basis for Usage
A9		Capital Eqpt.		Meniscus coater - cost of last unit purchased Etch station - standard equipment (This step will use same belt furnace as M13.)
A20	EACDP	Acid Disposal	gal	See M12
A16	B3688D B3736D	Maintenance Personnel	py	Apportioned to all process steps.
A20	C1032D	Electricity	kw	Meniscus coater only = 1.3×10^{-2}
A20	E100D E1328D ELMAS C1080D EPLIQ	DI H_2O HF Mask Liq N_2 Phosphorus Source	cu ft lb mℓ cu ft mℓ	See M13 See M13 See M13 See M13 Usage same as EBLIQ (M12).

JPL JET PROPULSION LABORATORY
California Institute of Technology
4800 Oak Grove Dr / Pasadena, Calif 91103

SOLAR ARRAY MANUFACTURING INDUSTRY COSTING STANDARDS

FORMAT B — COMPANY DESCRIPTION

Company Referent: WESTCO M

DESCRIPTIVE NAME
PILOT LINE MANUFACTURING OF SOLAR MODULES - SUB PROCESS SEQUENCE

0.	(b)	(Final) Product(s) Produced	BSF
	(a)	(Final) Process(es)	N^+ Diffusion
1.	(c)	Ideal Ratio(s) with units	1/1 - cm^2
	(b)	Intermediate Product(s)	DIFFWEB
	(a)	Process(es)	P^+ Diffusion
2.	(c)	Ideal Ratio(s) with units	1/1 - cm^2
	(b)	Intermediate Product(s)	
	(a)	Process(es)	
3.	(c)	Ideal Ratio(s) with units	
	(b)	Intermediate Product(s)	
	(a)	Process(es)	
4.	(c)	Ideal Ratio(s) with units	
	(b)	Intermediate Product(s)	
	(a)	Process(es)	
5.	(c)	Ideal Ratio(s) with units	
	(b)	Intermediate Product(s)	
	(a)	Process(es)	
6.	(c)	Ideal Ratio(s) with units	
	(b)	Intermediate Product(s)	
	(a)	Process(es)	
7.	(c)	Ideal Ratio(s) with units	
	(b)	Intermediate Product(s)	
	(a)	Process(es)	
8.	(c)	Ideal Ratio(s) with units	
	(b)	Intermediate Product(s)	
	(a)	Process(es)	
9.	(c)	Ideal Ratio(s) with units	
	(b)	Intermediate Product(s)	
	(a)	Process(es)	
	(c)	Ideal Ratio(s) with units	
		Purchased Product(s)	
		Supplier and Percentage	
		Supplier and Percentage	

PREPARED BY: R. B. Campbell

DATE:

JPL 3038-S R 5/80

Format B: Company Description (Continued) — Financial Parameters

Page ____Of ____

Note: In the LSA SAMICS context, leave this page blank; use default values of all company financial parameters.

Company Referent (From Front Side) ____________________

LSA SAMICS defaults and appropriate units are shown preprinted.

B-1 Percent of Capacity 100%	B-20 Startup Production Fraction 0.635 units/unit
B-2 (Financial) Leverage 1.2 $/$	B-21 Cash Balance Operation Time 0.06 yrs.
B-3 Debt Interest Rate 9.25%/yr.	B-22 Between Process Inventory Time 0 yrs.
B-4 Other Tax Rate 2%/yr.	B-23 Fiscal Hours Per Shift 8 hrs./shift
B-5 Insurance Rate 4%/yr.	B-24 Fiscal Minutes Per Fiscal Hour 60 min./hr.
B-6 Facility Life 40 yrs.	B-25 Fiscal Days Per Fiscal Week 7 days/wk.
B-7 Rate Of Return On Equity 20%/yr.	B-26 Fiscal Weeks Per Fiscal Year 52.1429 wks./yr.
B-8 Misc. Expense (as) Percentage Of Revenue 3%	B-27 Closed Weekdays Per Fiscal Year 20 days/yr.
B-9 Misc. Expense (as) Percentage Of Operating Expense 4%	B-28 Working Hours Per Person Per Shift 8 hrs./person/shift
B-10 Misc. Expense (as) Percentage Of Book Value 0%/yr.	B-29 Working Days Per Working Week 5 days/wk.
B-11 Facilities Tax Depreciation Method DDB	B-30 Paid Holidays Per Fiscal Year 8 days/yr.
B-12 Facilities Book Depreciation Method SL	B-31 Paid Vacation Days Per Fiscal Year 13.5 days/yr.
B-13 Facilities Inflation Rate Table 1975 8.0 • (yr. %/yr.)	B-32 Working Weeks Per Fiscal Year 52.1429 wks./yr. B-33 Average Paid Absenteeism Days Per Fiscal Year 17.5 days/yr.
B-14 Raw Materials Inventory Time 0.04 yrs.	B-34 Second Shift Wage Factor 1.15 ($/hr.)/($/hr.)
B-15 Processing Time Multiplier 1.0 min./min.	B-35 Third Shift Wage Factor 1.20 ($/hr.)/($/hr.)
B-16 Finished Goods Inventory Time 0.04 yrs.	B-36 Fourth Shift Wage Factor 1.20 ($/hr.)/($/hr.)
B-17 Accounts Receivable Turnover Time 0.10 yrs.	B-37 Number Of Shifts Per Day 3 shifts/day
B-18 Accounts Payable Turnover Time 0.09 yrs.	B-38 Facilities (Construction) Contingency Percentage 15%
B-19 Startup Direct Commodity Usage Fraction 1.25 units/unit	B-39 Equipment Contingency Percentage 15%

SOLAR ARRAY MANUFACTURING INDUSTRY COSTING STANDARDS
FORMAT C - INDUSTRY DESCRIPTION

JET PROPULSION LABORATORY
California Institute of Technology
4800 Oak Grove Dr. Pasadena CA 91109

C-1 Industry [Referent] WESTCORPM
Revision Number:

Note: Names given in brackets [ ] are the names of industry attributes requested by the SAMIS Computer Program.

C-2 [Descriptive . Name] Description of Industry MANUFACTURING OF SOLAR MODULES SUB-PROCESS

C-3 Result of Industry [Objective] (Eg: New PV Power Capability) 1 mw/yr

C-4 [Production . Units] (Eg: Peak Watts) 1mw/yr

DESCRIPTION OF THE FINAL PRODUCT OF THE INDUSTRY

C-5 [Final . Product . Reference] BSF Name Diffused Web

C-6 Production is Measured in [Final . Product . Units] (Eg: Modules) cm2

C-7 [Hardware . Performance] ______ (Units are C-4 Per C-6; Eg: Peak Watts per Module)

C-8 Product Design Description* ______

MAKERS OF THE FINAL PRODUCT OF THE INDUSTRY [MAKERS . LIST]

C-9 SAMIS Company [Company . Reference] WESTCOM [Market . Share] 100 %

SAMIS Company [Company . Reference] ______ [Market . Share] ______ %

SAMIS Company [Company . Reference] ______ [Market . Share] ______ %

PREPARED BY	COMPANY	DATE
R. B. Campbell	WESTINGHOUSE ELECTRIC CORPORATION	

* For LSA industries, include at least the following information on line C-8:

Cell Shape: Rectangular
Bare Cell Efficiency 14%
Cell Size: 2.5 cm x 9.8 cm
Encapsulated Cell Efficiency ---
Cells Per Module: 180
Packing Efficiency 96
Module Size: 40 cm x 120 cm
Module Efficiency 12.0%

Note: Production quantities are specified to SAMIS by the RUN . CONTROL: INDUSTRY . SIZE . RANGE vector.

JPL 3039-S R 6/81

283

SOLAR ARRAY MANUFACTURING INDUSTRY COSTING STANDARDS
FORMAT A - PROCESS DESCRIPTION

JET PROPULSION LABORATORY
California Institute of Technology
4800 Oak Grove Dr Pasadena, CA 91109

☐ A-1 Process [Referent] P2

Revision Number:

Note: Names given in brackets [ ] are the names of process attributes requested by the SAMIS Computer Program.

☐ A-2 [Descriptive . Name] of process BORON DIFFUSION - BASELINE

PART 1 - PRODUCT DESCRIPTION

☐☐ A-3 [Product . Referent] DIFFWEB

A-5 Unit of Measure [Product . Units] CM2

☐ A-4 Descriptive Name [Product . Name] DIFFUSED WEB

PART 2 - PROCESS CHARACTERISTICS

☐ A-6 [Output . Rate] (Not Thruput) 5559 Units (given on line A-5) Per Operating Minute

☐ A-7 [Inprocess . Inventory . Time] 80 Calendar Minutes

☐ A-8 [Duty . Cycle] .97 Operating Minutes Per Minute

☐ A-8a [Number . Of . Shifts . Per . Day] 3 Shifts

☐ A-8b [Personnel . Integerization . Override . Switch] Off (Off or On)

PART 3 - EQUIPMENT COST FACTORS [Machine . Description]

☐ A-9 Component [Referent]	DIFCE	SILR	ESTA3
☐ A-9a Component [Descriptive . Name]	Diffusion Furnace	Silox Reactor	Etch Station
☐ A-10 Base Year for Equipment Prices [Price . Year]	1980	1980	1980
☐ A-11 [Purchase . Cost . Vs . Quantity . Bought . Table] (Number Of and $ Per Component)	2 200,000	1 60,000	1 20,000
☐ A-12 Anticipated [Useful . Life] (Years)	7	7	7
☐ A-13 [Salvage . Value] ($ Per Component)	0	0	0
☐ A-14 [Removal . And . Installation . Cost] ($/Component)	3000	2000	2000
[Payment . Float . Interval]	0.0	0.0	0.0
[Inflation . Rate . Table]	IRTJ	IRTJ	IRTJ
[Equipment . Tax . Depreciation . Method]	DDB	DDB	DDB
[Equipment . Book . Depreciation . Method]	SL	SL	SL

84

A-15 Process Referent (From Front Side Line A-1) P2

PART 5a - BYPRODUCTS PRODUCED PER MACHINE PER MINUTE [Byproduct]

A-20 Catalog Number (Expense Item Referent)	A-22 Amount Produced Per Machine Per Minute [Amount . Per . Cycle]	A-23 Units	A-21 Byproduct Specifications
EACDP	4×10^{-3}	gal	Acid Disposal

PART 4 - FLOORSPACE PER MACHINE and PERSONNEL PER MACHINE PER SHIFT [Facility . Or . Personnel Requirement]

A-16 Catalog Number (Expense Item Referent)	A-18 Amount Required [Amount . Per . Machine]	A-19 Units	A-17 Requirement Description
A2064D	650	sq ft	Space
B3672D	2	py	Operator
B3688D	0.12	py	Mech. & Elec. Maint.
B3736D	0.12	py	Mech. & Elec. Maint.

PART 5b - DIRECT REQUIREMENTS PER MACHINE PER MINUTE [Utility . Or . Commodity Requirement]

A-20 Catalog Number (Expense Item Referent)	A-22 Amount Required Per Machine Per Minute [Amount . Per . Cycle]	A-23 Units	A-21 Requirement Specifications
C1032B	0.33	kw	Electricity
E1328D	0.08	lb	HF
ED100	0.066	cu ft	DI H_2O
EBB3D	.548	gm	BBr_3
C1080D	2.5×10^{3}	cu ft	Liq N_2
C1096D	5×10^{-4}	cu ft	Liq O_2

PART 6 - INTRA-INDUSTRY PRODUCT(S) REQUIRED

A-24 [Required . Product] (Reference)	A-28 [Yield] (%)	A-26 [Ideal . Ratio] Of Units Out/Units In	A-27 Units of A-26	A-25 Product Name
CLENWEB	99	1/1	cm^2/cm^2	

PREPARED BY	COMPANY	DATE	JPL USE ONLY
R. B. Campbell	WESTINGHOUSE ELECTRIC CORPORATION		
CHECKED BY	COMPANY	DATE	

286

PROCESS P2 (1)

Format A # and Description	Catalog #	Description	Usage/Units	Basis for Usage
A7		Time at station	80 min	SiO_2 coating - 30 min Diffusion - 30 min Etch - 20 min
A9-A14		Diffusion furnace	$400,000	One furnace dedicated to boron diffusion. Cost is vendor estimate.
		SiO_2 deposition	60,000	One unit required for P2 and P3. Prorate cost. $120,000 is vendor estimate.
		Etch station	20,000	Etch station similar to P1 - Engineering estimate.
A16-A19	A2096D	Space	650 sq ft	Based on vendor-supplied information.
	B3672D	Operator	2 PY	Process consists of placing loaded boat on oxide deposition unit input, removing loaded boat from unit and placing at diffusion furnace input. After diffusion, load etching apparatus and monitor process. Two persons can perform this task.
A20-A23	C1032B	Electricity	0.33 KWH/min	1 - 8 tube furnace at 2.2 KW/tube - 17.6 KW Drive on SiO_2 disposition unit - 0.3 KW Pumps on SiO_2 disposition unit - 0.7 KW Drive on etch station - 0.9 KW Pumps on etch station - 0.4 KW 19.9 KW or 0.33 $\frac{KWH}{min}$
	E1328D	HF	0.08 lb/min	Etching in 4 gal.tank;flushed every 4 hrs 7.6 ℓHF used each 4 hrs, 1150 gm/ℓ uses 36.4g/min or 0.08 lb/min.
	ED100	DIH_2O	0.066 $\frac{cu\ ft}{min}$	Usage is overflow in rinse tank. 2 l/min overflow or 0.066 cu ft/min

287

PROCESS P2 (2)

Format A # and Description	Catalog #	Description	Usage/Units	Basis for Usage
A-20-A-23 (cont)	EBB3D C1080D C1096D	B Br and diffusant Liquid N_2 Liquid O_2	0.219 gm 2.5×10^{-3} 5×10^{-4}	These usaqes are scaled directly 25 times that of one M process.
	C1128D	H_2O	$2.0 \frac{cu\ ft}{min}$	Vendor spec.
	EACDP	Acid disposal	$4 \times 10^{-3} \frac{gal}{min}$	Related to acid usage.

JET PROPULSION LABORATORY
California Institute of Technology
4800 Oak Grove Dr Pasadena, CA 91109

SOLAR ARRAY MANUFACTURING INDUSTRY COSTING STANDARDS
FORMAT A - PROCESS DESCRIPTION

A-1 Process [Referent] P3
Revision Number:

Note: Names given in brackets [ ] are the names of process attributes requested by the SAMIS Computer Program.

A-2 [Descriptive . Name] of process PHOSPHORUS DIFFUSION - BASELINE

PART 1 - PRODUCT DESCRIPTION

A-3 [Product . Referent] BSF

A-5 Unit of Measure [Product . Units] CM2

A-4 Descriptive Name [Product . Name] DIFFUSED WEB - BASELINE PROCESS

PART 2 - PROCESS CHARACTERISTICS

A-6 [Output . Rate] (Not Thruput) 5503 Units (given on line A-5) Per Operating Minute

A-7 [Inprocess . Inventory . Time] 80 Calendar Minutes

A-8 [Duty . Cycle] .98 Operating Minutes Per Minute

A-8a [Number . Of . Shifts . Per . Day] 3 Shifts

A-8b [Personnel . Integerization . Override . Switch] Off (Off or On)

PART 3 - EQUIPMENT COST FACTORS [Machine . Description]

A-9 Component [Referent]	DIFCE	SILR	ESTA4
A-9a Component [Descriptive . Name]	Diffusion Furnace	Silox Reactor	Etch Station
A-10 Base Year for Equipment Prices [Price . Year]	1980	1980	1980
A-11 [Purchase . Cost . Vs . Quantity . Bought . Table] (Number Of and $ Per Component)	2 200,000	1 60,000	1 20,000
A-12 Anticipated [Useful . Life] (Years)	7	7	7
A-13 [Salvage . Value] ($ Per Component)	0	0	0
A-14 [Removal . And . Installation . Cost] ($/Component)	3,000	2,000	2,000
[Payment . Float . Interval]	0.0	0.0	0.0
[Inflation . Rate . Table]	IRTJ	IRTJ	IRTJ
[Equipment . Tax . Depreciation . Method]	DDB	DDB	DDB
[Equipment . Book . Depreciation . Method]	SL	SL	SL

JPL 3037-S R 6/81

A-15 Process Referent (From Front Side Line A-1) P3

PART 5a - BYPRODUCTS PRODUCED PER MACHINE PER MINUTE [Byproduct]

A-20 Catalog Number (Expense Item Referent)	A-22 Amount Produced Per Machine Per Minute [Amount . Per . Cycle]	A-23 Units	A-21 Byproduct Specifications
EACDP	4×10^{-3}	gal	Acid Disposal

PART 4 - FLOORSPACE PER MACHINE and PERSONNEL PER MACHINE PER SHIFT [Facility . Or . Personnel Requirement]

A-16 Catalog Number (Expense Item Referent)	A-18 Amount Required [Amount . Per . Machine]	A-19 Units	A-17 Requirement Description
A2064D	650	sq ft	Space
B3672D	2	py	Operator
B3688D	0.12	py	Mech. & Elec. Maint.
B3736D	0.12	py	Mech. & Elec. Maint.

PART 5b - DIRECT REQUIREMENTS PER MACHINE PER MINUTE [Utility . Or . Commodity Requirement]

A-20 Catalog Number (Expense Item Referent)	A-22 Amount Required Per Machine Per Minute [Amount . Per . Cycle]	A-23 Units	A-21 Requirement Specifications
C1032B	0.12	kw	Electricity
E1328D	0.08	lb	HF
ED100	0.066	cu ft	DI H_2O
EPOCL	1.2×10^{-3}	lb	$POCl_3$
C1080D	2.5×10^{-3}	cu ft	Liq N_2
C1096D	5×10^{-4}	cu ft	Liq O_2
E1112D	0.55	cu ft	Argon

PART 6 - INTRA-INDUSTRY PRODUCT(S) REQUIRED

A-24 [Required . Product] (Reference)	A-28 [Yield] (%)	A-26 [Ideal . Ratio] Of Units Out/Units In	A-27 Units of A-26	A-25 Product Name
DIFFWEB	99	1/1	cm^2/cm^2	

PREPARED BY	COMPANY	DATE	JPL USE ONLY
R. B. Campbell	WESTINGHOUSE ELECTRIC CORPORATION		
CHECKED BY	COMPANY	DATE	

PROCESS P3 (1)

Format A # and Description	Catalog #	Description	Usage/Units	Basis for Usage
A7		Time at station	80 min	See A7 of P2.
A10-A14		Equipment		See A10-A14 of P2.
A16-A19		Direct requirement per machine.		See A16-A19 of P2.
A20-A23	E1112D	Argon	$0.55 \frac{cu\ ft}{min}$	Direct scaleup from M process.
	EPOCL	$POCl_3$ diffusant	$1.2 \times 10^{-3} \frac{lb}{min}$	
				All other commodities - see A20-A23 of P2.

SOLAR ARRAY MANUFACTURING INDUSTRY COSTING STANDARDS
FORMAT A - PROCESS DESCRIPTION

JET PROPULSION LABORATORY
California Institute of Technology
4800 Oak Grove Dr. Pasadena, CA 91109

☐ A-1 Process [Referent] P12
Revision Number:

Note: Names given in brackets [ ] are the names of process attributes requested by the SAMIS Computer Program.

☐ A-2 [Descriptive . Name] of process DLS BORON PLUS DLS MASK

PART 1 - PRODUCT DESCRIPTION

☐☐ A-3 [Product . Referent] DIFFWEB

A-5 Unit of Measure [Product . Units] CM2

☐ A-4 Descriptive Name [Product . Name] DIFFUSION OF BSF USING LIQUID SOURCE AND LIQUID MASK

PART 2 - PROCESS CHARACTERISTICS

☐ A-6 [Output . Rate] (Not Thruput) 5559 Units (given on line A-5) Per Operating Minute

☐ A-7 [Inprocess . Inventory . Time] 60 Calendar Minutes

☐ A-8 [Duty . Cycle] .97 Operating Minutes Per Minute

☐ A-8a [Number . Of . Shifts . Per . Day] 3 Shifts

☐ A-8b [Personnel . Integerization . Override . Switch] Off (Off or On)

PART 3 - EQUIPMENT COST FACTORS [Machine . Description]

☐ A-9 Component [Referent]	MENISCUS2	ETCHSTA2	BELTFCE
☐ A-9a Component [Descriptive . Name]	Meniscus Coaters for application of SiO_2 and liquid source	Station for etching diffused strips	Belt furnace for diffusion
☐ A-10 Base Year for Equipment Prices [Price . Year]	1980	1980	1980
☐ A-11 [Purchase . Cost . Vs . Quantity . Bought . Table] (Number Of and $ Per Component)	4 80,000	1 60,000	1 75,000
☐ A-12 Anticipated [Useful . Life] (Years)	7	7	7
☐ A-13 [Salvage . Value] ($ Per Component)	8,000	5,000	5,000
☐ A-14 [Removal . And . Installation . Cost] ($/Component)	5,000	2,000	3,000
[Payment . Float . Interval]	0.0	0.0	0.0
[Inflation . Rate . Table]	IRTJ	IRTJ	IRTJ
[Equipment . Tax . Depreciation . Method]	DDB	DDB	DDB
[Equipment . Book . Depreciation . Method]	SL	SL	SL

291

A-15 Process Referent (From Front Side Line A-1) P12

PART 5a - BYPRODUCTS PRODUCED PER MACHINE PER MINUTE [Byproduct]

A-20 Catalog Number (Expense Item Referent)	A-22 Amount Produced Per Machine Per Minute [Amount . Per . Cycle]	A-23 Units	A-21 Byproduct Specifications
EACDP	1.7×10^{-2}	gal	Acid Disposal

PART 4 - FLOORSPACE PER MACHINE and PERSONNEL PER MACHINE PER SHIFT [Facility . Or . Personnel Requirement]

A-16 Catalog Number (Expense Item Referent)	A-18 Amount Required [Amount . Per . Machine]	A-19 Units	A-17 Requirement Description
A2064D	800	sq ft	Space
B3672D	1	py	Operator
B3688D	0.12	py	Mech. & Elec. Maint.
B3736D	0.12	py	Mech. & Elec. Maint.

PART 5b - DIRECT REQUIREMENTS PER MACHINE PER MINUTE [Utility . Or . Commodity Requirement]

A-20 Catalog Number (Expense Item Referent)	A-22 Amount Required Per Machine Per Minute [Amount . Per . Cycle]	A-23 Units	A-21 Requirement Specifications
C1032D	0.14	kw	Electricity
E1328D	0.04	lb	HF
EBLIQ	0.25	mℓ	Liquid Source for Boron
ELMAS	0.25	mℓ	Liquid Source for Mask
ED100	0.066	cu ft	DI H_2O
C1080D	1.7×10^{-3}	cu ft	Liquid N_2

PART 6 - INTRA-INDUSTRY PRODUCT(S) REQUIRED

A-24 [Required . Product] (Reference)	A-28 [Yield] (%)	A-26 [Ideal . Ratio] Of Units Out/Units In	A-27 Units of A-26	A-25 Product Name
CLENWEB	99	1/1	cm^2/cm^2	

PREPARED BY	COMPANY	DATE	JPL USE ONLY
R. B. Campbell	WESTINGHOUSE ELECTRIC CORPORATION		
CHECKED BY	COMPANY	DATE	

PROCESS P12

Format A # and Description	Catalog #	Description	Usage/Units	Basis for Usage
A9		Meniscus Coater		Budgetary estimate for larger unit with self-contained drying.
		Etch Station		Vendor estimate (budgetary)
		Belt Furnace		Vendor estimate (budgetary)
A20	ACDP	Acid Disposal	1.7×10^{-2} gal	Price is vendor quote. Quantity based on 20X 1 mw usage.
A16	A2064D	Space	800 sq ft	Estimate based on equipment size
A16	B3672D	Operator	py	1 operator to coat and diffuse strips
A20	C1032D	Electricity	0.14 kw/min	Drive/Pump - etch station - 1.3 kw Drive/Pump - meniscus coater - 0.8 lw (X4) Belt Furance - heaters/blower - 4kw 6.1 kw or 0.1 kw/min
	E1328D	HF	.08 lb	see P2
	EBLIQ	Liquid Boron Source	.25 mℓ	25 x M12 usage
	ELMAS	Liquid Mask Source	.25 mℓ	25 x M12 usage
	ED100	DI H_2O	0.066 cu ft	See P2
	C1080D	Liquid N_2	7×10^{-4} cu ft	25 x M12 usage

JET PROPULSION LABORATORY
California Institute of Technology
4800 Oak Grove Dr. Pasadena, CA 91109

SOLAR ARRAY MANUFACTURING INDUSTRY COSTING STANDARDS
FORMAT A - PROCESS DESCRIPTION

☐ A-1 Process [Referent] P13
Revision Number:

Note: Names given in brackets [ ] are the names of process attributes requested by the SAMIS Computer Program.

☐ A-2 [Descriptive . Name] of process DLS MASK PLUS POCL3

PART 1 - PRODUCT DESCRIPTION

☐☐ A-3 [Product . Referent] BSF

A-5 Unit of Measure [Product . Units] CM2

☐ A-4 Descriptive Name [Product . Name] DIFFUSION OF FRONT JUNCTION USING POCL3 WITH LIQUID SOURCE MASK

PART 2 - PROCESS CHARACTERISTICS

☐ A-6 [Output . Rate] (Not Thruput) 5503 Units (given on line A-5) Per Operating Minute

☐ A-7 [Inprocess . Inventory . Time] 60 Calendar Minutes

☐ A-8 [Duty . Cycle] .97 Operating Minutes Per Minute

☐ A-8a [Number . Of . Shifts . Per . Day] 3 Shifts

☐ A-8b [Personnel . Integerization . Override . Switch] Off (Off or On)

PART 3 - EQUIPMENT COST FACTORS [Machine . Description]

☐ A-9 Component [Referent]	MENISCUS3	ETCHSTA3	DIFFCE
☐ A-9a Component [Descriptive . Name]	Meniscus coaters for application of SiO_2	Etch station	Diffusion furnace for phosphorus diffusion only
☐ A-10 Base Year for Equipment Prices [Price . Year]	1980	1980	1980
☐ A-11 [Purchase . Cost . Vs . Quantity . Bought . Table] (Number Of and $ Per Component)	2 80,000	1 60,000	1 400,000
☐ A-12 Anticipated [Useful . Life] (Years)	7	7	7
☐ A-13 [Salvage . Value] ($ Per Component)	8,000	5,000	20,000
☐ A-14 [Removal . And . Installation . Cost] ($/Component)	5,000	2,000	5,000
[Payment . Float . Interval]	0.0	0.0	0.0
[Inflation . Rate . Table]	IRTJ	IRTJ	IRTJ
[Equipment . Tax . Depreciation . Method]	DDB	DDB	DDB
[Equipment . Book . Depreciation . Method]	SL	SL	SL

A-15 Process Referent (From Front Side Line A-1) P13

PART 5a - BYPRODUCTS PRODUCED PER MACHINE PER MINUTE [Byproduct]

A-20 Catalog Number (Expense Item Referent)	A-22 Amount Produced Per Machine Per Minute [Amount . Per . Cycle]	A-23 Units	A-21 Byproduct Specifications
EACDP	1.7×10^{-2}	gal	Acid Disposal

PART 4 - FLOORSPACE PER MACHINE and PERSONNEL PER MACHINE PER SHIFT [Facility . Or . Personnel Requirement]

A-16 Catalog Number (Expense Item Referent)	A-18 Amount Required [Amount . Per . Machine]	A-19 Units	A-17 Requirement Description
A2064D	650	sq ft	
B3672D	1.0	py	Operator
B3688D	0.12	py	Mech. & Elec. Maint.
B3736D	0.12	py	Mech. & Elec. Maint.

PART 5b - DIRECT REQUIREMENTS PER MACHINE PER MINUTE [Utility . Or . Commodity Requirement]

A-20 Catalog Number (Expense Item Referent)	A-22 Amount Required Per Machine Per Minute [Amount . Per . Cycle]	A-23 Units	A-21 Requirement Specifications
C1032B	0.34	kw	Electricity
E1328D	0.04	lb	HF
ELMAS	0.25	mℓ	Liquid Mask Source
ED100	0.066	cu ft	DI H_2O
C1080D	1.7×10^{-3}	cu ft	Liq N_2
C1096D	5×10^{-4}	cu ft	Liq O_2
E1112D	0.55	cu ft	Argon
EPOCL	1.2×10^{-3}	lb	$POCl_3$

PART 6 - INTRA-INDUSTRY PRODUCT(S) REQUIRED

A-24 [Required . Product] (Reference)	A-28 [Yield] (%)	A-26 [Ideal . Ratio] Of Units Out/Units In	A-27 Units of A-26	A-25 Product Name
DIFFWEB	99	1/1	cm^2/cm^2	

PREPARED BY	COMPANY	DATE	JPL USE ONLY
R. B. Campbell	WESTINGHOUSE ELECTRIC CORPORATION		
CHECKED BY	COMPANY	DATE	

296

PROCESS P13

Format A # and Description	Catalog #	Description	Usage/Units	Basis for Usage
A9		Meniscus Coater Etch Station		See P12 See P12
A9		Diffusion Furnace		See P2
A20	EACDP	Acid Disposal	1.7×10^{-2} gal	See P12
A16	A2064D B3672D	Space Personnel	650 sq ft 1.0 py	Est. required for 2 meniscus coaters, furnace, and etch station Coat and load strips into diffusion furnace.
A20	C1032B	Electricity	0.34 kw/min	Drive/Pump - etch station - 1.3 kw Drive/Pump - meniscus coater - 0.8 kw (x2) Diffusion furnace (P2) 17.6 kw .34 kw/min
A20	E1328D ELMAS ED100 C1080D	HF Liquid Mask DI H_2O Liq N_2	0.08 lb 0.25 mℓ 0.066 cu ft 7×10^{-4} cu ft	Same usage as P12 Same usage as P12 Same usage as P12 Same usage as P12

PROCESS P13 Page 2

Format A # and Description	Catalog #	Description	Usage/Units	Basis for Usage
A20	C1096D	Liq O_2	5×10^{-4} cu ft	Same usage as P2
	E1112D	Argon	0.55 cu ft	Same usage as P2
	EPOCL	$POCl_3$	1.2×10^{-3} lb	Same usage as P2

JET PROPULSION LABORATORY
California Institute of Technology
4800 Oak Grove Dr. Pasadena CA 91109

SOLAR ARRAY MANUFACTURING INDUSTRY COSTING STANDARDS
FORMAT A - PROCESS DESCRIPTION

A-1 Process [Referent] P23
Revision Number:

Note: Names given in brackets [ ] are the names of process attributes requested by the SAMIS Computer Program.

A-2 [Descriptive . Name] of process DLS MASK PLUS DLS PHOS

PART 1 - PRODUCT DESCRIPTION

A-3 [Product . Referent] BSF

A-5 Unit of Measure [Product . Units] CM2

A-4 Descriptive Name [Product . Name] DIFFUSION OF FRONT JUNCTION WITH DLS MASK AND DLS PHOS

PART 2 - PROCESS CHARACTERISTICS

A-6 [Output . Rate] (Not Thruput)	5503	Units (given on line A-5) Per Operating Minute
A-7 [Inprocess . Inventory . Time]	60	Calendar Minutes
A-8 [Duty . Cycle]	.97	Operating Minutes Per Minute
A-8a [Number . Of . Shifts . Per . Day]	3	Shifts
A-8b [Personnel . Integerization . Override . Switch]	Off	(Off or On)

PART 3 - EQUIPMENT COST FACTORS [Machine . Description]

A-9 Component [Referent]	MENISCUS4	ETCHSTA4	
A-9a Component [Descriptive . Name]	Meniscus coaters for applying SiO_2 and liq phos.	Etch station	
A-10 Base Year for Equipment Prices [Price . Year]	1980	1980	
A-11 [Purchase . Cost . Vs . Quantity . Bought . Table] (Number Of and $ Per Component)	4 80,000	1 60,000	
A-12 Anticipated [Useful . Life] (Years)	7	7	
A-13 [Salvage . Value] ($ Per Component)	10,000	5,000	
A-14 [Removal . And . Installation . Cost] ($/Component)			
[Payment . Float . Interval]	0.0	0.0	0.0
[Inflation . Rate . Table]	IRTJ	IRTJ	IRTJ
[Equipment . Tax . Depreciation . Method]	DDB	DDB	DDB
[Equipment . Book . Depreciation . Method]	SL	SL	SL

A-15 Process Referent (From Front Side Line A-1) P23

PART 5a - BYPRODUCTS PRODUCED PER MACHINE PER MINUTE [Byproduct]

A-20 Catalog Number (Expense Item Referent)	A-22 Amount Produced Per Machine Per Minute [Amount . Per . Cycle]	A-23 Units	A-21 Byproduct Specifications
EACDP	1.7×10^{-2}	gal	Acid Disposal

PART 4 - FLOORSPACE PER MACHINE and PERSONNEL PER MACHINE PER SHIFT [Facility . Or . Personnel Requirement]

A-16 Catalog Number (Expense Item Referent)	A-18 Amount Required [Amount . Per . Machine]	A-19 Units	A-17 Requirement Description
A2064D	500	sq ft	Space
B3672D	1	py	Operator
B3672D	0.12	py	Mech. & Elec. Maint.
B3736D	0.12	py	Mech. & Elec. Maint.

PART 5b - DIRECT REQUIREMENTS PER MACHINE PER MINUTE [Utility . Or . Commodity Requirement]

A-20 Catalog Number (Expense Item Referent)	A-22 Amount Required Per Machine Per Minute [Amount . Per . Cycle]	A-23 Units	A-21 Requirement Specifications
C1032B	0.14	kw	Electricity
E1328D	.04	lb	HF
ELMAS	0.25	m	Liquid Source for Mask
EPLIQ	0.25	m	Liquid Source for Phosphorus
ED100	0.066	cu ft	DI H_2O
C1080D	1.7×10^{-3}	cu ft	Liq N_2
C1096D	5×10^{-4}	cu ft	Liq O_2

PART 6 - INTRA-INDUSTRY PRODUCT(S) REQUIRED

A-24 [Required . Product] (Reference)	A-28 [Yield] (%)	A-26 [Ideal . Ratio] Of Units Out/Units In	A-27 Units of A-26	A-25 Product Name
DIFFWEB	99	1/1	cm^2/cm^2	

PREPARED BY	COMPANY	DATE	JPL USE ONLY
R. B. Campbell	WESTINGHOUSE ELECTRIC CORPORATION		
CHECKED BY	COMPANY	DATE	

PROCESS P23

Format A # and Description	Catalog #	Description	Usage/Units	Basis for Usage
A9		Meniscus Coater Etch Station		See P12 Process uses same belt furnace as in P13
A20	EACDP	Acid Disposal	1.7×10^{-2} gal	See P13
A20	A2064D	Space	500 sq ft	Est. of space required for 4 meniscus coaters and etch station
A16	B3672D B3688D B3736D	Personnel Personnel Personnel	1 py .12 py .12 py	See P13 See P13 See P13
A20	C1032B E1328D ELMAS ED100	Electricity HF Mask DI H_2O	.14 kw 0.08 lb 0.25 mℓ 0.066 cu ft	See P12 See P12 See P12
	C1080D C1096D	Liq N_2 Liq O_2	7.4×10^{-4} cu ft 5×10^{-4} cu ft	See P13 See P13
	EPLIQ	Source for Mask	0.25	25x M23 usage

JET PROPULSION LABORATORY
California Institute of Technology
4800 Oak Grove Dr. / Pasadena, Calif. 91103

SOLAR ARRAY MANUFACTURING INDUSTRY COSTING STANDARDS

FORMAT B – COMPANY DESCRIPTION

Company Referent: WESTCO P

DESCRIPTIVE NAME
PILOT LINE MANUFACTURING OF SOLAR MODULES SUB-PROCESS

0.	(b)	(Final) Product(s) Produced	BSF
	(a)	(Final) Process(es)	N^+ Diffusion
	(c)	Ideal Ratio(s) with units	1/1 cm^2
1.	(b)	Intermediate Product(s)	DIFFWEB
	(a)	Process(es)	P^+ Diffusion
	(c)	Ideal Ratio(s) with units	1/1 cm^2
2.	(b)	Intermediate Product(s)	
	(a)	Process(es)	
	(c)	Ideal Ratio(s) with units	
3.	(b)	Intermediate Product(s)	
	(a)	Process(es)	
	(c)	Ideal Ratio(s) with units	
4.	(b)	Intermediate Product(s)	
	(a)	Process(es)	
	(c)	Ideal Ratio(s) with units	
5.	(b)	Intermediate Product(s)	
	(a)	Process(es)	
	(c)	Ideal Ratio(s) with units	
6.	(b)	Intermediate Product(s)	
	(a)	Process(es)	
	(c)	Ideal Ratio(s) with units	
7.	(b)	Intermediate Product(s)	
	(a)	Process(es)	
	(c)	Ideal Ratio(s) with units	
8.	(b)	Intermediate Product(s)	
	(a)	Process(es)	
	(c)	Ideal Ratio(s) with units	
9.	(b)	Intermediate Product(s)	
	(a)	Process(es)	
	(c)	Ideal Ratio(s) with units	
		Purchased Product(s)	
		Supplier and Percentage	
		Supplier and Percentage	

PREPARED BY: R. B. Campbell

DATE:

301

Format B: Company Description (Continued) – Financial Parameters

Note: In the LSA SAMICS context, leave this page blank; use default values of all company financial parameters.

Company Referent (From Front Side) ______________________

LSA SAMICS defaults and appropriate units are shown preprinted.

B-1 Percent of Capacity 100%	B-20 Startup Production Fraction 0.635 units/unit
B-2 (Financial) Leverage 1.2 $/$	B-21 Cash Balance Operation Time 0.06 yrs.
B-3 Debt Interest Rate 9.25%/yr.	B-22 Between Process Inventory Time 0 yrs.
B-4 Other Tax Rate 2%/yr.	B-23 Fiscal Hours Per Shift 8 hrs./shift
B-5 Insurance Rate 4%/yr.	B-24 Fiscal Minutes Per Fiscal Hour 60 min./hr.
B-6 Facility Life 40 yrs.	B-25 Fiscal Days Per Fiscal Week 7 days/wk.
B-7 Rate Of Return On Equity 20%/yr.	B-26 Fiscal Weeks Per Fiscal Year 52.1429 wks./yr.
B-8 Misc. Expense (as) Percentage Of Revenue 3%	B-27 Closed Weekdays Per Fiscal Year 20 days/yr.
B-9 Misc. Expense (as) Percentage Of Operating Expense 4%	B-28 Working Hours Per Person Per Shift 8 hrs./person/shift
B-10 Misc. Expense (as) Percentage Of Book Value 0%/yr.	B-29 Working Days Per Working Week 5 days/wk.
B-11 Facilities Tax Depreciation Method DDB	B-30 Paid Holidays Per Fiscal Year 8 days/yr.
B-12 Facilities Book Depreciation Method SL	B-31 Paid Vacation Days Per Fiscal Year 13.5 days/yr.
B-13 Facilities Inflation Rate Table 1975 8.0 * (yr. %/yr.)	B-32 Working Weeks Per Fiscal Year 52.1429 wks./yr.
	B-33 Average Paid Absenteeism Days Per Fiscal Year 17.5 days/yr.
B-14 Raw Materials Inventory Time 0.04 yrs.	B-34 Second Shift Wage Factor 1.15 ($/hr.)/($/hr.)
B-15 Processing Time Multiplier 1.0 min./min.	B-35 Third Shift Wage Factor 1.20 ($/hr.)/($/hr.)
B-16 Finished Goods Inventory Time 0.04 yrs.	B-36 Fourth Shift Wage Factor 1.20 ($/hr.)/($/hr.)
B-17 Accounts Receivable Turnover Time 0.10 yrs.	B-37 Number Of Shifts Per Day 3 shifts/day
B-18 Accounts Payable Turnover Time 0.09 yrs.	B-38 Facilities (Construction) Contingency Percentage 15%
B-19 Startup Direct Commodity Usage Fraction 1.25 units/unit	B-39 Equipment Contingency Percentage 15%

JET PROPULSION LABORATORY
California Institute of Technology
4800 Oak Grove Dr. Pasadena CA 91109

SOLAR ARRAY MANUFACTURING INDUSTRY COSTING STANDARDS
FORMAT C - INDUSTRY DESCRIPTION

☐ C-1 Industry [Referent] WESTCORPP
Revision Number:

Note: Names given in brackets [ ] are the names of industry attributes requested by the SAMIS Computer Program.

☐ C-2 [Descriptive . Name] Description of Industry MANUFACTURING OF SOLAR MODULES - SUB-PROCESS

☐ C-3 Result of Industry [Objective] (Eg: New PV Power Capability) 25 mw/yr

☐ C-4 [Production . Units] (Eg: Peak Watts) 25mw/yr

DESCRIPTION OF THE FINAL PRODUCT OF THE INDUSTRY

☐☐ C-5 [Final . Product . Reference] BSF Name Diffused Web

☐ C-6 Production is Measured in [Final . Product . Units] (Eg: Modules) cm2

☐ C-7 [Hardware . Performance] ______ (Units are C-4 Per C-6; Eg: Peak Watts per Module)

☐ C-8 Product Design Description* ______

MAKERS OF THE FINAL PRODUCT OF THE INDUSTRY [MAKERS . LIST]

☐ C-9 SAMIS Company [Company . Reference] WESTCO,M [Market . Share] 100 %

SAMIS Company [Company . Reference] ______ [Market . Share] ______ %

SAMIS Company [Company . Reference] ______ [Market . Share] ______ %

PREPARED BY	COMPANY	DATE
R. B. Campbell	WESTINGHOUSE ELECTRIC CORPORATION	

* For LSA industries, include at least the following information on line C-8:

Cell Shape:	Rectangular	Bare Cell Efficiency	14.0%
Cell Size:	2.5 cm x 9.8 cm	Encapsulated Cell Efficiency	---
Cells Per Module:	180	Packing Efficiency	96%
Module Size:	40 cm x 120 cm	Module Efficiency	12.0%

Note: Production quantities are specified to SAMIS by the RUN . CONTROL: INDUSTRY . SIZE . RANGE vector.

SOLAR ARRAY MANUFACTURING INDUSTRY COSTING STANDARDS
NEW EXPENSE ITEM SHEET

JET PROPULSION LABORATORY
California Institute of Technology
4800 Oak Grove Dr. Pasadena, CA 91109

EXPENSE ITEM ☒ NEW ☐ REVISED

Referent used on Format A, A-20 or A-16: EBLIQ
Name and Specifications: LIQUID DOPANT BORON
Specifications Continued: per data sheet 3-14-83
Units in which quantities are expressed: ml
Price Year: 1980
Inflation Rate (or code): 7 %/Year

Quantity	0.01	0.10
Price of this quantity	0.0021	0.015
Price/Unit	0.210	0.150

(Multiply number of units by 26 before entering as RQT for A2272I).

In storage, 100 units take 10 square feet of warehouse space.

Other indirect requirements:
____ units require ____ amount ____ units of ____ Catalog Number ____ description
____ units require ____ amount ____ units of ____ Catalog Number ____ description

Supplier: Allied Chemical
Address: 20 Peabody St., Buffalo, NY 14210
Supplier's Part Number(s): B150
Supplier's Catalog and Page Number(s): data sheet 3-14-83
Supplier's Salesperson and Phone Number:

EXPENSE ITEM: ☒ NEW ☐ REVISED

Referent used on Format A, A-20 or A-16: EPLIQ
Name and Specifications: LIQUID DOPANT PHOS
Specifications Continued: per data sheet 8-10-81
Units in which quantities are expressed: ml
Price Year: 1980
Inflation Rate (or code): 7 %/Year

Quantity	0.01	0.1
Price of this quantity	0.0021	0.015
Price/Unit	0.210	0.150

(Multiply number of units by 26 before entering as RQT for A2272I).

In storage, 100 units take 10 square feet of warehouse space.

Other indirect requirements:
____ units require ____ amount ____ units of ____ Catalog Number ____ description
____ units require ____ amount ____ units of ____ Catalog Number ____ description

Supplier: Allied Chemical
Address: 20 Peabody St., Buffalo, NY 14210
Supplier's Part Number(s): PX10
Supplier's Catalog and Page Number(s): data sheet 3-14-83
Supplier's Salesperson and Phone Number:

EXPENSE ITEM: ☒ NEW ☐ REVISED

Referent used on Format A, A-20 or A-16: ELMAS
Name and Specifications: LIQUID MASK
Specifications Continued: per data sheet 8-10-81
Units in which quantities are expressed: ml
Price Year: 1980
Inflation Rate (or code): 7 %/Year

Quantity	0.01	0.1
Price of this quantity	0.0025	0.018
Price/Unit	0.25	0.18

(Multiply number of units by 26 before entering as RQT for A2272I).

In storage, 100 units take 10 square feet of warehouse space.

Other indirect requirements:
____ units require ____ amount ____ units of ____ Catalog Number ____ description
____ units require ____ amount ____ units of ____ Catalog Number ____ description

Supplier: Diffusion Technology, Inc.
Address: 1090 Milpitas, Blvd., Milpitas, CA 95035
Supplier's Part Number(s): Spin Rite U1A
Supplier's Catalog and Page Number(s): data sheet 8-10-81
Supplier's Salesperson and Phone Number:

PREPARED BY	COMPANY	DATE	JPL USE ONLY
R. B. Campbell	WESTINGHOUSE ELECTRIC CORP.		
CHECKED BY	COMPANY	DATE	☐

308

JET PROPULSION LABORATORY
California Institute of Technology
4800 Oak Grove Dr. Pasadena CA 91109

SOLAR ARRAY MANUFACTURING INDUSTRY COSTING STANDARDS
NEW EXPENSE ITEM SHEET

EXPENSE ITEM ☒ NEW ☐ REVISED

EACDP — Referent used on Format A, A-20 or A-16
ACID DISPOSAL — Name and Specifications
Specifications Continued:
GAL — Units in which quantities are expressed
Quantity: gal
Price of this quantity: 1.91
Price/Unit: 1.91
1980 — Price Year
Inflation Rate (or code): ______ %/Year
(Multiply number of units by 26 before entering as RQT for A2272I).
In storage, 100 units take 3 square feet of warehouse space.
Other indirect requirements:
______ units require ______ amount ______ units of ______ Catalog Number ______ description
______ units require ______ amount ______ units of ______ Catalog Number ______ description
Supplier: Ecology Chem. & Ref. Co. Address: Brush Creek Rd.,Manor,PA 15665
Supplier's Part Number(s):
Supplier's Catalog and Page Number(s):
Supplier's Salesperson and Phone Number:

EXPENSE ITEM: ☒ NEW ☐ REVISED

ED100 — Referent used on Format A, A-20 or A-16
DI H20 — Name and Specifications
Specifications Continued: 18 meg ohm
CU FT — Units in which quantities are expressed
Quantity: cu ft
Price of this quantity: 0.073
Price/Unit: 0.073
19 — Price Year
Inflation Rate (or code): ______ %/Year
(Multiply number of units by 26 before entering as RQT for A2272I).
In storage, ______ units take ______ square feet of warehouse space.
Other indirect requirements:
______ units require ______ amount ______ units of ______ Catalog Number ______ description
______ units require ______ amount ______ units of ______ Catalog Number ______ description
Supplier: per ASEC Address:
Supplier's Part Number(s):
Supplier's Catalog and Page Number(s):
Supplier's Salesperson and Phone Number:

EXPENSE ITEM: ☒ NEW ☐ REVISED

EPOCL — Referent used on Format A, A-20 or A-16
POCL3 DIFFUSANT — Name and Specifications
Specifications Continued:
LBS — Units in which quantities are expressed
Quantity: 1
Price of this quantity: 5.00
Price/Unit: $5/lb
19 — Price Year
Inflation Rate (or code): ______ %/Year
(Multiply number of units by 26 before entering as RQT for A2272I).
In storage, 100 units take 5 square feet of warehouse space.
Other indirect requirements:
______ units require ______ amount ______ units of ______ Catalog Number ______ description
______ units require ______ amount ______ units of ______ Catalog Number ______ description
Supplier: Allied Chemical Address: 20 Peabody St.,Buffalo,NY 14210
Supplier's Part Number(s):
Supplier's Catalog and Page Number(s): catalog
Supplier's Salesperson and Phone Number:

PREPARED BY	COMPANY	DATE	JPL USE ONLY
R. B. Campbell	WESTINGHOUSE ELECTRIC CORP.		
CHECKED BY	COMPANY	DATE	☐

JPL 3037-1-S R 6/81

9950-892

JET PROPULSION LABORATORY
California Institute of Technology
4800 Oak Grove Dr Pasadena, CA 91109

SOLAR ARRAY MANUFACTURING INDUSTRY COSTING STANDARDS
NEW EXPENSE ITEM SHEET

EXPENSE ITEM ☒ NEW ☐ REVISED

EBB3D — Referent used on Format A, A-20 or A-16

BBR3 DIFFUSANT — Name and Specifications

Specifications Continued

G.M. — Units in which quantities are expressed

Quantity 1

Price of this quantity 0.85

Price/Unit

1980 — Price Year

%/Year — Inflation Rate (or code)

(Multiply number of units by 26 before entering as RQT for A2272I).

In storage, 100 units take 5 square feet of warehouse space.

Other indirect requirements:

units require ____ amount ____ units of ____ Catalog Number ____ description

units require ____ amount ____ units of ____ Catalog Number ____ description

Supplier TBD

Address

Supplier's Part Number(s)

Supplier's Catalog and Page Number(s)

Supplier's Salesperson and Phone Number

EXPENSE ITEM: ☐ NEW ☐ REVISED

Referent used on Format A, A-20 or A-16

Name and Specifications

Specifications Continued

Units in which quantities are expressed

Quantity

Price of this quantity

Price/Unit

19__ — Price Year

%/Year — Inflation Rate (or code)

(Multiply number of units by 26 before entering as RQT for A2272I).

In storage, ____ units take ____ square feet of warehouse space.

Other indirect requirements:

units require ____ amount ____ units of ____ Catalog Number ____ description

units require ____ amount ____ units of ____ Catalog Number ____ description

Supplier

Address

Supplier's Part Number(s)

Supplier's Catalog and Page Number(s)

Supplier's Salesperson and Phone Number

EXPENSE ITEM: ☐ NEW ☐ REVISED

Referent used on Format A, A-20 or A-16

Name and Specifications

Specifications Continued

Units in which quantities are expressed

Quantity

Price of this quantity

Price/Unit

19__ — Price Year

%/Year — Inflation Rate (or code)

(Multiply number of units by 26 before entering as RQT for A2272I).

In storage, ____ units take ____ square feet of warehouse space.

Other indirect requirements:

units require ____ amount ____ units of ____ Catalog Number ____ description

units require ____ amount ____ units of ____ Catalog Number ____ description

Supplier

Address

Supplier's Part Number(s)

Supplier's Catalog and Page Number(s)

Supplier's Salesperson and Phone Number

PREPARED BY	COMPANY	DATE	JPL USE ONLY
CHECKED BY	COMPANY	DATE	☐